

# Soil degradation and restoration in arid and semi-arid regions

**Edited by**

Kaibo Wang, Jianping Li, Zhengchao Zhou  
and Xunchang John Zhang

**Published in**

Frontiers in Environmental Science



## FRONTIERS EBOOK COPYRIGHT STATEMENT

The copyright in the text of individual articles in this ebook is the property of their respective authors or their respective institutions or funders. The copyright in graphics and images within each article may be subject to copyright of other parties. In both cases this is subject to a license granted to Frontiers.

The compilation of articles constituting this ebook is the property of Frontiers.

Each article within this ebook, and the ebook itself, are published under the most recent version of the Creative Commons CC-BY licence. The version current at the date of publication of this ebook is CC-BY 4.0. If the CC-BY licence is updated, the licence granted by Frontiers is automatically updated to the new version.

When exercising any right under the CC-BY licence, Frontiers must be attributed as the original publisher of the article or ebook, as applicable.

Authors have the responsibility of ensuring that any graphics or other materials which are the property of others may be included in the CC-BY licence, but this should be checked before relying on the CC-BY licence to reproduce those materials. Any copyright notices relating to those materials must be complied with.

Copyright and source acknowledgement notices may not be removed and must be displayed in any copy, derivative work or partial copy which includes the elements in question.

All copyright, and all rights therein, are protected by national and international copyright laws. The above represents a summary only. For further information please read Frontiers' Conditions for Website Use and Copyright Statement, and the applicable CC-BY licence.

ISSN 1664-8714  
ISBN 978-2-8325-3827-2  
DOI 10.3389/978-2-8325-3827-2

## About Frontiers

Frontiers is more than just an open access publisher of scholarly articles: it is a pioneering approach to the world of academia, radically improving the way scholarly research is managed. The grand vision of Frontiers is a world where all people have an equal opportunity to seek, share and generate knowledge. Frontiers provides immediate and permanent online open access to all its publications, but this alone is not enough to realize our grand goals.

## Frontiers journal series

The Frontiers journal series is a multi-tier and interdisciplinary set of open-access, online journals, promising a paradigm shift from the current review, selection and dissemination processes in academic publishing. All Frontiers journals are driven by researchers for researchers; therefore, they constitute a service to the scholarly community. At the same time, the *Frontiers journal series* operates on a revolutionary invention, the tiered publishing system, initially addressing specific communities of scholars, and gradually climbing up to broader public understanding, thus serving the interests of the lay society, too.

## Dedication to quality

Each Frontiers article is a landmark of the highest quality, thanks to genuinely collaborative interactions between authors and review editors, who include some of the world's best academicians. Research must be certified by peers before entering a stream of knowledge that may eventually reach the public - and shape society; therefore, Frontiers only applies the most rigorous and unbiased reviews. Frontiers revolutionizes research publishing by freely delivering the most outstanding research, evaluated with no bias from both the academic and social point of view. By applying the most advanced information technologies, Frontiers is catapulting scholarly publishing into a new generation.

## What are Frontiers Research Topics?

Frontiers Research Topics are very popular trademarks of the *Frontiers journals series*: they are collections of at least ten articles, all centered on a particular subject. With their unique mix of varied contributions from Original Research to Review Articles, Frontiers Research Topics unify the most influential researchers, the latest key findings and historical advances in a hot research area.

Find out more on how to host your own Frontiers Research Topic or contribute to one as an author by contacting the Frontiers editorial office: [frontiersin.org/about/contact](https://frontiersin.org/about/contact)

# Soil degradation and restoration in arid and semi-arid regions

## Topic editors

Kaibo Wang — Institute of Earth Environment, Chinese Academy of Sciences (CAS), China

Jianping Li — Ningxia University, China

Zhengchao Zhou — Shaanxi Normal University, China

Xunchang John Zhang — Grazinglands Research Laboratory, Agricultural Research Service (USDA), United States

## Citation

Wang, K., Li, J., Zhou, Z., Zhang, X. J., eds. (2023). *Soil degradation and restoration in arid and semi-arid regions*. Lausanne: Frontiers Media SA. doi: 10.3389/978-2-8325-3827-2

# Table of contents

04	<b>Editorial: Soil degradation and restoration in arid and semi-arid regions</b> Kaibo Wang, Jianping Li, Zhengchao Zhou and Xunchang John Zhang
07	<b>The roles for branch shelters and sheep manure to accelerate the restoration of degraded grasslands in northern China</b> Jing Liu, Rebecca L. Schneider, Stephen J. Morreale, Hongmei Wang, Ruixia Wang, Fang Wang and Zhigang Li
22	<b>Corrigendum: The roles for branch shelters and sheep manure to accelerate the restoration of degraded grasslands in northern China</b> Jing Liu, Rebecca L. Schneider, Stephen J. Morreale, Hongmei Wang, Ruixia Wang, Fang Wang and Zhigang Li
25	<b>Mechanisms of dust emissions from lakes during different drying stages in a semi-arid grassland in northern China</b> Shuai Qi, Xiaomeng Ren, Xiaohong Dang and Zhongju Meng
35	<b>Effect of slope shape on soil aggregate stability of slope farmland in black soil region</b> Yuxian Wang, Yingying Xu, Huiying Yang, Huibo Shen, Lei Zhao, Baoguo Zhu, Jiangxu Wang and Lifeng Guo
47	<b>Soil moisture and salinity dynamics of drip irrigation in saline-alkali soil of Yellow River basin</b> Yaqi Wang, Ming Gao, Heting Chen, Xiaoke Fu, Lei Wang and Rui Wang
59	<b>Nitrogen addition enhances terrestrial phosphorous retention in grassland mesocosms</b> Ellen Esch and Andrew S. MacDougall
68	<b>Long-term effects of soft rock amendment on changes of soil aggregate cementing agents of sandy soil by SEM-EDS</b> Zenghui Sun, Zhe Liu, Jichang Han, Huanyuan Wang, Haiou Zhang and Jiakun Yan
79	<b>Organic fertilizer has a greater effect on soil microbial community structure and carbon and nitrogen mineralization than planting pattern in rainfed farmland of the Loess Plateau</b> Yi Wang, Qianxue Li and Chunyue Li
92	<b>Phosphatase activities and available nutrients in soil aggregates affected by straw returning to a calcareous soil under the maize–wheat cropping system</b> Xiang-Jie Lin, Guang-Na Zhang, Zhen Wang, Qing-Dian Han and Peng Leng





## OPEN ACCESS

EDITED AND REVIEWED BY  
Yuncong Li,  
University of Florida, United States

\*CORRESPONDENCE  
Kaibo Wang,  
✉ wangkb@ieecas.cn

RECEIVED 04 October 2023  
ACCEPTED 12 October 2023  
PUBLISHED 17 October 2023

CITATION  
Wang K, Li J, Zhou Z and Zhang XJ (2023),  
Editorial: Soil degradation and restoration  
in arid and semi-arid regions.  
*Front. Environ. Sci.* 11:1307500.  
doi: 10.3389/fenvs.2023.1307500

COPYRIGHT  
© 2023 Wang, Li, Zhou and Zhang. This is  
an open-access article distributed under  
the terms of the [Creative Commons  
Attribution License \(CC BY\)](#). The use,  
distribution or reproduction in other  
forums is permitted, provided the original  
author(s) and the copyright owner(s) are  
credited and that the original publication  
in this journal is cited, in accordance with  
accepted academic practice. No use,  
distribution or reproduction is permitted  
which does not comply with these terms.

# Editorial: Soil degradation and restoration in arid and semi-arid regions

Kaibo Wang<sup>1\*</sup>, Jianping Li<sup>2</sup>, Zhengchao Zhou<sup>3</sup> and  
Xunchang John Zhang<sup>4</sup>

<sup>1</sup>State Key Laboratory of Loess and Quaternary Geology, Institute of Earth Environment, Chinese Academy of Sciences, Xi'an, China, <sup>2</sup>College of Agriculture, Ningxia University, Yinchuan, China, <sup>3</sup>School of Geography and Tourism, Shaanxi Normal University, Xi'an, China, <sup>4</sup>USDA-ARS Grazinglands Research Lab, El Reno, OK, United States

## KEYWORDS

arid and semi-arid areas, soil degradation, soil restoration, process and mechanism, soil remediation technology

## Editorial on the Research Topic

### Soil degradation and restoration in arid and semi-arid regions

Soil degradation is one of the huge challenges facing the human society, especially in arid and semi-arid regions (Amundson et al., 2015; Kraamwinkel et al., 2021). Soil degradation will lead to the loss of ecosystem functions, such as the decline in productivity and regulatory functions, the loss of species habitats, etc., causing the environment that was once suitable for living things unsuitable (Nunes et al., 2020; Rillig et al., 2023). Accurately understanding the process and mechanism of soil degradation in arid and semi-arid regions and developing technologies to curb soil degradation are of great significance for scientifically responding to land degradation, restoring and improving degraded lands, enhancing ecosystem wellbeing, and promoting the healthy development of human society.

This Research Topic contains eight articles, mainly involving two categories: soil degradation and degraded soil remediation. In addition, judging from the number of articles in the Research Topic, there is more research focusing on degraded soil remediation (five articles) than soil degradation (three articles). Although the articles in this Research Topic involve wind erosion, water erosion, salinization and other soil degradation types, compared with the more diverse soil degradation, the Research Topic is far from enough to understand the remediation of degraded soils. This Research Topic aims to attract more researchers to pay attention to soil degradation in arid and semi-arid regions and promote the remediation and management of degraded soil.

## Process and mechanism of soil degradation

Qi et al. investigated the effect of wind erosion on the surface dust emission of a dry lake in semi-arid grasslands in China. It was found that the surface sediment particles of intermittently dried and permanently dried lakes were mainly <63 μm, but the salt dust particles released from the surface of permanently dried lakes were finer. The concentration of salt dust released from intermittently dry surface is higher than that from permanently dry surface, with the salt ions mainly of Na<sup>+</sup>, Cl<sup>-</sup>, and SO<sub>4</sub><sup>2-</sup>. However, the dust flux from

intermittently dry surface is only 5%–15% of that from permanently dry land. The study revealed the wind erosion mechanisms of degraded lakes and provided reference data for soil desertification control in grassland areas.

Wang et al. demonstrated the effects of water erosion on the stability of soil aggregates and the loss of organic carbon in different slope shapes in the black soil region of northeast China. There was little difference in the fragmentation of soil aggregates between different slope shapes, and the fragmentation of soil aggregates was caused by the uneven expansion and contraction of clay particles. The soil erodibility of straight slope was lower than that of compound slope and concave slope, largely because soil organic carbon content of straight slope was greater than that of concave slope and compound slope. Soil organic carbon is preferably lost in the erosion of the top soil, resulting in the thinning of the black top soil layer and the decline of cultivated land quality.

Esch and MacDougall explored the retention mechanism of soil N and P in grassland ecosystem through microcosmic experiments. Compared with bare land, grassland can greatly reduce soil N loss, but slightly increase soil P loss. Moreover, most of the soil N loss occurred in the early growing season of grassland, while the soil P loss occurred in the late growing season. The addition of N reduces the loss of soil P obviously, but the addition of P has no effect on the loss of soil N. In addition, the difference in grassland function types had no significant effect on the loss of N and P. The authors concluded that soil nutrient loss in conventional agriculture can be mitigated by reducing N and P additions and changing the time of application.

## Process and mechanism of degraded soil remediation

Liu et al. proposed a technique for restoring degraded grassland based on the combination of branch mulching and sheep manure amendment. By combining two readily available and inexpensive resources, sheep manure and caragana branches, soil conditions can be significantly improved by the shelter of tree branches, and further to promote plant growth. Tree branch shelters shade and cool the soil and help maintain high soil water availability. The improvement of soil moisture promotes the conversion of manure nutrients and ultimately promotes the growth of grassland plants. In degraded grassland in northern China, when 60% of the ground is covered by branches, the average soil moisture content can be increased by 5 mm, and the plant yield can be doubled.

In view of the salinization of agricultural soil, Wang et al. took the Yellow River diversion irrigation area in the semi-arid region of northwest China as an example. By comparing the effects of flood irrigation and drip tube on the temporal and spatial distribution of soil water and salt in corn fields, they found that drip irrigation removes excess salt in the root zone through small-area irrigation and slow infiltration in compared with flood irrigation. A desalting zone with plenty water and little salt is formed near the drip head to create a suitable low-salt microenvironment for the normal growth of plants. The use of appropriate drip irrigation can achieve the purpose of water saving and salt control, and effectively enhanced crop productivity.

Sun et al. explored the effect and mechanism of soft rock addition to improve the soil aggregate structure of sandy soil in arid region. It was found that the soft rock addition could change the microstructure of the original sandy soil, which was dominated by a single granular barrier, promote the formation and development of soil, and form soil aggregates with good structural characteristics. Compared with aeolian sandy soil, the iron oxide in composite soil is fixed by combining with organic matter, which enhances the stability and development of soil aggregates, and thus improves the soil structure and productivity.

In response to the low phosphorus availability in calcareous soils in semi-arid regions of China, Lin et al. studied the effects of straw returning on soil phosphatase activity and available nutrients under a corn-wheat planting system. They reported high straw return rates led to a reduction of carbonate concentration by about 50% in 3.5 years. At the same time, the activity of soil phosphatase was significantly increased. The increase of substrate availability caused by straw returning to field may contribute to the improvement of soil phosphatase activity. The soil nutrition and phosphatase activity of calcareous soil could be improved with a high straw return rate.

Wang et al. research on farmland soil in the Chinese Loess Plateau showed that the application of organic fertilizer and the optimization of planting patterns can effectively improve the soil organic matter, nutrient content and microbial activity of the farmland, thus improving soil quality. After the application of organic fertilizer to the soil, it promoted the propagation of microorganisms and the soil carbon and nitrogen cycles, and increased the accumulation of soil nutrients. Reasonable crop rotation can achieve balanced utilization of soil nutrients and improve soil nutrient status. In dry farmland of the Loess Plateau, wheat and corn rotation combined with organic-inorganic fertilizer is an effective way to improve soil quality.

## Author contributions

KW: Writing–original draft. JL: Writing–original draft. ZZ: Writing–review and editing. XZ: Writing–review and editing.

## Funding

The author(s) declare financial support was received for the research, authorship, and/or publication of this article. This work was supported by the National Natural Science Foundation of China (42177339) and Shaanxi Province Science and Technology Activities for Overseas Students Selected Funding Project (2021015).

## Conflict of interest

The authors declare that the research was conducted in the absence of any commercial or financial relationships that could be construed as a potential conflict of interest.

## Publisher's note

All claims expressed in this article are solely those of the authors and do not necessarily represent those of their affiliated

organizations, or those of the publisher, the editors and the reviewers. Any product that may be evaluated in this article, or claim that may be made by its manufacturer, is not guaranteed or endorsed by the publisher.

## References

- Amundson, R., Berhe, A. A., Hopmans, J. W., Olson, C., Sztein, A. E., and Sparks, D. L. (2015). Soil science. Soil and human security in the 21st century. *Science* 348, 1261071. doi:10.1126/science.1261071
- Kraamwinkel, C. T., Beaulieu, A., Dias, T., and Howison, R. A. (2021). Planetary limits to soil degradation. *Commun. Earth Environ.* 2, 249. doi:10.1038/s43247-021-00323-3
- Nunes, F. C., de Jesus Alves, L., de Carvalho, C. C. N., Gross, E., de Marchi Soares, T., and Prasad, M. N. V. (2020). "Chapter 9 - soil as a complex ecological system for meeting food and nutritional security," in *Climate change and soil interactions*. Editors M. N. V. Prasad and M. Pietrzykowski (China: Elsevier), 229–269.
- Rillig, M. C., van der Heijden, M. G. A., Berdugo, M., Liu, Y. R., Riedo, J., Sanz-Lazaro, C., et al. (2023). Increasing the number of stressors reduces soil ecosystem services worldwide. *Nat. Clim. Change* 13, 478–483. doi:10.1038/s41558-023-01627-2



## OPEN ACCESS

EDITED BY  
Jianping Li,  
Ningxia University, China

REVIEWED BY  
Shaokun Wang,  
Northwest Institute of Eco-  
Environment and Resources (CAS),  
China  
Hao Qu,  
Cold and Arid Regions Environmental  
and Engineering Research Institute,  
Chinese Academy of Sciences, China

\*CORRESPONDENCE  
Zhigang Li,  
lizg001@sina.com

SPECIALTY SECTION  
This article was submitted to Soil  
Processes,  
a section of the journal  
Frontiers in Environmental Science

RECEIVED 04 November 2022  
ACCEPTED 02 December 2022  
PUBLISHED 04 January 2023

CITATION  
Liu J, Schneider RL, Morreale SJ,  
Wang H, Wang R, Wang F and Li Z  
(2023), The roles for branch shelters and  
sheep manure to accelerate the  
restoration of degraded grasslands in  
northern China.  
*Front. Environ. Sci.* 10:1089645.  
doi: 10.3389/fenvs.2022.1089645

COPYRIGHT  
© 2023 Liu, Schneider, Morreale, Wang,  
Wang, Wang and Li. This is an open-  
access article distributed under the  
terms of the [Creative Commons  
Attribution License \(CC BY\)](#). The use,  
distribution or reproduction in other  
forums is permitted, provided the  
original author(s) and the copyright  
owner(s) are credited and that the  
original publication in this journal is  
cited, in accordance with accepted  
academic practice. No use, distribution  
or reproduction is permitted which does  
not comply with these terms.

# The roles for branch shelters and sheep manure to accelerate the restoration of degraded grasslands in northern China

Jing Liu<sup>1,2</sup>, Rebecca L. Schneider<sup>3</sup>, Stephen J. Morreale<sup>3</sup>,  
Hongmei Wang<sup>1,2</sup>, Ruixia Wang<sup>4</sup>, Fang Wang<sup>5</sup> and Zhigang Li<sup>1,2\*</sup>

<sup>1</sup>School of Agriculture, Ningxia University, Yinchuan, Ningxia, China, <sup>2</sup>Ningxia Grassland and Animal Husbandry Engineering Technology Research Centre, Yinchuan, Ningxia, China, <sup>3</sup>Department of Nature Resources, College of Agriculture and Life Sciences, Cornell University, Ithaca, NY, United States, <sup>4</sup>Bajitan Nature Reserve Administration, Lingwu, Ningxia, China, <sup>5</sup>College of Geographical Sciences and Planning, Ningxia University, Yinchuan, Ningxia, China

New strategies are desperately needed for restoring the millions of hectares of degraded grasslands in arid and semiarid areas of northern China. This study evaluated using different combinations of manure amendments and shrub branch shelters for their impacts on soil moisture, nutrient availability, and plant growth over two growing seasons in a degraded grassland in Ningxia, China. A two-factor experiment was conducted, with three concentrations of 1.2 g m<sup>-2</sup>, 442 g m<sup>-2</sup>, and 884 g m<sup>-2</sup> native Tan sheep manure as the main plots. Cut caragana (*Caragana intermedia*) branches were used to create branch shelters covering 0%, 20%, 40%, and 60% of ground area, and these acted as sub-main plots. Soil water storage, soil temperature, manure decomposition, branch decomposition, soil nutrients, and plant growth were monitored for 2 years. Results indicated that soil water storage was significantly increased, and soil temperature decreased, under the 40% and 60% branch shelters. Decomposition rate of manure and shrub branches also increased with increasing soil water availability associated with the higher branch sheltering effects, although soil carbon and nitrogen concentrations were primarily driven by the decomposing manure. The combination of high levels of shrub branch shelter and manure application significantly enhanced plant production, although the bulk of the biomass was concentrated in one species, *Artemisia scoparia*. In conclusion, our study successfully demonstrated feasible and inexpensive solution for the restoration of degraded grasslands, which takes advantage of resources associated with overgrazing Tan sheep and *Caragana* shrub encroachment in arid and semiarid areas.

## KEYWORDS

caragana branch shelters, soil water availability, sheep manure decomposition, soil nutrients, plant growth, degraded grassland

# 1 Introduction

Grassland ecosystems account for approximately 40% of the Earth's surface (Luan et al., 2014), and fulfil important functions and services in agricultural systems (Liu et al., 2011). Grasslands provide the basis for agriculture with 3.38 billion ha (26%) used as livestock pasturing and 1.53 billion ha (12%) for cropland (Foley et al., 2011). However, due to climate change and human disturbance, grassland degradation has become a serious global ecological problem (Akiyama and Kawamura, 2007; Dong et al., 2019). Clearing of natural vegetation followed by chronic tillage for crops degrades soil structure, oxidizes soil organic matter, and kills the soil microbial communities that help bind the soil, resulting in increased erosion (Reichert et al., 2022). Overgrazing also kills the plants whose roots bind the soil and contribute to soil organic matter in grasslands (Klump et al., 2009). In summary, both systems lead to grassland degradation which has been described as an inverse succession that combines the deterioration of vegetation and soil (Gang et al., 2014). Therefore, many practices such as reseedling, fertilization, irrigation, organic amendments, and enclosure have been adopted to restore degraded grasslands (Zhang Q et al., 2021).

Presently, overgrazing is widely regarded as a major factor contributing to grassland degradation. However, with appropriate grazing practices, manure deposition and decomposition by livestock can play a positive role in grassland soil nutrient cycling and grassland restoration (Schuman et al., 2002), since about 50% (range 40%–60%) of total animal N excretion is voided in grasslands (Oenema and Tamminga, 2005). Numerous studies have demonstrated that returned or applied livestock manure to grasslands can effectively improve grassland soil fertility and productivity (Min et al., 2014; Duffková et al., 2015; Zhang et al., 2015; Bai et al., 2017). Moreover, livestock manure has high concentrations of easily-decomposable C and N compounds, providing readily-accessible nutrients to the soil micro- and macrobiota decomposers (Knops et al., 2002; Bakker et al., 2004). Conversely, chronic export of animal manure from the grassland ecosystem can result in deterioration of soil fertility and decline of grassland primary productivity (Xu et al., 2012). However, in degraded grassland systems, manure application alone is generally insufficient to restore the soil health and other types of amendments are needed. In particular, strategies are needed to improve soil water availability in these dry environments, since the activities of microbial manure decomposers are usually positively correlated with increasing soil moisture in arid areas (Zhu et al., 2020). Hence, the measures for improving soil water condition may have benefit for livestock manure decomposition and soil nutrient improvement in grazed grasslands.

In natural, undisturbed grasslands, the thick layer of leaf litter that forms across the surface has been shown to increase rain capture and shade and cool the soil (Deutsch et al., 2010). Similarly, the use of mulch and other surface organic

amendments is also gaining recognition for their value in shading and cooling soils, and reducing evaporative losses. For instance, addition of a thick layer of wood chips as mulch over the soil surface, can cool the soil, reduce evaporative loss, and enhance plant growth in arid areas (Li et al., 2018, 2019). Mulch is also used as a common landscaping practice, to prevent weed germination and growth, which it does by inhibiting light from reaching the surface (Cochran et al., 2009). Alternative strategies are needed that help shade and cool, but also allow some light penetration to help seed germination.

Previous research has shown that piling branches over the soil can shade and cool the soil yet allow seed germination and plant growth (Li et al., 2018, 2019; Leger et al., 2022). And unlike wood chip mulch, the sturdier longer branches facilitate the formation of a loose three-dimensional structure of material above the soil surface. One potential source of woody material, namely invading shrubs, may be a useful source of material for these amendments, while countering shrub encroachment, which has become another factor which is contributing to grassland degradation worldwide (Wilson et al., 2022). The proliferation of shrubs in grasslands can substantially change the pattern of soil water resources, which in turn leads to changes in the structure and function of the ecosystem (Jia et al., 2018; D'Odorico et al., 2012). Presently, about 10%–20% of arid and semi-arid grasslands are undergoing shrub encroachment (Watson et al., 2018). This phenomenon has been documented in southwestern North America (Caracciolo et al., 2016), the Mediterranean Basin (Maestre et al., 2009), Australia (Eldridge and Koen, 2003), and South Africa (Kerley and Whitford, 2009). Some grasslands in Inner Mongolia, Gansu, Ningxia, and other provinces of northern China are also exhibiting shrub encroachment (Wei et al., 2019). In eastern Ningxia, China, caragana (*Caragana intermedia*) were extensively planted in grasslands (accounting for about 33% of grassland area) for wind prevention and sand stabilization (Zheng et al., 2019). In the period immediately following planting, the caragana was deemed successful in stabilizing the sandy soils, however it was subsequently found to consume large amounts of water, decreasing overall soil water availability (Dan et al., 2020). As a result, with increasing time since planting of the caragana, a suite of problems occurs, including reduction in perennial herbs, water deficit, and soil degradation gradually developed in local grasslands (Zhao et al., 2020). Therefore, fire management and other measurements have being extensively adopted to reduce shrub encroachment for grassland restoration (Killgore et al., 2009; Wang et al., 2018; Wilcox et al., 2018). However, fire management may also cause environment pollution and waste of potentially valuable resources.

Interestingly, previous research has demonstrated that tree branch shelters were successful in achieving benefits to cool temperatures and increase soil moisture contents in forests





FIGURE 1

Shrub encroached grassland (A) in study site and schematic (B) and photo (C) showing layout of the experimental study site and plots. L, M and H in figure b are low, medium, and high amount of manure accumulated in grassland surface.

that had been thinned (Morreale and Sullivan, 2010). Even when laid directly atop forest soils coarse woody debris also has benefits in improving soil moisture, increasing soil organic matter, and reducing bulk density (Bulmer et al., 2007). Our earlier studies in semi-arid environments have also demonstrated that tree branch shelters effectively and immediately decrease evaporation, retain more precipitation, and enhance plant growth in desertified grassland soils (Li et al., 2018, 2019). Moreover, over longer term periods of three or more years, tree branch shelters were found to improve soil physical properties and increase soil nutrients of desertified grassland (Li et al., 2019). In addition, moderate shading level, for example <60%, had minimal negative effects on overall annual grassland net herbage accumulation (Dodd et al., 2005). Furthermore, unlike light organic materials such as straw and other herbaceous materials that may easily decompose in as little as 2 years even in more arid regions, woody materials (for instance shrub and tree branches) can last for years to decades (Weedon et al., 2009) when used for soil restoration. Therefore, woody materials have an additional advantage of reducing the cost of soil restoration over the long term, since constant re-application is not needed.

Given this framework, it is likely that caragana branches can also be viable for use as *in-situ* shelters to improve grassland soil moisture and jump-start restoration of degraded grasslands in Ningxia, where the climate is semi-arid and this shrub is abundant. We hypothesize that (a) caragana branch shelters can facilitate nutrient cycling of livestock manure in grassland by improving soil moisture availability, and (b) then enhancing plant growth *via* improving soil moisture and nutrient availability. The overall goal of this study was to evaluate the potential of utilizing various combinations of two readily available resources, caragana branch shelters and sheep manure, to improve the soil environment and support increased native plant productivity in highly degraded arid landscapes of northern China. The specific objectives of this study were to: (a) analyze the effect of using caragana branch shelters *versus* manure on the soil physical environment, including soil temperatures and soil water storage in the study site; (b) evaluate the interactive effects of different sheltering levels and amounts of manure amendment on decomposition rates of the two materials, as well as soil nutrient levels, and (c) evaluate interactive effects of manure and branch shelter



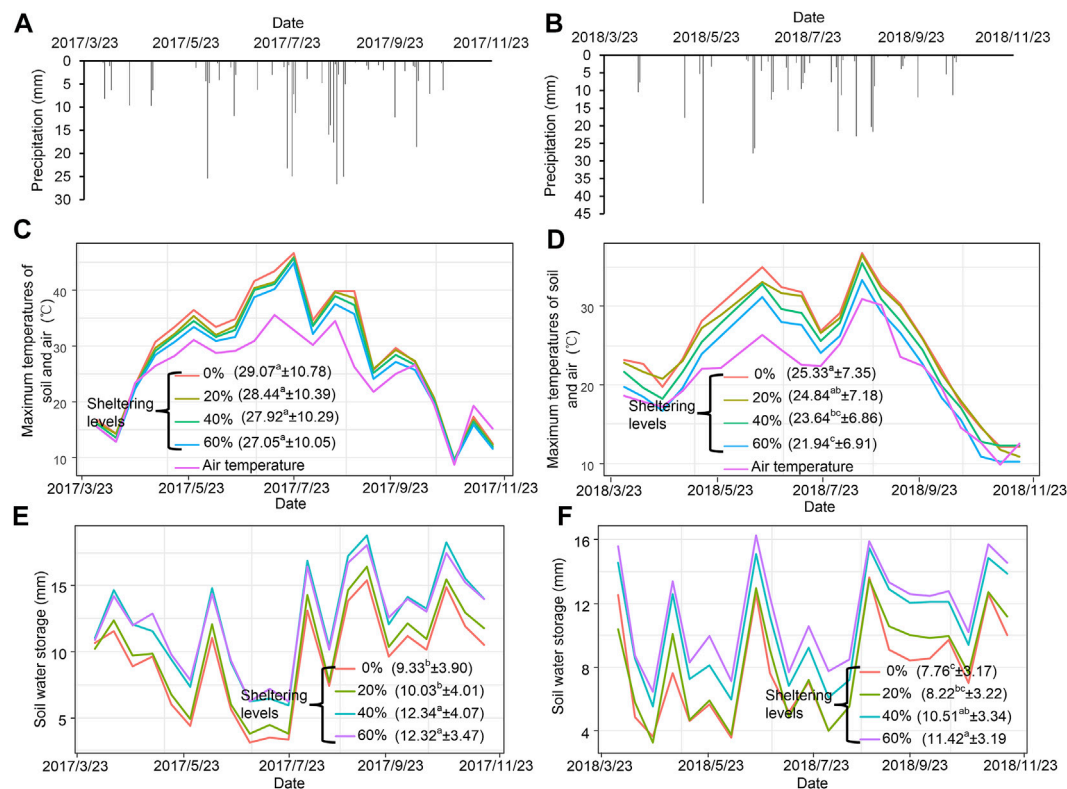


FIGURE 2

The precipitation (A,B) over the two growing seasons, and the maximum soil temperatures (C,D) and soil water storages (E,F) of degraded grassland under different branch sheltering levels in 2017 and 2018. Data in parentheses were average soil temperature  $\pm$ SE (C,D) and average soil water storage  $\pm$ SE (E,F), and different letters indicate significant differences among different treatments at the 0.05 level.

treatments on plant production, as indicated by biomass, average plant height, and cover.

## 2 Materials and methods

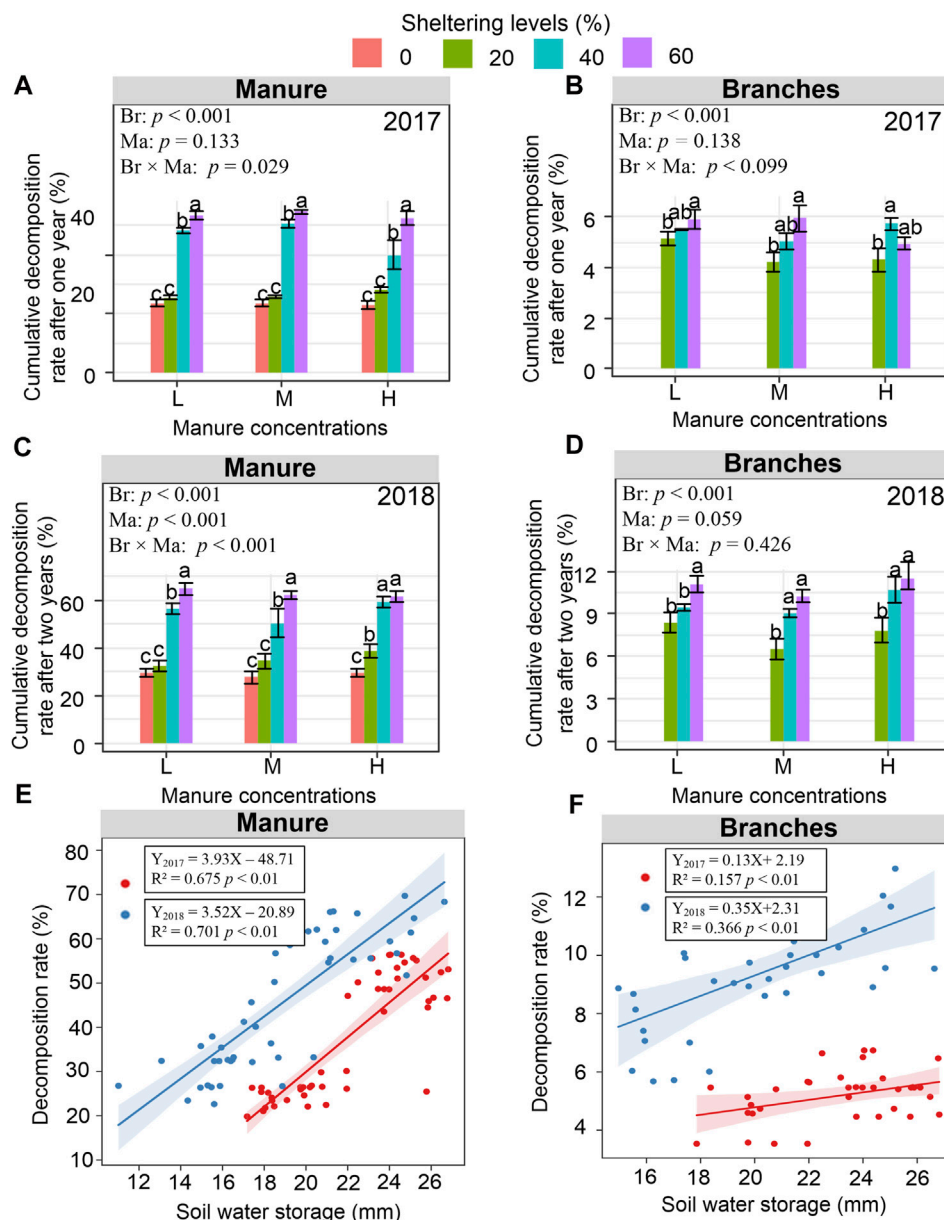
### 2.1 Site description

The study site is located in Yanchi County, Ningxia (106° 30'—107° 47' E, 37° 04'—38° 10' N), Northern China. The regional climate is a typical temperate continental and monsoonal climate. The average annual temperature is 8.1°C. The annual precipitation is 295 mm, and the average annual potential evapotranspiration is 2,132 mm, and the frost-free period is about 162 days (Zhang Y et al., 2021). The soil texture is primary sandy loam, and the soil characteristics of the 0–20 cm layer as follows: pH was 8.69, 0.18 g kg<sup>-1</sup> total N, 0.53 g kg<sup>-1</sup> total P, 2.29 g kg<sup>-1</sup> organic matter content. The natural vegetation of the site is desert steppe, and the plant species mainly consist of *Artemisia scoparia*, *Corispermum mongolicum*, *Heteropappus altaicus*, *Agropyron cristatum*,

*Salsola ruthenica*, *Agropyron mongolicum*, *Bassia dasyphylla*, and planted *Caragana intermedia*. However, caragana shrubs were extensively planted in grasslands (account for about 33% of 3,327 km<sup>2</sup> grassland area) for wind prevention and sand stabilization in this area, and the total above-ground caragana biomass (dry weight) in grassland can be as high as 8.4  $\times$  10<sup>4</sup> kg km<sup>-2</sup> (Zheng et al., 2019).

### 2.2 Field experiment design

The field experiment was set up in October in 2016 in a degraded 60 hm<sup>2</sup> grassland, and the measurements were conducted during the two subsequent growing seasons of 2017 and 2018. Prior to the experiment, this grassland was intensively grazed by Tan sheep, a native species to this region. The grazing density was 3–4 Tan sheep·hm<sup>-2</sup>, and the whole grassland was enclosed by fences with a gate. The vegetation of the site consisted of mixed grass species and shrub caragana. The cumulative amount of oven-dried (85°C) sheep manure was 872 g m<sup>-2</sup> at the gate and 1.2 g m<sup>-2</sup> at 800 m

**FIGURE 3**

Decomposition rates of manure (A,C) and caragana branches (B,D) under different treatments evaluated as % weight loss from the initial weight, as well as regressions of decomposition rate against soil water storage (mm) for manure treatments (E) and caragana treatment (F) in 2017 and 2018. Different letters above columns in Figs a, b, c, and d indicate significant differences among different sheltering levels in Figs a and b ( $p < 0.05$ ). Different  $p$  values in Figs a, b, c, and d indicate the effects of branch sheltering (Br), manure concentration (Ma), and their interaction (Br  $\times$  Ma) on decomposition by two-way ANOVAs.

from the gate, based on an initial sampling of the surface soil (0–5 cm depth) throughout the field.

In order to ensure the homogeneity both for soil properties and vegetation, all experimental plots were set up 200 m far away from the gate, i.e., at sites where the concentration of sheep manure was approximately  $442 \text{ g m}^{-2}$ . Then, a split-plot experiment was designed (Figure 1), and the main plots were

comprised of three treatments where the cumulative manure concentrations were  $1.2 \text{ g m}^{-2}$  (thus near to zero),  $442 \text{ g m}^{-2}$ , and  $884 \text{ g m}^{-2}$  for low (L), medium (M) and high (H) concentrations, respectively. Thus, for L, almost all manure had been removed from the plots, by shoveling. Whereas, for H, the manure removed from L plots were added into H plots. The M plots had no manure removed or added. The sub-main plots were

**TABLE 1** The evaluation of potential maximum C and N which decomposed sheep manure and caragana branches input to soil.

Treatments	The potential maximum C and N input to soil after 1 year (2017) decomposition (g kg <sup>-1</sup> )	The potential maximum C and N input to soil after 2 years (2018) decomposition (g kg <sup>-1</sup> )							
Manure concentrations	Sheltering levels (%)	C Input by manure	C Input by branches	N input by manure	N input by branches	C Input by manure	C Input by branches	N input by manure	N input by branches
L	0	<0.01	0.00	<0.01	0.00	<0.01	0.00	<0.01	0.00b
	20	<0.01	<0.01	<0.01	<0.01	<0.01	<0.01	<0.01	<0.01b
	40	<0.01	<0.01	<0.01	<0.01	<0.01	<0.01	<0.01	0.007 ± 0.00b
	60	<0.01	<0.01	<0.01	<0.01	<0.01	<0.01	<0.01	0.012 ± 0.00a
M	0	0.07 ± 0.00c	0.00	<0.01c	0.00	0.09 ± 0.01c	0.00	0.01 ± 0.00b	0.00b
	20	0.08 ± 0.00c	<0.01	<0.01c	<0.01	0.11 ± 0.01c	<0.01	0.01 ± 0.00a	<0.01b
	40	0.16 ± 0.00b	<0.01	0.01 ± 0.00b	<0.01	0.16 ± 0.02b	<0.01	0.01 ± 0.00b	0.006 ± 0.00a
	60	0.17 ± 0.02a	<0.01	0.01 ± 0.00a	<0.01	0.19 ± 0.01a	<0.01	0.01 ± 0.00a	0.010 ± 0.00a
H	0	0.15 ± 0.01c	0.00	0.01 ± 0.00c	0.00	0.19 ± 0.01b	0.00	0.01 ± 0.00b	0.00c
	20	0.18 ± 0.01c	<0.01	0.01 ± 0.00c	<0.01	0.24 ± 0.02b	<0.01	0.01 ± 0.00b	<0.01c
	40	0.25 ± 0.01b	<0.01	0.02 ± 0.01b	<0.01	0.37 ± 0.02a	<0.01	0.02 ± 0.00b	0.075 ± 0.00b
	60	0.33 ± 0.03a	<0.01	0.02 ± 0.00a	<0.01	0.38 ± 0.02a	<0.01	0.02 ± 0.00a	0.012 ± 0.00a

Different letters following means indicate significant differences among different sheltering levels at 0.05 level ( $p < 0.05$ ).

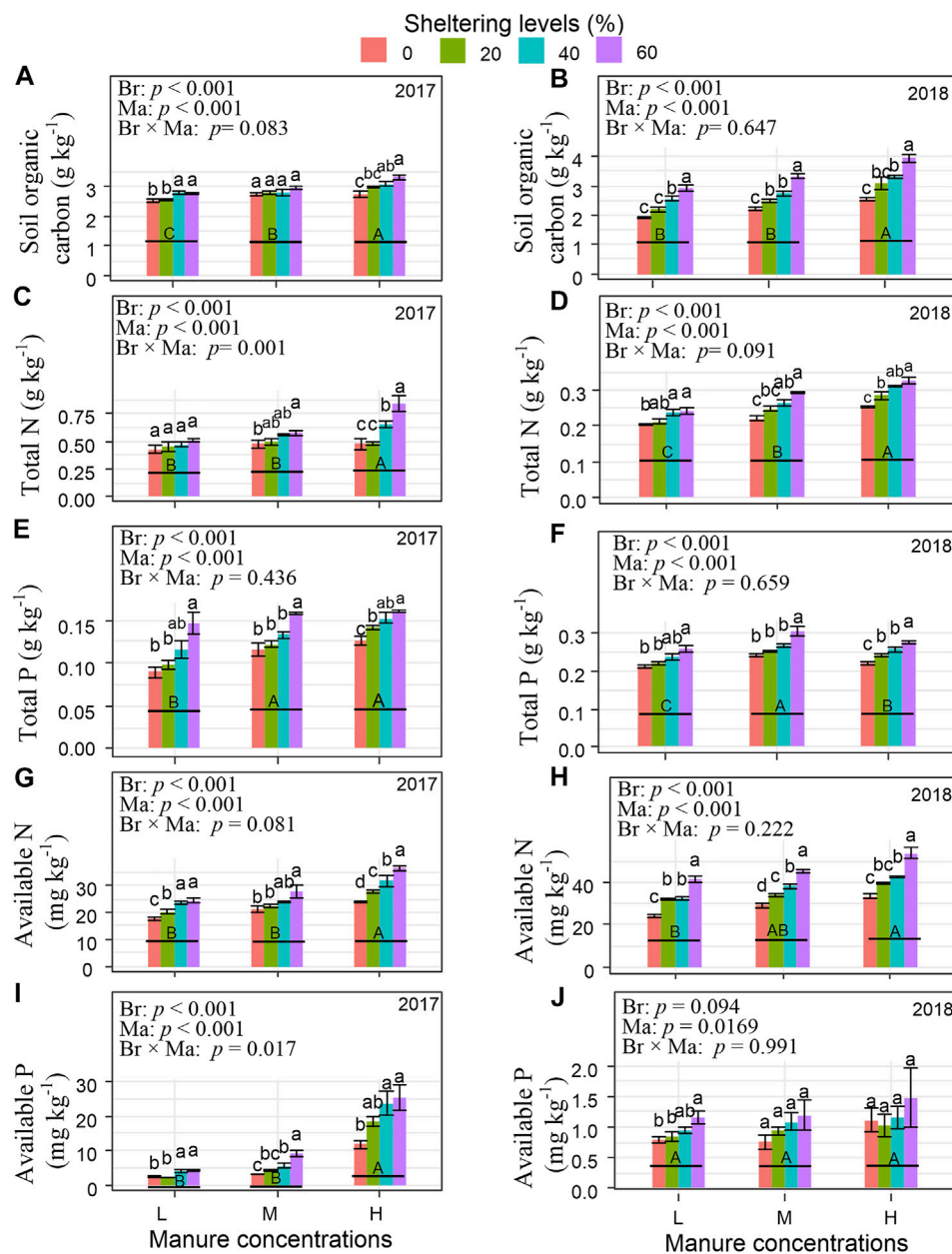


FIGURE 4

Soil organic carbon (A,B), total N (C,D), total P (E,F), available N (G,H), and available P (I,J) between 0–20 cm depth under different shrub branch sheltering levels and cumulative sheep manure concentrations in degraded grassland in 2017 and 2018. L, M, and H denote sheep manure with low, medium, and high concentration in grasslands. Different uppercase letters indicate significant differences among different concentrations of sheep manure ( $p < 0.05$ ), while lowercase letters indicate significant differences among different levels of shrub branch shelters ( $p < 0.05$ ). Different *p* values show the effects of branch sheltering (Br), manure concentration (Ma), and their interaction (Br × Ma) on soil nutrients by two-way ANOVAs.

comprised of four different branch shelters based on our previous studies (Li et al., 2018, 2019). Thus 0%, 20%, 40%, and 60% of grassland surface area were overlaid by the cut caragana branch shelters. Caragana branches of ~0.7 cm diameter were obtained from throughout the study site. Then branches, with length of ~1 m, were selected and layered over the soil surface, criss-

crossing to form a lattice type structure, after the manure plots were set up. The sheltering levels were adjusted and measured by LAI-2200C plant canopy analyzer (Li-COR Inc., United States) in October, when there was no aboveground plant foliage to interfere with the measurements. The branch shelter treatments were randomly distributed in each main block. The

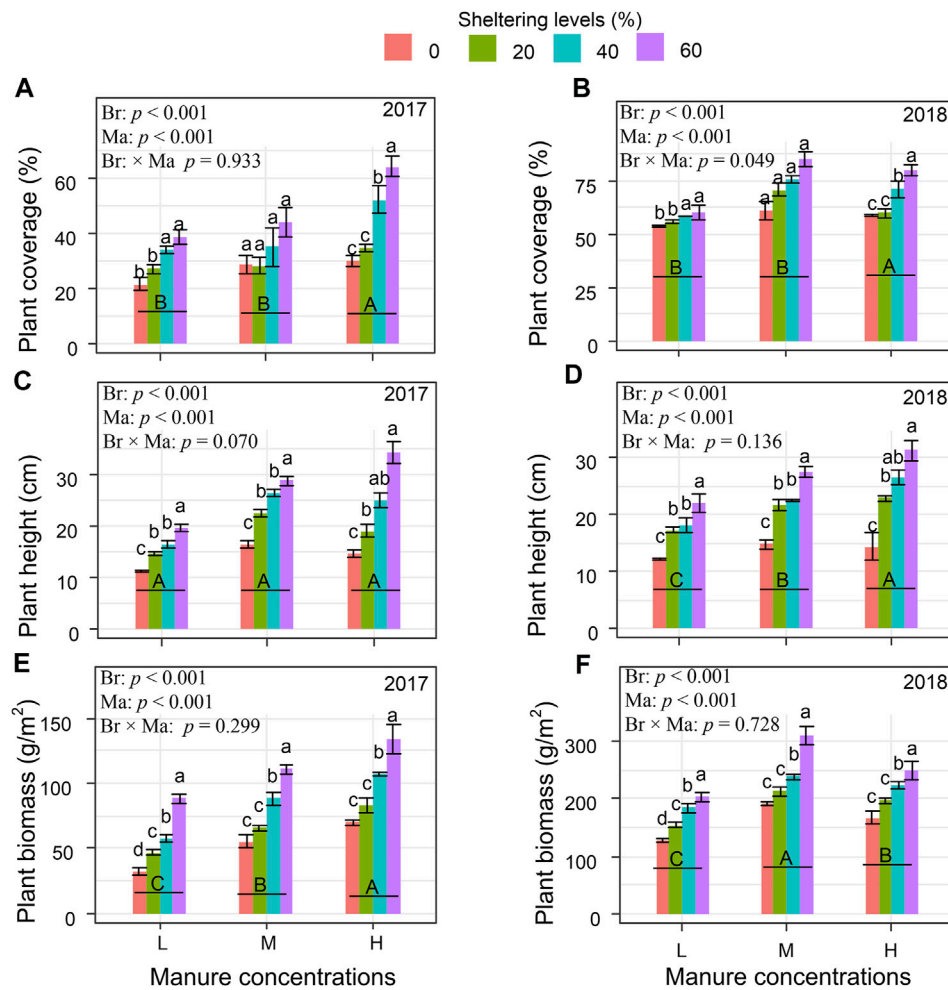


FIGURE 5

Plant coverage (A,B), height (C,D), and biomass (E,F) under different shrub branch sheltering levels and cumulative sheep manure concentrations in degraded grassland in 2017 and 2018. L, M, and H denote sheep manure with low, medium, and high concentration in grasslands. Different uppercase letters indicate significant differences among different concentrations of sheep manure ( $p < 0.05$ ), while lowercase letters indicate significant differences among different levels of shrub branch shelter ( $p < 0.05$ ). Different  $p$  values show the effects of branch sheltering (Br), manure concentration (Ma), and their interaction (Br  $\times$  Ma) on plant growth by two-way ANOVAs.

shelter treatments of 20%, 40%, and 60% surface coverage corresponded approximately to  $660 \text{ g m}^{-2}$ ,  $1,320 \text{ g m}^{-2}$ , and  $1980 \text{ g m}^{-2}$  (dry weight) caragana branches, respectively. Increasing extent of the branch shelters provided increasing amounts of shade, a thicker boundary layer above the soil surface which would act to reduce evaporative losses, as well as a greater amount of wood for potential decomposition into the plot.

In total, 12 treatments with four replicate plots per treatment were set up for the experiment. Each plot size was  $16 \text{ m}^2$  ( $4 \times 4 \text{ m}$ ), and each pair of plots were separated from each other by 2 m spacing, and 4 m alleys between the two main blocks. There was no grazing allowed in the field plots during the experimental period, and the whole experiment site was

enclosed with fences to prevent intrusion by Tan sheep and other large herbivores. The organic carbon content of manure and branch are  $198.55 \text{ g kg}^{-1}$  and  $453.94 \text{ g kg}^{-1}$ , respectively; the total N of manure and branch are  $12.27 \text{ g kg}^{-1}$  and  $14.82 \text{ g kg}^{-1}$ , respectively.

## 2.3 Monitoring of soil water content and associated soil temperature

The soil volumetric water content within the 0–20 cm soil layer was monitored using AZS - 100 Handheld Meter (Aozuo Ecology Instrumentation Ltd., Beijing China), but calibrated by the gravimetric method. Measurements were made every 10 days

from April to October both in 2017 and 2018. Finally, the soil water storage was calculated with the following equation:

$$SWS = VW \times H \quad (1)$$

where SWS (mm) is soil water storage; VW is volumetric water;  $H$  (mm) is soil depth = 200 mm.

Additionally, soil temperature at the depth of 20 cm was monitored at 14:00 h on the same day as the soil moisture measurements were made, using a soil thermometer (Changzhou Rui Ming Instrument and meter plant thermometer, Changzhou China).

## 2.4 Measurement of decompositions and nutrient inputs both for manure and caragana branches

Decomposition rates of manure and caragana branches were measured using nylon bags (with 2 mm mesh). For manure bags, 100 g oven-dried (85°C) and intact sheep manure were placed into a bag, then two bags were laid on the surface of the soil within each plot (totally, four sheltering levels  $\times$  3 manure concentrations  $\times$  2 sampling dates  $\times$  4 replicates = 96 bags). For branch bags, 100 g oven-dried (85°C) air-dried caragana branches (~0.7 cm in diameter and 10 cm in length) were placed into each bag, then two bags were placed into each plot for which there was branch sheltering (thus totally, three sheltering levels  $\times$  3 manure concentrations  $\times$  2 sampling dates  $\times$  4 replicates = 72 bags).

Both for manure and branches, one bag in each plot was collected at the end of September in 2017, and another was collected at the end of September in 2018. Then the decomposition rate was determined as the change in oven-dried weight loss determined after oven drying at 85°C. Organic carbon was assayed by the acidified potassium dichromate ( $K_2Cr_2O_7$ - $H_2SO_4$ ) heating method (Bao, 2013). Total nitrogen (N) was determined using the Kjeldahl procedure (Bao, 2013). Considering the influence of soil to interfere accurate evaluation for manure decomposition, ash correction was applied according to Rashid et al. (2017). Thus, a muffle furnace was used to determine ash content in bags by loss-on ignition at 550°C for 4 h, and the soil dry weight that contaminated the manure calculated as following equations:

$$CDW = \frac{AS_R - A_{IC}}{A_{SL}} \quad (2)$$

where CDW is soil dry weight (g) than contaminated the manure bag,  $AS_R$  is ash content (mg) that remained in manure bag,  $A_{IC}$  is the initial ash content (mg) in manure bag and  $A_{SL}$  is the soil ash content ( $mg\ g^{-1}$ ). After ash correction, cumulative decomposition rate of manure and branches, as well as the potential maximum C and N which manure and branches input into soil were evaluated with the following equations:

$$DR = 100 \times (DM_{initial} - DM_{end}) / DM_{initial}, \quad (3)$$

$$C_{released} \text{ or } N_{released} = DR \times DM_{initial} \times C_{content} \text{ or } N_{content} \times 0.001, \quad (4)$$

$$C_{input} \text{ or } N_{input} = \frac{C_{released} \text{ or } N_{released}}{BD \times S \times H}, \quad (5)$$

where, DR (%) is cumulative decomposition rate of manure or branches after one or 2 years;  $DM_{initial}$  ( $g\ m^{-2}$ ) is the initial dry matter weight of manure or sheltered branches in each plot;  $DM_{end}$  is the dry matter weight of manure or sheltered branches were decomposed after one or 2 years in each plot;  $C_{released}$  or  $N_{released}$  ( $g\ m^{-2}$ ) is cumulative released C or N from decomposed manure or branches after one or 2 years in each plot;  $C_{content}$  ( $g\ kg^{-1}$ ) or  $N_{content}$  ( $g\ kg^{-1}$ ) is the concentration of C or N in manure or branches;  $C_{input}$  ( $g\ kg^{-1}$ ) or  $N_{input}$  ( $g\ kg^{-1}$ ) is the potential maximum C or N which manure or branches cumulatively input into soil;  $BD$  ( $g\ cm^{-3}$ ) is soil bulk density, and in this study  $BD = 1.4\ g\ cm^{-3}$ ;  $S$  ( $m^2$ ) is soil area in calculation, and 1  $m^2$  soil area was applied in calculation in this study;  $H$  is soil depth,  $H = 20\ cm$  in this study.

## 2.5 Soil sampling and soil chemical property measurement

Samples were also collected at the end of September in both 2017 to 2018. Three soil samples between 0 and 20 cm were collected in each plot, and then mixed together to get about a 500-g composite sample for each plot. Four replicate samples were then analyzed from each composite for each treatment. Soil samples were sieved through a 2-mm mesh and oven-dried for chemical property analysis.

Soil organic carbon (SOC) was assayed by the acidified potassium dichromate ( $K_2Cr_2O_7$ - $H_2SO_4$ ) heating method (Bao, 2013). Total nitrogen (N) was determined using the Kjeldahl procedure (Bao, 2013); total phosphorus (P) was determined using  $H_2SO_4 + HClO_4$  digestion (Bao, 2013); available N was determined by the alkaline diffusion method (Bao, 2013); available P was extracted with 0.5 mol/L  $NaHCO_3$  (pH 8.5) (Bao, 2013).

## 2.6 Investigation of grassland vegetation

Within each plot, a  $1 \times 1\ m$  quadrat was set aside for analyzed vegetation in September in 2017 and again in 2018. The total coverage and average height of vegetation was evaluated according to point frame method (Byrne et al., 2011), then the aboveground biomass was harvested, dried at 60°C for 48 h, and weighed (Bloor, 2015).

## 2.7 Statistical analyses

Two-way ANOVAs were applied to detect the effects of shelters, sheep manure, and shelters  $\times$  manure on each



determined soil and plant index, respectively. And when the results of two-way ANOVAs shown interaction effect is significant, the simple effect analysis, thus One-way analysis of variance (ANOVA), was used to determine the difference between the effects of one factor at different levels of another factor. Regression analysis was applied to reveal the correlation of manure decomposition rate and soil water storage, as well as branch decomposition rate and soil water storage. Correlation analysis was used to reveal the relationships between plant growth parameters and tested soil properties. All above analyses were carried out using the “vegan” package in R. In all tests, a  $p$ -value  $\leq 0.05$  was considered significant.

### 3 Results

There was slightly more rainfall in 2018 (374.6 mm) than in 2017 (353.4 mm), however in 2017 it was distributed as smaller but more frequent storms throughout the growing season (Figures 2A, B). Average air temperature was hotter in 2017 than in 2018 (Figures 2C, D). Soil temperatures reached a maximum of 45°C in 2017, but maximums were 10° lower in 2018, at 35°C (Figures 2E, F).

#### 3.1 Effect of shelters on soil water storage and soil temperature of grassland

Branch shelters significantly decreased the average daily soil maximum temperature in both 2017 and 2018 (Figures 2C, D). Increasing the extent of branch shelter up to 60% resulted in 2°C cooler average soil temperatures in 2017, and in 3.4°C cooler soil temperatures in 2018, when compared with unsheltered exposed soil.

Soil water storage was overall slightly higher in 2017 than in 2018. There was a significant increase in average soil water storage associated with the 40% and 60% branch shelters as compared to the 0% Control in both 2017 and 2018 (Figures 2E, F). The 60% shelter increased the average soil water storage by 32% and 47.2% over the Controls in 2017 and 2018, respectively. The 20% branch shelter also increased soil water storage above the Control on several days, but was not statistically significant on average. In contrast, increasing the amount of sheep manure, without an associated shelter, was not found to significantly increase soil water storage or decrease soil temperature in either 2017 or 2018 ( $p > 0.05$ ) (Supplementary Figure S1).

#### 3.2 Effect of branch shelters on decomposition and nutrient releases of manure and branches

Two-way ANOVAs indicated that branch shelters significantly impacted both the manure and branch decomposition rates both in

2017 and 2018 ( $p < 0.001$ ), evaluated as % weight loss from the initial weight. Manure concentrations also significantly impacted its own decomposition in 2018 ( $p < 0.001$ ), and branch shelters  $\times$  manure concentrations significantly impacted manure decomposition as well both in 2017 and 2018 ( $p < 0.05$  or 0.001) (Figure 3). By the end of 2017, Control manure bags had lost ~25% of their initial mass, while treatments with shelters of 40% and 60% significantly increased the decomposition loss rate of the manure to roughly 50% (Figure 3A). In 2018, manure bags with 0% or 20% shelters had only lost an additional 5% of their initial weight but bags in the 40% and 60% shelters dramatically lost up to 65% of their initial weights (Figure 3C).

In contrast, caragana branches had very low decomposition rates, with less than 5% loss rate at the end of 2017 (Figure 3B). Branch bags had only lost an additional 5% more after the next 2018 growing season (Figure 3D). However, increasing density of the shelter did slightly increase the decomposition rate of the caragana bags. Further analysis showed that, as a whole, the decomposition rates of manure were increased with increasing branch sheltering levels both in 2017 and 2018. In addition, the decomposition rate of caragana branches also increased with increasing sheltering levels both in 2017 and 2018. Regression analysis revealed that both the manure decomposition and branch decomposition rates were positively correlated with soil water storage ( $p < 0.05$  or 0.01) (Figure 3E and Figure 3F).

The potential maximum C and N which manure and branches inputted into soil were estimated based on the rates of decomposition (Table 1). Branch treatments had no substantial effect in inputting C and N into soil during the whole experimental period. However, with increased sheltering levels, the potential of manure inputted C and N did increase. Manure had potential input of maximum C into the soil between 0.07–0.33 g kg<sup>-1</sup> in 2017 and 0.06 g kg<sup>-1</sup>–0.29 g kg<sup>-1</sup> C in 2018. Potential maximum inputs of Nitrogen into the soil from manure were 0.01–0.02 g kg<sup>-1</sup> both in 2017 and in 2018.

#### 3.3 Effect of branch shelters on soil nutrients of grassland

Overall, branch shelter, sheep manure, and branch shelter  $\times$  sheep manure generally had a positive effect on enhancing soil nutrients (Figure 4). However, patterns differed depending on year and on chemical species. SOC started with a low concentration of approximately 2.5 g kg<sup>-1</sup> in the Controls in 2017. SOC was significantly increased in the High manure treatments, when there were increases in branch sheltering levels. SOC responded more strongly to the increase in branch shelters in 2018 with a maximum concentration of 3.7 g kg<sup>-1</sup>g under High manure and 60% shelter. Increasing manure amounts, and especially increasing sheltering levels, resulted in increased concentrations of Total P, Available N, and Available P in both 2017 and 2018. However, Total N concentrations overall decreased by half in the second

year, whereas Available N almost doubled in the second year. In contrast, phosphorus concentrations exhibited the reverse pattern, with Total P increasing from year one to year two while Available P was reduced to less than 10% in the second year.

### 3.4 Effect of branch shelters on plant growth of grassland

Under the lowest manure treatment, and without branch shelters, plant growth at the end of 2017, was extremely low, measured respectively as average coverage (20%), average height (12 cm), and biomass ( $30 \text{ g m}^{-2}$ ) (Figures 5A, C, E). Without the addition of branch shelters, increasing the amount of sheep manure from Low to High in year 1, during the plant establishment phase, resulted in limited plant growth and only slightly increased plant biomass (Low avg  $32.1 \text{ g m}^{-2}$ ; High avg  $69.7 \text{ g m}^{-2}$ ; Figure 5E). Without shelters in year 2, the final biomass was approximately four-fold higher in the Low manure treatment (Avg  $128.4 \text{ g m}^{-2}$ ) as compared with year 1, but the plant growth was significantly higher in the Medium manure treatment (Avg  $167.4 \text{ g m}^{-2}$ ) and High manure treatment (Avg  $192 \text{ g m}^{-2}$ ) than Low manure treatment. Addition of branch shelters to the Low manure treatment, significantly increased the plant biomass production in year 1 as compared with no shelters (60% and Low manure in year 1: avg  $134.3 \text{ g m}^{-2}$ ).

When manure and shelter treatments were combined, there were impressive increases in production. During the plant establishment phase in year 1, High amounts of manure combined with 60% sheltering level resulted in an average  $134.3 \text{ g m}^{-2}$  of biomass (Figure 5E), and by the end of year 2, biomass under Medium manure had reached  $238.4 \text{ g m}^{-2}$  and  $310.9 \text{ g m}^{-2}$  under the 40% and 60% shelters respectively (Figure 5F). Plant biomass in year two under High manure was comparable or slightly lower than Medium manure, under the same sheltering levels. Similar patterns were observed for the two other indices of plant response, i.e., plant coverage and plant height. However in all cases, plant biomass was dominated by, or consisted solely of one native annual species, *Artemisia scoparia*.

Correlation analysis revealed that all tested soil properties positively correlated with plant height and biomass ( $p < 0.01$ ), yet not correlated with plant coverage ( $p > 0.05$ ) in 2017 (Table 2). However, in 2018, all tested soil properties (except available P) were positively correlated with plant coverage, height, and biomass ( $p < 0.01$  or  $0.05$ ; Table 2).

## 4 Discussion

Overall, the results of this study demonstrated that combining two readily available and inexpensive resources, sheep manure and caragana branches in the form of a branch shelter, can significantly improve the soil environment and foster native plant growth in the severely degraded grassland soils, such as those of Ningxia, China. The branch shelters act to shade and cool the soil, and help maintain significantly higher soil moisture availability. This pattern was consistent across the two growing seasons. Addition of manure significantly increased the availability of nitrogen and phosphorus for plant growth. Application of manure alone, which is the traditional amendment approach, only had a minor effect on soil properties and plant growth, even at the highest levels. In contrast, increasing the branch sheltering level up to 60%, at the lowest manure rate, doubled plant production which suggests that limited water availability may be a stronger driver in these semi-arid environments. In fact, after 2 years, treatments with the highest amounts of both branch shelters and manure amendments combined resulted in a nearly doubling of the soil organic carbon and greatly boosted plant production to  $311 \text{ g m}^{-2}$  ( $3,110 \text{ kg ha}^{-1}$ ) by the end of year 2. Continued observations of the plants after the study ended indicated that they maintained enhanced production under the amendments in the subsequent year as well.

Notably, plant biomass in the treatment plots was dominated by a single native annual, wormwood *Artemisia scoparia*. Although the substantial increase in plant production can help jumpstart ecosystem processes and begin the self-healing of the grassland, additional inputs would likely be needed, either in the form of seeds or seedlings, to more quickly re-establish the diverse grassland flora

TABLE 2 The correlations between plant growth parameters and soil properties.

Year	Plant growth parameters	SWS	SOC	TN	TP	AN	AP
2017	Plant coverage	0.184	-0.008	0.056	-0.053	0.006	-0.124
	Plant height	0.527**	0.666**	0.532**	0.507**	0.583**	0.526**
	Plant biomass	0.667**	0.815**	0.653**	0.809**	0.809**	0.674**
2018	Plant coverage	0.349*	0.609**	0.624**	0.759**	0.630**	0.310*
	Plant height	0.471**	0.802**	0.783**	0.788**	0.836**	0.368*
	Plant biomass	0.422**	0.663**	0.660**	0.868**	0.715**	0.232

SWS, mean soil water storage; SOC, soil organic carbon; TN, total N; TP, total P; AN, available N; AP, available P. \* $p < 0.05$ , \*\* $p < 0.01$ .

communities key to a stable and resilient ecosystem. This simple and inexpensive solution employing readily available amendment materials has strong potential for application in other severely degraded landscapes. The research findings also provide new insights into the valuable benefits of a different form of organic amendment, namely branch shelters derived from encroaching shrubs, to help restored degraded grasslands.

In arid and semiarid regions, agricultural production is being exacerbated by increasing droughts associated with climate change (Pachauri and Meyer 2014). Hence, improvement of soil water capture and availability is pivotal in these water-limited regions and our research provides useful new insights about the role and efficacy of woody amendments in this regard. This study demonstrated that soil water availability can be significantly increased by the use of branch shelters in degraded soils. Our previous research demonstrated that branch shelters combined with woodchip incorporation into the soil could increase average soil water content by as much as 5 mm above the unamended soil, (from 7 to 11 mm in year 2012 and 11–16 mm in the same plots 3 years later) and by ~2 mm above the unamended soil in the woodchip treatment without branches in the same time periods (Li et al., 2019). This was a substantial improvement in soil water availability given the annual rainfall of ~150 mm during both growing seasons. In comparison, the current study demonstrated that only using branch shelters, with no woodchip incorporation, had an average increase of ~3.5 mm in soil water storage, under conditions of more than twice the total rainfall, and also decreased the maximum soil temperatures by at least 2°. Although less effective at improving soil moisture than the combined branch plus woodchips, the branch shelters alone are a simpler solution to implement than incorporation of woodchips into the soil. The successful use of branch shelters provides a new and complementary type of organic amendment, along with mulch, composts, and woodchip incorporation, that can help to restore degraded grasslands.

The impacts of the woody amendments are apparently complicated by the specific temperature and precipitation regimes experienced in a given year. The study year 2018 was significantly cooler and only slightly drier than 2017, which may explain why the branch shelter treatments exhibited greater success in reducing soil temperatures and increasing soil water storage in the second year. But, when the results of all these studies are integrated, it is clear that woody amendments can play a key role in restoring grassland soils, with significant reductions in soil temperatures and increases in soil water availability. These results can be achieved with just the use of branch shelters, with greater benefits achieved by combining shelters with woodchip or manure incorporation into the soil.

A few other studies have also corroborated this finding. For example, the use of long plum tree branches increased soil moisture in the jujube orchard in the Loess Plateau of China (Yang et al., 2010). Even loose piles of wood latticed above the

forest floor achieved similar benefits of cooler temperatures and higher soil moisture contents (Morreale and Sullivan, 2010). It is likely that the use of branch shelters retains soil moisture through a combination of processes including increasing the boundary layer thickness, which acts to reduce evaporation, and by shading (Flerchinger et al., 2003; Fuchs and Hadas, 2011). However, more research is needed to understand the underlying mechanisms so that appropriate restoration applications can be developed. For example, plastic branch shelters may not provide the same benefits as wood branches, because they can't absorb and release water and contribute to evaporative cooling. In a similarly vein, our previous research showed that rubber woodchips did not provide the same benefits as true woodchips incorporated into the soil because they couldn't absorb and then release water (Menzies-Pluer et al., 2020).

In all, the utility of small branch material for ecological restoration is particularly useful given that shrub encroachment has become a global nuisance contributing to grassland degradation. For instance, previous studies have showed that caragana growth depleted or even exhausted soil water of the grassland in our study site (Zhao et al., 2020). Historically, these invasive shrubs are removed mechanically, or herbicides and fire are used to destroy the shrubs (Killgore et al., 2009; Wang et al., 2018). However, our study suggests that shrubs can be cut and used for shelter for grassland restoration in the future.

This study also revealed that utilizing Tan sheep manure as a soil amendment proved to be a vital strategy for soil nutrient enhancement in a region where this material is widely available. Previous studies have shown that 75%–95% of the nitrogen of the forages consumed by grazing livestock is returned to the grassland in the form of both manure and urine (Cai et al., 2014). Schuman et al. (2002) also reported that manure deposition by grazing livestock has a significant impact on grassland soil nutrient cycling. However, as has been demonstrated elsewhere, manure decomposition and increased nutrient availability were positively correlated with soil water availability (Zhu et al., 2020). In this study, branch shelter levels of 40%–60% significantly improved soil water content and accelerated manure decomposition, and manure decomposition rate was significantly positively correlated with soil water condition. Manure inputs of C and N into the soil increased as branch sheltering levels increased, and with inputs ranging from 0.07–0.33 g kg<sup>-1</sup> C in 2017 and 0.06 g kg<sup>-1</sup>–0.29 g kg<sup>-1</sup> C in 2018, and maximum N inputs were 0.01–0.02 g kg<sup>-1</sup> both in 2017 and in 2018. It is acknowledged that the manure used in this study was already 1 year old when it was re-distributed and the experiment started. Much of the nutrients are leached out and/or volatilized after the first few weeks and months post animal defecation (Zhu et al., 2020), so decomposition rates and nutrient inputs of fresher manure would likely be more extreme.

In contrast, decomposition rates of the caragana branches were extremely slow, at approximately 3–6% weight loss per year.

They were therefore a limited source of nutrients to the soil and their key role appeared to be increasing soil moisture retention. Serendipitously, the low decomposition rate of branches also translated to a low-cost application for soil restoration underscoring our previous observation that one of the advantages of woody amendments over other organic materials is that the benefits achieved are maintained more than 5 years post implementation (Li et al., 2019). So, we speculate that shrub branch shelters will also benefit grassland restoration for a comparatively long period without requiring replenishment.

Ultimately, our study demonstrated that the use of shrub branch shelters and sheep manure had significant positive effects on plant growth in this degraded grassland. Under the combined treatment of High manure levels and 40–60% coverage by branch shelters, aboveground plant biomass reached  $\sim 300 \text{ g m}^{-2}$  in the second year. This biomass is comparable to levels reported from short-grass prairie steppes of comparable climate in the western Great Plains (Reeves et al., 2021). The current condition of the soil at this site is so degraded that, when unamended, there are insufficient nutrients and water to allow plants to get established and grow. The system had degraded to such a level that it had reached a new stable state or equilibrium condition (Scheffer et al., 2015). Inputs were needed to jumpstart the ecosystem to a different equilibrium. So, this is a feasible solution for plant production in grassland in arid and semiarid areas of China, since water and soil nutrients are regarded as most limiting factors for plant/crop production in these areas (Wang et al., 2016). Actually, this research also found that caragana branch shelter significantly improved soil water content and reduced soil temperature in a degraded grassland, and created a beneficial environment for reseeded forage growth (Zhang R et al., 2021). Our previous studies had also demonstrated that poplar branch shelters improved soil water condition and enhanced plant growth in arid areas (Li et al., 2018, 2019). Similarly, Fehmi et al. (2020) showed that adding a thin layer of wood chips on the surface increased plant growth. Besides, return of livestock manure in typical grasslands (Zhang et al., 2015), alpine grasslands (Min et al., 2014), dry grasslands (Duffková et al., 2015), and desertified grasslands (Bai et al., 2017) had also showed the effectively potential in improving productivity. Wang et al. (2016) also found that, dry matter accumulation and rainfall use efficiency of crop significantly increased as chicken manure application rate increasing (from  $750 \text{ g m}^{-2}$ – $2,250 \text{ g m}^{-2}$ ) in semiarid areas of China. Our experimental design allowed us to separate the influence of the two different amendment types and demonstrated that it was the combination of cooler temperatures, higher moisture availability and increased nutrients that resulted in the highest plant production. Actually, there was also a very similar study demonstrated that woody branch shelter combined with a thin layer of

compost can improve success rates of revegetation in dryland ecosystems by moderating the soil microclimate (such as improving soil moisture and enhancing soil nutrients) (Leger et al., 2022). In this study, the correlation analysis also showed that plant growth was significantly influenced by all tested indices including soil water, soil organic carbon, Total N, Total P, Available N, and Available P during whole period. In conclusion, this study revealed that the improved soil moisture promoted the transformation of manure nutrients and finally enhanced plant growth of grassland (Bang et al., 2005; Aarons et al., 2009; Saarijärvi and Virkajärvi, 2009).

## 5 Conclusion

This study demonstrated that 40%–60% cover of shrub branch shelters effectively increased soil water availability of degraded grassland, and consequently promoted decomposition of manure and shrub branches. The soil C and N were substantially inputted by decomposed manure rather than shrub branches, while the low decomposition rate of branches also means low-cost application in soil restoration. The combination of shrub branch shelter and manure application also enhanced plant growth *via* improving soil water availability and soil nutrients. In summary, our study provided a template using shrub branches and livestock manure to restore degraded grassland in arid and semiarid areas.

## Data availability statement

The raw data supporting the conclusions of this article will be made available by the authors, without undue reservation.

## Author contributions

ZL designed the research. JL and ZL performed the research and wrote the manuscript. RLS and SJM wrote the manuscript. HW, RW, and FW analyzed the data. All authors contributed to the article and approved the submitted version.

## Funding

This work was supported by the Key Research and Development Plan of Ningxia (2021BEG03010; 2021BEB04002), Ningxia Natural Science Foundation (2022AAC05013), the National Natural Science Foundation of China (32,260348; 42067022) and the Science and Technology Research Project of Ningxia Higher Education Institutions (NGY2018008).

## Conflict of interest

The authors declare that the research was conducted in the absence of any commercial or financial relationships that could be construed as a potential conflict of interest.

## Publisher's note

All claims expressed in this article are solely those of the authors and do not necessarily represent those of their affiliated

organizations, or those of the publisher, the editors and the reviewers. Any product that may be evaluated in this article, or claim that may be made by its manufacturer, is not guaranteed or endorsed by the publisher.

## Supplementary material

The Supplementary Material for this article can be found online at: <https://www.frontiersin.org/articles/10.3389/fenvs.2022.1089645/full#supplementary-material>

## References

- Akiyama, T., and Kawamura, K. (2007). Grassland degradation in China: Methods of monitoring, management and restoration. *Grassl. Sci.* 53, 1–17. doi:10.1111/j.1744-697X.2007.00073.x
- Aarons, S. R., O'Connor, C. R., Hosseini, H. M., and Gourley, C. J. P. (2009). Dung pads increase pasture production, soil nutrients and microbial biomass carbon in grazed dairy systems. *Nutr. Cycl. Agroecosyst.* 84, 81–92. doi:10.1007/s10705-008-9228-5
- Bai, Y., Wei, Z., Lv, S., Yan, R., Wu, R., Wang, T., et al. (2017). Effects of fertilizer application on the yield of forage and nutrient content on desert grassland. *Grassl. Prataculture* 29, 10–16. CNKI:SUN:NMCY.0.2017-02-002
- Bakker, E. S., Olff, H., Boekhoff, M., Gleichman, J. M., and Berendse, F. (2004). Impact of herbivores on nitrogen cycling: Contrasting effects of small and large species. *Oecologia* 138, 91–101. doi:10.1007/s00442-003-1402-5
- Bang, H. S., Lee, J. H., Kwon, O. S., Na, Y. E., Jang, Y. S., and Kim, W. H. (2005). Effects of paracoprid dung beetles (Coleoptera: Scarabaeidae) on the growth of pasture herbage and on the underlying soil. *Appl. Soil Ecol.* 29, 165–171. doi:10.1016/j.apsoil.2004.11.001
- Bao, S. (2013). *Soil and agricultural chemistry analysis*. Beijing: China Agriculture Press.
- Bloor, J. M. G. (2015). Additive effects of dung amendment and plant species identity on soil processes and soil inorganic nitrogen in grass monocultures. *Plant Soil* 396, 189–200. doi:10.1007/s11104-015-2591-5
- Bulmer, C., Venner, K., and Prescott, C. (2007). Forest soil rehabilitation with tillage and wood waste enhances seedling establishment but not height after 8 years. *Can. J. For. Res.* 37, 1894–1906. doi:10.1139/X07-063
- Byrne, K. M., Lauenroth, W. K., Adler, P. B., and Byrne, C. M. (2011). Estimating aboveground net primary production in grasslands: A comparison of nondestructive methods. *Rangel. Ecol. Manag.* 64, 498–505. doi:10.2111/REM-D-10-00145.1
- Cai, Y., Wang, X., Tian, L., Zhao, H., Lu, X., and Yan, Y. (2014). The impact of excretal returns from yak and Tibetan sheep dung on nitrous oxide emissions in an alpine steppe on the qinghai-Tibetan plateau. *Soil Biol. Biochem.* 76, 90–99. doi:10.1016/j.soilbio.2014.05.008
- Caracciolo, D., Istanbuloglu, E., Noto, L. V., and Collins, S. L. (2016). Mechanisms of shrub encroachment into Northern Chihuahuan Desert grasslands and impacts of climate change investigated using a cellular automata model. *Adv. Water Resour.* 91, 46–62. doi:10.1016/j.advwatres.2016.03.002
- Cochran, D. R., Gilliam, C. H., Eakes, D. J., Wehtje, G. R., Knight, P. R., and Olive, J. (2009). Mulch depth affects weed germination. *J. Environ. Hortic.* 27, 85–90. doi:10.24266/0738-2898-27.2.85
- Dan, Y., Du, L. T., Wang, L., Ma, L. L., Qiao, C. L., Wu, H. Y., et al. (2020). Effects of planted shrub encroachment on evapotranspiration and its components in desert steppe: A case study in Yanchi county, Ningxia hui autonomous region. *Acta Ecol. Sin.* 40, 5638–5648. doi:10.5846/stxb201910032066
- Deutsch, E. S., Bork, E. W., and Willms, W. D. (2010). Soil moisture and plant growth responses to litter and defoliation impacts in Parkland grasslands. *Agric. Ecosyst. Environ.* 135, 1–9. doi:10.1016/j.agee.2009.08.002
- Dodd, M. B., McGowan, A. W., Power, I. L., and Thorrold, B. S. (2005). Effects of variation in shade level, shade duration and light quality on perennial pastures. *N. Z. J. Agric. Res.* 48, 531–543. doi:10.1080/00288233.2005.9513686
- D'Odorico, P., Okin, G. S., and Bestelmeyer, B. (2012). A synthetic review of feedbacks and drivers of shrub encroachment in arid grasslands. *Ecolhydrology* 5, 520–530. doi:10.1002/eco.259
- Dong, C., Wang, W., Liu, H., Xu, X., and Zeng, H. (2019). Temperate grassland shifted from nitrogen to phosphorus limitation induced by degradation and nitrogen deposition: Evidence from soil extracellular enzyme stoichiometry. *Ecol. Indic.* 101, 453–464. doi:10.1016/j.ecolind.2019.01.046
- Duffková, R., Hejčman, M., and Libichová, H. (2015). Effect of cattle slurry on soil and herbage chemical properties, yield, nutrient balance and plant species composition of moderately dry arrhenatherion, grassland. *Agric. Ecosyst. Environ.* 213, 281–289. doi:10.1016/j.agee.2015.07.018
- Eldridge, D. J., and Koen, T. B. (2003). Detecting environmental change in eastern Australia: Rangeland health in the semi-arid woodlands. *Sci. Total Environ.* 310, 211–219. doi:10.1016/S0048-9697(02)00641-1
- Fehmi, J. S., Rasmussen, C., and Gallery, R. E. (2020). Biochar and woodchip amendments alter restoration outcomes, microbial processes, and soil moisture in a simulated semi-arid ecosystem. *Restor. Ecol.* 28, 355–364. doi:10.1111/rec.13100
- Flerchinger, G. N., Sauer, T. J., and Aiken, R. A. (2003). Effects of crop residue cover and architecture on heat and water transfer at the soil surface. *Geoderma* 116, 217–233. doi:10.1016/S0016-7061(03)00102-2
- Foley, J. A., Ramankutty, N., Brauman, K. A., Cassidy, E. S., Gerber, J. S., Johnston, M., et al. (2011). Solutions for a cultivated planet. *Nature* 478, 337–342. doi:10.1038/nature10452
- Fuchs, M., and Hadas, A. (2011). Mulch resistance to water vapor transport. *Agric. Water Manag.* 98, 990–998. doi:10.1016/j.agwat.2011.01.008
- Gang, C., Zhou, W., Chen, Y., Wang, Z., Sun, Z., Li, J., et al. (2014). Quantitative assessment of the contributions of climate change and human activities on global grassland degradation. *Environ. Earth Sci.* 72, 4273–4282. doi:10.1007/s12665-014-3322-6
- Jia, X., Shao, M., Yu, D., Zhang, Y., and Binley, A. (2018). Spatial variations in soil-water carrying capacity of three typical revegetation species on the Loess Plateau, China. *Agric. Ecosyst. Environ.* 273, 25–35. doi:10.1016/j.agee.2018.12.008
- Kerley, G. I. H., and Whitford, W. G. (2009). Can kangaroo rat graminivory contribute to the persistence of desertified shrublands. *J. Arid Environ.* 73, 651–657. doi:10.1016/j.jaridenv.2009.01.001
- Killgore, A., Jackson, E., and Whitford, W. G. (2009). Fire in chihuahuan desert grassland: Short-term effects on vegetation, small mammal populations, and faunal pedoturbation. *J. Arid Environ.* 73, 1029–1034. doi:10.1016/j.jaridenv.2009.04.016
- Klumpp, K., Fontaine, S., Attard, E., Le Roux, X., Gleixner, G., and Soussana, J. F. (2009). Grazing triggers soil carbon loss by altering plant roots and their control on soil microbial community. *J. Ecol.* 97, 876–885. doi:10.1111/j.1365-2745.2009.01549.x
- Knops, J. M. H., Bradley, K. L., and Wedin, D. A. (2002). Mechanisms of plant species impacts on ecosystem nitrogen cycling. *Ecol. Lett.* 5, 454–466. doi:10.1046/j.1461-0248.2002.00332.x
- Leger, A. M., Ball, K. R., Rathke, S. J., and Blankinship, J. C. (2022). Mulch more so than compost improves soil health to reestablish vegetation in a semiarid rangeland. *Restor. Ecol.* 30, e13698. doi:10.1111/rec.13698
- Li, Z., Schneider, R. L., Morreale, S. J., Xie, Y., Li, C., and Li, J. (2018). Woody organic amendments for retaining soil water, improving soil properties and



enhancing plant growth in desertified soils of Ningxia, China. *Geoderma* 310, 143–152. doi:10.1016/j.geoderma.2017.09.009

Li, Z., Schneider, R. L., Morreale, S. J., Xie, Y., Li, J., Li, C., et al. (2019). Using woody organic matter amendments to increase water availability and jump-start soil restoration of desertified grassland soils of Ningxia, China. *Land Degrad. Dev.* 30, 1313–1324. doi:10.1002/ldr.3315

Liu, K., Sollenberger, L. E., Newman, Y. C., Vendramini, J. M. B., Interrante, S. M., and White-Leech, R. (2011). Grazing management effects on productivity, nutritive value, and persistence of "Tifton 85" Bermudagrass. *Crop Sci.* 51, 353–360. doi:10.2135/cropsci2010.02.0122

Luan, J., Cui, L., Xiang, C., Wu, J., Song, H., Ma, Q., et al. (2014). Different grazing removal enclosures effects on soil C stocks among alpine ecosystems in east Qinghai-Tibet Plateau. *Ecol. Eng.* 64, 262–268. doi:10.1016/j.ecoleng.2013.12.057

Maestre, F. T., Bowker, M. A., Puche, M. D., Hinojosa, M. B., Martínez, I., García-Palacios, P., et al. (2009). Shrub encroachment can reverse desertification in semi-arid Mediterranean grasslands. *Ecol. Lett.* 12, 930–941. doi:10.1111/j.1461-0248.2009.01352.x

Menzies-Pluer, E. G., Schneider, R. L., Morreale, S. J., Liebig, M. A., Li, J., Li, C. X., et al. (2020). Returning degraded soils to productivity: An examination of the potential of coarse woody amendments for improved water retention and nutrient holding capacity. *Water Air Soil Pollut.* 231, 15. doi:10.1007/s11270-019-4380-x

Min, X., Ma, Y., Li, S., and Wang, Y. (2014). Effects of sheep manure on productivity and nutrition of soil for *Poa pratensis* cv. Qinghai pasture. *Pratacultural Sci.* 31, 1039–1044. doi:10.11829/j.issn.1001-0629.2013-0572

Morreale, S. J., and Sullivan, K. L. (2010). Community-level enhancements of biodiversity and ecosystem services. *Front. Earth Sci. China* 4, 14–21. doi:10.1007/s11707-010-0015-7

Oenema, O., and Tamminga, S. (2005). Nitrogen in global animal production and management options for improving nitrogen use efficiency. *Sci. China. C Life Sci.* 48, 871–887. doi:10.1007/BF03187126

Pachauri, R. K., and Meyer, L. A. (2014). "Contribution of working groups I, II and III to the fifth assessment report of the intergovernmental panel on climate change," in *Climatic change 2014 synthesis report* (Geneva: IPCC).

Rashid, M. I., Lantinga, E. A., Brussaard, L., and de Goede, R. G. M. (2017). The chemical convergence and decomposer control hypotheses explain solid cattle manure decomposition in production grasslands. *Appl. Soil Ecol.* 113, 107–116. doi:10.1016/j.apsoil.2017.02.009

Reeves, C. R., Hanberry, B. B., Wilmer, H., Kaplan, N. E., and Lauenroth, W. K. (2021). An assessment of production trends on the Great Plains from 1984 to 2017. *Rangel. Ecol. Manag.* 78, 165–179. doi:10.1016/j.rama.2020.01.011

Reichert, J. M., Gubiani, P. I., dos Santos, D. R., Reinert, D. J., Aita, C., and Giacomini, S. J. (2022). Soil properties characterization for land-use planning and soil management in watersheds under family farming. *Int. Soil Water Conservation Res.* 10, 119–128. doi:10.1016/j.iswcr.2021.05.003

Saarijärvi, K., and Virkajärvi, P. (2009). Nitrogen dynamics of cattle dung and urine patches on intensively managed boreal pasture. *J. Agric. Sci.* 147, 479–491. doi:10.1017/S0021859609008727

Scheffer, M., Carpenter, S. R., Dakos, V., and van Nes, E. H. (2015). Generic indicators of ecological resilience: Inferring the chance of a critical transition. *Annu. Rev. Ecol. Syst.* 46, 145–167. doi:10.1146/annurev-ecolsys-112414-054242

Schuman, G. E., Janzen, H. H., and Herrick, J. E. (2002). Soil carbon dynamics and potential carbon sequestration by rangelands. *Environ. Pollut.* 116, 391–396. doi:10.1016/S0269-7491(01)00215-9

Wang, G., Li, J., Sujith, R., David, D., Gonzales, H. B., and Sankey, J. B. (2018). Post-fire redistribution of soil carbon and nitrogen at a grassland–shrubland ecotone. *Ecosystems* 22, 174–188. doi:10.1007/s10021-018-0260-2

Wang, X., Jia, Z., Liang, L., Yang, B., Ding, R., Nie, J., et al. (2016). Impacts of manure application on soil environment, rainfall use efficiency and crop biomass under dryland farming. *Sci. Rep.* 6, 20994. doi:10.1038/srep20994

Watson, P. A., Alexander, H. D., and Moczygemba, J. D. (2018). Coastal prairie recovery in response to shrub removal method and degree of shrub encroachment. *Rangel. Ecol. Manag.* 72, 275–282. doi:10.1016/j.rama.2018.11.005

Weedon, J. T., Cornwell, W. K., Cornelissen, J. H. C., Zanne, A. E., Wirth, C., and Coomes, D. A. (2009). Global meta-analysis of wood decomposition rates: A role for trait variation among tree species? *Ecol. Lett.* 12, 45–56. doi:10.1111/j.1461-0248.2008.01259.x

Wei, N., Zhao, L. P., Tan, S. T., and Zhao, F. R. (2019). Research progress on shrub encroachment in grasslands. *Ecol. Sci.* 38, 208–216. doi:10.14108/j.cnki.1008-8873.2019.06.030

Wilcox, B. P., Birt, A., Fuhlendorf, S. D., and Archer, S. R. (2018). Emerging frameworks for understanding and mitigating woody plant encroachment in grassy biomes. *Curr. Opin. Environ. Sustain.* 32, 46–52. doi:10.1016/j.cosust.2018.04.005

Wilson, B. S., Jensen, W. E., Houseman, G. R., Jameson, M. L., Reichenborn, M. M., Watson, D. F., et al. (2022). Cattle grazing in CRP grasslands during the nesting season: Effects on avian abundance and diversity. *J. Wildl. Manage.* 86. doi:10.1002/jwmg.22188

Xu, S., Sayer, E. J., Eisenhauer, N., Lu, X., wang, J., and Liu, C. (2021). Aboveground litter inputs determine carbon storage across soil profiles: A meta-analysis. *Plant Soil* 462, 429–444. doi:10.1007/s11104-021-04881-5

Xu, Z., Gao, L., Wang, L., Cheng, S., Zhang, X., and Wu, J. (2012). Impacts of dung combustion on carbon cycle of grassland ecosystem. *Resour. Sci.* 34, 1062–1069. doi:10.1007/7588(2012)06-1062-08

Yang, Z., Wang, Y., Zhao, Y., Li, P., and Dan, X. (2010). Influence of branch cover and water retaining agent on soil water. *J. Irrigation Drainage* 29, 97–99. doi:10.1016/S1002-0160(10)60014-8

Zhang, Q., Liu, K., Shao, X., Li, H., He, Y., Sirimuji, Wang B., et al. (2021). Microbes require a relatively long time to recover in natural succession restoration of degraded grassland ecosystems. *Ecol. Indic.* 129, 107881. doi:10.1016/j.ecolind.2021.107881

Zhang, R., Li, J., Peng, W., Wang, F., and Li, Z. (2021). Effects of mulching with caragana (*Caragana intermedia*) branches on soil moisture content and temperature and reseeded forage biomass in desertified grassland in Ningxia Province, China. *Acta Pratacultural Sin.* 30, 58–67. doi:10.11686/cyxb2020172

Zhang, Y., Xie, Y., Ma, H., Zhang, J., Jing, L., Wang, Y., et al. (2021). The responses of soil respiration to changed precipitation and increased temperature in desert grassland in northern China. *J. Arid Environ.* 193, 104579. doi:10.1016/j.jaridenv.2021.104579

Zhang, Y., Yang, S., Fu, M., Cai, J., Zhang, Y., Wang, R., et al. (2015). Sheep manure application increases soil exchangeable base cations in a semi-arid steppe of Inner Mongolia. *J. Arid. Land* 7, 361–369. doi:10.1007/s40333-015-0004-5

Zhao, Y., Yu, L., Zhou, Y., Wang, H., Ma, Q., and Qi, L. (2020). Soil moisture dynamics and deficit of desert grassland with anthropogenic introduced shrub encroachment in the eastern Ningxia, China. *Acta eco. Sin.* 40, 1305–1315. doi:10.5846/stxb201812152735

Zheng, Q., Du, L., Gong, F., Dan, Y., and Wang, L. (2019). Landscape characteristics of caragana intermedia plantation based on GF-1 remote sensing image in Yanchi. *J. southwest For. Univ. Nat. Sci.* 39, 152–159. doi:10.11929/j.swfu.201808028

Zhu, Y., Merbold, L., Leitner, S., Pelster, D. E., Okoma, S. A., Ngetich, F., et al. (2020). The effects of climate on decomposition of cattle, sheep and goat manure in Kenyan tropical pastures. *Plant Soil* 451, 325–343. doi:10.1007/s11104-020-04528-x





## OPEN ACCESS

EDITED AND REVIEWED BY  
Jianping Li,  
Ningxia University, China

\*CORRESPONDENCE  
Zhigang Li,  
✉ lizg001@sina.com

SPECIALTY SECTION  
This article was submitted  
to Soil Processes,  
a section of the journal  
Frontiers in Environmental Science

RECEIVED 05 January 2023  
ACCEPTED 18 January 2023  
PUBLISHED 03 February 2023

CITATION  
Liu J, Schneider RL, Morreale SJ, Wang H,  
Wang R, Wang F and Li Z (2023),  
Corrigendum: The roles for branch  
shelters and sheep manure to accelerate  
the restoration of degraded grasslands in  
northern China.  
*Front. Environ. Sci.* 11:1138449.  
doi: 10.3389/fenvs.2023.1138449

COPYRIGHT  
© 2023 Liu, Schneider, Morreale, Wang,  
Wang, Wang and Li. This is an open-access  
article distributed under the terms of the  
Creative Commons Attribution License  
(CC BY). The use, distribution or  
reproduction in other forums is permitted,  
provided the original author(s) and the  
copyright owner(s) are credited and that  
the original publication in this journal is  
cited, in accordance with accepted  
academic practice. No use, distribution or  
reproduction is permitted which does not  
comply with these terms.

# Corrigendum: The roles for branch shelters and sheep manure to accelerate the restoration of degraded grasslands in northern China

Jing Liu<sup>1,2</sup>, Rebecca L. Schneider<sup>3</sup>, Stephen J. Morreale<sup>3</sup>,  
Hongmei Wang<sup>1,2</sup>, Ruixia Wang<sup>4</sup>, Fang Wang<sup>5</sup> and Zhigang Li<sup>1,2\*</sup>

<sup>1</sup>School of Agriculture, Ningxia University, Yinchuan, Ningxia, China, <sup>2</sup>Ningxia Grassland and Animal Husbandry Engineering Technology Research Centre, Yinchuan, Ningxia, China, <sup>3</sup>Department of Nature Resources, College of Agriculture and Life Sciences, Cornell University, Ithaca, NY, United States, <sup>4</sup>Baijitan Nature Reserve Administration, Lingwu, Ningxia, China, <sup>5</sup>College of Geographical Sciences and Planning, Ningxia University, Yinchuan, Ningxia, China

## KEYWORDS

caragana branch shelters, soil water availability, sheep manure decomposition, soil nutrients, plant growth, degraded grassland

## A Corrigendum on

The roles for branch shelters and sheep manure to accelerate the restoration of degraded grasslands in northern China

by Liu J, Schneider R. L, Morreale S. J, Wang H, Wang R, Wang F and Li Z (2023). *Front. Environ. Sci.* 10: 1089645. doi: 10.3389/fenvs.2022.1089645

The original article contained a previous version of the manuscript. The article has now been corrected to show the most updated version that includes all the corrections detailed below.

In the original article, there was an error as Table 2 was not included in the text. The table and its caption appear below.

In the original article, there was an error in the phrasing of a sentence in the **Abstract**. This sentence previously stated: “Strategies are desperately needed for restoring the millions of hectares of degraded grasslands which have been simultaneously impacted by overgrazing and Caragana shrub encroachment in arid and semiarid areas of northern China.” The corrected sentence appears below:

“New strategies are desperately needed for restoring the millions of hectares of degraded grasslands in arid and semiarid areas of northern China.”

In the original article, there was an error in one of the words in the **Abstract**. The word previously stated: “*Artemis*”. The corrected word appears below:

TABLE 2 The correlations between plant growth parameters and soil properties.

Year	Plant growth parameters	SWS	SOC	TN	TP	AN	AP
2017	Plant coverage	0.184	−0.008	0.056	−0.053	0.006	−0.124
	Plant height	0.527**	0.666**	0.532**	0.507**	0.583**	0.526**
	Plant biomass	0.667**	0.815**	0.653**	0.809**	0.809**	0.674**
2018	Plant coverage	0.349*	0.609**	0.624**	0.759**	0.630**	0.310*
	Plant height	0.471**	0.802**	0.783**	0.788**	0.836**	0.368*
	Plant biomass	0.422**	0.663**	0.660**	0.868**	0.715**	0.232

SWS, mean soil water storage; SOC, soil organic carbon; TN, total N; TP, total P; AN, available N; AP, available P. \* $p < 0.05$ , \*\* $p < 0.01$ .

### “Artemisia”

In the original article, there was an error in one of the words in section **I Introduction**. The word previously stated: “bill”. The corrected sentence appears below:

### “billion”

In the original article, there was an error in a sentence in section **I Introduction**. This sentence previously stated: “This litter has been shown to be a key contributor to the development of soil organic content in the soil profile to 1 m depth (Xu et al., 2021).” This sentence should be deleted.

In the original article, Rashid et al., 2017 was not cited in the article and a change in paragraph wording was not included in section **2 Materials and methods**, sub-section *2.4 Measurement of decompositions and nutrient inputs both for manure and Caragana branches*, paragraph 2. This paragraph previously stated: “Both for manure and branches, one bag in each plot was collected at the end of September in 2017, and another was collected at the end of September in 2018. Then the decomposition rate was determined as the change in oven-dried weight loss determined after oven drying at 85°C. Organic carbon was assayed by the acidified potassium dichromate ( $K_2Cr_2O_7-H_2SO_4$ ) heating method (Bao, 2013). Total nitrogen (N) was determined using the Kjeldahl procedure (Bao, 2013). Meanwhile, cumulative decomposition rate of manure and branches, as well as the potential maximum C and N which manure and branches input into soil were evaluated with the following equations:

$$DR = 100 \times (DM_{initial} - DM_{end}) / DM_{initial} \quad (2)$$

$$C_{released} \text{ or } N_{released} = DR \times DM_{initial} \times C_{content} \text{ or } N_{content} \times 0.001 \quad (3)$$

$$C_{input} \text{ or } N_{input} = \frac{C_{released} \text{ or } N_{released}}{BD \times S \times H} \quad (4)$$

where,  $DR$  (%) is cumulative decomposition rate of manure or branches after one or 2 years;  $DM_{initial}$  ( $g\ m^{-2}$ ) is the initial dry matter weight of manure or sheltered branches in each plot;  $DM_{end}$  is the dry matter weight of manure or sheltered branches were decomposed after one or 2 years in each plot;  $C_{released}$  or  $N_{released}$  ( $g\ m^{-2}$ ) is cumulative released C or N from decomposed manure or branches after one or 2 years in each plot;  $C_{content}$  ( $g\ kg^{-1}$ ) or  $N_{content}$  ( $g\ kg^{-1}$ ) is the concentration of C or N in manure or branches;  $C_{input}$  ( $g\ kg^{-1}$ ) or  $N_{input}$  ( $g\ kg^{-1}$ ) is the potential maximum C or N which manure or branches cumulatively input into soil;  $BD$  ( $g\ cm^{-3}$ ) is soil bulk density, and in this study  $BD = 1.4\ g\ cm^{-3}$ ;  $S$  ( $m^2$ ) is soil area in

calculation, and  $1\ m^2$  soil area was applied in calculation in this study;  $H$  is soil depth,  $H = 20\ cm$  in this study.” The corrected sentence and citation appear below:

“Both for manure and branches, one bag in each plot was collected at the end of September in 2017, and another was collected at the end of September in 2018. Then the decomposition rate was determined as the change in oven-dried weight loss determined after oven drying at 85°C. Organic carbon was assayed by the acidified potassium dichromate ( $K_2Cr_2O_7-H_2SO_4$ ) heating method (Bao, 2013). Total nitrogen (N) was determined using the Kjeldahl procedure (Bao, 2013). Considering the influence of soil to interfere accurate evaluation for manure decomposition, ash correction was applied according to Rashid et al. (2017). Thus, a muffle furnace was used to determine ash content in bags by loss-on-ignition at 550°C for 4 h, and the soil dry weight that contaminated the manure calculated as following equations:

$$CDW = \frac{AS_R - A_{IC}}{A_{SL}} \quad (2)$$

where  $CDW$  is soil dry weight ( $g$ ) than contaminated the manure bag,  $AS_R$  is ash content ( $mg$ ) that remained in manure bag,  $A_{IC}$  is the initial ash content ( $mg$ ) in manure bag and  $A_{SL}$  is the soil ash content ( $mg\ g^{-1}$ ). After ash correction, cumulative decomposition rate of manure and branches, as well as the potential maximum C and N which manure and branches input into soil were evaluated with the following equations:

$$DR = 100 \times (DM_{initial} - DM_{end}) / DM_{initial} \quad (3)$$

$$C_{released} \text{ or } N_{released} = DR \times DM_{initial} \times C_{content} \text{ or } N_{content} \times 0.001, \quad (4)$$

$$C_{input} \text{ or } N_{input} = \frac{C_{released} \text{ or } N_{released}}{BD \times S \times H}, \quad (5)$$

where,  $DR$  (%) is cumulative decomposition rate of manure or branches after one or 2 years;  $DM_{initial}$  ( $g\ m^{-2}$ ) is the initial dry matter weight of manure or sheltered branches in each plot;  $DM_{end}$  is the dry matter weight of manure or sheltered branches were decomposed after one or 2 years in each plot;  $C_{released}$  or  $N_{released}$  ( $g\ m^{-2}$ ) is cumulative released C or N from decomposed manure or branches after one or 2 years in each plot;  $C_{content}$  ( $g\ kg^{-1}$ ) or  $N_{content}$  ( $g\ kg^{-1}$ ) is the concentration of C or N in manure or branches;  $C_{input}$  ( $g\ kg^{-1}$ ) or  $N_{input}$  ( $g\ kg^{-1}$ ) is the potential maximum C or N which manure or branches cumulatively input into soil;  $BD$  ( $g\ cm^{-3}$ ) is soil bulk density, and in this study  $BD = 1.4\ g\ cm^{-3}$ ;  $S$  ( $m^2$ ) is soil area in

calculation, and 1 m<sup>2</sup> soil area was applied in calculation in this study;  $H$  is soil depth,  $H = 20$  cm in this study.”

In the original article, there was an error in Figure 6 as published. Figure 6 should be removed.

In the original article, there was an error in **section 2 Materials and methods**, sub-section 2.7 *Statistical analyses*, paragraph 1. This sentence previously stated: “One-way analysis of variance (ANOVA) tests was used to compare soil water content, soil surface temperature, soil chemical properties, decomposition rates of manure and caragana branches, and plant growth among treatments in each year, respectively. Tukey HSD tests were used to make *post hoc* multiple pairwise comparisons among all treatments, when data showed homogeneity of variance. Two-way ANOVAs were applied to detect the effects of shelters, sheep manure, and shelters  $\times$  manure on each determined soil and plant index, respectively. Regression analysis was applied to reveal the correlation of manure decomposition rate and soil water storage, as well as branch decomposition rate and soil water storage. Redundancy analysis (RDA) was run to reveal major drivers of soil properties affecting plant growth. All above analyses were carried out using the “vegan” package in R. In all tests, a  $p$ -value  $\leq 0.05$  was considered significant.” The corrected sentence appears below:

“Two-way ANOVAs were applied to detect the effects of shelters, sheep manure, and shelters  $\times$  manure on each determined soil and plant index, respectively. And when the results of two-way ANOVAs shown interaction effect is significant, the simple effect analysis, thus One-way analysis of variance (ANOVA), was used to determine the difference between the effects of one factor at different levels of another factor. Regression analysis was applied to reveal the correlation of manure decomposition rate and soil water storage, as well as branch decomposition rate and soil water storage. Correlation analysis was used to reveal the relationships between plant growth parameters and tested soil properties. All above analyses were carried out using the “vegan” package in R. In all tests, a  $p$ -value  $\leq 0.05$  was considered significant.”

In the original article, there was an error in a sentence in section **3 Results**, sub-section 3.4 *Effect of branch shelters on plant growth of grassland*. This sentence previously stated: “Redundancy analysis was performed to illustrate relationships between plant growth and soil properties at depth of 0–20 cm. All tested soil parameter were

significantly influencing plant growth both in 2017 and 2018 ( $p < 0.05$ ; Figure 6)”. The corrected sentence appears below:

“Correlation analysis revealed that all tested soil properties positively correlated with plant height and biomass ( $p < 0.01$ ), yet not correlated with plant coverage ( $p > 0.05$ ) in 2017 (Table 2). However, in 2018, all tested soil properties (except available P) were positively correlated with plant coverage, height, and biomass ( $p < 0.01$  or  $0.05$ ; Table 2).”

In the original article, there was an error in a sentence in section **4 Discussion**, page 13. This sentence previously stated: “In this study, the RDA model also showed that plant growth was significantly influenced by all tested indices including soil water, soil organic carbon, Total N, Total P, Available N, and Available P during whole period.” The corrected sentence appears below:

“In this study, the correlation analysis also showed that plant growth was significantly influenced by all tested indices including soil water, soil organic carbon, Total N, Total P, Available N, and Available P during whole period.”

In the original article, there was an error in a sentence in section **Conclusion**. This sentence previously stated: “In summary, our study provided a template for restoration of degraded grassland simultaneously incurred by overgrazing and shrub encroachment in arid and semiarid areas.” The corrected sentence appears below:

“In summary, our study provided a template using shrub branches and livestock manure to restore degraded grassland in arid and semiarid areas.”

The authors apologize for these errors and state that this does not change the scientific conclusions of the article in any way. The original article has been updated.

## Publisher's note

All claims expressed in this article are solely those of the authors and do not necessarily represent those of their affiliated organizations, or those of the publisher, the editors and the reviewers. Any product that may be evaluated in this article, or claim that may be made by its manufacturer, is not guaranteed or endorsed by the publisher.



## OPEN ACCESS

EDITED BY  
Kaibo Wang,  
Institute of Earth Environment (CAS), China

REVIEWED BY  
Baicheng Niu,  
Qinghai Normal University, China  
Eric Josef Ribeiro Parteli,  
University of Duisburg-Essen, Germany

\*CORRESPONDENCE  
Zhongju Meng,  
✉ mengzhongju@126.com

SPECIALTY SECTION  
This article was submitted to Soil  
Processes,  
a section of the journal  
Frontiers in Environmental Science

RECEIVED 29 November 2022  
ACCEPTED 23 December 2022  
PUBLISHED 06 January 2023

CITATION  
Qi S, Ren X, Dang X and Meng Z (2023),  
Mechanisms of dust emissions from lakes  
during different drying stages in a semi-  
arid grassland in northern China.  
*Front. Environ. Sci.* 10:1110679.  
doi: 10.3389/fenvs.2022.1110679

COPYRIGHT  
© 2023 Qi, Ren, Dang and Meng. This is an  
open-access article distributed under the  
terms of the [Creative Commons  
Attribution License \(CC BY\)](#). The use,  
distribution or reproduction in other  
forums is permitted, provided the original  
author(s) and the copyright owner(s) are  
credited and that the original publication in  
this journal is cited, in accordance with  
accepted academic practice. No use,  
distribution or reproduction is permitted  
which does not comply with these terms.

# Mechanisms of dust emissions from lakes during different drying stages in a semi-arid grassland in northern China

Shuai Qi<sup>1</sup>, Xiaomeng Ren<sup>2</sup>, Xiaohong Dang<sup>1</sup> and Zhongju Meng<sup>1\*</sup>

<sup>1</sup>College of Desert Control Science and Engineering, Inner Mongolia Agricultural University, Hohhot, China,

<sup>2</sup>Inner Mongolia Meteorological Institute, Hohhot, China

Semi-arid playas are important to grassland ecosystem species as an important source of global dust emissions. However, there is a lack of data on dust emissions during the different drying stages of grassland playas. In this study, we initially conducted the field experiments on two types of surfaces (intermittently dried and permanently dried) in playas located in semi-arid regions in northern China, and we measured dust emissions at five wind speeds in spring when wind erosion was frequent. The results showed that the intermittently dried surface was more prone to wind erosion, which was primarily due to the formation of a loose and fragile salt crust on the surface. In addition, the proportion of salt in the dust was higher than that for the permanently dried surfaces. Nevertheless, the total horizontal dust flux (1.13–2.3 g/cm<sup>2</sup>·min) from the intermittently dried surface was only 5%–15% that of the permanently dried surface (7.47–42.86 g/cm<sup>2</sup>·min). The dust content varied linearly with the height of the intermittently dried surface, and varied exponentially with the height of the permanently dried surface. The particles collected on the intermittently dried surface were larger (<63 μm) than those collected on the permanently dried surface (<10 μm), and the unit mass concentration of each ion (mainly Na<sup>+</sup>, Cl<sup>-</sup>, and SO<sub>4</sub><sup>2-</sup>) in the salt dust was also higher for the intermittently dried surface than for the permanently dried surface. Although salt dust was continuously released from the intermittently dried surface, the total amount released each time was limited. These results indicate that to attenuate the damage of salt dust storms, priority should be given to protecting permanently dried surfaces and reducing the supply of salt dust particles at the surface.

## KEYWORDS

grassland playa, wind erosion, salt crust, salt dust, desertification of land

## Introduction

Wind erosion caused by the drying of salt lakes is one of the sources of dust release in arid and semi-arid regions and even globally (Gill et al., 2002; Abuduwaili et al., 2010; Baddock et al., 2011; Motaghi et al., 2020; Van Pelt et al., 2020), accounting for about 30% of global dust emissions (Sweeney et al., 2016). According to current studies on dust emissions, landscapes that exist in semi-arid and arid regions such as the Gobi Desert (Wang et al., 2006b; Wang et al., 2008), salt and dry lakes, ephemeral stream depressions, seasonal marshes, and alluvial fans (Derbyshire et al., 1998), emit dust in different seasons (Varga, 2012). About 100–300 million tons of dust are emitted into the atmosphere each year (Varga et al., 2014). These landform units are commonly found in the western United States (Bowen

and Johnson, 2015; Collins et al., 2018), North Africa (Prospero et al., 2002; Mahowald et al., 2006), Central Asia (Ziyadeh et al., 2018), and northern China (Tao et al., 2020; Hao and Li, 2021). There are hundreds of lakes with areas of greater than 50 km<sup>2</sup> in northern China, and under the drastic climate change and unreasonable human development, a large number of these lakes have shrunk and become dry lake beds. These lake beds are generally flatter and have lower slopes (Chun et al., 2017), no vegetation cover, and a surface composed of loose salt-rich sedimentary particles (Yang L.-R. et al., 2007; Liu et al., 2010). These surfaces are exposed to windy conditions year-round and are highly susceptible to wind erosion, leading to unavoidable air pollution and environmental problems in arid and semi-arid regions (Shao et al., 2011; Von Holdt et al., 2017). The chemical composition and particle size composition of salt dust storms are different from those of ordinary dust storms. Salt dust storms contain high concentrations of sulfate, chloride, and some harmful metal particles with strong adsorption (Abuduwaili et al., 2010), which usually lead to a decline in soil productivity, affect plant photosynthesis and cause respiratory diseases in animals and humans (Liu et al., 2010; Ziyadeh et al., 2018). The chemical composition and particle size of the dried salt lake surface sediments also lead to the formation of aerosols that are suspended in the air for long periods, which have a serious impact on the local environment and can even be carried farther away before deposition, affecting a much wider area (Wang et al., 2012b). Therefore, the threat of such dust is greater than that of normal dust storms originating in the desert and Gobi regions. Based on previous studies, salinized particles play an important role in the atmospheric, climatic and biogeochemical cycles (Stout et al., 2009; Lee et al., 2012; Cheng et al., 2022), and the emission and dispersion of salt dust have become a hot research topic (Liu et al., 2010).

Numerous studies have been conducted on dry lakes using methods such as surface sampling (Shahabinejad et al., 2019), wind tunnel simulations (Liu et al., 2021), and remote sensing techniques (Cheng et al., 2022); however, these studies mainly focused on areas such as palm lakes in deserts, saline areas in degraded agricultural lands, and alluvial fans in the Gobi Desert (Gill et al., 2002; Yang L.-R. et al., 2007), as well as surface sediment characteristics. Wind erosion of dry lakes in grassland areas has been insufficiently studied, especially the horizontal flux transport of sediments at different heights. Grassland lakes, as an important part of grassland ecosystems, are now facing serious challenges, and a large number of these lakes have degraded and dried up (Meng et al., 2018). QeHan Lake dried up in 2002. Wind erosion of the surface consisting of loose salt-containing particles provides a sufficient source of sand, seriously damaging the local pasture and greatly affecting the lives and productivity of herders. However, due to the lack of pollution monitoring stations around the dry lakes in QeHan, there is limited information about how the area is directly affected by dust events. Therefore, we selected the dry salt lakes in QeHan, located on the Inner Mongolia Plateau, as the research area. Furthermore, we measured the surface sediment transport characteristics and wind erosion material in two different stages (intermittent drying and permanent drying) to reveal the wind erosion law in the different drying stages of grassland lakes. In addition, we aimed to provide reference data for soil wind erosion vacancies and desertification control of degraded lakes in grassland areas.

## Materials and methods

### Study area

QeHan Lake (114°45'–115°04'E, 43°22'–43°29'N) is a closed salt lakes located in the northern part of the Otindag sandy land region on the Inner Mongolia Plateau. QeHan relies on the Engel River for recharge, and the ecological environment is very fragile and sensitive to global climate change (Niu et al., 2005). Due to the influence of long-term high temperatures, the arid climate and excessive human economic activities during the past 40 years (Wang et al., 2006a; Yang X. et al., 2007), the grassland has been severely degraded, the sandy land has intensified, and the lakes have shrunk severely, making this one of the most serious areas of desertification in northern China (Chun et al., 2018). The study area is influenced by the East Asian summer monsoon and the East Asian winter monsoon (Tada et al., 2016; Li et al., 2017). The summer has maximum temperature of 39.1°C and winter has a minimum temperature of −42.2°C. The annual average temperature is 2.3°C. The annual precipitation is around 280 mm, and is mainly concentrated in July–September. The evaporation is around 2000 mm, the annual average wind speed is 3.5 m/s, and the number of windy days reaches 45 days. QeHan West Lake completely dried up in 2002, and a large area of the lake bed is now exposed. This area is rich in sand-sourced material, and high winds occur frequently every year, making it a huge source of sand and dust.

### Method

The field data were collected on 25–26 April, 2021 in the area where strong dust storms occurred, and almost all of northern China received dust storms during this period, so our results are representative of the dust transport in this region.

### Surface sampling

We randomly selected five locations and collected surface (0–5 cm) soil samples from two types of ground surfaces before the windy day on April 25, these two surfaces were defined according to the local river recharge. The first type of surface, seasonal alternation of wetting and drying as intermittently dried surface, and the other surface far away from the center of the lake and near the lake shore, the surface always keep dried loose situation as permanently dried surface. A total of 10 samples were collected. As shown in Figure 1, on the intermittently dried surface, a significant amount of salt frosts was attached to the top of the soil crust, while the permanently dried surface was composed of loose sediments without significant salt particles. The water content, ion contents, and particle size of the surface samples were measured to provide basic data for investigating wind and sand transport in the region.

### Wind speed

The wind speed was measured five times using a three-cup anemometer at heights of 10, 30, 50, 100, and 200 cm at the two sampling sites, and the duration of each observation was up to 60 min.



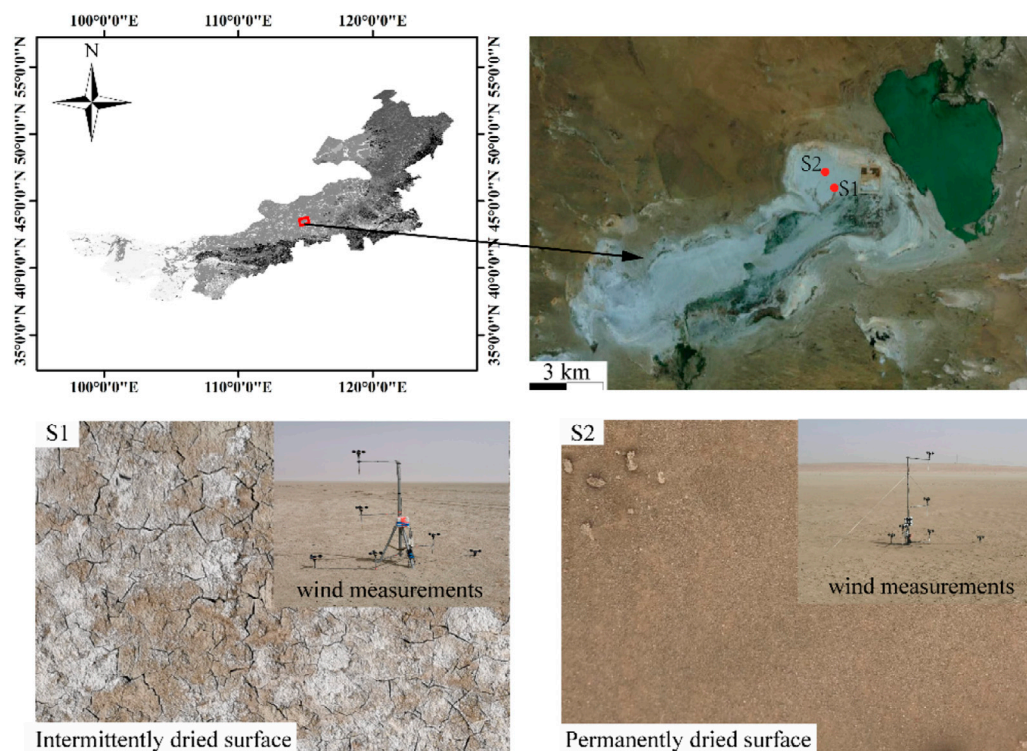


**FIGURE 1**  
Location of the study region.

## Sediment transport

To determine the sediment transport characteristics on the playa surface, we used a homemade rotatable step sediment sampler to continuously measure the sediment transport within 50 cm. The sampler collected blowing sand in 2 cm × 2 cm sections. An electronic balance with a precision of .01 g was used to weight the collected sediment, and the field measurements were conducted five times during the occurrence of a severe sandstorm on 26 April 2021. Because the intermittently dry surface contained crusts and the sediment transport was limited, we combined the sand transport during periods one and two into one, and the sand transport during periods three, four, and five into a total of two sets of transport data. Five transport datasets were collected for the permanently dry surface.

## Particle size and ion determination

We analyzed the particle size distribution and salt content of the collected sediments at the Key Laboratory of the State Forestry and Grassland Administration for the Conservation and Restoration of Desert Ecosystems, Inner Mongolia Agricultural University, using a German Flying laser grain size meter and a Swiss Aptar 930 ion chromatograph. One surface sample was collected from each site, and the samples collected at a height of 50 cm were analyzed. We classified the particle size into five classes: PM10 (<10 μm), clay and silt (<63 μm), very fine sand (63–125 μm), fine sand (125–250 μm) and

sand (>250 μm); we analyzed the contents of 10 soluble salt ions: Li<sup>+</sup>, Na<sup>+</sup>, Mg<sup>2+</sup>, K<sup>+</sup>, Ca<sup>2+</sup>, F<sup>-</sup>, Cl<sup>-</sup>, NO<sub>3</sub><sup>-</sup>, PO<sub>4</sub><sup>2-</sup>, and SO<sub>4</sub><sup>2-</sup>.

## Data processing

The vertical profile of  $u_z$ , the horizontal wind velocity (m/s) at height  $z$  (cm), can be described by the law of the wall (Zhang et al., 2017):

$$u_z = \frac{u^*}{K} \ln \frac{z}{z_0} \quad (1)$$

$$u_z = a + b \ln Z \quad (2)$$

$$z_0 = \exp(-a/b) \quad (3)$$

$$u^* = Kb \quad (4)$$

where  $u_z$  is the velocity at height  $z$  (m/s);  $K$  is the von Karman's constant (.4);  $z$  is the measurement height (cm);  $a$  and  $b$  are regression coefficients;  $u^*$  is the shear velocity (m/s); and  $z_0$  is the aerodynamic roughness (cm).

Mathematical models of the horizontal sediment flux were used to reflect the sand transport fluxes from the different surfaces. These models mainly focused on linear functions, exponential functions.

$$Q_T = \sum_{i=2}^{50} q_z \quad (5)$$

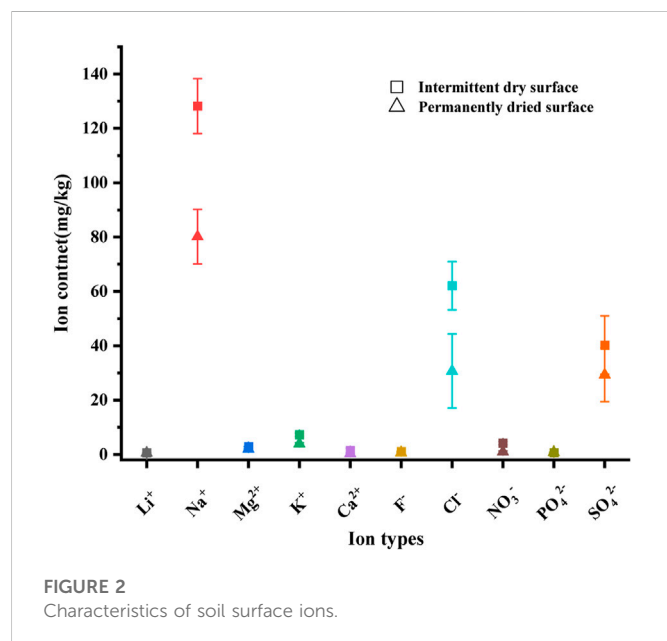
$$Q = az + b \quad (6)$$

$$Q = ae^{-bz} \quad (7)$$



TABLE 1 Characteristics of surface soil grain size distribution and moisture content.

Surface type	Grain size content (%)					Soil moisture (%)	pH
	<10 $\mu\text{m}$	10–63 $\mu\text{m}$	63–125 $\mu\text{m}$	125–250 $\mu\text{m}$	>250 $\mu\text{m}$		
Intermittent dry surface	70.24 $\pm$ 8.11	29.76 $\pm$ 6.55	—	—	—	.32 $\pm$ .1	8.83 $\pm$ .04
Permanently dried surface	80.13 $\pm$ 7.29	15.03 $\pm$ 3.21	.05 $\pm$ .07	2.55 $\pm$ 2.23	2.24 $\pm$ 1.49	.29 $\pm$ .07	8.80 $\pm$ .02

FIGURE 2  
Characteristics of soil surface ions.

where  $Q_T$  is the total sediment transport rate at a height of 50 cm;  $q_z$  is the sediment transport at height  $z$  in sediment collection chamber  $i$ .  $Q$  is the amount of sand transported in a certain height layer ( $\text{g}/\text{cm}^2 \text{min}^{-1}$ );  $z$  is the height (cm);  $a$  and  $b$  are the wind and sand circulation coefficients.

## Result

### Characteristics of surface soil

The surface characteristics of the two soils are presented in Table 1 and Figure 2. The intermittently dry surface was entirely composed of clay and chalk, and the permanently dry surface contained a small proportion of sand and gravel. The soil moisture content of the intermittently dry surface was slightly higher. The ions on both surfaces were mainly  $\text{Na}^+$ ,  $\text{Cl}^-$ , and  $\text{SO}_4^{2-}$ , and the contents of the other ions were low. The contents of all of the ions were greater on the intermittently dried surface than on the permanently dried surface (Liu et al., 2010).

### Wind velocity during the field measurement periods

The surface characteristics affect the near-surface wind speed and also dust emissions, and the wind speed profiles in the study area all conform to a log-linear function ( $R^2 > .95$ ), and all these measurements in Figure 3 were performed during sediment

transport events (i.e., sediment was being transported during the time of the measurements of  $u^*$ ) (Table 2). The roughness of the intermittently dried surfaces was calculated as .05–.07 cm, and it was only slightly affected by wind speed changes. The roughness of the permanently dried surfaces was .06–.37 cm and changed with the wind speed. Similarly, the friction velocity of the intermittently dried surface was .60–1.16 m/s, which was greater than that of the intermittently dried surfaces. The friction velocity increased with increasing wind speed from both types of surfaces. This indicates that the intermittent dried surface was more prone to wind erosion.

### Horizontal sediment flux at different heights

The vertical distribution of the horizontal fluxes of the sediment from the intermittently dry and permanently dry surfaces at different wind speeds differed significantly (Figure 4). The measured dust fluxes from the permanently dry surfaces were 6.62–18.64 times higher than those from the intermittently dry surface (Figure 4A). Less dust was emitted from the intermittent drying surface in a lower height range, and it varied little with height. The dust transport varied linearly with wind speed for the intermittently dried surface ( $R^2 > .92$ ), while the dust emission from the permanently dried surface decreases varied significantly and exponentially with height at different wind speeds ( $R^2 > .91$ ) (Figure 4B; Table 2). This indicates that the erodible surface particle supply was an important factor controlling the horizontal dust flux at different heights, and the permanently dried surface provide more dust during salt dust storms.

### Grain size frequency of aeolian sediment

Figure 5 shows the distribution characteristics of the sediments at different heights for both surfaces in the field. The frequency curves of the sediments were multi-peaked during the dust storms, and the particle size characteristics of both surfaces did not vary significantly with height. The main particles transported from the intermittently dried surface were clay <10  $\mu\text{m}$  (49.93%–74.52%), followed by gravel >250  $\mu\text{m}$  (mean of 22.56%) (Figure 5A), and the main particles transported from the permanently dried surface sediments were clay <10  $\mu\text{m}$  (72.87%–87.83%), followed by 10–63  $\mu\text{m}$  powder particles (mean of 15.61%) (Figure 5B). This indicates that the particles released from the intermittently dried surface were more dispersed and coarser than those released from the permanently dried surface. This means that the unstable secondary particles produced by the aggregation of fine salt particles were easily polished and decomposed during wind-blown sand activity and more suspended particles (<63  $\mu\text{m}$ ) were released.

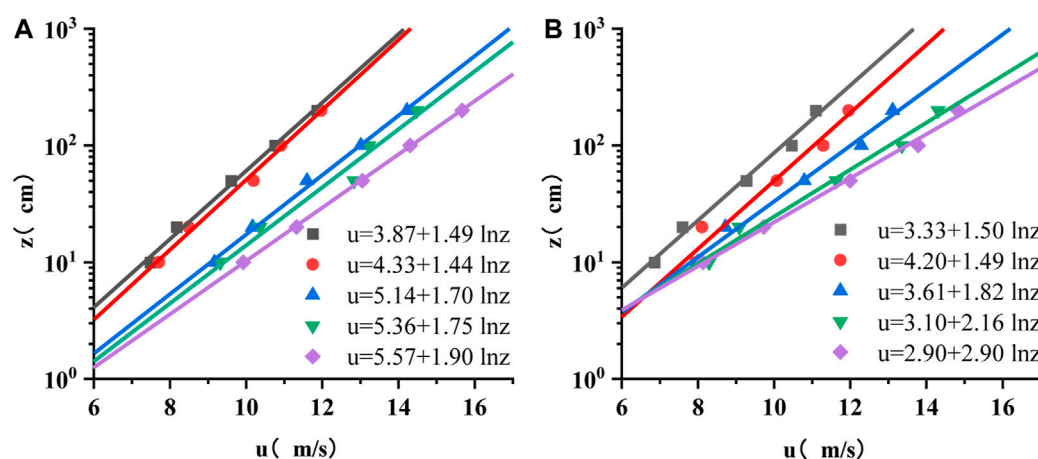


FIGURE 3

Five field observations of wind speed profiles on two types of surfaces,  $R^2 > .95$ ,  $p < .05$ .

TABLE 2 Aerodynamic roughness length ( $z_0$ , cm), calculated shear velocity ( $u^*$ , m/s), and total transport rate ( $Q_T$ ) at the two field measurement sites.

Sites	Wind speed (m/s) at 2 m	$z_0$ (cm)	$u^*$ (m/s)	$Q_T$ (g/cm <sup>2</sup> ·min)	Sediment model
Intermittent dry surface	11.86	.07	.60	1.13	$Q = -.0004 z_0 + .01113$
	11.97	.05	.58		
	14.22	.05	.68	2.30	$Q = -.0004 z_0 + .0189$
	14.48	.05	.70		
	15.67	.05	.76		
Permanent dry surface	11.09	.11	.60	2.98	$Q = .5927e^{-.223z_0}$
	11.96	.06	.60	4.49	$Q = .8374e^{-.22z_0}$
	13.11	.14	.73	7.04	$Q = 1.2157e^{-.181z_0}$
	14.31	.24	.86	17.74	$Q = 2.3025e^{-.135z_0}$
	14.82	.37	1.16	18.07	$Q = 2.719e^{-0.173z_0}$

## Salt content of sediments

The water-soluble salt ions in the sediment transported from the two types of surfaces were emitted at different horizontal heights (Figure 6). The ions contained in the horizontal transport flux of the surface sediments in the study area were mainly  $\text{Na}^+$ ,  $\text{Cl}^-$ , and  $\text{SO}_4^{2-}$ , and the contents of the water-soluble ions such as  $\text{Li}^+$ ,  $\text{Mg}^{2+}$ ,  $\text{K}^+$ ,  $\text{Ca}^{2+}$ ,  $\text{F}^-$ ,  $\text{NO}_3^-$ , and  $\text{PO}_4^{2-}$  were much lower than those of the above three ions. By comparing the sediment ion transport fluxes from the two surfaces, we found that the ion contents, as well as the total salinity, of the sediment released from the intermittently dried surface, were greater than that of the sediment released from the permanently dried surface at almost all height. The ion contents from the intermittently dried surface initially increased and then decreased (Figure 6A) within the measurable height (16 cm), and the highest salt content (182.93 mg/kg) was measured at a height of 10 cm. The ion contents from the permanently dried surface (Figure 6B) initially decreased within a height of 14 cm, increased from 14 to 22 cm, and decreased from 22 to 33 cm, and the maximum salt content was

152 mg/kg. This indicates that the horizontal sediment released from the intermittently dried surface contained a high concentration of salts and that the soluble salt particles were released before the soil particles during the drying process.

## Discussion

### Friction threshold velocity of surface characteristics

The physical characteristics of the surface, texture, and structure and the presence of undisturbed crust at the test site have a strong influence on both the friction velocity and roughness (Van Pelt et al., 2020). The friction velocity is generally considered to be the dominant factor controlling the horizontal deposition fluxes during wind erosion events and is generally influenced by surface roughness, soil moisture, soil particle size, and crusting (Buyantogtokh et al., 2021). In this study, we found that the frictional velocity and roughness of the

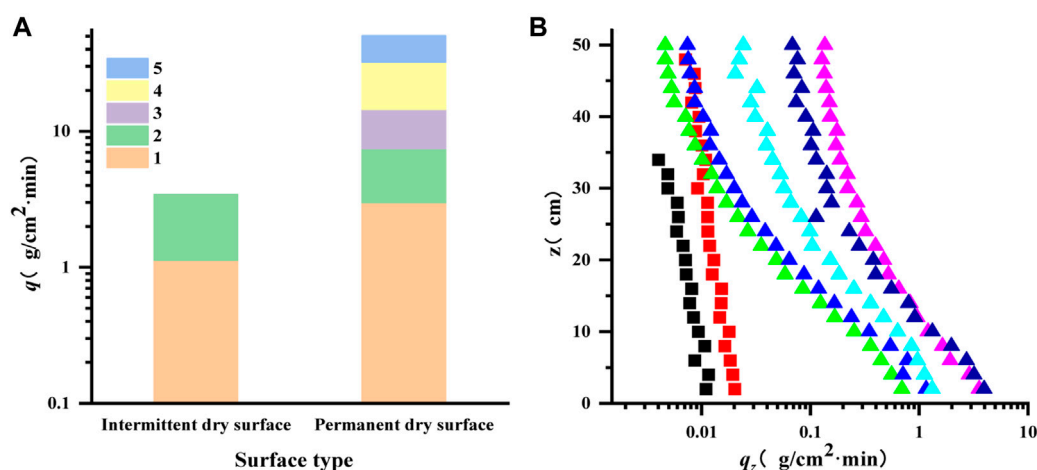


FIGURE 4

Horizontal sediment flux at different heights, (B) The squares represent salt dust emissions from the intermittently surface at wind speeds and the triangles represent salt dust emissions at five wind speeds.

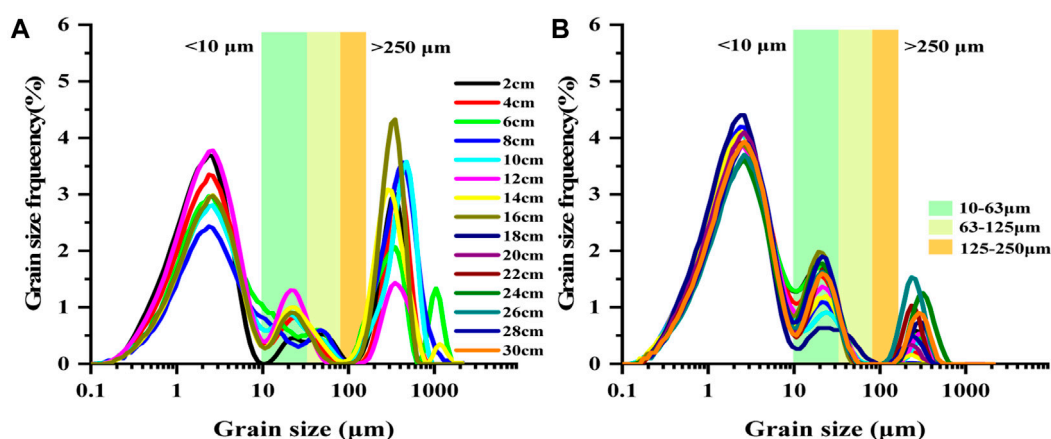


FIGURE 5

Grain size frequency of aeolian sediment on two surfaces.

intermittently dried surface (crusted) were smaller than those of the permanently dried (activated) surface, which is inconsistent with the common finding that crusting can increase the surface roughness and the frictional threshold velocity (Webb et al., 2016). We speculate that this inconsistency is related to the salt material on the surface, which was composed of sulfate, chloride, and sodium salts that formed a loose (McCord et al., 2001; Nield et al., 2016) and a fluffy thin layer of crust. These relatively low mass salt particles were more susceptible to wind erosion. When the loose particles on the surface were blown away, a relatively hard surface crust remained (Bu et al., 2015), so the friction velocity and roughness of the intermittently dried surface were smaller. The friction velocity and roughness are important factors controlling the horizontal sediment flux (Sankey et al., 2009; Baddock et al., 2011), but their importance varies in different systems (Webb et al., 2016). On the intermittently dried surface, there was a limited supply of salt dust, so the friction velocity and roughness played a secondary role in determining horizontal sediment flux (O'Brien and

McKenna Neuman, 2012). The sediment flux can be increased by interference (Baddock et al., 2011), and changes in the size of sediment particles on the soil surface affect the friction velocity and roughness (Tegen et al., 2002).

## Characteristics of surface dust emission

Grain size has a strong influence on dust emission and transport (Zhang et al., 2022). Particle removal from the surface and transport is influenced by surface wind forces and properties (Zobeck et al., 2013; Cheng et al., 2017). Finer soil particles generally either remain suspended in the air or are carried further away (Mahmoodabadi and Ahmadbeigi, 2012), while coarser particles remain on the soil surface (Mahmoodabadi and Cerdà, 2013). Based on analyzed of both the surface particles and the transported sediment particles, we found that the >250 μm particles collected from the intermittently dried land

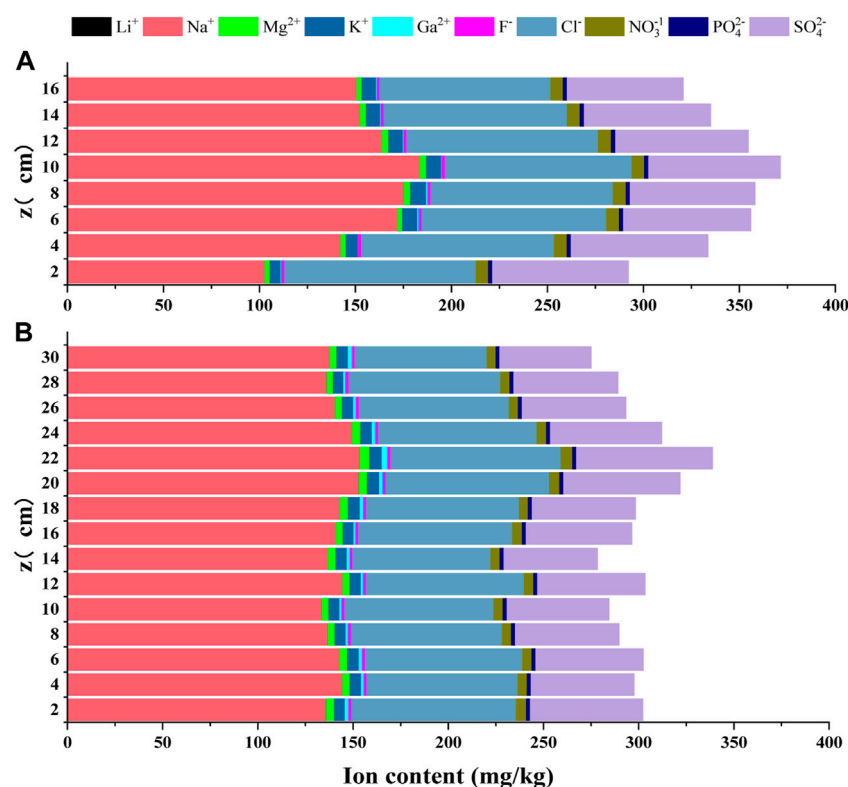


**FIGURE 6**  
Vertical horizontal ion flux of sediment.

surface were not found in the surface sampling, so they must have come from the transit airflow. (Kok et al., 2012). showed that 63–500  $\mu\text{m}$  particles move in a transigratory manner at the surface, and this movement is extremely destructive to the surface, Sand-carrying winds carry gravel, causing the initial release of the fragile salt aggregates from the surface by polishing the crust surface. The limited supply of dust in the sand-carrying winds cause coarsening of the particles, but for the permanently dry surface, where the dust supply is sufficient, the effect of such limited particles on the dust coarsening is not significant. Alternatively, some of the larger particles in the sand-carrying winds produce a higher effective recovery factor on the rigid bed surface due to collision with the surface, and these particles can reach higher heights, whereas the permanently dried surface (loose particles) weakens kinetic energy and was converted to release of smaller particles to higher heights, so that there was no gravel on the intermittently dried surface and large particles are found in sediment transport, whereas permanently dried surface dust has fewer large particles (Kamath and Parteli, 2021).

The difference in the salt and dust emissions from the two surfaces clearly indicates that intermittently dried surfaces have limited material available for wind erosion due to the presence of crusts, greatly reducing the sediment carryover and thus weakening the intensity of the wind erosion and dust storms (Zhang et al., 2016). The functional relationship in the dust emission model of incompletely erodible bed (intermittently dried surface) was a linear function, and the slope is the same at different wind speeds, so that the flux of sediment was in a stable state, and the dust emission of completely erodible bed (permanently dried surface) was

exponential model. This was consistent with Sandesh Kamath's (Kamath et al., 2022) numerical simulation results and experimental conclusions. The number of sand available on the ground has a great influence on the dust flux (Kamath and Parteli, 2021). However, we found that the sediments released from the intermittently dry surfaces had higher salt concentrations than those released from the permanently dried surface, which corresponds to the salt concentrations of both surfaces. Evaporation is the main factor affecting the mineral composition of the surface in arid and semi-arid regions, and continuous dryness and wetness lead to the formation of mineral surfaces that are unstable and continuous dryness and wetness lead to the formation of mineral surfaces that are unstable and are changed by wind and precipitation, varying at different times and in different regions (Liu et al., 2010). Evaporation transports the solution to the soil surface. As water evaporates, ions remain on the surface and crystallize when the ion concentration was saturated (Dai et al., 2015; Altausen et al., 2019) where salt-rich surface was formed, and the frequency of intermittently dried surface water transport was higher than that of the permanently dried surface, so the surface salt concentration was higher. In general wind erosion mainly cause salt dispersion from the crustal surface (Dai et al., 2022); however, wind erosion and salt accumulation occur simultaneously, especially on intermittently dried surfaces, where water-soluble ions continuously replenish the salt loss due to wind erosion through epilimnion aggregation, providing an inexhaustible source for salt dust storms (Liu et al., 2010; Motaghi et al., 2020), so, the concentration of salt dust collected on intermittently dried surface was higher. We measured the salt

concentration in the dust from the intermittently dried surface of 2.67%–5.25%. The results of the permanently dried surface releasing salt dust concentration of .03%–2% were similar to the results measured in the Wang wind tunnel (Wang et al., 2012a). Although intermittently dried surfaces continuously release high concentrations of salt dust, their salt dust emissions are only 5%–15% of those from permanently dried surfaces; thus, priority should be given to protecting permanently dried surfaces during the windy season to reduce dust emissions.

## Conclusion

Our results confirm that the characteristics and mechanisms of surface sediment transport are different during the different phases of playa surface drying, which is crucial because lakes are important landscapes in northern China. Previous studies have shown that the Gobi Desert is an important source of dust in northern China, and our results confirm that dry lakes are also major sources of dust, thus filling the previous knowledge gap. The main conclusions of this study are as follows.

1. The wind speed curve of the playa surface during the dust storm can be expressed as a logarithmic linear function. The friction velocity of the intermittently dried crust surface was .58–.76 m/s, and the aerodynamic roughness was .05–.07 cm. The friction velocity of the permanently dried surface was .6–1.16 m/s, and the aerodynamic roughness was .06–.37 cm. The fragile salt crust on the intermittently dried surface was more prone to wind erosion than the permanently dried surface.
2. During the observation period, the two sediment transport fluxes from the intermittently dried surface were 1.13 g/cm<sup>2</sup>·min and 2.3 g/cm<sup>2</sup>·min, respectively, and the sediment transport flux conformed to a linear function. The sediment transport fluxes from the permanently dried surface were 7.47 g/cm<sup>2</sup>·min and 42.86 g/cm<sup>2</sup>·min, respectively, and the sediment transport flux conformed to an exponential function. The salt dust released from the permanently dried surface was 6.62–18.64 times greater than that released from the intermittently dried surface.
3. The sand-carrying wind had a great influence on the salt particles released from the intermittently dried surface, but it had little effect on the soil particles released from the permanently dried surface. Although the two types of surface sediment particles were mainly <63 μm, accounting for about 71.45%–96.02%, the salt dust particles released from the permanently dried surface were finer. The salt ions were mainly Na<sup>+</sup>, Cl<sup>−</sup>, and SO<sub>4</sub><sup>2−</sup>, and the concentrations of salt dust released from the intermittently surface were higher than those of the permanently dry surface.

## References

- Abuduwalli, J., Liu, D., and Wu, G. (2010). Saline dust storms and their ecological impacts in arid regions. *J. Arid Land* 2, 144–150. doi:10.3724/sp.j.1227.2010.00144
- Altausen, D., Ge, Y., Abuduwalli, J., Ma, L., Abdullaev, S., and Hofer, J. (2019). Lakes in arid land and saline dust storms. *E3S Web Conf.* 99, 01007. doi:10.1051/e3sconf/20199901007
- Baddock, M. C., Zobeck, T. M., Van Pelt, R. S., and Fredrickson, E. L. (2011). Dust emissions from undisturbed and disturbed, crusted playa surfaces: Cattle trampling effects. *Aeolian Res.* 3, 31–41. doi:10.1016/j.aeolia.2011.03.007
- Bowen, M. W., and Johnson, W. C. (2015). Holocene records of environmental change in High Plains playa wetlands, Kansas, US. *Holocene* 25, 1838–1851. doi:10.1177/0959683615591356
- Bu, C., Zhao, Y., Hill, R. L., Zhao, C., Yang, Y., Zhang, P., et al. (2015). Wind erosion prevention characteristics and key influencing factors of bryophytic soil crusts. *Plant Soil* 397, 163–174. doi:10.1007/s11104-015-2609-z
- Buyantogtokh, B., Kurosaki, Y., Tsunekawa, A., Tsubo, M., Gantsetseg, B., Davaadorj, A., et al. (2021). Effect of stones on the sand saltation threshold during natural sand and

Our results showed that the transport rate and salt concentration of weathered sediments on the surface of a playa were very high, especially under strong wind conditions. Due to the limited height of our sand sampler, if particles were collected at a higher height, we believe that a better explanation for the emission of surface dust particles and the salt concentration could be obtained.

## Data availability statement

The original contributions presented in the study are included in the article/supplementary material, further inquiries can be directed to the corresponding author.

## Author contributions

SQ: Conceptualization, methodology, writing original draft; XR: Writing–review and editing; XD reviewed and revised the manuscript; ZM: Conceptualization, supervision, project administration.

## Funding

This research was supported by the National Natural Science Foundation of China (42067015), and the Natural Science Foundation of Inner Mongolia Autonomous Region (2020MS03038), Desert Ecosystem Conservation and Restoration Innovation Team, and Improvement Innovation Team of Desertification Control (BR22-13-03).

## Conflict of interest

The authors declare that the research was conducted in the absence of any commercial or financial relationships that could be construed as a potential conflict of interest.

## Publisher's note

All claims expressed in this article are solely those of the authors and do not necessarily represent those of their affiliated organizations, or those of the publisher, the editors and the reviewers. Any product that may be evaluated in this article, or claim that may be made by its manufacturer, is not guaranteed or endorsed by the publisher.



- dust storms in a stony desert in Tsogt-Ovoo in the Gobi Desert, Mongolia. *J. Arid Land* 13, 653–673. doi:10.1007/s40333-021-0072-7
- Cheng, H., Liu, C., Li, J., Zou, X., Liu, B., Kang, L., et al. (2017). Wind erosion mass variability with sand bed in a wind tunnel. *Soil Tillage Res.* 165, 181–189. doi:10.1016/j.still.2016.08.013
- Cheng, Y.-B., Dickey, H., Yimam, Y. T., Schmid, B., Paxton, B., Schreuder, M., et al. (2022). Land surface parameterization at exposed playa and desert region to support dust emissions estimates in southern California, United States. *Remote Sens.* 14, 616. doi:10.3390/rs14030616
- Chun, X., Su, R., Liu, J., Liang, W., Yong, M., and Ulambadrakh, K. (2017). Climatic implications on variations of QeHan Lake in the arid regions of Inner Mongolia during the recent five decades. *Environ. Monit. Assess.* 189, 14. doi:10.1007/s10661-016-5721-5
- Chun, X., Yong, M., Liu, J., and Liang, W. (2018). Monitoring land cover change and its dynamic mechanism on the QeHan Lake basin, inner Mongolia, North China, during 1977–2013. *Environ. Monit. Assess.* 190, 205. doi:10.1007/s10661-018-6582-x
- Collins, J. D., Gill, T. E., and Langford, R. (2018). Characterizing formation processes of Rimrock Lake, a Late Pleistocene-Holocene playa, Harney Basin, south-eastern Oregon, USA, using an end-member mixing analysis. *J. Quat. Sci.* 33, 721–737. doi:10.1002/jqs.3048
- Dai, J., Zhang, G., Liu, L., Shi, P., Zhang, H., Han, X., et al. (2022). Effects of efflorescence and subflorescence by different salts on soil physical properties and aeolian erosion. *Catena* 215, 106323. doi:10.1016/j.catena.2022.106323
- Dai, S., Shin, H., and Santamarina, J. C. (2015). Formation and development of salt crusts on soil surfaces. *Acta Geotech.* 11, 1103–1109. doi:10.1007/s11440-015-0421-9
- Derbyshire, E., Meng, X., and Kemp, R. A. (1998). Provenance, transport and characteristics of modern aeolian dust in Western Gansu Province, China, and interpretation of the Quaternary loess record. *Quat. loess Rec.* 39, 497–516. doi:10.1006/jare.1997.0369
- Gill, T. E., Gillette, D. A., Niemeyer, T., and Winn, R. T. (2002). Elemental geochemistry of wind-erodible playa sediments, Owens Lake, California. *Owens Lake, Calif.* 189, 209–213. doi:10.1016/s0168-583x(01)01044-8
- Hao, S., and Li, F. (2021). Water sources of the typical desert vegetation in Ebinur Lake basin. *Acta Geogr. Sin.* 76, 1649–1661. doi:10.1007/s11442-022-1987-4
- Kamath, S., and Parteli, E. J. (2021). Toward a large-scale particle-based parallel simulator of Aeolian sand transport, including a model for mobile sand availability. *EPJ Web Conf.* 249, 13004. doi:10.1051/epjconf/202124913004
- Kamath, S., Shao, Y., and Parteli, E. J. R. (2022). Scaling laws in aeolian sand transport under low sand availability. *Geophys. Res. Lett.* 49, e2022GL097767. doi:10.1029/2022gl097767
- Kok, J. F., Parteli, E. J., Michaels, T. I., and Karam, D. B. (2012). The physics of wind-blown sand and dust. *Rep. Prog. Phys.* 75, 106901. doi:10.1088/0034-4885/75/10/106901
- Lee, J. A., Baddock, M. C., Mbu, M. J., and Gill, T. E. (2012). Geomorphic and land cover characteristics of aeolian dust sources in West Texas and eastern New Mexico, USA. *Aeolian Res.* 3, 459–466. doi:10.1016/j.aeolia.2011.08.001
- Li, X., Cheng, H., Tan, L., Ban, F., Sinha, A., Duan, W., et al. (2017). The East Asian summer monsoon variability over the last 145 years inferred from the Shihua Cave record, North China. *Sci. Rep.* 7, 7078. doi:10.1038/s41598-017-07251-3
- Liu, B., Wang, Z., Niu, B., and Qu, J. (2021). Large scale sand saltation over hard surface: A controlled experiment in still air. *J. Arid Land* 13, 599–611. doi:10.1007/s40333-021-0104-3
- Liu, D., Abuduwaili, J., Lei, J., Wu, G., and Gui, D. (2010). Wind erosion of saline playa sediments and its ecological effects in Ebinur Lake, Xinjiang, China. *Environ. Earth Sci.* 63, 241–250. doi:10.1007/s12665-010-0690-4
- Mahmoodabadi, M., and Ahmadbeigi, B. (2012). Dry and water-stable aggregates in different cultivation systems of arid region soils. *Arabian J. Geosciences* 6, 2997–3002. doi:10.1007/s12517-012-0566-x
- Mahmoodabadi, M., and Cerdà, A. (2013). WEPP calibration for improved predictions of interrill erosion in semi-arid to arid environments. *Geoderma* 204–205, 75–83. doi:10.1016/j.geoderma.2013.04.013
- Mahowald, N. M., Muhs, D. R., Levis, S., Rasch, P. J., Yoshioka, M., Zender, C. S., et al. (2006). Change in atmospheric mineral aerosols in response to climate: Last glacial period, preindustrial, modern, and doubled carbon dioxide climates. *J. Geophys. Res. Atmos.* 111. doi:10.1029/2005jd006653
- Mccord, T. B., Orlando, T. M., Teeter, G., Hansen, G. B., Sieger, M. T., Petrik, N. G., et al. (2001). Thermal and radiation stability of the hydrated salt minerals epsomite, mirabilite, and natron under Europa environmental conditions. *J. Geophys. Res. Planets* 106, 3311–3319.
- Meng, Z., Dang, X., Gao, Y., Ren, X., Ding, Y., and Wang, M. (2018). Interactive effects of wind speed, vegetation coverage and soil moisture in controlling wind erosion in a temperate desert steppe, Inner Mongolia of China. *J. Arid Land* 10, 534–547.
- Motaghi, F. A., Hamzehpour, N., Abasiyan, S. M. A., and Rahmati, M. (2020). The wind erodibility in the newly emerged surfaces of Urmia Playa Lake and adjacent agricultural lands and its determining factors. *Catena* 194, 104675. doi:10.1016/j.catena.2020.104675
- Nield, J. M., Mckenna Neuman, C., O'Brien, P., Bryant, R. G., and Wiggs, G. F. S. (2016). Evaporative sodium salt crust development and its wind tunnel derived transport dynamics under variable climatic conditions. *Aeolian Res.* 23, 51–62. doi:10.1016/j.aeolia.2016.09.003
- Niu, S. L., Jiang, G. M., Wan, S. Q., Liu, M. Z., Gao, L. M., and Li, Y. G. (2005). Ecophysiological acclimation to different soil moistures in plants from a semi-arid sandland. *J. Arid Environ.* 63, 353–365. doi:10.1016/j.jaridenv.2005.03.017
- O'Brien, P., and Mckenna Neuman, C. (2012). A wind tunnel study of particle kinematics during crust rupture and erosion. *Geomorphology* 173–174, 149–160. doi:10.1016/j.geomorph.2012.06.005
- Prospero, J. M., Ginoux, P., Torres, O., Nicholson, S. E., and Gill, T. E. (2002). Environmental characterization of global sources of atmospheric soil dust identified with the nimbus 7 total ozone mapping spectrometer (toms) absorbing aerosol product. *Rev. Geophys.* 40, 2–1–2–31231. doi:10.1029/2000rg000095
- Sankey, J. B., Germino, M. J., and Glenn, N. F. (2009). Relationships of post-fire aeolian transport to soil and atmospheric conditions. *Aeolian Res.* 1, 75–85. doi:10.1016/j.aeolia.2009.07.002
- Shahabinejad, N., Mahmoodabadi, M., Jalalian, A., and Chavoshi, E. (2019). The fractionation of soil aggregates associated with primary particles influencing wind erosion rates in arid to semiarid environments. *Geoderma* 356, 113936. doi:10.1016/j.geoderma.2019.113936
- Shao, Y., Wyrwoll, K.-H., Chappell, A., Huang, J., Lin, Z., Mctainsh, G. H., et al. (2011). Dust cycle: An emerging core theme in Earth system science. *Aeolian Res.* 2, 181–204. doi:10.1016/j.aeolia.2011.02.001
- Stout, J. E., Warren, A., and Gill, T. E. (2009). Publication trends in aeolian research: An analysis of the Bibliography of Aeolian Research. *Geomorphology* 105, 6–17. doi:10.1016/j.geomorph.2008.02.015
- Sweeney, M. R., Zlotnik, V. A., Joeckel, R. M., and Stout, J. E. (2016). Geomorphic and hydrologic controls of dust emissions during drought from Yellow Lake playa, West Texas, USA. *J. Arid Environ.* 133, 37–46. doi:10.1016/j.jaridenv.2016.05.007
- Tada, R., Zheng, H. B., and Clift, P. D. (2016). Evolution and variability of the Asian monsoon and its potential linkage with uplift of the Himalaya and Tibetan Plateau. *Prog. Earth Planet. Sci.* 3, 4. doi:10.1186/s40645-016-0080-y
- Tao, S., Fang, J., Ma, S., Cai, Q., Xiong, X., Tian, D., et al. (2020). Changes in China's lakes: Climate and human impacts. *Natl. Sci. Rev.* 7, 132–140. doi:10.1093/nsr/nwz103
- Tegen, I., Harrison, S. P., Kohfeld, K., Prentice, I. C., Coe, M., and Heimann, M. (2002). Impact of vegetation and preferential source areas on global dust aerosol: Results from a model study. *J. Geophys. Res. Atmos.* 107, AAC 14–21. doi:10.1029/2001jd000963
- Van Pelt, R. S., Tatarko, J., Gill, T. E., Chang, C., Li, J., Eibedingil, I. G., et al. (2020). Dust emission source characterization for visibility hazard assessment on Lordsburg Playa in Southwestern New Mexico, USA. *Geoenvironmental Disasters* 7, 34. doi:10.1186/s40677-020-00171-x
- Varga, G. J. H. G. B. (2012). Spatio-temporal distribution of dust storms-a global coverage using. *NASA TOMS aerosol Meas.* 61, 275.
- Varga, G., Ujvari, G., and Kovacs, J. (2014). Spatiotemporal patterns of saharan dust outbreaks in the mediterranean basin. *Aeolian Res.* 15, 151–160. doi:10.1016/j.aeolia.2014.06.005
- Von Holdt, J., Eckardt, F., and Wiggs, G. (2017). Landsat identifies aeolian dust emission dynamics at the landform scale. *Remote Sens. Environ.* 198, 229–243. doi:10.1016/j.rse.2017.06.010
- Wang, X., Chen, F., and Dong, Z. (2006a). The relative role of climatic and human factors in desertification in semiarid China. *Glob. Environ. Change* 16, 48–57. doi:10.1016/j.gloenvcha.2005.06.006
- Wang, X., Hua, T., Zhang, C., Lang, L., and Wang, H. (2012a). Aeolian salts in Gobi deserts of the Western region of Inner Mongolia: Gone with the dust aerosols. *Atmos. Res.* 118, 1–9. doi:10.1016/j.atmosres.2012.06.003
- Wang, X., Hua, T., Zhang, C., Qian, G., and Luo, W. (2012b). Salts in the clay playas of China's arid regions: Gone with the wind. *Environ. Earth Sci.* 68, 623–631. doi:10.1007/s12665-012-1765-1
- Wang, X., Xia, D., Wang, T., Xue, X., and Li, J. (2008). Dust sources in arid and semiarid China and southern Mongolia: Impacts of geomorphological setting and surface materials. *Geomorphology* 97, 583–600. doi:10.1016/j.geomorph.2007.09.006

- Wang, X., Zhou, Z., and Dong, Z. (2006b). Control of dust emissions by geomorphic conditions, wind environments and land use in northern China: An examination based on dust storm frequency from 1960 to 2003. *Geomorphology* 81, 292–308. doi:10.1016/j.geomorph.2006.04.015
- Webb, N. P., Galloza, M. S., Zobeck, T. M., and Herrick, J. E. (2016). Threshold wind velocity dynamics as a driver of aeolian sediment mass flux. *Aeolian Res.* 20, 45–58. doi:10.1016/j.aeolia.2015.11.006
- Yang, L.-R., Yue, L.-P., and Li, Z.-P. (2007a). The influence of dry lakebeds, degraded sandy grasslands and abandoned farmland in the arid inlands of northern China on the grain size distribution of East Asian aeolian dust. *Environ. Geol.* 53, 1767–1775. doi:10.1007/s00254-007-0782-y
- Yang, X., Ding, Z., Fan, X., Zhou, Z., and Ma, N. (2007b). Processes and mechanisms of desertification in northern China during the last 30 years, with a special reference to the Hunshandake Sandy Land, eastern Inner Mongolia. *Catena* 71, 2–12. doi:10.1016/j.catena.2006.10.002
- Zhang, Z., Dong, Z., Li, J., Qian, G., and Jiang, C. (2016). Implications of surface properties for dust emission from gravel deserts (gobis) in the Hexi Corridor. *Geoderma* 268, 69–77. doi:10.1016/j.geoderma.2016.01.011
- Zhang, Z., Dong, Z., and Wu, G. (2017). Field observations of sand transport over the crest of a transverse dune in northwestern China Tengger Desert. *Soil Tillage Res.* 166, 67–75. doi:10.1016/j.still.2016.10.010
- Zhang, Z., Zhang, Y., and Pan, K. (2022). Characteristics of Aeolian sediments transported above a gobi surface. Characteristics of Aeolian sediments transported above a gobi surface. *Atmos. Chem. Phys.* doi:10.5194/acp-2022-485
- Ziyadeh, A., Karimi, A., Hirmas, D. R., Kehl, M., Lakzian, A., Khademi, H., et al. (2018). Spatial and temporal variations of airborne dust fallout in Khorasan Razavi Province, Northeastern Iran. *Geoderma* 326, 42–55. doi:10.1016/j.geoderma.2018.04.010
- Zobeck, T. M., Baddock, M., Scott Van Pelt, R., Tatarko, J., and Acosta-Martinez, V. (2013). Soil property effects on wind erosion of organic soils. *Aeolian Res.* 10, 43–51. doi:10.1016/j.aeolia.2012.10.005



## OPEN ACCESS

EDITED BY  
Kaibo Wang,  
Institute of Earth Environment (CAS), China

REVIEWED BY  
Xingyi Zhang,  
Key Laboratory of Mollisols Agroecology,  
Northeast Institute of Geography and  
Agroecology (CAS), China  
Mikhail Komissarov,  
Institute of Biology, UFA Federal Research  
Centre (RAS), Russia

\*CORRESPONDENCE  
Huibo Shen,  
✉ shenhuibo@163.com

SPECIALTY SECTION  
This article was submitted to  
Soil Processes,  
a section of the journal  
Frontiers in Environmental Science

RECEIVED 19 December 2022  
ACCEPTED 19 January 2023  
PUBLISHED 20 February 2023

CITATION  
Wang Y, Xu Y, Yang H, Shen H, Zhao L,  
Zhu B, Wang J and Guo L (2023), Effect of  
slope shape on soil aggregate stability of  
slope farmland in black soil region.  
*Front. Environ. Sci.* 11:1127043.  
doi: 10.3389/fenvs.2023.1127043

COPYRIGHT  
© 2023 Wang, Xu, Yang, Shen, Zhao, Zhu,  
Wang and Guo. This is an open-access  
article distributed under the terms of the  
[Creative Commons Attribution License](#)  
(CC BY). The use, distribution or  
reproduction in other forums is permitted,  
provided the original author(s) and the  
copyright owner(s) are credited and that  
the original publication in this journal is  
cited, in accordance with accepted  
academic practice. No use, distribution or  
reproduction is permitted which does not  
comply with these terms.

# Effect of slope shape on soil aggregate stability of slope farmland in black soil region

Yuxian Wang<sup>1</sup>, Yingying Xu<sup>1</sup>, Huiying Yang<sup>1</sup>, Huibo Shen<sup>1\*</sup>, Lei Zhao<sup>1</sup>,  
Baoguo Zhu<sup>2</sup>, Jiangxu Wang<sup>3</sup> and Lifeng Guo<sup>4</sup>

<sup>1</sup>Qiqihar Branch of Heilongjiang Academy of Agricultural Sciences, Qiqihar, China, <sup>2</sup>Jiamusi Branch, Heilongjiang Academy of Agricultural Sciences, Jiamusi, China, <sup>3</sup>Heilongjiang Academy of Agricultural Sciences, Harbin, China, <sup>4</sup>Heilongjiang Province Institute of Meteorological Science, Harbin, China

Slope erosion in the black soil region of Northeast China is complex and specific. In order to effectively control soil erosion and protect scarce black soil resources, it is necessary to reveal the law of soil erosion and the influence of basic units of soil structure on its erosion process. This paper used three treatments in the Le Bissonnais (LB) method to determine soil aggregate stability parameters and soil erodibility K values based on particle size composition. By establishing a mathematical fitting of the slope erosion rate along the slope length, it is found that the sinusoidal function fitting can better characterize the periodic law of the slope erosion rate of the long and gentle slope cultivated land in the typical black soil region. The research shows that the primary mechanism of black soil aggregate breakage is dissipation and mechanical disturbance, while the damage caused by clay expansion is the least.

## KEYWORDS

black soil, soil erosion, combined erosion, cultivated land with long gentle slope, slope length, aggregate

## 1 Introduction

Soil erosion is a significant soil degradation phenomenon that threatens the sustainable use of land productivity and, thus, food security. The problem of water and soil erosion in the Yangtze River Economic Belt, the Loess Plateau, and the black soil area in Northeast China is still severe. Among them, the phenomenon of soil and water loss in sloping farmland in the black soil region of Northeast China is particularly prominent and needs to be solved urgently (Chen et al., 2021).

Cultivated land is the fundamental guarantee for human survival and development. As an essential link in the transformation process of land resource utilization, nature has become the focus of the current human population, resources, and environmental issues (van den Bergh et al., 1999; Bromley, 1995). The area of cultivated land in the black soil region of Northeast China is about 18.5 million hectares. Sloping cultivated land is a vital cultivated land resource in the black soil region, accounting for 59.3% of the cultivated land area in the black soil region of Northeast China. It is widely distributed and has long gentle slopes. Due to its natural advantages, such as fertile soil and reasonable structure, it has become an essential agricultural soil (Rana et al., 2022), which is significant to China's food security. However, due to extensive development and utilization, high-quality cultivated land resources have been degraded, and the thickness of the black soil layer in Northeast China is decreasing year by year (Fan et al., 2004; Xu et al., 2018; Zhizhen et al., 2018). Compared with other soil erosion regions in China, the soil erosion in the black soil region of Northeast China is mainly affected by various external forces of erosion that are replaced by seasons and superimposed in space. In

addition, the ubiquitous topography of rivers and hills in the black soil area and the everyday use of farming along the ridges leading to the complexity and particularity of slope erosion in the black soil area. Therefore, it is urgent to reveal the law of soil erosion and the influence of the basic units of soil structure on its erosion process, effectively control soil erosion and protect the scarce black soil resources.

Many scholars believe that the Le Bissonnais (LB) method is more suitable for analyzing the stability of soil aggregates than other methods (Lal et al., 2000) believe that the degradation of any soil is first manifested in the destruction of the soil aggregate structure (Ojeda et al., 2008) studied the stability of calcareous soil aggregates. Many studies in China have used the LB method to study the stability of soil aggregates in iron-rich soils and hilly loess areas (Ma et al., 2022). Furthermore, discuss the stability of water-stable soil aggregates under different vegetation types in loess hilly areas, showing the applicability of the Le Bissonnais method in this soil type (An et al., 2013; Jakik et al., 2015; Wu et al., 2017).

The occurrence of slope soil erosion is accompanied by the destruction of aggregates (Roth and Eggert, 1994; Bissonnais, 1996). The breakage of soil aggregates significantly impacts the whole process of soil erosion, and the stability of aggregates is closely related to the degree of soil erosion. In particular, it significantly impacts the slope erosion process, surface runoff seepage storage and erosion resistance (Madari et al., 2005; Hu et al., 2007). Aggregate fragmentation plays an essential role in soil separation, providing primary material for raindrop splash erosion and runoff erosion, but erosion sediment is also the primary carrier of soil nutrients (Wuddivira et al., 2009; Shen et al., 2019). In addition, studies on the effects of tillage erosion, wind erosion, and most water erosion on soil aggregate fragmentation and physical and chemical properties are mainly based on surface soil (Breshears et al., 2003; Wirtz et al., 2012).

Many scholars have researched the relationship between the slope erosion process and soil aggregate stability and the mutual influence mechanism (Huang et al., 2022; Mo et al., 2022). (Fang, 2005) research shows that soil erosion mainly destroys surface macro aggregates and increases the loss rate of macro aggregates. Due to the runoff migration on the slope, the content of macro aggregates in the sedimentary area is high (Zhang et al., 2011) pointed out that the stability of surface soil aggregates along the longitudinal slope showed fluctuations, but the rules were not obvious. The variation of aggregate stability parameters along the slope length shows apparent differences caused by the different soil erosion resistance at different parts of the slope. In the erosion process of black soil, hydraulic erosion mainly destroys macroaggregates and preferentially migrates macroaggregates (Yan et al., 2008). Aggregates with a diameter >1.0 mm are less susceptible to migration. Raindrops will break up aggregates of >1.0 mm in size, and the loss characteristics will change with the loss ratio of aggregates of each size (Yang et al., 2008). The aggregates with a particle size of <1.0 mm are prone to displacement under raindrops, showing prominent enrichment characteristics.

Many scholars have researched the relationship between the slope erosion process and the stability of soil aggregates and the mutual influence mechanism. The stability of surface soil aggregates along the longitudinal slope shows fluctuations, but the law is not apparent. This study takes the soil of slope farmland in a typical black soil area as the research object. This paper uses three processing operations in the LB method to simulate heavy rain, slight rainfall, raindrop splash and

runoff disturbance, respectively. Moreover, the stability of slope cultivated land's surface and subsurface soil aggregates was measured and analyzed. Discuss the fragmentation characteristics of soil aggregates under different wet treatments, and analyze the soil aggregates of typical eroded black soil. To clarify slope soil aggregate stability distribution characteristics and its relationship with soil physical and chemical properties. The soil erodibility K value and soil organic carbon content were calculated based on the geometric particle size to clarify the variation characteristics of the leading quality factors of black soil slope cultivated land. It provides a scientific basis for revealing the dynamic change mechanism of soil erodibility and provides particular theoretical support for preventing and controlling soil and water loss in sloping farmland in black soil areas.

## 2 Materials and methods

### 2.1 The study region

The typical black soil area in Northeast China is an important agricultural production area in China. From west to east, it is divided into typical black soil sub-regions of Eastern Mongolia, Sonnen and Sanjiang, accounting for 28.5%, 63.8% and 7.7% of the typical black soil area, respectively. The reclamation period is 30–100 years. The terrain is higher in the northeast than in the southwest, and the typical terrain is full of mountains and rivers. Corn and soybeans are mainly grown. It has the remarkable characteristics of a typical compound erosion area in the world, and high-intensity rainfall in summer, autumn and early spring are prone to high-intensity soil erosion. Freezing and thawing are frequent in late autumn and early winter, followed by snowmelt erosion. The thickness of the black soil layer in China in the 1950 s was 50–80 cm, and now it is decreasing at a rate of 3–10 mm per year, down to 20–40 cm in 2000. In some severe areas, the soil parent material is exposed, and the production capacity is lost.

Keshan Farm belongs to the Qiqihar Branch of Heilongjiang Land Reclamation Bureau. It was originally a large-scale mechanical farm of the Mechanical Corps, located in Nehe City and Keshan County. Keshan Farm is located in the northern part of the typical black soil sub-region of Songnen, and belongs to the core area of the typical black soil region transitioning from the southwestern foot of the Lesser Khingan Mountains to the Songnen Plain. The geographic location is 125°07'40"–125°37'30" east longitude, 48°11'15"–48°24'07" north latitude. The altitude is between 250 and 383 m. The slope is long and gentle, and the slope of the sloping cultivated land is mostly 1°–3°, and the slope length is mostly 500–2000 m, and the longest is 4,000 m. Chuanmangang has obvious landform features. The temperate continental monsoon climate has a large temperature difference between the four seasons, the annual average temperature is 1.9°C, and the average annual precipitation is 503 mm. The precipitation from June to September accounts for 80.4% of the annual precipitation. The soil texture is silty clay with a particle composition (United States Department of Agriculture) sand, silt, and clay content of 14.2%, 40.7%, and 45.2%, respectively. The average thickness of the black soil layer is 20–40 cm, which is a typical thick-bed black soil area.

The fifth subfield of Keshan Farm was selected for reclamation for nearly 70 years, with an average slope length of about 2,200 m and a typically long and gentle slope farmland with an average slope of 1.5°



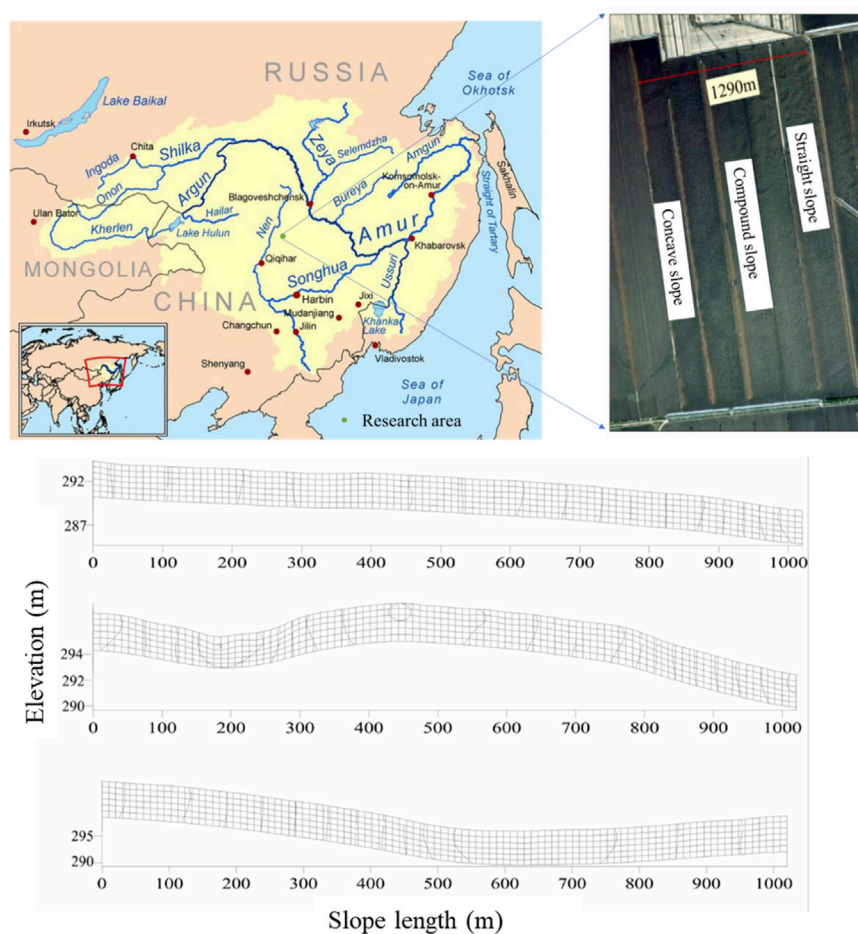


**FIGURE 1**  
Location and slope topography of the study area.

along the slope direction. Based on remote sensing images and topographical features, the cultivated land with long and gentle slopes adjacent to space was selected for an on-the-spot investigation. Straight slopes, concave slopes, and concave-straight compound slopes with the same planting history, adjacent spatial locations, and a slope length of 1,020 m were selected as the research objects (Figure 1). The slope is ridged and cultivated in rotation along the slope. The rotation crops are potatoes (*Solanum tuberosum*) and corn (*Zea mays*). The tillage direction is the same as the runoff direction, the soil is prepared in autumn, and the seeds are sown on demand in spring.

## 2.2 Method

### 2.2.1 Sampling method

Soil samples were collected in early May 2019 (before planting), after the spring thaw period. Straight slopes, concave slopes and concave-straight compound slopes were sampled every 30 m along the longitudinal section of the slope. The sampling depth is 30 cm, the sampling length is 1,020 m, and 34 sampling points are collected on each slope (Zhang et al., 2009) determined through statistical analysis of many experiments that soil samples with a distance of 0.75–5 m

between sampling points are independent. The mixed sample composed of more than five independent soil samples can represent the attributes of the sampling point, and the sampling diameter does not affect its representativeness when the diameter of the sampler is 38–86 mm. Therefore, in this study, a soil drill with a diameter of 5 cm was used to drill into the slope perpendicular to the horizontal plane to collect soil samples.

Given that the plots are adjacent in space and have the same planting history, there is no significant difference in soil thickness. The soil was collected by ring cutter to measure soil bulk density, total porosity, capillary porosity and soil moisture content. The LB method was used to determine soil water-stable aggregates' content to measure cultivated land soil quality.

### 2.2.2 Determination of aggregate stability

Determination steps of Le Bissonnais method (Guo et al., 2010a): Collect undisturbed soil samples and put them into disposable plastic boxes. After being brought back to the laboratory, the soil was gently peeled along the gaps in the natural structure of the soil into a soil mass with a diameter of about 10–12 mm, and the thick root system and stones of the plants were removed. The soil samples were sieved, and the 5–3 mm particle size was taken for testing. In order to eliminate the influence of initial water content, the prepared soil samples were



dried at 40°C for 24 h before determining aggregate stability to standardize their water content. The FW treatment simulated the disintegration of aggregates in the soil under the condition of rapid wetting (such as summer rainstorms, irrigation, etc.). It mainly reflected the dissipation mechanism of aggregate disintegration. The SW treatment reflects the disintegration of aggregates caused by soil clay swelling during slow soil wetting. WS treatment applies ethanol to wet the agglomerates. Because of the characteristics of ethanol itself and its interaction with soil, the dispersion of aggregates and the swelling of clay particles were significantly reduced, mainly reflecting the disintegration of aggregates under mechanical disturbance.

① Fast wet treatment (FW). Weigh 5–10 g of soil aggregates that have been pre-dried and passed through a 5–3 mm sieve. Pour 50 mL of deionized water into a 250 mL beaker, pour the soil sample into the beaker slowly, and immerse it in the deionized water. After standing for 10 min, remove the supernatant, and use a washing bottle filled with ethanol to gently flush the treated soil sample into a 0.05 mm sieve submerged in ethanol. Simultaneously, shake the sieve helically in ethanol five times with even force to separate the soil aggregates. Subsequently, the agglomerates on the sieve were washed into an evaporating dish and dried at 40°C for 48 h. The dried soil samples were passed through 2, 1, 0.5, 0.2, 0.1, and 0.05 mm sieves and weighed to the nearest 0.0001 g.

② slow wet treatment (SW). Samples are consistent as FW. Place the aggregates on filter paper on a 3 cm sponge pad. Control the height of the water surface to be 0.2–0.5 cm lower than the surface of the sponge, and saturate it for 60 min (the specific saturation time is determined according to the nature of the soil). Then wash it into a 0.05 mm sieve submerged in ethanol with a washing bottle filled with ethanol, and the rest of the sieving steps are the same as above.

③ Mechanical shock treatment (WS). Samples are consistent as FW. Inject 50 mL of ethanol into a beaker with a capacity of 250 mL, slowly pour the prepared soil sample into the beaker, and immerse it in ethanol. After standing for 10 min, the supernatant was removed, and the treated soil sample was transferred to a 250 mL Erlenmeyer flask with 50 mL of deionized water, and the deionized water was added to 200 mL. Subsequently, the Erlenmeyer flask was shaken ten times by inversion, and the supernatant was removed after standing for 30 min. Using a washing bottle filled with ethanol, gently wash the treated soil sample into a 0.05 mm sieve submerged in ethanol, and the rest of the steps are the same as above.

### 2.2.3 Characteristic parameters of soil aggregates

Determination of physical and chemical properties of soil: Soil bulk density, capillary porosity (ring knife method), Soil organic carbon (hydration thermal potassium dichromate sulfuric acid method) (McBride, 2022).

The mean mass diameter (MWD) and geometric mean diameter (GMD) are calculated by Eqs 1, 2 formula (Khan et al., 2022):

$$MWD = \frac{\sum_{i=1}^n \bar{x}_i w_i}{\sum_{i=1}^n w_i} \quad (1)$$

$$GMD = \exp \frac{\sum_{i=1}^n w_i \ln \bar{x}_i}{\sum_{i=1}^n w_i} \quad (2)$$

In the formula,  $\bar{x}_i$  is the average diameter of soil particle size (mm);  $w_i$  is the proportion of different soil size aggregates to the total aggregates.

The formula for calculating the fractal dimension of soil aggregates is as follows Eqs 3, 4:

$$\frac{W(r < R_i)}{W_T} = \left[ \frac{\bar{R}_i}{R_{max}} \right]^{3-D} \quad (3)$$

Take the base 10 logarithm of both sides:

$$\frac{\lg W(r < R_i)}{W_T} = (3 - D) \lg \frac{\bar{R}_i}{R_{max}} \quad (4)$$

In the formula: D is the fractal dimension of each particle size distribution of soil water-stable aggregates; W is the cumulative mass with a diameter less than  $R_i$ ;

$W_T$  is the total mass;

$R_i$  is the average diameter of soil particles between two adjacent particle sizes  $R_i$  and  $R_{i+1}$ ;

$R_{max}$  is the average diameter of the largest particle size soil particle.

Soil erodibility factor K adopts a model of global soil erodibility (without considering soil particle size composition, in the case of organic matter, soil infiltration and other indicators), only the geometric mean particle size (GMD) is considered to estimate the soil erodibility K value, and the specific calculation formula is as follows:

$$K = 7.954 \{ 0.0017 + 0.0494 \exp [ - \frac{1}{2} ( (\log(MWD) + 1.675) / 0.6986 )^2 ] \} \quad (5)$$

After correction, it is used to estimate the soil erodibility value in eastern China.

$$K = -0.00911 + 0.55066 K_{formula} \quad (6)$$

The Relative Dissipation Index (RSI) and the Relative Mechanical Fragmentation Index (RMI) respectively represent the degree of destruction of soil aggregates by dissipation and mechanical destruction. The higher the values of RSI and RMI, the higher the sensitivity of soil aggregates to the effects of dissipation and mechanical oscillations (Wang et al., 2022).

$$RSI = \frac{MWD_{SW} - MWD_{FW}}{MWD_{SW}} \quad (7)$$

$$RMI = \frac{MWD_{SW} - MWD_{WS}}{MWD_{SW}} \quad (8)$$

where:  $MWD_{SW}$ ,  $MWD_{FW}$  and  $WD$  represent the average weight diameter of aggregates under SW, FW and WD treatment, respectively.

## 3 Results

### 3.1 The particle size distribution characteristics of soil aggregates

On straight slopes, concave slopes, and concave-straight compound slopes, there were significant differences in the particle size distribution of soil aggregates with different treatments of the LB method (Figure 2). Except for the aggregate percentage of 2–1 mm particle size did not

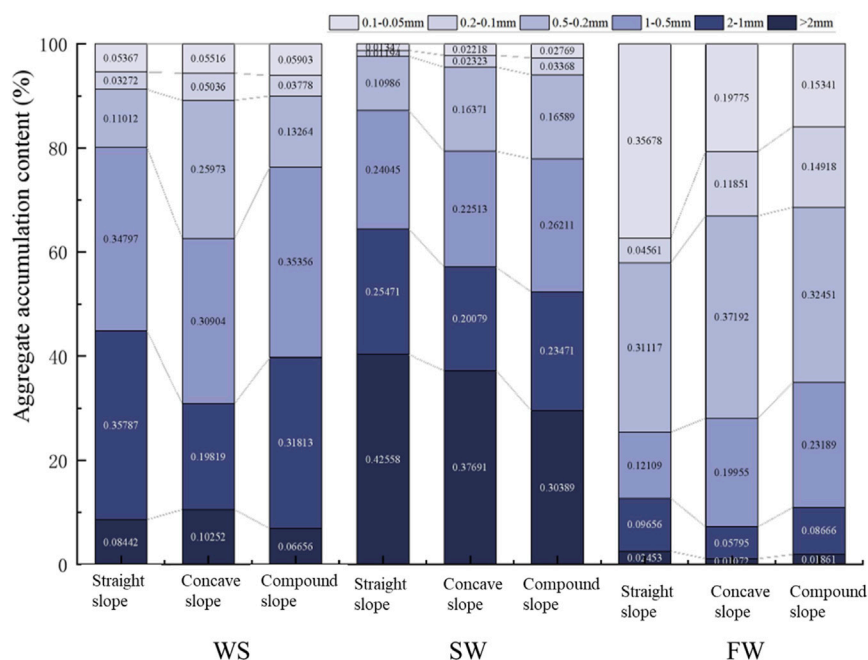


FIGURE 2

Size distribution of aggregates under different treatment methods of LB method: Cumulative particle size content of aggregates under different treatment methods.

reach a significant level between SW and WS treatments, there were significant differences in the aggregate content of other particle sizes ( $p < 0.01$ ). After FW treatment, the particle size distribution of water-stable aggregates is relatively dispersed, mainly 1–0.5 mm, 0.5–0 mm and 0.1–0.05 mm. The percentages ranged from 12.6% to 24.0%, 32.5%–38.8% and 15.9%–37.3%, respectively. Compared with the SW and WS methods, the difference is most evident in the particle size distribution of 0.1–0.05 mm, and the content of aggregates broken into the 0.1–0.05 mm particle size is 11.17 and 4.2 times that of the SW and WS treatments, respectively. After WS treatment, the water-stable aggregates were mainly concentrated in the 1–0.5 mm particle size, and the percentage ranged from 31.6% to 36.5%. The second was concentrated at 2–1 mm, with a percentage range of 20.3%–36.2%. The primary performance is that the particle size of the >2 mm aggregate is broken down to the particle size of 2–0.5 mm. After SW treatment, the particle size of soil aggregates was relatively concentrated, mainly distributed in >2 mm particle size, and the percentage ranged from 29.5% to 40.3%. It is the most significant percentage of >2 mm particle size among the three treatments, four times and 21 times that of WS and FW treatments, respectively. The percentage of <0.2 mm particle size is tiny, ranging from 2.4% to 5.9%. Under the three treatments of the LB method, the proportion of soil aggregates with particle size >2 mm after aggregate crushing was SW > WS > FW. The proportion of aggregates mainly broken into the 2–1 mm size fraction is WS > SW > FW, the same as that of the aggregates broken into the 1–0.5 mm size fraction. The proportion of 0.5–0.2 mm size aggregates is FW > WS > SW, which is the same as that of <0.2 mm size aggregates. It indicated that the FW treatment disintegrated most large aggregates into smaller ones. The FW treatment had the most significant effect on aggregate disintegration, while the SW treatment had the most negligible effect. Because of this, torrential rain or heavy rain is the

most fundamental driving force for the loss of cultivated land or bare land in the black soil region of Northeast China.

A particle size >0.25 mm is generally believed to be an important indicator of soil erodibility. However, previous studies have shown that under simulated rainfall conditions, runoff depth, soil erosion volume and soil stability >0.2 mm aggregate content are negatively correlated after 30 min (Barthès and Roose, 2002). The LSD test showed that at the three particle size levels of >0.2 mm, >0.5 mm, and >1 mm, there were significant differences ( $p < 0.01$ ) among the accumulated aggregate content of each corresponding size under the three treatments. Judging from the accumulation content of aggregates at the three particle size levels, the SW and WS treatments differed significantly from the FW treatments. At the >0.2 mm particle size, the difference between SW and WS is minimal. Nevertheless, as the particle size increases, the difference becomes more considerable. This law of soil aggregate fragmentation is reflected in the minor variation between different slope shapes. The three treatment methods were paired with T-tests among the three slopes, and the significant differences were 0.677, 0.861 and 0.876, respectively. It shows that different slope shapes have no significant effect on the percentage content of the particle size after the aggregates are broken, so the straight slope is used for the analysis below.

### 3.2 Effect of soil aggregate stability along slope length distribution

Since the runoff on the slope is mainly concentrated in the surface soil, the 0–10 cm soil layer on the slope is now analyzed (Figure 3). The SW in the LB method was used to simulate the SW process of light rain on the slope. The soil aggregates were broken into

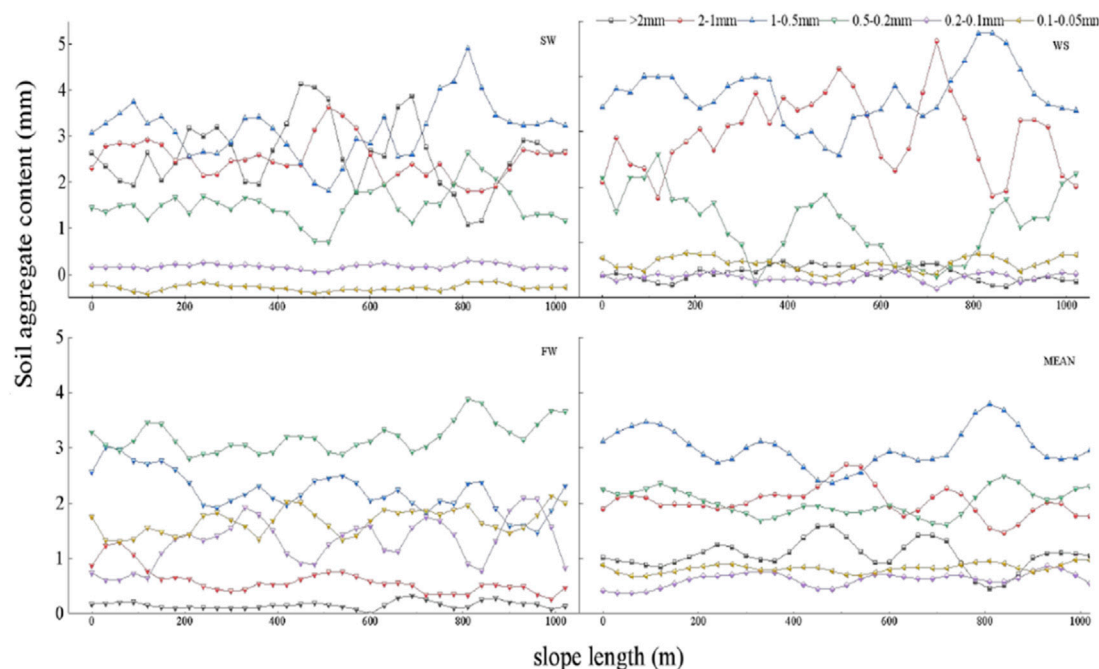


FIGURE 3

The distribution of the particle size content of soil water-stable aggregates along the slope length.

aggregates  $>0.2$  mm, and the fluctuation along the slope length was noticeable. The central particle size distribution along the slope length was 1–0.5 mm size and  $>2$  mm size alternately, which indicated the difference in slope soil resistance to dissipation. Among them, the 1–0.5 mm and 0.5–0.2 mm particle size distributions showed consistent fluctuations on the slope, and both showed the opposite fluctuation trend to the  $>2$  mm particle size distribution along the slope length. The content of 0.2–0.05 mm particle size is less, and the distribution along the slope is more uniform, with less fluctuation. WS simulated the process of raindrop splashing and runoff disturbance on the slope. The soil aggregates were mainly broken at the 2–0.2 mm particle size, and the 2–1 mm and 0.5–0.2 mm particle size distribution along the slope length fluctuated more than SW. The distribution of  $>2$  mm and  $<0.2$  mm particle size fragmentation along the slope length showed a consistent pattern, both relatively gentle. The  $>2$  mm particle size was less on the slope, indicating that the  $>2$  mm particle size aggregates were mainly split under the impact of raindrops.

Compared with the clay expansion and mechanical crushing effects of SW and WS treatments, the dissipation effect of simulated rainstorms under FW treatment significantly increased the content of 0.2–0.1 mm and 0.1–0.05 mm grain size on the slope, and there were fluctuations along the slope length. Trend. The contents of  $>2$  mm and 2–1 mm particle size were small, and the soil aggregates were mainly concentrated in  $<1$  mm. It shows that under the action of air explosion, the aggregates of slope aggregates are mainly broken down to  $<1$  mm particle size. The ability of aggregates to resist damage is relatively weak, and the resistance ability of all points on the slope is relatively consistent with that of light rain, raindrop splash and runoff disturbance. Furthermore, the more small particle aggregates on the slope surface, the more substances that can be splashed and carried by raindrops are more likely to be transported

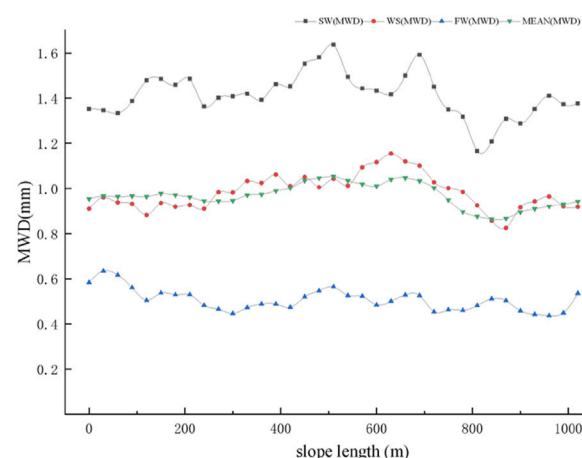


FIGURE 4

Distribution of soil aggregate stability along slope length.

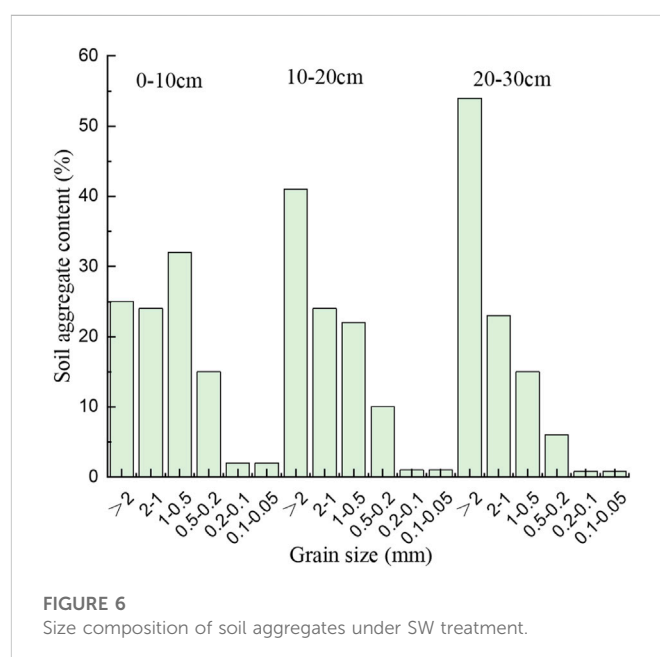
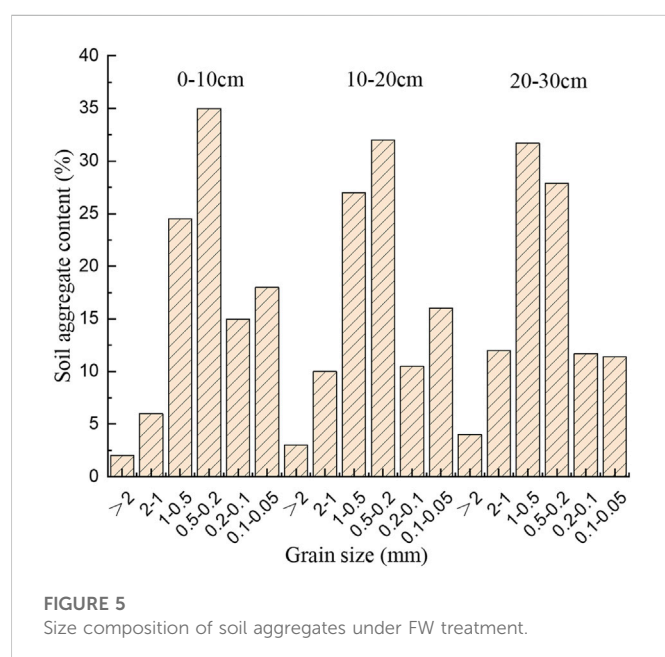
and migrated by runoff, resulting in severe soil erosion. However, under the action of SW and WS, the broken particle size distribution of surface aggregates showed undulating changes along the slope length, indicating that the soil in different parts of the slope is susceptible to uneven expansion and mechanical breakage; there are differences between the two.

After the slope soil experienced a series of freeze-thaw cycles, the stability of aggregates showed noticeable differences under simulated rainfall erosion conditions. Furthermore, with the change in slope length, the stability of aggregates showed a fluctuating trend with the slope length (Figure 4). Under SW treatment, the stability of

**TABLE 1** The stability of soil aggregates and the correlation of each parameter.

Parameter	Organic carbon	Bulk density	Total porosity	Capillary porosity
MWD <sub>FW</sub>	0.408*	−0.377	0.338	−0.341*
MWD <sub>SW</sub>	0.370*	−0.590	0.532	−0.096
MWD <sub>WS</sub>	0.455**	−0.068	−0.015	−0.026

Note: \* indicates a significant correlation at the 0.05 level (two-sided). \*\*Indicates a significant correlation at the 0.01 level (two-sided), n = 35.



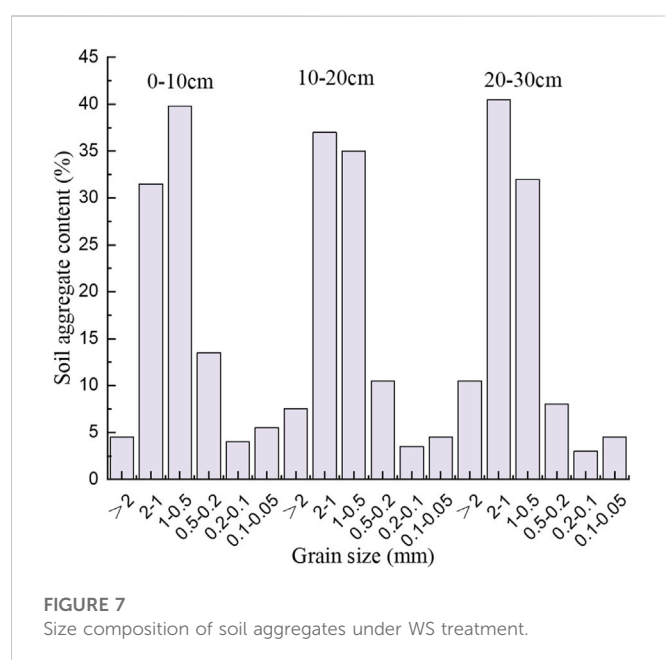
aggregates on the slope surface was the most stable ( $1.09 \text{ mm} \leq \text{MWD} < 1.69 \text{ mm}$ ). However, the stability was the lowest under FW treatment ( $0.40 \text{ mm} \leq \text{MWD} < 0.73 \text{ mm}$ ). Under the WS treatment, the erosion was moderate ( $0.99 \text{ mm} \leq \text{MWD} < 1.31 \text{ mm}$ ), and the entire slope showed a uniform change trend. The stability of soil aggregates in slope soil was the worst under air explosion, but the stability fluctuation trend was relatively gentle. It shows that the results of resistance to dissipation at each position on the slope are the smallest and equal. During the wetting process, the soil aggregates are due to the compression of the enclosed air inside the aggregates, resulting in an increase in the internal pressure of the aggregates and the breakdown of the aggregates. The characteristic index of soil porosity (adequate capillary pore size and total pore size) and the increase of soil porosity will provide more places for the confined air required for “air explosion”, thus promoting the trend of aggregate fragmentation. That is, the distribution of soil pores directly affects the strength of aggregate stability. There was a clear negative correlation between aggregate stability (MWD<sub>FW</sub>) and soil pore condition. As capillary porosity increases, the stability of soil aggregates decreases. To a certain extent, it proves the existence of the “air explosion” phenomenon. Along the slope length direction, the total and capillary porosity variability on the slope is 2.9% and 9.0%, respectively, which belongs to weak variability. The variability of the porosity of the aggregates on the slope before breaking is small, so the distribution of aggregates broken along the slope due to the difference in pore size

under the action of FW is small. The fluctuation trend of soil aggregate stability on the slope surface is slight.

### 3.3 Distribution characteristics of soil aggregate stability along the profile

Table 1 shows the relationship between soil properties and aggregate stability under different methods. Under the fast-wetting treatment of the LB method (FW, simulating the summer rainstorm scenario), the aggregates of each soil layer depth (0–10 cm, 10–20 cm and 20–30 cm) on the slope were damaged to a certain extent, and the large aggregates collapsed. A solution to finer aggregates (Figure 5). The particle size of aggregates is mainly concentrated in  $<1 \text{ mm}$ , and the cumulative percentages in the 0–10 cm, 10–20 cm, and 20–30 cm soil layers are 91.86%, 87.16% and 84.29%, respectively, and the particle size  $>2 \text{ mm}$  only accounts for 2.45%. The content of aggregates  $>0.2 \text{ mm}$  in each soil layer was not significantly different, indicating that soil aggregates at all depths were destroyed after FW treatment. However, with the increase of soil depth, the conversion ratio of  $>0.5 \text{ mm}$  soil aggregates to large aggregates increased. The 0–20 cm soil aggregates were broken in the same way under the FW treatment, but the 20–30 cm soil aggregates were broken differently than the upper soil. It shows that the effect of air explosion on the soil damage of the 0–20 cm





soil layer in the black soil region of Northeast China is more prominent.

The aggregates treated with SW have apparent advantages in the proportion of  $>2$  mm, 2–1 mm, 1–0.5 mm, and 0.5–0.2 mm, accounting for 97% of the total. It shows that the original 5–3 mm large aggregates were mainly broken into  $>0.2$  mm aggregates under SW treatment (Figure 6). The particle size of  $>2$  mm aggregates increased significantly with soil depth. In the 20–30 cm soil layer, the particle size of aggregates  $>2$  mm accounted for more than 50%, and the distribution of aggregates was relatively uniform except for the soil aggregates  $>0.2$  mm in the 0–10 cm soil layer. The damage of the soil aggregates in the lower layer decreased step by step and broke down step by step, indicating that it was under the action of clay expansion. The soil aggregates in the upper layer were more easily broken than in the lower layer, and the transformation ratio of soil aggregates in the lower layer to macroaggregates was significantly higher than that in the upper layer.

The water-stable aggregates in the WS treatment were mainly concentrated in the 2–0.5 mm particle size, and the cumulative proportions of each soil layer were 70.58%, 71.14%, and 72.79%, respectively. It shows that the original 5–3 mm large aggregates are mainly broken down to 2–0.5 mm aggregates under WS treatment (Figure 7). Under each depth of soil layer, the aggregate content tends to be normally distributed, that is, there are more aggregates with a size of 2–0.5 mm. Furthermore, with it as the centre, it decreases step by step to both sides, but with the increase of soil layer, it also shows the trend of shifting to large particle size. Overall, the distribution of crushed aggregates was relatively similar, indicating that the impact of mechanical vibration treatment on each soil layer of cultivated soil aggregates was equivalent. The difference from the SW treatment was that the mechanically disturbed soil aggregates severely damaged the particle size aggregates  $>2$  mm, mainly breaking down to  $<2$  mm particle size. Unlike the FW treatment, the proportion of  $<0.2$  mm aggregates was small. It shows that under the action of disintegration under mechanical disturbance, the degree of fragmentation of cultivated soil aggregates is moderate.

**TABLE 2** Aggregate stability at different soil depths.

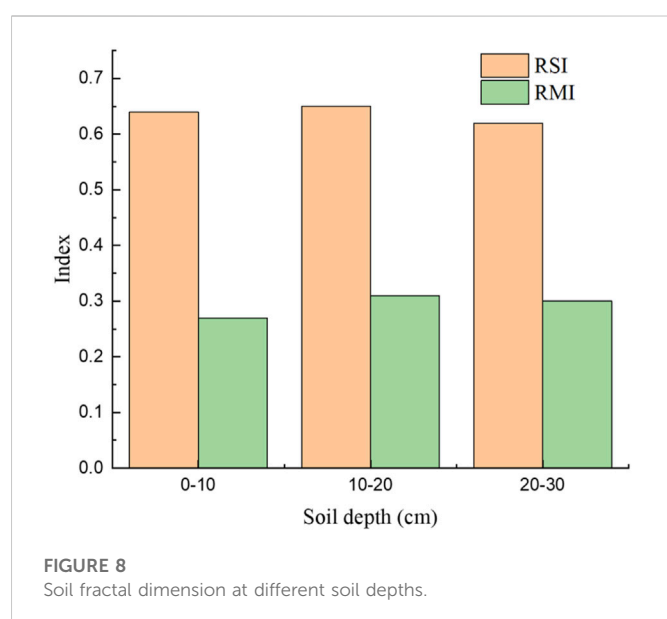
	0–10 cm		10–20 cm		20–30 cm	
	MWD/ mm	CV/ %	MWD/ mm	CV/ %	MWD/ mm	CV/ %
SW	0.62–1.54	20.40	0.88–2.06	18.80	1.25–1.98	11.20
WA	0.42–1.10	19.40	0.86–1.22	12.70	0.80–2.30	22.80
FW	0.28–0.68	17.76	0.33–0.71	15.70	0.35–0.95	23.60

The stable state of soil aggregates in different soil layers was different due to different treatments of aggregates (Table 2). Under FW treatment, the stability of soil aggregates at different depths was mostly at an unstable level ( $0.4 < \text{MWDFW} < 0.8$ ). Under the WS and SW treatments, except for the 0–10 cm soil layer, the aggregate stability was above the stable level ( $\text{MWD}_{\text{sw}}, \text{MWD}_{\text{ws}} > 0.8$ ). The results showed that the stability of soil aggregates was the strongest after the SW treatment. The second is the pre-wetting and shaking treatment. After the rapid wetting treatment, the stability and corrosion resistance of the aggregates are the weakest. It can be seen that the dissipation effect caused by rapid wetting and the mechanical disturbance effect caused by pre-wetting oscillation are the main effects of soil aggregate destruction.

Among all the soil samples on the slope, 95% had the largest MWD after SW treatment, and 5.88% had the largest aggregate MWD after WS treatment. However, only 0.98% of the samples had the largest MWD after FW treatment. The performance is  $\text{MWD}_{\text{SW}} > \text{MWD}_{\text{WS}} > \text{MWD}_{\text{FW}}$ . The aggregates treated with FW had the lowest MWD, i.e., the aggregates were most destructive. The aggregate MWD value of SW treatment was the largest, and the aggregate damage was the least. There were significant differences in the MWD values of the aggregates treated with FW, WS and SW in the Le Bissonnais method. However, the MWD values of aggregates in different soil layers have the same variation after treatment. The  $\text{MWD}_{0-10 \text{ cm}} < \text{MWD}_{10-20 \text{ cm}} < \text{MWD}_{20-30 \text{ cm}}$  among different soil layers under the three failure mechanisms showed that the structure of soil aggregates in the 20–30 cm soil layer was the most stable, while the 0–10 cm soil layer had the worst stability.

Under SW treatment, the average weight diameters ( $\text{MWD}_{0-10 \text{ cm}}, \text{MWD}_{10-20 \text{ cm}}$  and  $\text{MWD}_{20-30 \text{ cm}}$ ) of soil aggregates in each soil layer were 1.18, 1.44, and 1.66, respectively. The soil aggregates in the lower layer increased by 21.8% and 11.2%, respectively compared with the upper layer. It shows that the 10–20 and 20–30 cm soil layers are less sensitive to aggregate breakage caused by simulating the wetness of light rain in the field than the 0–10 cm soil layer, that is, the soil erosion resistance of the 10–30 cm soil layer is significantly better than that of 0–10 cm soil layer. Under the FW treatment, the average weight diameters of aggregates in the 0–10, 10–20, and 20–30 cm soil layers were 0.42, 0.51, and 0.62, respectively, and the stability was the worst. The soil aggregate stability of the lower layer was 11.9% and 22.2% higher than that of the upper layer, respectively, and the difference was most evident between 0–20 cm and 20–30 cm. It shows that the 20–30 cm soil layer is less sensitive to air explosion than the 0–20 cm soil layer. That is, the corrosion resistance is significantly enhanced. Under WS processing, the mean weight diameters ( $\text{MWD}_{0-10 \text{ cm}}, \text{MWD}_{10-20 \text{ cm}}$  and  $\text{MWD}_{20-30 \text{ cm}}$ ) of the aggregates in each soil layer





were 0.86, 0.98 and 1.1, respectively. The soil aggregate stability of the lower layer was 14.0% and 11.9% higher than that of the upper layer. The susceptibility of different soil layers to soil erosion was comparable under simulated field mechanical disturbance. That is, relative to the pre-wetting disturbance, and there is no noticeable difference in the corrosion resistance of each soil layer. It shows that the soil aggregates in the 0–10 cm soil layer are more sensitive to the damage of light rain in the field, and the soil aggregates in the 0–20 cm soil layer are more sensitive to air explosion. Each soil layer's susceptibility to soil aggregate damage was equivalent under mild mechanical vibration and other conditions.

There were differences in the fractal dimension of soil aggregates among different soil layers among the treatments. However, the variation trends were not the same (Figure 8). The average fractal dimensions of the 0–10, 10–20, and 20–30 cm soil layers under the SW treatment were 2.36, 1.95, and 1.85, respectively. The average fractal dimensions of the 0–10, 10–20, and 20–30 cm soil layers under WS treatment were 2.47, 2.39, and 2.36, respectively. The average fractal dimensions of the 0–10, 10–20, and 20–30 cm soil layers under the FW treatment were 2.73, 2.70, and 2.70, respectively. Both showed a decreasing trend with the increase of the soil layer. It indicated that the degree and effects of the three treatments on the soil structure were different and changed with the depth of the soil layer. However, in the soil profile under FW treatment, the soil fractal dimension  $D$  was unchanged in each soil layer, and the value range was small. However, the fractal dimension of the soil in the slow-moisture treatment gradually decreases and changes obviously with the depth of the profile.

### 3.4 The impact of soil aggregate fragmentation on the main factors of soil quality

The soil erodibility  $K$  value in the black soil region of Northeast China was estimated using the modified geometric particle size model, which can be used as an estimation model for soil erodibility  $K$  value in

eastern China. As a comprehensive relative index of soil water erosion resistance, the more significant the  $K$  value, the more unstable the aggregates and the more prone to erosion. Conversely, the stronger the soil erosion resistance. The soil erodibility of the slopes in the study area was analyzed (Table 3), and it was found that the soil erodibility of each slope showed that the  $K$  value of the straight slope was the smallest. The variability was the most minuscule (14.8%). Composite and concave slopes had similar  $K$  values, with a variability of 22.4% and 21.0%, respectively. The variation range of soil  $K$  value of the three slopes is 0.008–0.043, and the average value is 0.018 (Keli et al., 2007) research shows that China's  $K$  value of soil erodibility is relatively concentrated in the 0.001–0.04. The overall soil erodibility in the study area belongs to medium variation (16%–32%), and the  $K$  value of soil erodibility decreases significantly with the increase of soil depth. It shows that with the increase of the depth of the soil layer, the ability of soil erosion resistance is gradually enhanced.

The  $K$  value of soil erodibility is closely related to aggregates, and rainfall erosion further affects the potential erodibility of soil and the final soil erosion process (Zhu et al., 2022). The Pearson correlation analysis was performed on the soil erodibility, aggregate size and SOC, as shown in Table 3. The soil erodibility  $K$  value was positively correlated with the aggregate content of 0.5–0.2 mm, 0.2–0.1 mm, and 0.1–0.05 mm, and the correlation coefficients were 0.317, 0.394, and 0.319, respectively ( $p < 0.01$ ). The results showed that fine particles could clog soil pores during precipitation when the  $<0.5$  mm particle size content increases. In turn, it hinders the infiltration of soil moisture, increases surface runoff, accelerates surface runoff and sand production, and enhances soil erosion capacity. The erodibility  $K$  value was negatively correlated with the particle size of  $>2$  mm and 2–1 mm aggregates, and the correlation coefficients were 0.211 and 0.192, respectively ( $p < 0.01$ ). It shows that the large particles have intense anti-erosion media stripping and transport ability, and the soil's anti-corrosion ability is strong. The erodibility  $K$  value was significantly negatively correlated with the organic carbon content (Table 3), with a correlation coefficient of 0.261 ( $p < 0.01$ ). This shows that soil organic carbon can enhance the bonding between soil particles and water, mainly showing a significant negative correlation between the  $<1$  mm particle size and SOC content. It shows that SOC promotes soil water stability and the formation of aggregates, which is beneficial to the stability of soil structure and enhances soil erosion resistance.

## 4 Discussion

According to the average value of the particle size distribution on the slope under the three treatments, the particle composition is mainly  $>2$  mm. Among them, the 1–0.5 mm and 0.5–0.2 mm particle sizes showed similar fluctuation trends.  $>2$  mm, 2–1 mm particle size showed a similar trend. The particle size distribution of  $>1$  mm and the particle size distribution of 1–0.2 mm showed opposite trends in the slope fluctuation trend. It shows that rainfall erosion mainly breaks  $>2$  mm, 2–1 mm grain size into 1–0.2 mm grain size. Thus, abundant loose aggregate particles are provided for raindrop splash erosion and runoff erosion, which is the primary source of erosion materials in soil erosion. The particle size distribution of aggregates on the slope surface after crushing directly affects the impact of raindrops and runoff on the initiation and transportation of soil particles. The difference in particle size

TABLE 3 Correlation between slope soil erodibility K value, SOC and each particle size.

	K	SOC	>2 mm	2-1 mm	1-0.5 mm	0.5–0.2 mm	0.2–0.1 mm	0.1–0.05 mm
K	1	–0.261**	–0.211*	–0.192*	0.190	0.317**	0.394**	0.319**
SOC	–0.261**	1	–0.091	–0.043	–0.270**	–0.314**	–0.287**	–0.320**

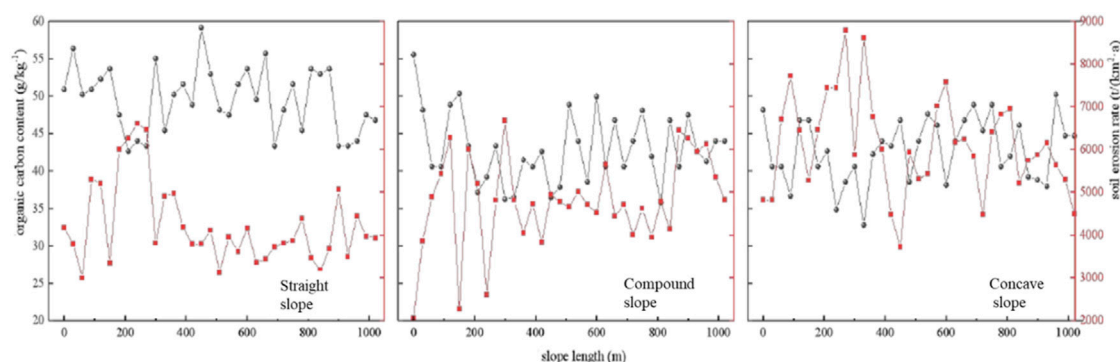


FIGURE 9  
Distribution characteristics of soil SOC and soil erosion rate along the slope length.

distribution will lead to the difference in the sediment carried by the runoff scouring process, leading to the erosion-sedimentation fluctuation law on the slope surface. There is a periodic change law of ebb and flow or similarity among the grain fractions on the slope along the slope length. Although it does not precisely match the fluctuation trend of erosion intensity of slope farmland, the fundamental trends reflected by the two are similar.

Under simulated light rain conditions, the stability of aggregates on the slope surface fluctuated most obviously along the slope length. Agglomerates break up due to uneven expansion and contraction of soil clay particles. Studies have shown that the fracture mechanism can only be expressed when the soil contains many clay minerals with expansive lattices. The internal structure of the agglomerates produces fine cracks (cracks), which leads to the breakage of the agglomerates. The clay mineral montmorillonite and clay content (37%) in the soil are relatively high; the main clay mineral is montmorillonite. Its expansion and contraction are substantial, and montmorillonite aggregates are more sensitive to the stress generated by expansion. Although less destructive, it is better than rapid wetting for differentiating unstable soils between different locations on a slope.

Under the conditions of simulated raindrop impact and runoff disturbance, the stability of aggregates on the slope surface is between the two. When the external mechanical damage kinetic energy is significant enough, soil aggregates combined with dissipation or clay expansion will disperse and break aggregates. It shows that the cementation effect of soil organic matter on aggregates is dominant (excluding the destruction effect of dissipation and clay expansion). Thick-layer black soil has a high content of organic matter and clay, both cementing substances. It dramatically enhances the cementation ability between soil aggregates and plays an essential role in the formation and stability of soil aggregate structure. Analysis of the correlation between aggregate stability parameters and soil organic carbon content showed that organic carbon was significantly

correlated with its stability (MWDWS) under mechanical disturbance. It is confirmed that the soil aggregates on the slope will destroy the cohesion of soil organic matter during mechanical disturbance and crushing. The organic carbon content enhances its ability to resist mechanical damage. Along the slope length direction, the variability of organic carbon on the slope is 8.7%, which is weak variability. Therefore, under mechanical disturbance, there is little difference in the distribution of aggregate breakage along the slope.

Regardless of the destruction method, after the aggregates experienced rainfall, the aggregates were broken into smaller particles. Nutrients mainly exist in the soil in an adsorption or organic state, and most soil flow is fine particles. Since the fine particles have a larger specific surface area, they have a more substantial adsorption effect on nutrients. Therefore, it can be inferred that the enormous loss of fine particles in the slope runoff accompanies the enormous loss of soil nutrients. In the long-term rainfall erosion process, with the continuous development of runoff, the sediment content carried by it has been in the mutual conversion state of “saturated-unsaturated”. Due to the combined effect of erosion and deposition, the nutrient content inevitably erodes and deposits continuously with the runoff and sediment on the slope, and finally presents a trend of fluctuating changes.

By analyzing the changes of organic carbon along the length of the three slopes: straight slope, concave slope and compound slope, it was found that the average value of soil organic carbon content (SOC) on the slope was 46.58 g/kg-1. The variation range is 26.76–68.09 g/kg-1. There was a significant difference in the content of SOC in different slope shapes ( $p \leq 0.01$ ). The SOC content of each slope shape is mainly as follows: open slope < compound slope < straight slope. The SOC content of the straight slope is 1.04 and 1.11 times that of the composite and concave slopes. The soil SOC content of the concave slope with the highest soil erosion rate is the lowest. Straight slopes with the lowest soil erosion rates have the highest

average concentrations. The erosion intensity and SOC content of the composite slope is in between. In terms of the change along the slope length, the soil SOC content generally showed a high-low-high variation trend. Contrary to the change in soil erosion rate along the slope length, the site with a higher soil erosion rate corresponds to lower soil SOC content and *vice versa* (Figure 9).

The variation trend of slope soil SOC and soil erosion intensity is opposite to that of slope distribution, reflecting that the spatial distribution of soil erosion intensity directly affects the distribution of slope soil organic carbon distribution. Analyzing the reasons, soil organic carbon mainly exists in soil aggregates in a close combination of organic and inorganic substances. The migration and transformation of soil particles mainly accompany it. The study of slope soil is mainly based on the erosion-transport process, and the soil erosion-transport process is also the process of soil SOC transport. The SOC accumulated on the soil surface is easily lost with the migration of the surface soil. This will cause a large amount of fertile soil on the surface of the cultivated land, and the soil and its nutrients will be lost through runoff and sediment. The remaining content of cultivated land is reduced, and the black soil layer is thinned, resulting in barren soil and a decline in cultivated land quality.

## 5 Conclusion

This paper uses three processing methods of the LB method to clarify the crushing characteristics of soil aggregates under different damage effects. The breaking mechanism of typical black soil aggregates was clarified, and the distribution characteristics of the stability of soil aggregates in different parts and layers along the slope were analyzed. Furthermore, the response of slope soil erodibility K value and soil SOC content loss to slope surface was discussed. The main conclusions are as follows.

- (1) Overall, the aggregate stability showed  $MWDSW > MWDWS > MWDFW$ .
- (2) The analysis of the aggregates in the topsoil layer (0–10 cm) found that the fluctuation trends along the slope length among the various grain sizes on the slope did not completely match. However, the fundamental trends reflected by the two were similar.

## References

- An, S. S., Darboux, F., and Cheng, M. (2013). Revegetation as an efficient means of increasing soil aggregate stability on the Loess Plateau (China)[J]. *Geoderma* 209, 75–85. doi:10.1016/j.geoderma.2013.05.020
- Barthès, B., and Roose, E. (2002). Aggregate stability as an indicator of soil susceptibility to runoff and erosion; validation at several levels. *Catena* 47, 133–149. doi:10.1016/S0341-8162(01)00180-1
- Bissonnais, Y. L. (1996). Aggregate stability and assessment of soil crustability and erodibility: I. Theory and methodology. *Eur. J. Soil Sci.* 47, 425–437. doi:10.1111/j.1365-2389.1996.tb01843.x
- Breshears, D. D., Whicker, J. J., and Johansen, M. P., (2003). Wind and water erosion and transport in semi-arid shrubland, grassland and forest ecosystems: Quantifying dominance of horizontal wind-driven transport. *Earth Surf. Process. Landforms* 28, 1189–1209. doi:10.1002/esp.1034
- D. W. Bromley (1995). *Handbook of environmental economics*. 1st Edition. Elsevier. Available at: <https://www.amazon.com/Handbook-Environmental-Economics-Daniel-Bromley/dp/1557866414>.
- Chen, R., Yan, D., Wen, A., Shi, Z., Chen, J., Liu, Y., et al. (2021). The regional difference in engineering-control and tillage factors of Chinese Soil Loss Equation[J]. *J. Mt. Sci.* 18 (3), 658–670. doi:10.1007/s11629-020-6268-z
- (3) Under the three failure mechanisms,  $MWD0-10\text{ cm} < MWD10-20\text{ cm} < MWD20-30\text{ cm}$  is reflected among different soil layers.
- Fan, H., Cai, Q., and Wang, H. (2004). Soil erosion environment in the black soil region of NortheastNortheast China. *J. Soil Water Conservation* 18, 5. doi:10.1016/j.envsci.2010.07.004
- Fang, H. (2005). Study on erosion and sedimentation characteristics of black soil in slope cultivated land by  $^{137}\text{Cs}$  tracing technique. *J. Ecol.* 25, 7. doi:10.1016/S1002-0160(06)60044-1
- Guo, M., Zheng, F., An, S., Liu, Y., Wang, B., and Darboux, F. (2010a). Application of Le Bissonnais method to study soil aggregate stability in the Hilly-gully region. *Sci. Soil Water Conservation* 8, 68–73. doi:10.5846/stxb201301160103
- Hu, Z., Yizhong, L., Zhichen, Y., and Baoguo, L. (2007). Effects of conservation tillage on soil aggregate characteristics in north China plain. *Chin. Agric. Sci.* 40, 7. doi:10.1016/j.still.2012.06.007
- Huang, B., Zhu, M., Liu, Z., Sheng, M., Chen, M., Yang, Q., et al. (2022). The formation of small macro-aggregates induces soil organic carbon stocks in the restoration process used on cut slopes in alpine regions of China. *Land Degrad. Dev.* 33, 3283–3293. doi:10.1002/ldr.4388
- Jakik, O., Kodeová, R., Kubi, A., Stehliková, I., Drábek, O., and Kapička, A. (2015). Soil aggregate stability within morphologically diverse areas[J]. *Catena* 127, 287–299. doi:10.1016/j.catena.2015.01.010

## Data availability statement

The original contributions presented in the study are included in the article/supplementary material, further inquiries can be directed to the corresponding author.

## Author contributions

All authors were responsible for designing the framework of the entire manuscript from topic selection to solution to experimental verification.

## Funding

Heilongjiang Academy of Agricultural Sciences Innovation Project Grant (CX23GG11, 2020FJZX029), Qiqihar Science and Technology Program Key Project (ZDGG-202208).

## Conflict of interest

The authors declare that the research was conducted in the absence of any commercial or financial relationships that could be construed as a potential conflict of interest.

## Publisher's note

All claims expressed in this article are solely those of the authors and do not necessarily represent those of their affiliated organizations, or those of the publisher, the editors and the reviewers. Any product that may be evaluated in this article, or claim that may be made by its manufacturer, is not guaranteed or endorsed by the publisher.

- Keli, Z., Wenying, P., and Hongli, Y. (2007). Soil erodibility value and its estimation in China. *Acta Soil Sci.* 44, 7.
- Khan, F. U., Khan, A. A., Li, K., Xu, X., Adnan, M., Fahad, S., et al. (2022). Influences of long-term crop cultivation and fertilizer management on soil aggregates stability and fertility in the loess plateau, northern China. *J. Soil Sci. Plant Nutr.*, 1–12. doi:10.1007/s42729-021-00744-1
- Lal, R., Lal, L., and Lal, S. (2000). Physical management of soils of the tropics: Priorities for the 21st century. *Soil Sci.* 165, 191–207. doi:10.1097/00010694-200003000-00002
- Ma, R., Hu, F., Xu, C., Liu, J., and Zhao, S. (2022). Response of soil aggregate stability and splash erosion to different breakdown mechanisms along natural vegetation restoration. *Catena* 208, 105775. doi:10.1016/j.catena.2021.105775
- Madari, B., Machado, P., Torres, E., Andrade, A., and Valencia, L. (2005). No tillage and crop rotation effects on soil aggregation and organic carbon in a Rhodic Ferralsol from southern Brazil. *Soil. Tillage Res.* 80, 185–200. doi:10.1016/j.still.2004.03.006
- Mcbride, M. B. (2022). Estimating soil chemical properties by diffuse reflectance spectroscopy: Promise versus reality. *Eur. J. Soil Sci.* 73, e13192. doi:10.1111/ejss.13192
- Mo, J., Feng, J., He, W., Liu, Y., Cao, N., Tang, Y., et al. (2022). Effects of polycyclic aromatic hydrocarbons fluoranthene on the soil aggregate stability and the possible underlying mechanism. *Environ. Sci. Pollut. Res.* 7, 1–11. doi:10.1007/s11356-022-22855-7
- Ojeda, G., Alcaniz, J. M., and Bissonnais, Y. L. (2008). Differences in aggregate stability due to various sewage sludge treatments on a Mediterranean calcareous soil. *Agric. Ecosyst. Environ.* 125, 48. doi:10.1016/j.agee.2007.11.005
- Rana, S., Cheng, X., Wu, Y., Hu, C., Jemim, R. S., Liu, Z., et al. (2022). Evaluation of soil and water conservation function in the Wugong mountain meadow based on the comprehensive index method[J]. *Heliyon* 8 (12), e11867. doi:10.1016/j.heliyon.2022.e11867
- Roth, C. H., and Eggert, T. (1994). Mechanisms of aggregate breakdown involved in surface sealing, runoff generation and sediment concentration on loess soils. *Soil. Tillage Res.* 32, 253–268. doi:10.1016/0167-1987(94)90024-8
- Shen, C., Wang, Y., Zhao, L., Xu, X., Yang, X., and Liu, X. (2019). Characteristics of material migration during soil erosion in sloped farmland in the black soil region of Northeast China[J]. *Trop. Conserv. Sci.* 12, 1940082919856835. doi:10.1177/1940082919856835
- Van Den Bergh, J., Jeroen, C., and Verbruggen, H. (1999). Spatial sustainability, trade and indicators: An evaluation of the 'ecological footprint. *Ecol. Econ.* 29, 61–72. doi:10.1016/s0921-8009(99)00032-4
- Wang, J., Deng, Y., Li, D., Liu, Z., Wen, L., Huang, Z., et al. (2022). Soil aggregate stability and its response to overland flow in successive Eucalyptus plantations in subtropical China. *Sci. Total Environ.* 807, 151000. doi:10.1016/j.scitotenv.2021.151000
- Wirtz, S., Seeger, M., and Ries, J. B. (2012). Field experiments for understanding and quantification of rill erosion processes. *Catena* 91, 21–34. doi:10.1016/j.catena.2010.12.002
- Wu, X., Wei, Y., Wang, J., Di, W., and Cai, C. (2017). Effects of soil physicochemical properties on aggregate stability along a weathering gradient. *Catena* 156, 205–215. doi:10.1016/j.catena.2017.04.017
- Wuddivira, M. N., Stone, R. J., and Ekwue, E. I. (2009). Clay, organic matter, and wetting effects on splash detachment and aggregate breakdown under intense rainfall. *Soil Sci. Soc. Am. J.* 73, 226–232. doi:10.2136/sssaj2008.0053
- Xu, X., Zheng, F., Wilson, G. V., He, C., Lu, J., and Bian, F. (2018). Comparison of runoff and soil loss in different tillage systems in the Mollisol region of Northeast China. *Soil Tillage Res.* 177, 1–11. doi:10.1016/j.still.2017.10.005
- Yan, S., Xiaoping, Z., Aizhen, L., Wenfeng, L., and Xueming, Y. (2008). Soil loss form analysis of black soil slope cultivated land—taking a rainfall as an example. *Dryland Agric. Res.* 26, 6.
- Yang, Z., Enheng, W., and Xiangwei, C. (2008). Characteristics of black soil splash erosion and aggregate sorting under simulated rainfall conditions. *J. Soil Water Conservation* 22, 4. doi:10.1371/journal.pone.0154591
- Zhang, G. H., Liu, Y. M., Han, Y. F., and Zhang, X. C. (2009). Sediment transport and soil detachment on steep slopes: I. Transport capacity estimation. *Soil Sci. Soc. Am. J.* 73, 1291–1297. doi:10.2136/sssaj2008.0145
- Zhang, X., Zheng, F., Bin, W., and Juan, A. (2011). Relationship between soil aggregate stability and organic matter in sloping cultivated land in black soil area with different reclamation years. *J. Shaanxi Normal Univ.* 34, 695. doi:10.1081/CSS-120018969
- Zhizhen, F., Fenli, Z., Wei, H., Li, G., and Xu, X. (2018). Impacts of mollic epipedon thickness and overloaded sediment deposition on corn yield in the Chinese Mollisol region. *Agric. Ecosyst. Environ.* 257, 175. doi:10.1016/j.agee.2018.02.010
- Zhu, M., He, W., Liu, Y., Chen, Z., Dong, Z., Zhu, C., et al. (2022). Characteristics of Soil Erodibility in the Yinna Mountainous Area, Eastern Guangdong Province, China[J]. *Int. J. Environ. Res. Public Health.* 19 (23), 15703. doi:10.3390/ijerph192315703



## OPEN ACCESS

## EDITED BY

Yuncong Li,  
University of Florida, United States

## REVIEWED BY

Yiming Wang,  
Institute of Soil Science (CAS), China  
Yanbing Qi,  
Northwest A&F University, China

## \*CORRESPONDENCE

Rui Wang,  
✉ amwangrui@126.com

## SPECIALTY SECTION

This article was submitted to Soil  
Processes,  
a section of the journal  
Frontiers in Environmental Science

RECEIVED 23 December 2022

ACCEPTED 02 March 2023

PUBLISHED 10 March 2023

## CITATION

Wang Y, Gao M, Chen H, Fu X, Wang L and  
Wang R (2023), Soil moisture and salinity  
dynamics of drip irrigation in saline-alkali  
soil of Yellow River basin.  
*Front. Environ. Sci.* 11:1130455.  
doi: 10.3389/fenvs.2023.1130455

## COPYRIGHT

© 2023 Wang, Gao, Chen, Fu, Wang and  
Wang. This is an open-access article  
distributed under the terms of the  
Creative Commons Attribution License  
(CC BY). The use, distribution or  
reproduction in other forums is  
permitted, provided the original author(s)  
and the copyright owner(s) are credited  
and that the original publication in this  
journal is cited, in accordance with  
accepted academic practice. No use,  
distribution or reproduction is permitted  
which does not comply with these terms.

# Soil moisture and salinity dynamics of drip irrigation in saline-alkali soil of Yellow River basin

Yaqi Wang<sup>1</sup>, Ming Gao<sup>1</sup>, Heting Chen<sup>1</sup>, Xiaoke Fu<sup>1</sup>, Lei Wang<sup>2</sup> and  
Rui Wang<sup>1\*</sup>

<sup>1</sup>School of Agriculture, Ningxia University, Yinchuan, China, <sup>2</sup>School of Ecology and Environment, Ningxia University, Yinchuan, China

Soil secondary salinization in the Yellow River Diversion Irrigation Area of Northwest China seriously threatens local agricultural production. Drip irrigation technology is one of the largest contributors to low-yielding saline-alkali land; however, research on the high spatio-temporal scale variability of soil moisture and salinity in drip irrigation is still lacking. Herein, four treatments, CK (flood irrigation, 900 mm), W1 (small volume drip irrigation, 360 mm), W2 (medium volume drip irrigation, 450 mm), and W3 (large volume drip irrigation, 540 mm), were set up to investigate the characteristics and laws of soil moisture and salinity under different irrigation methods. The results showed that the soil moisture of drip irrigation was 5.02%–17.88% (W1), 7.36%–21.06% (W2), and 13.79%–27.88% (W3) higher than that of flood irrigation, resulting in a vertical distribution of soil moisture being low at the top and high at the bottom. Under drip irrigation, the soil salinity formed a desalination zone centered on the drip emitter and this zone gradually expanded to deeper soil with continuous drip irrigation, gradually transforming the soil from surface aggregation type to the bottom accumulation type. The desalination rates of W1, W2, and W3 were 18.46%, 20.84%, and 22.94%, respectively, whereas the salt leaching rate of CK was slower and the salt distribution was not uniform; therefore, the desalination rate was only 5.32%. By precisely controlling the irrigation water volume and flow, drip irrigation significantly reduced surface evaporation and subsurface leakage of water and improved water use efficiency, thus increasing grain yield. Compared with flood irrigation, the yield increase rates of W1, W2, and W3 were 6.6%, 16.18%, and 18.32%, respectively. Therefore, drip irrigation with an appropriate irrigation volume in the saline land in northern Ningxia can improve water saving, salt suppression, and maize yield.

## KEYWORDS

saline-alkali soil, soil moisture, soil salinity, drip irrigation, flood irrigation

## 1 Introduction

Soil salinization is a major global environmental problem with severe negative impacts on crop planting and sustainable agricultural development in arid and semi-arid regions (Chhabra, 2004; Ashraf, 2007). In saline-alkali areas with high groundwater tables, the movement of water and salt to the surface caused by capillary upwelling and high evaporation is the main cause of salinization (Northey et al., 2006). The Yellow River



Diversion Irrigation Agricultural Area is located in the semi-arid region of Northwest China. People have diverted water from the Yellow River for hundreds of years allowing the Yellow River Basin in ancient China to achieve prosperity in agriculture and the development of civilization under climatic conditions with an average annual precipitation of only 200 mm (Wang et al., 1993; Xiong et al., 1996). However, excessive irrigation leads to the accumulation of salt in groundwater and secondary salinization, and insufficient fertilization leads to a decrease in water and fertilizer use efficiency and fertilizer use efficiency, resulting in agricultural non-point source pollution (Liu et al., 2014; Wang et al., 2014). At present, hundreds of years of irrigation by the Yellow River have raised the groundwater table, and the dry and high evaporation climate conditions in this region have further exacerbated the local soil salinization process, seriously threatening normal agricultural production (Wang et al., 1993; Xiong et al., 1996).

The essence of saline soil improvement measures is to regulate the movement of soil water and salt, to promote the downward leaching of soil salt, and to prevent salt from migrating upward to the surface with the soil solution due to transpiration (Guan et al., 2019; Stavi et al., 2021; Gu et al., 2022). The traditional water-saving measure is to remove soil salt by flooding before sowing, but this method wastes valuable water resources and increases the risk of environmental pollution (Pimentel et al., 2004). Drip irrigation can accurately control the amount of water and nutrients applied to the soil, ensuring adequate levels of water, nutrients and aeration in the soil-root zone (Burt and Isbell, 2005; Rajak et al., 2006). Drip irrigation also removes excess salt from the root zone through small area irrigation and slow infiltration, forming a desalination zone with sufficient water and less salt near the emitter, creating a suitable low-salinity microenvironment for the normal growth of plants (Burt and Isbell, 2005). It has become a key irrigation technology in the promotion of water conservation, salt suppression, and productivity improvement in saline-alkali land (Stavi et al., 2021) and is one of the most effective methods for developing low-yield salinized farmland, being widely used in salinized farmlands globally. Nevertheless, improper drip irrigation methods can cause in many problems, particularly in highly saline soils (Darwish et al., 2005). Therefore, when designing a drip irrigation system for planting crops in saline-alkali soils, the amount and timing of drip irrigation must be carefully optimized.

Proper management and evaluation of drip irrigation requires a good understanding of salt movement patterns and crop water consumption. However, the mechanism of this water-salt transport is not well understood, especially because research on the strong variability of soil moisture and salinity at the spatial and temporal levels is lacking. Therefore, it is an urgent need to study the distribution characteristics and laws of soil moisture and salinity under different irrigation methods. To improve the theory of water-salt movement and drip irrigation regulation, and realize the sustainable development and utilization of saline soil by drip irrigation technology, this study carried out field experiments on salinized soils of different degrees in the Yellow River Irrigation Area of Ningxia. This study mainly focused on: 1) the spatial and temporal dynamic transport of soil water and salt under drip irrigation, 2) plant responses to different drip irrigation systems, and 3) clarifying the desalination mechanism under drip irrigation scheduling.

## 2 Methods and materials

### 2.1 Site description

The experiment was carried out in the Saline Land Water-saving and Salt-control Technology Demonstration Area (38°84'N, 106°57'E, 1,100 m), in Pingluo County, Ningxia Hui Autonomous Region, Northwest China. The whole region has a temperate continental semi-arid climate, with an annual average temperature of 9.5 °C, a minimum temperature of −22.6 °C, and a maximum temperature of 37.8 °C. The annual sunshine hours were 2,900 h, and the frost-free period was 180 days. The mean annual precipitation and potential evaporation (PE) were 180 mm and 1900 mm, respectively. The soil type was saline-irrigated silt with a medium loam texture. The physical and chemical properties of the initial soil are listed in Table 1. Before the experiment, the groundwater had an average depth of 1.4 m, a pH of 8.4, and an electrical conductivity (EC) of 15 dS m<sup>−1</sup>.

### 2.2 Experimental design

The experiment was conducted from April 2022 to September 2022, and the test crop was silage maize (*Zea mays* L.) of variety Dajingjiu 26. The planting method was set in wide (60 cm) and narrow (40 cm) with a planting density of 22 × 50 cm (Figure 1). Based on the local traditional irrigation quota and fertilization habits, four treatments were set up: 1) CK (traditional flood irrigation, 900 mm of irrigation during the growth season), 2) W1 (360 mm of drip irrigation during the growth season), 3) W2 (450 mm of drip irrigation throughout the growing season), and 4) W3 (540 mm of drip irrigation throughout the growing season). Each treatment was repeated three times, and a total of 12 plots (randomly arranged) were set up with an area of 20 × 20 m<sup>2</sup>.

### 2.3 Fertilization management and irrigation scheduling

The flood irrigation treatment (CK) used urea, superphosphate, and potassium sulfate as fertilizers. The amounts of N, P, and K were 400 kg N ha<sup>−1</sup>, 200 kg P<sub>2</sub>O<sub>5</sub> ha<sup>−1</sup>, and 225 kg K<sub>2</sub>O ha<sup>−1</sup>, respectively, of which 65% N was used as base fertilizer and 35% as topdressing. Rotary tillage was carried out at a depth of 20–25 cm immediately after the application of base fertilizer. The remaining urea was top dressed twice during the maize growth period as required. The drip irrigation treatments (W1, W2, and W3) used water-soluble fertilizer (24-12-14) specialized for maize drip irrigation. There were 10 times of irrigation in the maize growing season, including 7 times of drip irrigation fertilization. The total fertilization amount was the same as that of CK, and the specific fertilization and irrigation were shown in Table 2.

Irrigation water was pumped from an irrigation canal connected to the Yellow River with a pH, EC, and SAR<sub>e</sub> of 7.5, 0.8 dS m<sup>−1</sup>, and 1.87 mmol L<sup>−1</sup>, respectively. The drip irrigation system was composed of a solenoid valve, pressure meter, flow meter, screen

TABLE 1 Basic physical and chemical properties of the initial soil.

Soil layer	Soil mechanical composition (%)			Soil bulk density	EC <sub>e</sub>	pH	SAR <sub>e</sub>
(cm)	<0.002 mm	0.002–0.05 mm	0.05–2 mm	(g cm <sup>-3</sup> )	(dS m <sup>-1</sup> )		(mmol L <sup>-1</sup> )
0–10	0.82	90.76	8.42	1.36	2.81	8.62	21.87
10–20	0.44	94.33	5.23	1.46	2.74	8.73	21.64
20–30	1.13	91.36	7.52	1.46	2.65	8.64	21.41
30–40	1.22	86.58	12.20	1.55	2.45	8.52	21.20
40–50	0.96	88.98	12.06	1.57	2.47	8.68	21.42
50–60	0.67	87.89	11.44	1.53	2.40	8.50	20.80
60–70	0.77	82.83	18.40	1.58	2.38	8.65	20.99
70–80	0.84	74.52	24.64	1.56	2.26	8.46	20.36
80–90	1.32	71.48	29.20	1.58	2.24	8.63	20.54
90–100	1.75	65.64	32.61	1.55	2.14	8.47	19.92

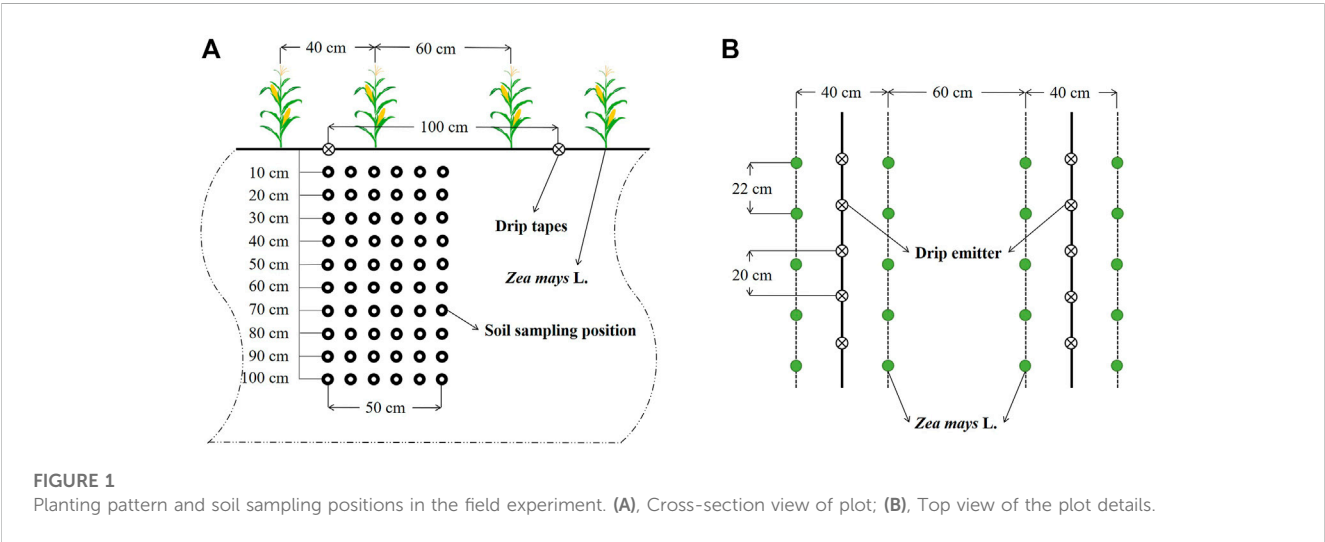


TABLE 2 Irrigation and fertilization during growing seasons of maize (*Zea mays* L.).

Treatment	Irrigation amount during growing seasons of maize (mm)					Fertilization rates(kg ha <sup>-1</sup> )		
	Seedling	Jointing	Flowering	Maturation	Total	N	P <sub>2</sub> O <sub>5</sub>	K <sub>2</sub> O
CK	180	270	270	180	900	400	200	225
W1	70	110	110	70	360	400	200	225
W2	90	135	135	90	450	400	200	225
W3	110	160	160	110	540	400	200	225

filter, fertilizer tank, and drip lines. Each treatment (three plots) was independently installed using a drip irrigation field control system to control the irrigation quota. Drip irrigation pipes were arranged in narrow rows, with one pipe for every two rows of maize (Figure 1).

The distance between the drip irrigation emitters was 20cm, and the flow rate of the emitters was 1.27 L h<sup>-1</sup>. As in the local high-yielding maize fields, field management included weeding and insecticide control.

## 2.4 Soil sample collection and analysis

The entire experimental period was divided into Stage A (end of April to end of May), Stage B (end of May to end of June), Stage C (end of June to end of July), and Stage D (end of July to early September) during the maize growing season to collect the soil samples. For each sample, sites near the drip emitter were randomly selected in each plot, and soil samples were collected using an auger with a diameter of 4.0 cm in and a height of 15 cm. Samples were collected at distances of 0, 10, 20, 30, 40, and 50 cm from the emitters, and at sampling depths of 10, 20, 30, 40, 50, 60, 70, 80, 90, and 100 cm (Figure 1). Sixty soil samples were obtained from each sampling site. The distribution of soil sampling points for the flood irrigation treatment was similar that of the drip irrigation treatments, with 60 soil samples were randomly selected from each plot. After removing the surface organic impurities and fine roots from fresh samples, the soil water content was determined using the oven-drying method. The remaining soil subsamples were air-dried and sieved through a 1 mm sieve, and then three replicates were mixed into one sample to make a saturated soil slurry extract using the standard method (Robbins and Wiegand, 1990). The pH and  $EC_e$  were measured using a conductivity meter (DDS-12A, REX) and a pH meter (PHS-3C, REX), respectively.  $Na^+$ ,  $Ca^{2+}$  and  $Mg^{2+}$  were measured using an inductively coupled plasma optical emission spectrometer (Optima 5300DV), and  $SAR_e$  (sodium adsorption ratio) was calculated as follows:

$$SAR_e = \frac{Na^+}{[(Mg^{2+} + Ca^{2+})/2]^{0.5}} \quad (1)$$

where the concentration of each cation is in  $mmol L^{-1}$ .

The soil desalination rate (SDR) was used to characterize the desalination process under different treatments:

$$SDR = \frac{S_0 - S_i}{S_0} \times 100\% \quad (2)$$

Where SDR is the soil desalination rate (%),  $S_0$  is the initial soil  $EC_e$  ( $dS m^{-1}$ ),  $S_i$  is the soil  $EC_e$  for each soil layer at different stages ( $dS m^{-1}$ ).

## 2.5 Plant sample collection and analysis

At the mature stage of maize, three maize plants were randomly selected from each plot to measure their plant height and stem diameter. In this way, nine maize plants are collected from each treatment, and a total of 36 maize plants are collected. After on-site measurement, the whole plant shall be sampled and transported back to the laboratory immediately, dried to constant weight at  $70^\circ C$ , measured the weight of dry matter and 1,000 grains on the ground, and then calculated the grain yield. Based on the aboveground dry matter mass and grain yield, the nutritional quality index of silage maize was calculated using the following formula:

$$N = Y/M \quad (3)$$

Where  $N$  is the nutritional quality index of silage maize (%),  $Y$  is the grain yield ( $kg ha^{-1}$ ), and  $M$  is the aboveground dry matter mass per unit area ( $kg ha^{-1}$ ). The water use efficiency in the maize growth

season was calculated according to the following equation (Zhang et al., 2019):

$$WUE = Y/ET \quad (4)$$

Where  $WUE$  is the water use efficiency ( $kg ha^{-1} mm^{-1}$ ),  $Y$  is the grain yield ( $kg ha^{-1}$ ), and  $ET$  is the maize evapotranspiration during the growth period (mm) calculated by the soil water balance equation (Zhang et al., 2019) as:

$$ET = I + P + \Delta S + G - R - L - E \quad (5)$$

Where  $ET$  is the maize evapotranspiration during the growth period (mm),  $I$  is the amount of irrigation (mm),  $P$  is the total precipitation (mm) collected by the field rain gauge.  $\Delta S$  is the change in soil water storage (mm) estimated using the space-weighted mean method,  $G$  is the contribution of groundwater (mm),  $R$  is the surface runoff (mm),  $L$  is the underground leakage (mm) calculated by soil leakage water monitor, and  $E$  is the evaporation of surface water (mm) monitored by the micro-Lysimeter evaporator. Because the terrain of the test area was flat and the average depth of maize roots was much greater than the average depth of groundwater,  $G$  and  $R$  were ignored in this study.

## 2.6 Statistical analyses

All data were recorded and classified in Microsoft Office Excel 2016, and analysis of variance (ANOVA) was performed using IBM SPSS Statistics ver.19.0 (IBM Co., Armonk, NY, United States). Tukey's honestly significant difference (HSD) test was used to determine significant differences between the means at  $p \leq 0.05$ . Figures were created using Origin 2022 (Origin Lab Co., Northampton, MA, United States).

## 3 Results

### 3.1 Soil moisture dynamic movement

Changes in the spatial distribution of soil moisture with sampling time are shown in Figure 2. The soil moisture distribution changed significantly with the irrigation measures, indicating that irrigation changed the soil moisture infiltration characteristics. In Stage A, the wetted area under the drip emitters of the drip irrigation treatments (W1, W2, and W3) expanded both horizontally and vertically, and the water content of the 0–40 cm soil layer under W1, W2, and W3 increased by 3.78%–27.09%, 3.17%–37.79%, and 6.86%–44.87%, respectively, compared with CK. At the end of Stages B, C, and D, the soil wet zone continued to expand horizontally and vertically, and the soil water content in the 0–100 cm soil layer increased by 3.13%–6.36%, 3.28%–8.51%, and 5.01%–9.35%, respectively, compared with Stage A. The soil water content in the 0–20 cm soil layer of the drip irrigation treatment was significantly higher than that of CK, and the W1, W2, and W3 treatments were 5.02%–17.88%, 7.36%–21.06%, and 13.79%–27.88% higher than that of CK, respectively. Overall, irrigation increased soil moisture, resulting in a vertical distribution of soil moisture being low at the top and

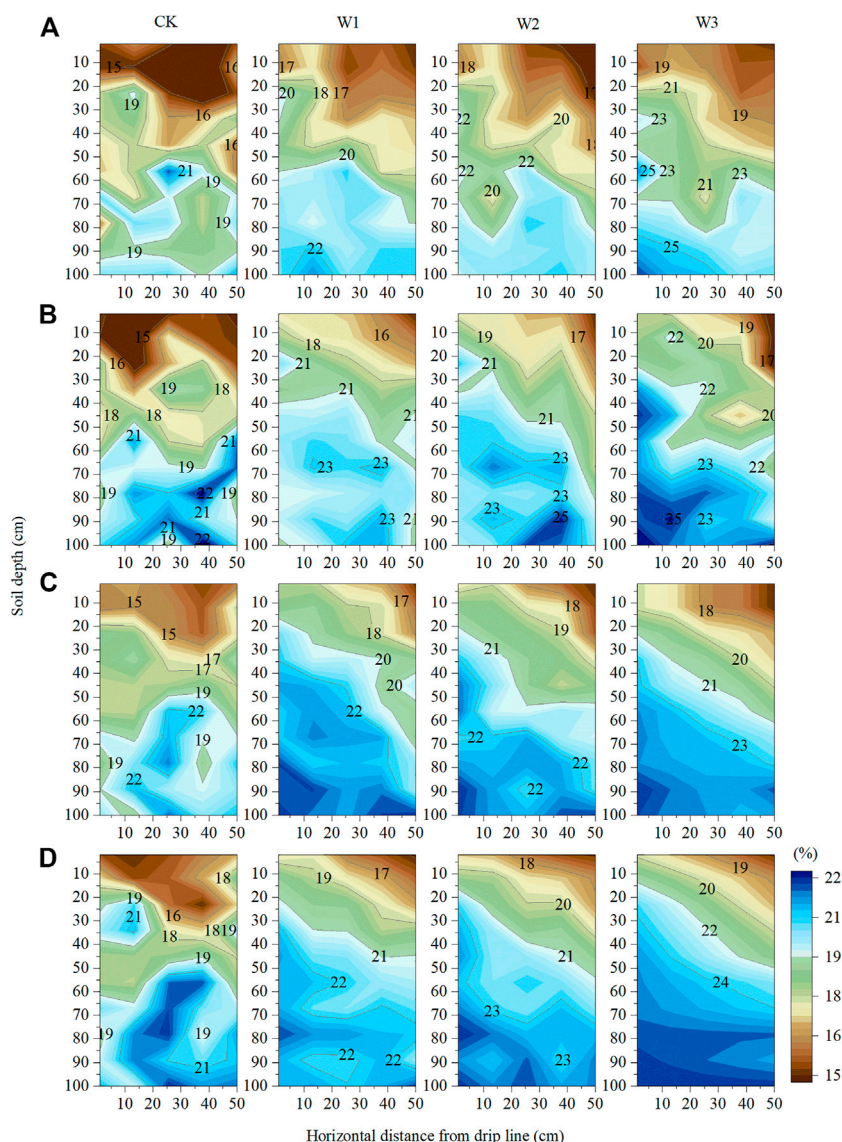


FIGURE 2

Spatial distribution of soil water (mass water content). (A), Stage A, end of April to end of May; (B), Stage B, end of May to end of June; (C), Stage C, end of June to end of July; (D), Stage D, end of July to early September.

high at the bottom. The water content of the shallow soil in the flood irrigation treatment was significantly lower than that in the drip irrigation treatment. This is because the frequent side flow of irrigation water causes strong surface evaporation, indicating that drip irrigation has a better effect on maintaining surface soil moisture.

### 3.2 Soil salinity dynamic movement

The spatial distribution of  $EC_e$  at different stages is shown in Figure 3, demonstrating the trend in soil salinity during the growing season. Soil moisture movement controls the redistribution of soil salts. Owing to the small amount of irrigation at Stage A, the soil salinity in the 0–40 cm soil layer of each treatment did not change much during this period. Nevertheless, starting from Stage B, the soil

salinity decreased sharply to lower levels in all treatments; in particular, the  $EC_e$  of the 0–20 cm soil layer in the W3 treatment decreased by 5.68% compared with other treatments. In Stage C, compared with the CK, the desalination zone gradually appeared 0–40 cm below the drip emitters in the drip irrigation treatments, and the soil salts gradually leached to the deep layer. At the end of Stage D, with continuous irrigation, the soil desalination zone continued to expand, and its lower boundary edge further moved from 30–50 cm to 70–90 cm. There was a clear decreasing trend in soil salinity in the 0–100 cm soil layer under the drip irrigation treatments. Compared with CK, the  $EC_e$  of 0–40 cm soil layer in W1, W2, and W3 decreased by 23.53%–32.57%, 26.49%–35.64%, and 26.30%–36.86%, respectively. In general, with the prolongation of the maize growth period, the soil salts gradually leached down with soil water infiltration under the drip irrigation treatments and gradually formed a desalination zone centered on the drip



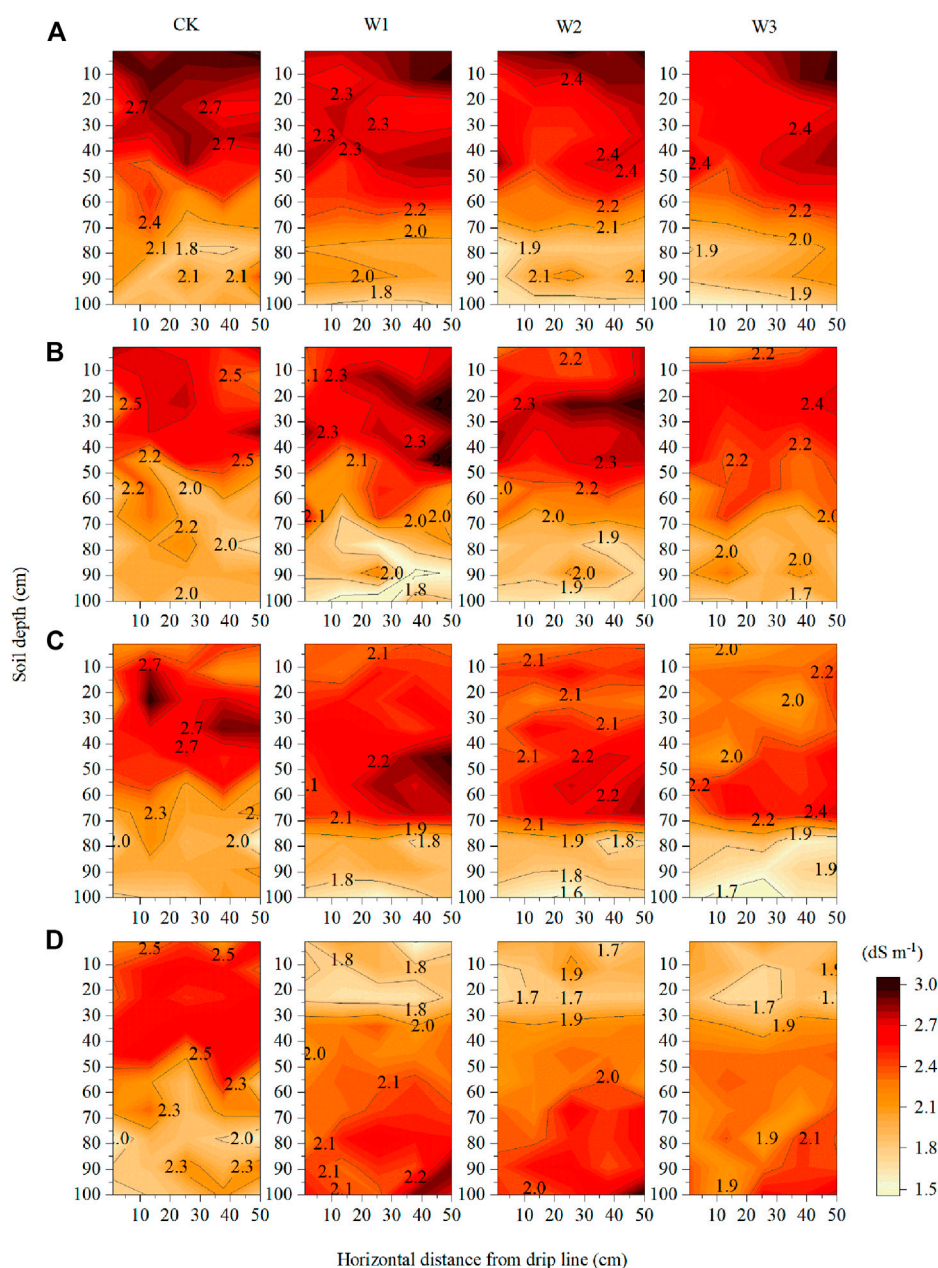


FIGURE 3

Spatial distribution of soil salinity (electrical conductivity of saturated extract). (A), Stage A, end of April to end of May; (B), Stage B, end of May to end of June; (C), Stage C, end of June to end of July; (D), Stage D, end of July to early September.

emitters. In contrast, the soil salt leaching rate of CK was lower, and the salt distribution was uneven.

### 3.3 Soil pH and sodium adsorption ratio

Table 3 shows the trends in soil pH and SAR<sub>e</sub> at the later stage of the field trial (end of Stage D). Except for the 10–20 cm soil layer, the drip irrigation treatments significantly reduced the soil pH value of each soil layer by 0.72%–2.13%, 0.83%–3.33%, and 0.81%–3.39% in W1, W2, and W3, respectively, compared with CK. When irrigation

water removed salts from the surface soil, the pH of the 0–40 cm soil layer was significantly higher than that of the 40–80 cm soil layer. Similar to the soil EC<sub>e</sub>, it showed the vertical distribution characteristics of low salt content in the upper soil layer and high salt content in the lower soil layer as a whole, and the deep soil layer SAR<sub>e</sub> was significantly higher than that of the shallow soil. The soil SAR<sub>e</sub> values of the drip irrigation treatments were significantly lower than those of CK by 1.4%–6.63% (W1), 1.63%–7.02% (W2), and 1.43%–7.02% (W3). Consequently, the effect of salt washing of drip irrigation was positive, but the difference between the drip irrigation treatments was insignificant.



TABLE 3 Soil pH and sodium adsorption ratio of different soil layers.

	Soil layer (cm)	Treatment			
		CK	W1	W2	W3
pH	0-10	8.52dA	8.34eB	8.34eB	8.32eB
	10-20	8.37fA	8.38dA	8.38dA	8.37dA
	20-30	8.52bcdA	8.34eB	8.33eB	8.32eB
	30-40	8.48eA	8.34eB	8.33eB	8.32eB
	40-50	8.55abA	8.49abB	8.27fC	8.26fC
	50-60	8.52cdA	8.51aAB	8.49abB	8.49aB
	60-70	8.55abA	8.46cB	8.46cB	8.45cB
	70-80	8.57aA	8.50aB	8.49aBC	8.48abC
	80-90	8.54abcdA	8.47cB	8.47bcB	8.47bcB
	90-100	8.55abcA	8.47bcB	8.47bcB	8.47bcB
SAR <sub>c</sub> (mmol L <sup>-1</sup> )	0-10	17.90cA	16.76dB	16.76cB	16.75bB
	10-20	17.90cA	16.75dB	16.76cB	16.76bB
	20-30	17.93bcA	16.77dB	16.79cB	16.79bB
	30-40	17.90cA	16.71dB	16.71cB	16.72bB
	40-50	17.96abA	16.79cdB	16.7cB	16.7bB
	50-60	17.91bcA	17.04cB	17.30bB	17.04bB
	60-70	17.95abcA	17.34bB	17.34abB	17.41aB
	70-80	18.00aA	17.36bB	17.52abB	17.57aB
	80-90	17.94bcA	17.68aB	17.55abB	17.68aB
	90-100	17.96abA	17.67aB	17.67aB	17.67aB

Note: Different lowercase letters in the same column indicate significant differences between different soil layers, and different capital letters in the same row indicate significant differences between different irrigation patterns at  $p < 0.05$ .

### 3.4 Soil desalination

As illustrated in Table 4, there were significant differences in soil salinity and desalination rate in the different soil layers of each treatment. At the start of the field experiment, there were no significant differences in soil salinity between the treatments. At the later stage of the field experiment, there was a significant difference in the soil salts among the treatments. In the 0–10 cm, 10–20 cm, 20–30 cm and 40–50 cm soil layers, the soil salinity of the drip irrigation treatments was significantly lower than CK, but the difference was not significant between the drip irrigation treatments. As the soil layer deepened, the difference in soil salinity between treatments gradually decreased. Overall, the soil salinity of CK showed a trend of high up and low down, while that of the drip irrigation treatments showed the reverse trend. Compared with the drip irrigation treatments, the overall desalination efficiency of CK was lower, and the desalination rate of each soil layer was unevenly distributed, with an average of only 5.32%. The desalination rates of W1, W2, and W3 were 18.46%, 20.84%, and 22.94%, respectively. The drip irrigation treatments significantly reduced soil salinity in the tillage layer (0–40 cm), and the desalination rates were 32.45% (W1), 35.01%

(W2), and 36.23% (W3), respectively. Notably, with the deepening of the soil layer, the soil became denser, the porosity decreased, and the soil desalination rate gradually decreased. Especially in the 90–100 cm soil layer, the soil desalination rate became negative, and the soil salinity tended to increase.

### 3.5 Crop water consumption

As shown in Table 5, the soil water storage ( $\Delta S$ ) varied from 36.59 to 45.59 mm throughout the growing season, and there was no significant difference among the treatments. Compared with the flood irrigation treatment, the drip irrigation treatments produced uniform infiltration flow and reduced underground leakage ( $L$ ) by precisely controlling the volume and flow of irrigation water. Due to the frequent flow of surface irrigation water caused by large amounts of flood irrigation, the surface evaporation ( $E$ ) of CK was significantly higher than that of the drip irrigation treatments by 57.64%–68.29%, while there was no significant difference between the drip irrigation treatments. It can be seen that underground leakage and surface evaporation of CK accounted for 35.8% of

TABLE 4 Soil salinity and desalination rate of different soil layers.

Soil depth (cm)		Treatment			
		CK	W1	W2	W3
0-10	Initial soil salinity (g kg <sup>-1</sup> )	10.34aA	10.22aA	10.41aA	10.4aA
	Soil salinity at end of growth (g kg <sup>-1</sup> )	8.86abcA	6.39cB	6.25cdB	6.32 cB
	SDR (%)	14.37%	37.39%	40.01%	39.16%
10-20	Initial soil salinity (g kg <sup>-1</sup> )	9.91abA	9.93abA	9.87bA	9.94abA
	Soil salinity at end of growth (g kg <sup>-1</sup> )	9.42abA	6.48cB	6.26cdB	6.29cB
	SDR (%)	4.82%	34.69%	36.57%	36.70%
20-30	Initial soil salinity (g kg <sup>-1</sup> )	9.45cdA	9.42cA	9.5bcA	9.42bcA
	Soil salinity at end of growth (g kg <sup>-1</sup> )	9.45abA	6.15cB	5.86dB	5.73dB
	SDR (%)	−0.05%	34.60%	38.30%	39.17%
30-40	Initial soil salinity (g kg <sup>-1</sup> )	9.51bcdA	9.56bcA	9.41bcA	9.58bcA
	Soil salinity at end of growth (g kg <sup>-1</sup> )	9.85aA	7.35abB	7.04abcBC	6.71bcC
	SDR (%)	−3.60%	23.11%	25.17%	29.91%
40-50	Initial soil salinity (g kg <sup>-1</sup> )	9.63bcA	9.64bcA	9.59bA	9.65bcA
	Soil salinity at end of growth (g kg <sup>-1</sup> )	9.46abA	7.16bcB	7.32abB	7.15abB
	SDR (%)	1.59%	25.55%	23.72%	25.78%
50-60	Initial soil salinity (g kg <sup>-1</sup> )	9.13dA	9.2cA	8.99cdA	9.2cA
	Soil salinity at end of growth (g kg <sup>-1</sup> )	8.05cdeA	7.63abAB	6.88bcB	7.1abAB
	SDR (%)	11.87%	16.99%	23.47%	22.71%
60-70	Initial soil salinity (g kg <sup>-1</sup> )	8.54eA	8.56dA	8.5deA	8.55dA
	Soil salinity at end of growth (g kg <sup>-1</sup> )	8.18bcdA	7.62abAB	7.37abB	7.01abB
	SDR (%)	4.15%	10.99%	13.20%	17.97%
70-80	Initial soil salinity (g kg <sup>-1</sup> )	7.82fA	7.88eA	7.69fA	7.88efA
	Soil salinity at end of growth (g kg <sup>-1</sup> )	6.79eB	7.74aA	7.39abAB	7.09abAB
	SDR (%)	13.09%	1.77%	3.91%	9.89%
80-90	Initial soil salinity (g kg <sup>-1</sup> )	8.12efA	8.09deA	8.17efA	8.09deA
	Soil salinity at end of growth (g kg <sup>-1</sup> )	7.68cdeA	7.63abA	7.68aA	7.19abA
	SDR (%)	5.44%	5.62%	5.63%	11.11%
90-100	Initial soil salinity (g kg <sup>-1</sup> )	7.34gA	7.27fA	7.49gA	7.26fA
	Soil salinity at end of growth (g kg <sup>-1</sup> )	7.23deA	7.71abA	7.61abA	7.48 aA
	SDR (%)	1.51%	−6.08%	−1.59%	−3.01%
	Average soil desalination rate (%)	5.32%	18.46%	20.84%	22.94%

Note: Different lowercase letters in the same column indicate significant differences between different soil layers, and different capital letters in the same row indicate significant differences between different irrigation patterns at  $p < 0.05$ .

irrigation water and rainfall, significantly higher than W1 (32.61%), W2 (28.73%), and W3 (23.88%). Compared with traditional flood irrigation, drip irrigation significantly improved the water use efficiency of maize. The water use efficiency of W1 and W2 was the highest, reaching 23.88–25.68 kg ha<sup>-1</sup> mm<sup>-1</sup>, followed by W3, and CK was the lowest at only 15.98 kg ha<sup>-1</sup> mm<sup>-1</sup>.

### 3.6 Crop growth and yield

It can be seen from Table 6 that different treatments had no significant effect on maize plant height, stem diameter, and aboveground biomass, but the drip irrigation treatments significantly increased maize grain yield, with a general trend of

**TABLE 5** Maize (*Zea mays* L.) evapotranspiration components and water use efficiency.

Treatment	<i>I</i> (mm)	<i>P</i> (mm)	$\Delta S$ (mm)	<i>L</i> (mm)	<i>E</i> (mm)	$(L + E)/(I + P)$ (%)	ET (mm)	WUE (kg ha <sup>-1</sup> mm <sup>-1</sup> )
CK	900	169	40.16a	20.00a	424.3a	41.57a	664.8a	15.98c
W1	360	169	36.59a	11.33b	115.0b	32.61b	439.3d	25.68a
W2	450	169	45.59a	12.67b	134.7b	28.73b	517.3c	23.88a
W3	540	169	45.41a	15.00 ab	154.0b	23.88b	585.4b	21.37b

Note: *I* is the irrigation amount, *P* is the precipitation during the maize growing season,  $\Delta S$  is the change in soil water storage in the 0–100 cm soil layer, *L* is the underground leakage, *E* is the evaporation of surface water, ET is the maize evapotranspiration during the growth period, and WUE is the water use efficiency. Different lowercase letters in the same column indicate significant differences between treatments, as described below.

**TABLE 6** Maize (*Zea mays* L.) growth indicators in different treatments.

Treatment	Plant height (cm)	Stem diameter (mm)	Aboveground biomass (kg ha <sup>-1</sup> )	Grain yield (kg ha <sup>-1</sup> )	Nutritional quality index (%)	Grain yield increase rate over CK (%)
CK	287.8a	19.70a	57299a	10572c	18.47b	-
W1	292.2a	19.54a	58553a	11270bc	19.25ab	6.60%
W2	288.4a	20.42a	59549a	12349ab	20.74a	16.81%
W3	327.1a	19.90a	60101a	12509a	20.82a	18.32%

Note: Different lowercase letters in the same column indicate significant differences between different irrigation patterns at  $p < 0.05$ .

W3≥W2≥W1≥CK. Compared with CK, the grain yield increase rates of W1, W2, and W3 were 6.6%, 16.18%, and 18.32%, respectively, indicating that drip irrigation significantly increased maize grain yield, and the yield increase effect was better with the increase of irrigation quota. According to the calculation of the nutritional quality index from maize grain yield and aboveground biomass, the drip irrigation treatments significantly improved the nutritional quality of silage maize, and the nutritional quality indices of W2 and W3 were 10.73%–12.31%, and 11.30%–14.97% higher than that of CK, respectively. Thus, under the condition of high-frequency water-fertilizer drip irrigation, the water and fertilizer supply can better meet the water and fertilizer needs of maize growth, improving the grain yield and nutritional quality of silage maize.

## 4 Discussion

### 4.1 Soil desalination process

Irrigation schedules play an important role in controlling the soil moisture and salinity in irrigated arid areas (Ren et al., 2019). Many studies have been carried out in arid and semi-arid areas on the technology of combining drip irrigation with water and fertilizer to form a water-saving irrigation technology system (Zheng et al., 2016; Wang et al., 2018; Hou et al., 2019). In this study, the water content of the soil layers changed significantly with time under different irrigation patterns and gradually increased with increasing soil depth, demonstrating that the irrigation measures significantly improved the soil water infiltration performance. Compared with traditional flood irrigation, drip irrigation of medium and large volumes significantly increased the soil water content of shallow

(0–20 cm) and deep (70–100 cm) soils, indicating that high-frequency drip irrigation replenished the water loss of shallow soils due to high evaporation and transpiration in arid and semi-arid areas, thus maintaining the surface soil moisture at a high level (Dong et al., 2021). Therefore, the large amount of low-frequency irrigation water treated by flood irrigation and the high-frequency uniform irrigation water treated by drip irrigation may be the main reason for the difference in soil water content between the two treatments. The uniform and stable infiltration of irrigation water under drip irrigation increased the water content of deep soil and maintained the high content of soil water under the high evaporation climate environment. However, in the traditional flood irrigation treatment, owing to the large amount of irrigation water used simultaneously, the irrigation water tended to accumulate on the soil surface, which made the irrigation water prone to uneven underground leakage, which was not conducive to water infiltration and lead to uneven distribution of soil water (Figure 2). In addition, flood irrigation treatment resulted in evaporation loss of a large amount of water, increased evapotranspiration of farmland, reduced water use efficiency (Table 5) and wasted valuable water resources.

Soil water movement drives the diffusion of soil salinity, whereas  $EC_e$  reflects the total amount of soil ions, which decreases with the leaching of soil salts by drip irrigation (Qi et al., 2018; Su et al., 2022). Consistent with previous research (Dong et al., 2022), our study observed a significant decrease in soil salinity under drip irrigation as the irrigation intervention continued from stages A to D (Figure 3). This is because the soil salts were dissolved by the infiltrating water during the drip irrigation process, and the high-frequency underground leachate diffused downward smoothly, gradually forming a desalination zone centered on the drip emitter. This finding is consistent with

those of other studies showing that soil salts accumulate around the desalination zone under drip irrigation conditions (Burt and Isbell, 2005). One interesting finding is that with the infiltration of water, soil salinity gradually migrated to deeper soil layers, and the characteristics of soil salinity gradually changed from a surface aggregation pattern to a bottom accumulation pattern (Figure 3; Table 5), forming the vertical distribution characteristics of the upper lower and lower higher as a whole. A possible explanation for this might be that the blocked downward movement of salts was caused by the compacted and reduced porosity of the deep soil, and the close distance to the groundwater table, where the salts in groundwater can easily enter the soil through capillary action (Shah et al., 2011; Sun et al., 2022). Another important finding was the uneven distribution of water and soil salinity across soil layers under flood irrigation treatment, which indicating that under the flood irrigation condition, the irrigation water was easy to accumulate on the surface, and cannot form uniform underground seepage in the soil, resulting in the uneven distribution of salt in the soil, and ultimately reducing the soil desalination efficiency.

During the desalination process, the soil pH value decreased significantly in the 0–50 cm soil layer (Table 3), indicating that irrigation measures reduced shallow soil alkalization. In contrast to earlier findings (Dong et al., 2021), drip irrigation could increase the soil pH within a certain range by moving the soil salts. These differences may be partly explained by the fact that the change in pH was not only the result of an exchange reaction between  $H^+$  and  $Na^+$ , but also that the transport of soil moisture in the irrigated soil can change the multi-ion composition of the soil, thus affecting the change of soil pH; the specific reasons for this need to be further studied. In this study, with the extension of the maize growing season, the soil  $SAR_e$  decreased gradually (Table 3), which was similar to the distribution of soil  $EC_e$ . Previous studies have interpreted this phenomenon as that under saline water conditions, because  $Na^+$  has a lower charge and smaller hydration radius than  $Ca^{2+}$  and  $Mg^{2+}$ , it is less likely to be adsorbed by soil colloids and migrate downwards during drip irrigation (Zhao et al., 2019), so  $Na^+$  leaches more than  $Mg^{2+}$  and  $Ca^{2+}$  (White, 2005). Therefore, in the process of soil desalination in this study, more  $Na^+$  was leached and less  $Mg^{2+}$  and  $Ca^{2+}$  were washed away during the soil desalination process, resulting in a lower  $SAR_e$  calculated with  $Na^+$  as the numerator and  $Mg^{2+}$  and  $Ca^{2+}$  as the denominators. Furthermore, the  $SAR_e$  of each soil layer in the drip irrigation treatments was significantly lower than that in the flood irrigation treatment, indicating that the steady and continuous infiltration flow of drip irrigation accelerated the leaching of soil ions and significantly inhibited the process of soil salinization.

## 4.2 Plant responses

Water plays an indispensable role in plant growth, and improving water use efficiency in arid regions is an effective way to increase productivity (Qu et al., 2020). This study found that the surface evaporation of CK was nearly four times that of W1 (Table 5), indicating that the surface evaporation of traditional flood irrigation was greatly increased by frequent horizontal flow

because of the large amount of irrigation water spread on the farmland at one time. It is worth noting that the amount of underground leakage under flood irrigation was significantly higher than that under drip irrigation. The reason may be that the terrain of this area was flat, and there was no surface runoff during irrigation. Therefore, a large amount of flood irrigation water accumulated on the surface, causing uneven infiltration, damaging the soil structure, and forming gaps and tunnels connected with groundwater in many places, thus increasing the underground leakage flow. These gaps and tunnels were likely responsible for salts that had leached into the groundwater returning to the surface with transpiration at the end of the maize growth season, causing soil re-salinization (Li et al., 2021). However, under the drip irrigation treatment, the irrigation water conducted a small amount of high frequency drip irrigation on the soil, without surface water accumulation, maintaining the soil structure, so the underground seepage flow was low. Overall, nearly half (41.57%) of the total input water was lost from the farmland ecosystem in the diffuse irrigation treatment, which was significantly higher than that in the drip irrigation treatments, significantly reducing the water use efficiency. Similar to other studies in the dry and saline inland areas of Northwest China (Wang et al., 2012), this study found that drip irrigation treatments reduced deep leakage and surface evaporation, and improved the water use efficiency of farmland by uniformly distributing water and precisely controlling water volume.

In this experiment, maize varieties were used as silage. Plant height and stem diameter are the key characteristics of maize growth, and the quality of aboveground dry matter mass is an important indicator of maize silage yield (Rüegg et al., 1998), and the nutritional quality of silage maize depends on the proportion of grain yield and aboveground dry matter mass (Lima et al., 2022). This study found that there were no significant differences in plant height, stem diameter and aboveground dry matter mass between irrigation modes (Table 4); however, compared with the traditional flood irrigation, the drip irrigation treatments significantly increased the grain yield and improved the nutritional quality and economic value of silage maize. With the increase in irrigation amount, the yield increase effect of drip irrigation treatments was greater than that of the flood irrigation treatment. In addition, the water use efficiency of maize differed significantly between irrigation modes, with the highest water use efficiency achieved by small-volume drip irrigation, followed by medium-volume drip irrigation, large-volume drip irrigation, and flood irrigation treatment. In summary, the irrigation frequency, fertilizer ratio and application amount of irrigation water under the drip irrigation treatment were consistent with the law of fertilizer and water demand of maize (Fan et al., 2020). Drip irrigation treatments could provide sufficient nutrients and water for the middle and later stages of maize growth, promote the nutrient absorption of maize roots, reduce the evapotranspiration of farmland water, improve the water use efficiency of maize, thus improve the yield of maize and nutritional quality. In this test, it was found that the medium and large water drip irrigation treatment was the best in terms of soil water content,

salt content and maize yield. Compared with the traditional flood irrigation treatment, the soil water content under the medium and large water drip irrigation treatment was increased by 14%–21% (Figure 2), the soil salt was reduced by 21%–23% (Table 4), and the grain yield was increased by 17%–18% (Table 6). Therefore, the initial recommended irrigation water in Yellow River basin was 450–540 mm.

## 5 Conclusion

Drip irrigation significantly improves the infiltration performance of soil water. Through uniform infiltration of irrigation water and precise water and fertilizer control, soil salts were smoothly infiltrated into deeper soil, gradually forming a desalination zone centered on the drip emitter, which gradually changed the soil salinity characteristics from the surface aggregation mode to the bottom aggregation mode, thus significantly reducing surface evaporation and underground leakage, and improving water utilization efficiency and yield. In contrast, flood irrigation led to an uneven distribution of soil water and salt, poor desalination, and a significantly lower water use efficiency and yield than drip irrigation. Therefore, using drip irrigation with an appropriate irrigation volume in the Yellow River irrigated regions can achieve the goal of water saving and salt control, whilst effectively improving land productivity. However, our study was limited by the short duration of the research, which is only 1 year. Soil improvement in saline-alkali land is a long-term process. In the future, long-term and continuous drip irrigation is required to observe its long-term impact on soil structure, water, salinity and plant growth.

## Data availability statement

The raw data supporting the conclusion of this article will be made available by the authors, without undue reservation.

## References

- Ashraf, M. (2007). Variation in nutritional composition and growth performance of some halophytic species grown under saline conditions. *Afr. J. Range Forage Sci.* 24 (1), 19–23. doi:10.2989/102201107780178203
- Burt, C. M., and Isbell, B. (2005). Leaching of accumulated soil salinity under drip irrigation. *Trans. ASAE* 48 (6), 2115–2121. doi:10.13031/2013.20097
- Chhabra, R. (2004). Classification of salt-affected soils. *Arid Land Res. Manag.* 19 (1), 61–79. doi:10.1080/15324980590887344
- Darwish, T., Attallah, T., El Moujabber, M., and Khatib, N. (2005). Salinity evolution and crop response to secondary soil salinity in two agro-climatic zones in Lebanon. *Agric. Water Manag.* 78 (1–2), 152–164. doi:10.1016/j.agwat.2005.04.020
- Dong, S., Wan, S., Kang, Y., and Li, X. (2021). Establishing an ecological forest system of salt-tolerant plants in heavily saline wasteland using the drip-irrigation reclamation method. *Agric. Water Manag.* 245, 106587. doi:10.1016/j.agwat.2020.106587
- Dong, S., Wang, G., Kang, Y., Ma, Q., and Wan, S. (2022). Soil water and salinity dynamics under the improved drip-irrigation scheduling for ecological restoration in the saline area of Yellow River basin. *Agric. Water Manag.* 264, 107255. doi:10.1016/j.agwat.2021.107255
- Fan, J., Lu, X., Gu, S., and Guo, X. (2020). Improving nutrient and water use efficiencies using water-drip irrigation and fertilization technology in Northeast China. *Agric. Water Manag.* 241, 106352. doi:10.1016/j.agwat.2020.106352
- Gu, Y. Y., Zhang, H. Y., Liang, X. Y., Fu, R., Li, M., and Chen, C. J. (2022). Effect of different biochar particle sizes together with bio-organic fertilizer on rhizosphere soil microecological environment on saline-alkali land. *Front. Environ. Sci.* 1156. doi:10.3389/fenvs.2022.949190
- Guan, Z., Jia, Z., Zhao, Z., and You, Q. (2019). Dynamics and distribution of soil salinity under long-term mulched drip irrigation in an arid area of northwestern China. *Water* 11 (6), 1225. doi:10.3390/w11061225
- Hou, Y., Wang, Z., Ding, H., Li, W., Wen, Y., Zhang, J., et al. (2019). Evaluation of suitable amount of water and fertilizer for mature grapes in drip irrigation in extreme arid regions. *Sustainability* 11 (7), 2063. doi:10.3390/su11072063
- Li, Y., Li, M., Liu, H., and Qin, W. (2021). Influence of soil texture on the process of subsurface drainage in saturated-unsaturated zones. *Int. J. Agric. Biol. Eng.* 14 (1), 82–89. doi:10.25165/j.ijabe.20211401.5699
- Lima, L. M., Bastos, M. S., Ávila, C. L., Ferreira, D. D., Casagrande, D. R., and Bernardes, T. F. (2022). Factors determining yield and nutritive value of maize for silage under tropical conditions. *Grass Forage Sci.* 77 (3), 201–215. doi:10.1111/gfs.12575
- Liu, R., Kang, Y., Zhang, C., Pei, L., Wan, S., Jiang, S., et al. (2014). Chemical fertilizer pollution control using drip fertigation for conservation of water quality in Danjiangkou Reservoir. *Nutrient Cycl. Agroecosyst.* 98 (3), 295–307. doi:10.1007/s10705-014-9612-2
- Nortney, J., Christen, E., Ayars, J., and Jankowski, J. (2006). Occurrence and measurement of salinity stratification in shallow groundwater in the Murrumbidgee

## Author contributions

YW and RW contributed to the design of the study, and YW wrote the first draft of the manuscript. MG, HC, and XF conducted field sampling, laboratory analysis and statistical analysis. LW wrote sections of the manuscript. All authors contributed to manuscript revision, read, and approved the submitted version.

## Funding

This study was funded by the National key research and development program of China (2021YFD1900600).

## Acknowledgments

We would like to thank other Ningxia University students who participated in the field and data collection and were not listed in the author list.

## Conflict of interest

The authors declare that the research was conducted in the absence of any commercial or financial relationships that could be construed as a potential conflict of interest.

## Publisher's note

All claims expressed in this article are solely those of the authors and do not necessarily represent those of their affiliated organizations, or those of the publisher, the editors and the reviewers. Any product that may be evaluated in this article, or claim that may be made by its manufacturer, is not guaranteed or endorsed by the publisher.



- Irrigation Area, south-eastern Australia. *Agric. Water Manag.* 81 (1–2), 23–40. doi:10.1016/j.agwat.2005.04.003
- Pimentel, D., Berger, B., Filiberto, D., Newton, M., Wolfe, B., Karabinakis, E., et al. (2004). Water resources: Agricultural and environmental issues. *BioScience* 54 (10), 909–918. doi:10.1641/0006-3568(2004)054[0909:wraaei]2.0.co;2
- Qi, Z., Feng, H., Zhao, Y., Zhang, T., Yang, A., and Zhang, Z. (2018). Spatial distribution and simulation of soil moisture and salinity under mulched drip irrigation combined with tillage in an arid saline irrigation district, northwest China. *Agric. Water Manag.* 201, 219–231. doi:10.1016/j.agwat.2017.12.032
- Qu, W., Tan, Y., Li, Z., Aarnoudse, E., and Tu, Q. (2020). Agricultural water use efficiency—A case study of inland-river basins in northwest China. *Sustainability* 12 (23), 10192. doi:10.3390/su122310192
- Rajak, D., Manjunatha, M., Rajkumar, G., Hebbara, M., and Minhas, P. (2006). Comparative effects of drip and furrow irrigation on the yield and water productivity of cotton (*Gossypium hirsutum* L.) in a saline and waterlogged vertisol. *Agric. Water Manag.* 83 (1–2), 30–36. doi:10.1016/j.agwat.2005.11.005
- Ren, D., Wei, B., Xu, X., Engel, B., Li, G., Huang, Q., et al. (2019). Analyzing spatiotemporal characteristics of soil salinity in arid irrigated agro-ecosystems using integrated approaches. *Geoderma* 356, 113935. doi:10.1016/j.geoderma.2019.113935
- Robbins, C., and Wiegand, C. (1990). *Field and laboratory measurements*: Asce.
- Rüegg, W., Richner, W., Stamp, P., and Feil, B. (1998). Accumulation of dry matter and nitrogen by minimum-tillage silage maize planted into winter cover crop residues. *Eur. J. Agron.* 8 (1–2), 59–69. doi:10.1016/s1161-0301(97)00013-0
- Shah, S., Vervoort, R., Suweis, S., Guswa, A. J., Rinaldo, A., and Van Der Zee, S. (2011). Stochastic modeling of salt accumulation in the root zone due to capillary flux from brackish groundwater. *Water Resour. Res.* 47 (9). doi:10.1029/2010wr009790
- Stavi, I., Thevs, N., and Priori, S. (2021). Soil salinity and sodicity in drylands: A review of causes, effects, monitoring, and restoration measures. *Front. Environ. Sci.* 330, 712831. doi:10.3389/fenvs.2021.712831
- Su, F., Wu, J., Wang, D., Zhao, H., Wang, Y., and He, X. (2022). Moisture movement, soil salt migration, and nitrogen transformation under different irrigation conditions: Field experimental research. *Chemosphere* 300, 134569. doi:10.1016/j.chemosphere.2022.134569
- Sun, G., Zhu, Y., Gao, Z., Yang, J., Qu, Z., Mao, W., et al. (2022). Spatiotemporal patterns and key driving factors of soil salinity in dry and wet years in an arid agricultural area with shallow groundwater table. *Agriculture* 12 (8), 1243. doi:10.3390/agriculture12081243
- Wang, Z., Zhu, S., and Yu, R. (1993). *Saline soil in China*. Beijing: Science Press.
- Wang, R., Kang, Y., Wan, S., Hu, W., Liu, S., Jiang, S., et al. (2012). Influence of different amounts of irrigation water on salt leaching and cotton growth under drip irrigation in an arid and saline area. *Agric. Water Manag.* 110, 109–117. doi:10.1016/j.agwat.2012.04.005
- Wang, R., Wan, S., Kang, Y., and Dou, C. (2014). Assessment of secondary soil salinity prevention and economic benefit under different drip line placement and irrigation regime in northwest China. *Agric. Water Manag.* 131, 41–49. doi:10.1016/j.agwat.2013.09.011
- Wang, Z., Bian, Q., Zhang, J., and Zhou, B. (2018). Optimized water and fertilizer management of mature jujube in Xinjiang arid area using drip irrigation. *Water Sci. Technol.* 10 (10), 1467. doi:10.3390/w10101467
- White, R. E. (2005). *Principles and practice of soil science: The soil as a natural resource*. John Wiley & Sons.
- Xiong, S., Xiong, Z., and Wang, P. (1996). Soil salinity in the irrigated area of the Yellow River in Ningxia, China. *Arid Land Res. Manag.* 10 (1), 95–101. doi:10.1080/15324989609381423
- Zhang, T., Zhan, X., He, J., and Feng, H. (2019). Moving salts in an impermeable saline-sodic soil with drip irrigation to permit wolfberry production. *Agric. Water Manag.* 213, 636–645. doi:10.1016/j.agwat.2018.11.011
- Zhao, X., Xia, J., Chen, W., Chen, Y., Fang, Y., and Qu, F. (2019). Transport characteristics of salt ions in soil columns planted with *Tamarix chinensis* under different groundwater levels. *Plos One* 14 (4), e0215138. doi:10.1371/journal.pone.0215138
- Zheng, H., Chuan, L., Zhao, J., Sun, S., and Zhang, J. (2016). *Overview of water and fertilizer integration development*. Atlantis Press, 273–277.



## OPEN ACCESS

## EDITED BY

Kaibo Wang,  
Chinese Academy of Sciences (CAS),  
China

## REVIEWED BY

Zhenhong Wang,  
Guizhou University, China  
Yi Wang,  
Chinese Academy of Sciences (CAS),  
China

## \*CORRESPONDENCE

Andrew S. MacDougall,  
✉ asm@uoguelph.ca

RECEIVED 14 January 2023

ACCEPTED 06 April 2023

PUBLISHED 13 April 2023

## CITATION

Esch E and MacDougall AS (2023),  
Nitrogen addition enhances terrestrial  
phosphorous retention in  
grassland mesocosms.  
*Front. Environ. Sci.* 11:1144268.  
doi: 10.3389/fenvs.2023.1144268

## COPYRIGHT

© 2023 Esch and MacDougall. This is an  
open-access article distributed under the  
terms of the [Creative Commons  
Attribution License \(CC BY\)](#). The use,  
distribution or reproduction in other  
forums is permitted, provided the original  
author(s) and the copyright owner(s) are  
credited and that the original publication  
in this journal is cited, in accordance with  
accepted academic practice. No use,  
distribution or reproduction is permitted  
which does not comply with these terms.

# Nitrogen addition enhances terrestrial phosphorous retention in grassland mesocosms

Ellen Esch and Andrew S. MacDougall\*

Department of Integrative Biology, University of Guelph, Guelph, ON, Canada

Nitrogen (N) and phosphorus (P) are fundamental for plant biomass production in grasslands, are often co-limiting, and have become major freshwater pollutants. By factorially applying gradients of N and P to field-based grassland mesocosms, we tested for saturating thresholds of plant uptake as nutrients increase and whether simultaneous and potentially additive growing-season demand reduces flows of dissolved nutrients to subsurface leachate. We quantified the seasonality of nutrient losses, differences in uptake by functional group (grasses, forbs), the impacts of increasing nutrients on root:shoot ratios, and contrasted vegetated and unvegetated treatments to isolate edaphic influences. Overall, most added nutrients were retained by plants and soil—80% for N and 99% for P. Co-limitation dynamics were powerful but asymmetrical with N additions reducing P in leachate, but P having little influence on N. N retention was primarily influenced by season—most N was lost prior to peak biomass when plant demand was presumably lower. Nutrients reduced root:shoot ratios by increasing foliage but with no detectable effect on retention, possible because root biomass remained unchanged. Similarly, there was no impact of functional group on nutrient loss. Despite substantial plant uptake, leachate concentrations of N and P still exceeded regional levels for safe drinking water and prevention of algal blooms. This work reveals how nutrient co-limitation can accelerate the capture of P by N in grasslands, indicating that plant uptake can significantly reduce dissolved subsurface nutrients. However, the off-season flows of N and the failure to meet regional water-quality standards despite capture levels as high as 99% reveal that vegetative-based solutions to nutrient capture by grasslands are important but likely insufficient without complementary measures that reduce inputs.

## KEYWORDS

buffer strips, co-limitation, mesocosm, nutrient leaching, nutrient retention, sustainable agriculture

## Introduction

Nutrient retention by plants is a critical ecosystem function, especially given dramatic anthropogenic increases in the inputs of nitrogen (N) and phosphorous (P) (Cordell et al., 2009; Stevens et al., 2015). This includes agricultural fertilization, which has increased crop yields in the past century but with accelerating environmental impacts (Sobota et al., 2015; McCann et al., 2021). The sole intent of fertilization is to trigger yield increases in crops, but a “retention gap” often occurs where upwards of 30%–50% of annually applied soluble inorganic fertilizer can be lost to leaching or

volatilization (Bouwman et al., 2002; Good and Beatty, 2011; Mueller et al., 2012). This gap has resulted in N and P becoming major global pollutants, driven in part by their yearly addition to often nutrient-saturated farm soils (Drinkwater and Snapp, 2007). Reducing nutrient losses on farms will require a more complete understanding of the capacity for maximum plant uptake, by crops and by downslope amendments such as permanent-cover buffers (Blann et al., 2009; Noble et al., 2023).

The retention of N and P by plant uptake is often stoichiometrically regulated—they are required in combination and in different ratios, and are typically co-limiting such that the availability of one affects the uptake of the other (Elser et al., 2007; Harpole et al., 2011; Li et al., 2016). As such, the maximum capacity for plants to retain nutrients on farms may be determined in part by the availability of one or both nutrients (Greenwood et al., 2008; Hou et al., 2020). The power of N-P co-limitation for plant growth has been illustrated in global grasslands, with N-P additions on five continents increasing annual biomass by 48% compared to N alone (21% increase) and P alone (no detectable impact) (Carroll et al., 2022). This co-dependency suggests the potential for synergistic uptake, where their combined addition (as typically occurs in agriculture) triggers higher retention than would occur by adding one or the other in isolation. A challenge for maximizing co-dependent uptake, however, is that the magnitude and timing of uptake can vary widely by seasonal life stage (Niklas et al., 2005; Li et al., 2016; Deng et al., 2017; Jiang et al., 2019). Unfortunately, most farm nutrients are applied in single early-season pulses when plant demand is low. As well, uptake at peak biomass can be constrained in nutrient-saturated soils because resource limitations often shift to water, light, or other nutrients—declining root:shoot ratios may be associated with less nutrient demand (Harpole et al., 2017; Cleland et al., 2019). Given these complexities, the occurrence of “retention gaps” on farms is unsurprising, with more efficient and possibly complete utilization of soil nutrients by plants being dependent on the temporal dynamics of stoichiometric uptake that can be difficult to determine (e.g., Penuelas et al., 2012).

Here, we use field-based grassland mesocosms to test these issues, exploring resource co-limitation, plant uptake, and the retention of nutrients from entering subsurface leachate. Foremost we measure nutrient loss in leachate across factorial gradients of added N and P, using application rates comparable to intensive agriculture (range: 0–20 g m<sup>-2</sup>). We quantify whether co-limitation impacts on retention are explicitly related to how N and P combine to affect overall plant production, on allocation to roots *versus* shoots, on whether N and P demands vary seasonally based on reductions of nutrient loads in leachate, and whether community composition (7 species of grasses, 7 species of forbs including 4 legumes, or a 14 species mix of both) alters these outcomes. We partner these treatments with unvegetated mesocosms with or without nutrients, to untangle background effects of soil processes on N and P flow rates (Burwell et al., 1977; Noble et al., 2023). Finally, we explore management implications, focusing on how early-season application, temporal patterns of biomass production by grassland, and species composition variously shape leachate concentrations, relative to established groundwater standards derived to protect drinking water and prevent algal blooms.

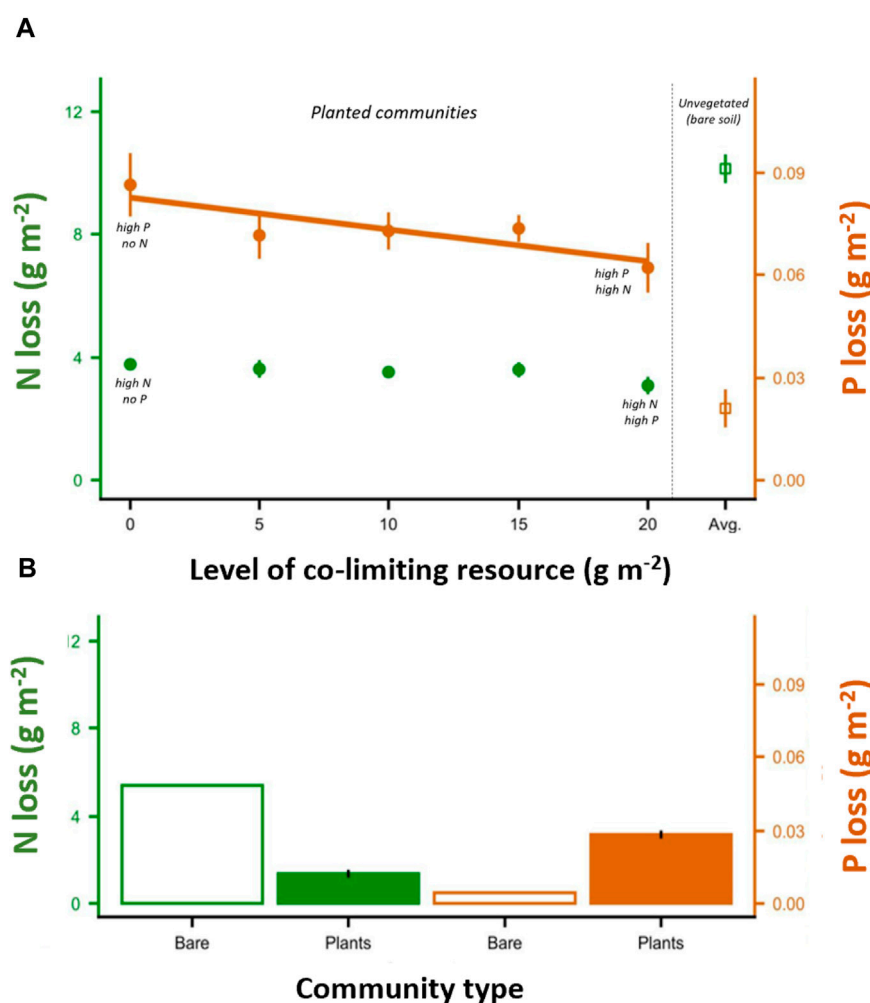
## Materials and methods

### Experiment design

Two hundred grassland mesocosms were established in 2018 with differing plant communities (4 levels including unvegetated) and nutrient additions (10 levels) at the rare Charitable Research Reserve (Cambridge, ON, Canada; 43° 22' N, 80° 21' W). Mesocosms were established in 19 L plastic buckets designed to capture leachate from the experimental plant communities (Supplementary Figure S1). A drainage spout was installed using a 50 cm 5/8" inner diameter hose at the base of each mesocosm. These mesocosms were filled 30 cm of soil on top of a 5 cm layer of 3/4" inch aggregate stone to facilitate drainage. Sieved soil was acquired from the top 20 cm of an agricultural field, retired in 2007 from long-term corn-soy-wheat rotations (Harvey and MacDougall, 2014; 2015; 2018). After 2007, succession happened naturally, and the site is now characterized by oldfield taxa especially *Solidago*, *Trifolium*, and *Symphyotrichum* spp. The soils are well-drained luvisolic St Jacobs Loams (Agriculture and Agri-Food Canada, 2004). Filled mesocosms were arranged so that the drainage hose fed via gravity into a hand-dug hole (Supplementary Figure S1). Collection bags were attached to the end of each drainage hose.

Mesocosms were seed planted on 5 June 2018, with one of three randomly allocated experimental grassland communities plus a no-plant control. Grassland communities were all grasses (7 species: *Bromus inermis*, *Dactylis glomerata*, *Echinochloa esculenta*, *Lolium multiflorum*, *Lolium perenne*, *Phleum pratense*, *Sorghum drummondii*), all grassland forbs including legumes (7 species: *Achillea millefolium*, *Brassica napus*, *Brassica oleracea*, *Medicago sativa*, *Trifolium hybridum*, *Trifolium pratense*, *Trifolium repens*), or a 14-species combination of both (referred to as “both” for brevity in the figures). The unvegetated control treatment was unplanted. Mesocosms were hand weeded to maintain community composition. After planting, all mesocosms were watered daily for 2 weeks including the unvegetated controls.

Ten nutrient treatments began on 19 June 2018 once seeds had germinated. The treatments had variable N levels with constant P (0, 5, 10, or 15 g N m<sup>-2</sup>; 20 g P m<sup>-2</sup>), variable P levels with constant N (20 g N m<sup>-2</sup>; 0, 5, 10, or 15 g P m<sup>-2</sup>), both N and P at high levels (20 g N m<sup>-2</sup>; 20 g P m<sup>-2</sup>), or control levels with no N and P added (0 g N m<sup>-2</sup>; 0 g P m<sup>-2</sup>). The gradients of nutrient addition were designed to encapsulate i) recommended rates for crop fertilization [16.2 g N m<sup>-2</sup> for corn (Ontario Ministry of Agriculture Food and Rural Affairs, 2018)], ii) levels of N and P commonly used in ecological nutrient studies [10 g N m<sup>-2</sup> and 10 g P m<sup>-2</sup> (Borer et al., 2017)], and iii) to maintain symmetrical levels of N and P addition. Fertilizer was added as urea (N) or triple super phosphate (P). After fertilizing, mesocosms were only watered to ensure plant survival. This was necessary in July which experienced a period without precipitation (Figure 1). As before, all mesocosms including the no-plant controls were equally watered. All watering events during this frame were adjusted to ensure that no water would percolate through the entire mesocosm and be lost as leachate. Treatments with plants (all grasses, all forbs, grasses and forbs) had 2 replicates per each nutrient treatment across 3 blocks for a total of 180 mesocosms (3 vegetated treatments X 10 nutrients treatments X 2 replicates X

**FIGURE 1**

Nutrient loss with shifting levels of co-limiting resources, for high P with increasing levels of N and for high N with increasing levels of P. For P, increasing levels of N reduces P levels in subterranean leachate (**A**). In contrast, N levels in leachate are unaffected by increased levels of P addition (**A**). For unvegetated mesocosms, N losses are significantly higher compared to vegetated mesocosms, indicating the importance of plant uptake on N (**A,B**). Unexpectedly, P levels in leachate were lower in mesocosms lacking vegetation (**A,B**). Error bars represent = 1 SE, and trendlines show significant linear relationships. In (**A**), N = 9 for mesocosms with plants, and N = 5 for bare soil mesocosms. In (**B**), N = 9 for mesocosms with plants, and N = 1 for bare soil.

3 blocks = 180). Treatments without plants had 2 replicates per nutrient treatment within only 1 block for a total of 20 mesocosms (180 + 20 = 200 total).

## Leachate sampling and processing

Leachate collection began starting 19 June 2018 and occurred three times, approximately every 3 weeks (**Figure 1**). Collections encompassed i) 19 June–10 July (21 days, 9.5 cm ambient precipitation), ii) 10 July–5 August (26 days, 8.0 cm), and iii) 5 August–22 August (17 days, 21.1 cm). Leachate was processed by lowering the pH to 2.0 with hydrochloric acid to preserve the sample until processing, and then refrigerated up to 48 h until analysis.

Leachate was analyzed for total N and total P at SGS Agri-Food Laboratories (Guelph, ON, Canada). Nitrogen was determined by

NO—cadmium reduction ([Standard Methods, 2006](#)) and Kjeldahl N ([Standard Methods, 2005](#)) to 0.05 mg/L. In some instances, the level

Of N present in the samples was below the detectable level of 0.5. In these cases, N was recorded

As 0 mg/L. Total P was determined by inductively coupled plasma—mass spectrometry (U.S. EPA. 1994) to 0.003 mg/L. Below the detection limit, P was recorded as 0 mg/L.

Total N and total P leached throughout the experiment was approximated by taking the product of each collection period's leachate nutrient concentrations by the maximum volume of leachate collected within the collection period. There was no difference in mean volume of leachate collected between the 4 communities at any collection date, and there was high correlation between the mean and maximum volume collected ( $r = 0.97$ ). Given that this experiment was not designed to precisely measure the volume of leachate, but rather the nutrient concentrations, the maximum volume at each date is used to reduce

any error associated with spillage of leachate in transportation to the laboratory. Statistical significance remained unchanged regardless if volume mean or max was used, or if total potential leachate (based on rainfall amount during each collection period) was used. This value is equivalent to a “loadings” basis to facilitate comparisons between this experiment and water quality reports and recommendations.

## Biomass harvesting

At the conclusion of the experiment, above- and below-ground biomass were harvested separately to obtain the aboveground:belowground ratio (AG: BG). The aboveground fraction was clipped at the soil surface, oven dried at 40°C for 48 h and weighed. Roots were collected by passing the entire mesocosm's soil through a sieve (1 mm diameter), after which collected roots were washed free of dirt, oven dried, and weighed. Biomass measurements are g per mesocosm, which is equivalent to  $0.07 \text{ m}^{-2}$ .

## Soil and plant chemistry

On a subset of the treatments (treatments =  $0 \text{ g N m}^{-2} + 0 \text{ g P m}^{-2}$ ;  $0 \text{ g N m}^{-2} + 20 \text{ g P m}^{-2}$ ;  $20 \text{ g N m}^{-2} + 0 \text{ g P m}^{-2}$ ;  $20 \text{ g N m}^{-2} + 20 \text{ g P m}^{-2}$ ), two soil cores (2.5 cm diameter, 10 cm depth) were collected at the conclusion of the experiment. Cores were stored at 4°C until analysis, sieved to remove roots and plant biomass, air dried, and homogenized using a coffee grinder. After processing, soil available P was determined using the Mehlich 3 procedure (Frank et al., 2012). Aboveground biomass collected from the same subset of treatments was homogenized using a Wiley Mill, after which we used a sulfuric acid digestion and determined foliar % P colorimetrically with ammonium molybdate (Ogdahl et al., 2013).

## Statistical analysis

Analyses were performed at the block-level, averaging over two replicate mesocosms for a total  $n = 100$  (90 experimental, 10 no-plant controls). Averaging was necessary to account for missing data, particularly during the second leachate collection time point during which multiple mesocosms did not produce leachate.

Analyses were performed on two different subsets of the 10 experimental fertilizer levels. The “variable N” experiment consisted of plots where N fertilizer levels varied (0, 5, 10, 15, 20  $\text{g N m}^{-2}$ ) and P fertilizer was held constant (always at 20  $\text{g P m}^{-2}$ ). The “variable P” experiment consisted of plots where P fertilizer levels varied (0, 5, 10, 15, 20  $\text{g P m}^{-2}$ ) and N fertilizer was held constant (always at 20  $\text{g N m}^{-2}$ ). Treatments where no N nor P was added were used as a comparative measure, similarly with plots with a no-plant addition control.

For the leachate analysis in mesocosms grown with plants, concentration of N and P at each time point was analyzed in a 2-way ANOVA where community type and fertilizer treatment were fixed factors. Above- and below-ground biomass and their ratio were also evaluated within the same 2-way ANOVA. Significance of all

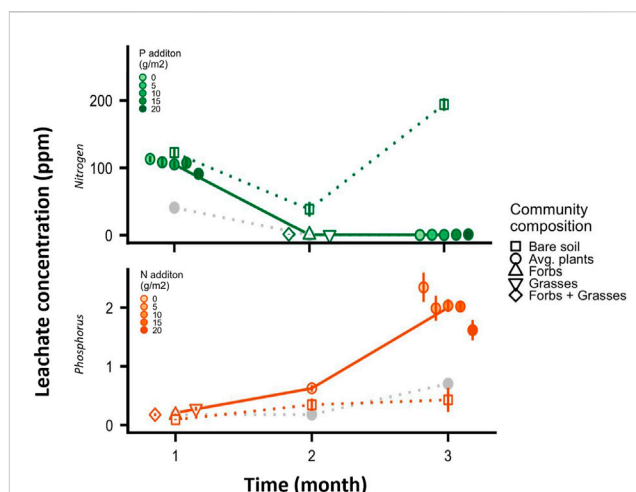


FIGURE 2

Average concentration by time of nitrogen and phosphorus in leachate, for N losses with increasing P addition and P losses with increasing N addition. Temporal patterns for bare soil mesocosms (square points) and nutrient control mesocosms (grey points,  $0 \text{ g N m}^{-2}$  and  $0 \text{ g P m}^{-2}$ ) are shown for comparative purposes. Error bars = 1 SE, and trendlines show the average trend in nutrient losses for the focal mesocosms (solid line) as well as the bare soil and nutrient controls (dashed). Most N was lost early in the year prior to peak plant growth, regardless of P levels. Most P was lost later in the growing season, when mesocosm biomass was at its peak.

factors was evaluated with Type II tests using the Anova function in the car package (Fox and Weisberg, 2011). When there was a significant community type  $\times$  nutrient interaction, separate linear models evaluating the effect of the variable nutrient on a response variable were run each community type. When there was a significant, main effect of community type, Tukey's post-hoc tests were run evaluating the response variable against the 3 community types.

We used a piecewise structural equation modeling (SEM) approach to assess the importance of biomass and leachate responses to fertilizer addition for each community type. Given that biomass production could play both explanatory and response roles, we used piecewise SEMs to disentangle the role of each variable (Grace et al., 2010). Specifically, we used the *piecewiseSEM* package (Lefcheck, 2016) to investigate how added N and P impacts nutrient retention via direct (fertilizer rate) and indirect (mediated by biomass uptake) pathways. We tested if community composition significantly varied, and finding a better association with an unconstrained model, we fitted unique models to each community type. In all cases, the initial model included the following links: 1) Total N leached is affected by N fertilizer rate, biomass production, and above:belowground ratio, 2) Total P leached is affected by P fertilizer rate, biomass production, and above:belowground ratio, 3) biomass production is affected by N and P fertilizer rates 4) above:belowground ratio is affected by N and P fertilizer rates. Importantly, our initial model did not include links between N addition and P loss, or P addition and N loss, because we had no *a priori* expectation, or any biological hypothesis, that would directly link these outcomes. After specifying our initial model, we refined our model by dropping non-significant links ( $p <$



0.05) in a stepwise fashion beginning with the least significant until the  $\Delta\text{AICc}$  between subsequent models was  $<2$ . Final model fits indicated good fit with the data for all communities (grasses: Fisher's  $C = 13.52$ ,  $p = 0.484$ ; forbs: Fisher's  $C = 10.5$ ,  $p = 0.398$ ; both: Fisher's  $C = 16.74$ ,  $p = 0.403$ ) where  $p$ -value  $>0.05$  indicates good model fit (Shipley, 2009). The relative importance of direct effects is given by standardized coefficients for each path, and indirect effects can be determined by multiplying standardized coefficients.

Data analyses were performed using R version 3.5.1 (R Core Team, 2018). Leachate levels were compared with regional standards for standing non-running surface water (Canada, 2004), of 10 ppm (comparable to 10 mg L<sup>-1</sup>) for N and 0.02 ppm (comparable to 0.02 mg L<sup>-1</sup>) for P. Both have been shown to be minimum thresholds for triggering significant impacts on drinking water quality and aquatic processes including algal blooms (see Noble et al., 2023).

## Results

### Regulation of N loss by treatment

Overall N loss was not influenced by P additions (Figure 1; Supplementary Table S1). Temporally, nearly all N loss occurred before grassland plants had reached maturity (Figure 2). The period of greatest N loss was during the first month (average 105.0 mg L<sup>-1</sup> in leachate across all treatments with 20 g N m<sup>-2</sup> added—Figure 2). During this period, we did see evidence of co-limitation dynamics where P additions slightly reduced N losses (Figure 2; Supplementary Table S1), but the effect was not sufficiently strong to influence overall N loss (Figure 1; Supplementary Table S1). Following the first month, leaching losses of N dropped (Figure 2, average 0.5 mg L<sup>-1</sup> loss for both the second and third month). During the second month, we saw that communities dominated by grasses had less leaching than communities with both grasses and forbs (Supplementary Table S1, Tukey's post-hoc,  $p = 0.046$ ). During the third month, adding P actually increased N leaching losses (Supplementary Table S1, linear post-hoc  $p = 0.009$ ). The nearly undetectable levels of N leaching during the second and third months, however, left the total N leaching losses unaffected by adding P or manipulating community composition (Supplementary Table S1). Supplemental results show that greater N additions meant more N loss overall, but the magnitude of this effect was much smaller than the overall temporal patterns linked to plant development and uptake (Supplementary Figure S2A; Supplementary Table S1). Bare soil mesocosms lost more N than did any treatment with plants present (Figure 1). N loss occurred even in mesocosms where no N was applied ( $\sim 2$  g m<sup>-2</sup> total throughout the experiment; Figure 1B, Figure 2A).

### Regulation of P loss by treatment

Overall P leaching was reduced by N additions (Supplementary Table S1; Figure 1A, brown points). This trend emerged after the first month (Supplementary Table S1). Temporally, P loss accelerated throughout the growing season (Figure 2B). During the first month, we found that grass communities had higher P

losses than those with only forbs (Supplementary Table S1, Tukey's post-hoc  $p = 0.027$ ) or with grasses and forbs growing together (Tukey's post-hoc  $p = 0.038$ ). Supplemental results show that adding more P meant greater P loss (Supplementary Figure S2B; Supplementary Table S1). Unexpectedly, bare soil mesocosms lost less P than did any treatment even with plants present—rather than retaining P by plant uptake, the presence of vegetation increased P loss to leachate (Figure 1).

## Functional groups and root:shoot allocation with nutrients

There was no overall effect of functional group on nutrient loss across our three experimental plant communities, although vegetation (compared to bare soil controls) consistently reduced N losses and facilitated P losses (Figure 1). The different functional groups did vary in the magnitude to which biomass production and allocation patterns mechanistically influenced overall nutrient leaching (Figure 3). In grass communities, N additions increased plant biomass that subsequently led to higher P demand and less P lost in leachate (Figure 3). In contrast, N additions had little direct effect on forb biomass production, and therefore did not influence overall P leaching (Figure 3). In all cases, fertilizer application shifted allocation towards greater relative investment in shoots (Figure 3). While relative reduced root allocation was a consequence of N addition, this did not result in increased N leaching likely because total root biomass did not change—changes to root:shoot ratios strictly involved changes in foliar biomass.

## Discussion

Overall, we observed significant retention of nutrients in mesocosm grassland, based on nutrients added as a one-time early-season input comparable to typical agricultural management. Nutrient concentrations detected in leachate during the growing season revealed the capture of  $\sim 80\%$  added N and  $\sim 99\%$  retention of added P. The mechanisms of retention, however, differed substantially and involved both vegetative and soil-based processes. First, the interaction between N and P were highly asymmetric—N additions reduced P leaching but there was no reciprocal effect of P additions on N loss. Second, there were significant temporal influences on both nutrients but in the opposite direction: nearly all N loss occurred before the mesocosm grassland had reached maturity while P loss was highest at peak biomass. Finally, we observed proportional linkages between higher application rates and greater leaching losses, especially for N. There was no overall effect of functional group among our three experimental plant communities. In total, our work shows that terrestrial nutrient retention can be immediately increased by establishing permanent vegetation cover and leveraging co-limitation dynamics to maximize biomass production—plants reduced N leaching to negligible levels as they matured, with N-driven biomass growth creating greater P demands and therefore reduced P leaching. On the other hand, despite these trends, nutrient concentrations in

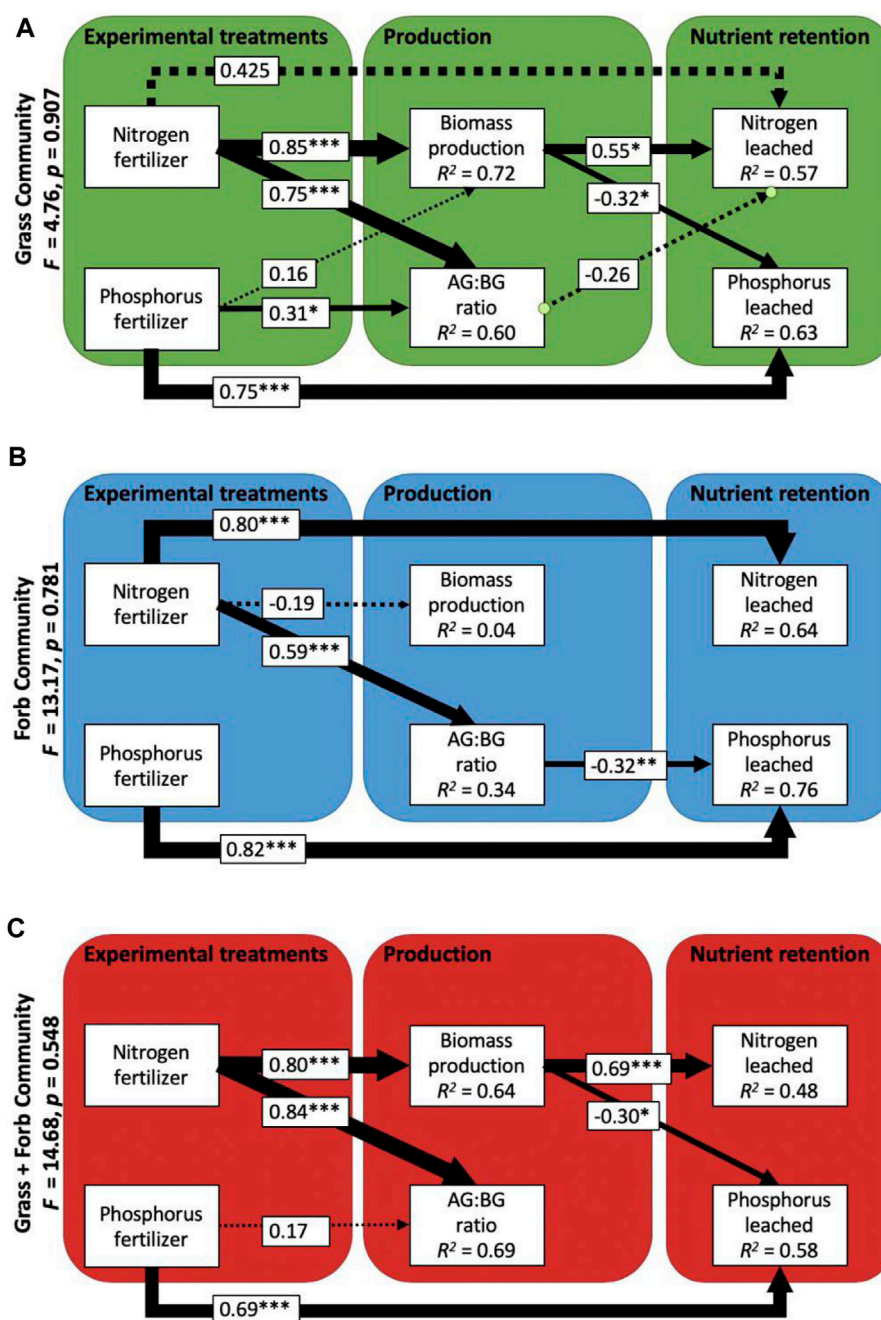


FIGURE 3

Best-fit path models showing the links between experimental N and P additions, biomass production, ratios between above and belowground biomass (AG: BG), and amounts of N and P leached within the grass (A), forb (B) and grass + forb (C) communities. Arrow thickness is proportional to the standardized path coefficients, with the directionality and size given within boxes along the arrow. Asterisks indicate significance level of linkages (\* $<0.05$ , \*\* $<0.01$ , \*\*\* $<0.001$ ), and dashed lines are used when significance of paths is  $>0.05$ .  $R^2$  values are given within the boxes containing endogenous variables.

leachate still exceeded regional standards for water quality (even with  $\sim 99\%$  capture of P). These results strongly suggest that nutrient uptake by grasslands, while highly effective (e.g., planted riparian grassland buffers), is unlikely to stem nutrient losses in conventional agriculture, without complementary measures that reduce the amounts added and adjust the time of application towards periods of peak plant activity.

We observed strikingly different models of nutrient retention for N and P, both functionally and temporally. For N, plant maturity was the largest factor controlling retention, such that low plant biomass early in the growing season coincided with the greatest losses to leachate. Early season leachate concentrations for N, sometimes exceeding  $105 \text{ mg L}^{-1}$ , were well above recommended guidelines for safe drinking water ( $<10 \text{ mg L}^{-1}$ ) (Canada, 2019).

Following the first month, leaching losses of N dropped to negligible levels (average  $0.5 \text{ mg L}^{-1}$  loss for both) in accordance with previous work showing that inorganic N is readily taken up by phenologically active plants (Hooper and Vitousek, 1998).

During the second month, we saw that communities dominated by grasses had slightly lower leaching than communities with both grasses and forbs, potentially because grasses may have had faster root biomass production than forbs although this was not tested. The nearly undetectable levels of N leaching during the second and third months, however, left the total N leaching losses unaffected by adding P or community composition. Our soils do not appear to be strongly P limited given that P addition did not significantly increase biomass production, so perhaps it is not surprising that P additions did not reduce N loss. The ability of plants to uptake N, and therefore reduce leaching losses throughout a growing season, was contrasted by the patterns seen in the bare soil mesocosms. Not surprisingly, fertilized bare soil lost up to 2.5 x more N than any treatment with plants present.

Temporally, total N loss corresponded in part with precipitation, with the first and third collection dates associated with appreciably more rainfall than the second (Supplementary Figure S3). This observation aligns with previous work showing that precipitation pulses can facilitate nutrient movement during the growing season (Congreves et al., 2016; Bowles et al., 2018; Noble et al., 2023). Finally, N loss to leachate occurred even in mesocosms where no N was applied. Soil used in this experiment had been farmed and fertilized for decades until 2007, suggesting nutrient legacies given that nutrient cessation occurred more than a decade prior to our experiment (see also Mazzorato et al., 2022). They may also reflect N loss associated with microbial decomposition (e.g., Craine et al., 2007), although we did not quantify N volatilization rates. Regardless, these results for N loss suggest that retention is best maximized by the presence of mature, phenologically active vegetation.

For P, in nearly all cases including both vegetated and unvegetated mesocosms, retention was at least 99% based on the difference between levels of fertilization and levels measured in leachate. This finding supports previous reports of P being typically less mobile than N via binding to soil (Burwell et al., 1977; Noble et al., 2023). However, three notable findings emerged from our work, despite the high levels of retention for P. Foremost, we found that overall P loss was reduced by N additions suggesting strong nutrient co-limitation. There were lower levels of P remaining in the soil at the conclusion of the experiment when N was added (Supplementary Figure S4), showing that N additions further limit P leaching losses. Mechanistically, more plant biomass (driven by N additions) likely meant higher demand, and thus uptake, for P. Alternatively, N additions have been shown to increase root and soil phosphatase activity (Marklein and Houlton 2012; Deng et al., 2017), which can also facilitate plant P uptake although we did not evaluate enzyme production here. While foliar plant %P was reduced with added N (Supplementary Figure S5), accounting for additional biomass production meant that P held in plant tissues was still greater when N was added. The temporal signature of P loss reinforces that biomass production demands P, and compliments previous findings of widespread N and P co-limitation on primary production (Elser et al., 2007; Harpole et al., 2017; Carroll et al.,

2022). It also provides new evidence that co-limitation dynamics can impact nutrient retention in nutrient-rich systems.

Second, we found that plants appeared to facilitate small amounts of P loss based on comparisons with bare-soil mesocosms. Given the sensitivity of P solubility to pH (e.g., Penn and Camberato, 2019), one possible explanation is the acidification of the rhizosphere by plant activity. Plant-derived acidification can occur by a range of possible mechanisms, including ammonium uptake, root exudation, and oxidization (Hinsinger, 2001). Consequentially, this may lead to greater P loss later once plants have developed root systems, an effect that may be magnified in the relatively confined area of the mesocosm containers (Supplementary Figure S1). This effect also appears to vary by vegetation type. During the first month, we found that grasses had higher P losses than communities grown with only forbs or with grasses and forbs, potentially because grass dominated communities established roots more quickly. An alternative possibility for unexpectedly high flows of P to subsurface water is macropores, which can form on clay-dominated soils during periods of summer drought (Noble et al., 2023). However, none were observed in our mesocosms.

Third, regardless of P retention approaching 100% the quantity of P leached from the system still exceeded levels necessary to maintain uncontaminated freshwater based on a threshold of  $0.02 \text{ mg L}^{-1}$  (Canada, 2004). This was true even when supplemental P was not added to the mesocosms—during the third month, P averaged  $2.0 \text{ mg L}^{-1}$  in leachate with fertilization and  $0.60 \text{ mg L}^{-1}$  without. While surface flows and sediment loss are the primary mechanisms by which P moves from terrestrial to aquatic systems (Gaynor and Findlay, 1995), these results show that P loss via leaching pathways cannot be disregarded as a threat to water quality (Noble et al., 2023). Given that we saw that adding more P fertilizer meant more P loss (Supplementary Figure S1B), we conclude that P leaching can be lowered by reducing P inputs.

The strong connection between plant growth and nutrient uptake is to be expected, given the need for both N and P for photosynthesis. However, we did not observe higher retention with greater functional group richness despite predictions that niche complementarity may elevate community-level nutrient foraging (Tilman et al., 1997; Cardinale et al., 2011). The greatest driver of vegetative-based retention was whether the plant community was present or absent, with the functional composition of our three communities being relatively unimportant. We did see some limited trends relating the presence of grasses or forbs. Communities grown with grasses had stronger biomass responses to N fertilizer additions, which subsequently was linked to less P loss via greater plant demand and uptake for P. In contrast, N additions had little direct effect on forb biomass production, and therefore did not influence overall P leaching. The forb community contained several N fixing species, which may have contributed to the lower sensitivity of biomass production to added N (You et al., 2017). Fertilizer application also shifted allocation towards greater relative investment in shoots, would be expected as mineral nutrient additions increased (Bloom et al., 1985; Ziter and MacDougall, 2013; Borer et al., 2014; Cleland et al., 2019; Eskelinen et al., 2022). However, this did not result in increased N leaching possibly because root biomass remained unchanged.

To conclude, these results reveal the potential for herbaceous vegetation to capture large percentages on dissolved plant-available

forms of N and P at shallow depths in soils (30 cm deep), including feedbacks where higher N triggers elevated uptake of P (Cooper et al., 2017). This is consistent with numerous studies showing the effectiveness of farm and forest buffers for nutrient capture (e.g., Blann et al., 2009; Weigelhofer et al., 2012; Noble et al., 2023). It also reveals a paradoxical dynamic where nutrient additions could potentially act to stem nutrient losses in some circumstances, at least for dissolved P (Yang et al., 2018). Our factorial isolation of the relative effects of vegetation and soil was helpful to isolate retention mechanisms, given that non-vegetative factors can also seasonally affect nutrient flows (e.g., drought-soil interactions in summer). Our non-vegetative plots showed that higher N flows occurred even without N addition, while also showing unexpectedly lower flows with P compared to vegetated mesocosms. The former is consistent with findings of high influxes of dissolved nutrients into open waters when plants are seasonally inactive (Noble et al., 2023). Finally, we also observed that nutrient concentrations in leachate often exceeded regional water-quality standards even with P capture at 99%. Clearly, vegetation alone cannot solve nutrient losses on managed landscapes unless partnered with measures that better match peak uptake with the timing, amount, and ratio of added nutrients (Noble et al., 2023).

## Data availability statement

The raw data supporting the conclusion of this article will be made available by the authors, without undue reservation.

## Author contributions

All authors contributed to the study conception and design. EE, assisted by AM, conceived the ideas and designed methodology; EE collected and analysed the data; EE and AM co-wrote the

manuscript. All authors contributed critically to the drafts and gave final approval for publication.

## Acknowledgments

We thank Kristin Doherty, Bernal Arce, Lauren Janke, Daniel Noble, Brock Roth, and the *rare* Charitable Research Reserve. Support provided by the Food From Thought research program funded by a Canada First Research Excellence Fund to the University of Guelph.

## Conflict of interest

The authors declare that the research was conducted in the absence of any commercial or financial relationships that could be construed as a potential conflict of interest.

## Publisher's note

All claims expressed in this article are solely those of the authors and do not necessarily represent those of their affiliated organizations, or those of the publisher, the editors and the reviewers. Any product that may be evaluated in this article, or claim that may be made by its manufacturer, is not guaranteed or endorsed by the publisher.

## Supplementary material

The Supplementary Material for this article can be found online at: <https://www.frontiersin.org/articles/10.3389/fenvs.2023.1144268/full#supplementary-material>

## References

- Agriculture and Agri-Food Canada (2004). *Canadian soil information system: National soil database*. Canada: Agriculture and Agri-Food Canada.
- Blann, K. L., Anderson, J. L., Sands, G. R., and Vondracek, B. (2009). Effects of agricultural drainage on aquatic ecosystems: A review. *Crit. Rev. Environ. Sci. Tech.* 39, 909–1001. doi:10.1080/10643380801977966
- Bloom, A. J., Chapin, F. S., and Mooney, H. A. (1985). Resource limitation in plants - an economic analogy. *Annu. Rev. Ecol. Syst.* 16, 363–392. doi:10.1146/annurev.es.16.110185.002051
- Borer, E. T., Grace, J. B., Harpole, W. S., MacDougall, A. S., and Seabloom, E. W. (2017). A decade of insights into grassland ecosystem responses to global environmental change. *Nat. Ecol. Evol.* 1, 0118. doi:10.1038/s41559-017-0118
- Borer, E. T., Seabloom, E. W., Gruner, D. S., Harpole, W. S., Hillebrand, H., Lind, E. M., et al. (2014). Herbivores and nutrients control grassland plant diversity via light limitation. *Nature* 508, 517–520. doi:10.1038/nature13144
- Bouwman, A. F., Boumans, L. J. M., and Batjes, N. H. (2002). Estimation of global NH<sub>3</sub> volatilization loss from synthetic fertilizers and animal manure applied to arable lands and grasslands. *Glob. Biogeochem. Cycles* 16, 8–1–8–14. doi:10.1029/2000gb001389
- Bowles, T. M., Atallah, S. S., Campbell, E. E., Gaudin, A. C. M., Wieder, W. R., and Grandy, A. S. (2018). Addressing agricultural nitrogen losses in a changing climate. *Nat. Sustain.* 1, 399–408. doi:10.1038/s41893-018-0106-0
- Burwell, R. E., Schuman, G. E., Heinemann, H. G., and Spomer, R. G. (1977). Nitrogen and phosphorus movement from agricultural watersheds. *J. Soil Water Conservation* 32, 226–230.
- Canada, E. (2004). *Canadian guidance framework for the management of phosphorus in freshwater systems*. Ottawa: Environment Canada. Ecosystem health: Science-based solutions
- Canada, G. (2019). *Guidelines for Canadian drinking water quality: Guideline technical document-nitrate and nitrite*. Canada: Agriculture and Agri-Food Canada.
- Cardinale, B. J., Matulich, K. L., Hooper, D. U., Byrnes, J. E., Duffy, E., Gamfeldt, L., et al. (2011). The functional role of producer diversity in ecosystems. *Am. J. Bot.* 98 (3), 572–592. doi:10.3732/ajb.1000364
- Carroll, O., Batzer, E., Bharath, S., Borer, E. T., Campana, S., Esch, E., et al. (2022). Nutrient identity modifies the destabilising effects of eutrophication in grasslands. *Ecol. Letts* 25, 754–765. doi:10.1111/ele.13946
- Cleland, E. E., Lind, E. M., DeCrappeo, N. M., DeLorenzo, E., Wilkins, R. A., Adler, P. B., et al. (2019). Belowground biomass response to nutrient enrichment depends on light limitation across globally distributed grasslands. *Ecosystems* 22, 1466–1477. doi:10.1007/s10021-019-00350-4
- Congreves, K. A., Dutta, B., Grant, B. B., Smith, W. N., Desjardins, R. L., and Wagner-Riddle, C. (2016). How does climate variability influence nitrogen loss in temperate agroecosystems under contrasting management systems? *Agric. Ecosyst. Environ.* 227, 33–41. doi:10.1016/j.agee.2016.04.025
- Cooper, R. J., Hama-Aziz, Z., Hiscock, K. M., Lovett, A. A., Dugdale, S. J., Sunnenberg, G., et al. (2017). Assessing the farm-scale impacts of cover crops and non-inversion tillage regimes on nutrient losses from an arable catchment. *Agric. Ecosyst. Environ.* 237, 181–193. doi:10.1016/j.agee.2016.12.034
- Cordell, D., Drangert, J. O., and White, S. (2009). The story of phosphorus: Global food security and food for thought. *Glob. Environ. Change-Human Policy Dimensions* 19, 292–305. doi:10.1016/j.gloenvcha.2008.10.009
- Craine, J. M., Morrow, C., and Fierer, N. (2007). Microbial nitrogen limitation increases decomposition. *Ecology* 88, 2105–2113. doi:10.1890/06-1847.1



- Deng, Q., Hui, D. F., Dennis, S., Reddy, K. C., and Xu, X. (2017). Responses of terrestrial ecosystem phosphorus cycling to nitrogen addition: A meta-analysis. *Glob. Ecol. Biogeogr.* 26, 713–728. doi:10.1111/geb.12576
- Drinkwater, L. E., and Snapp, S. (2007). Nutrients in agroecosystems: Rethinking the management paradigm. *Adv. Agron.* 92, 163–186. doi:10.1016/S0065-2113(04)92003-2
- Elser, J. J., Bracken, M. E. S., Cleland, E. E., Gruner, D. S., Harpole, W. S., Hillebrand, H., et al. (2007). Global analysis of nitrogen and phosphorus limitation of primary producers in freshwater, marine and terrestrial ecosystems. *Ecol. Lett.* 10, 1135–1142. doi:10.1111/j.1461-0248.2007.01113.x
- Eskelinen, A., Harpole, W. S., Jessen, M. T., Virtanen, R., and Hautier, Y. (2022). Light competition drives herbivore and nutrient effects on plant diversity. *Nature* 611, 301–305. doi:10.1038/s41586-022-05383-9
- Fay, P. A., Prober, S. M., Harpole, W. S., Knops, J. M., Bakker, J. D., Borer, E. T., et al. (2015). Grassland productivity limited by multiple nutrients. *Nat. Plants* 1, 15080. doi:10.1038/nplants.2015.80
- Fox, J., and Weisberg, S. (2011). *An R companion to applied regression*. second edition. Thousand Oaks, CA: Sage.
- Frank, K., Beegle, D., and Denning, J. (2012). “Phosphorus. North central regional research publication No. 221 (revised),” in *Recommended chemical soil test procedures for the North Central Region* (United States: University Of Missouri).
- Gaynor, J. D., and Findlay, W. I. (1995). Soil and phosphorus loss from conservation and conventional tillage in corn production. *Am. Soc. Agron. Crop Sci. Soc. Am. Soil Sci. Soc. Am.* 24, 734–741. doi:10.2134/jeq1995.00472425002400040026x
- Good, A. G., and Beatty, P. H. (2011). Fertilizing nature: A tragedy of excess in the commons. *Plos Biol.* 9, e1001124. doi:10.1371/journal.pbio.1001124
- Grace, J. B., Anderson, T. M., Olff, H., and Scheiner, S. M. (2010). On the specification of structural equation models for ecological systems. *Ecol. Monogr.* 80, 67–87. doi:10.1890/09-0464.1
- Greenwood, D. J., Karpinet, T. V., Zhang, K., Bosh-Serra, A., Boldrini, A., and Karawulova, L. (2008). A unifying concept for the dependence of whole-crop N: P ratio on biomass: Theory and experiment. *Ann. Bot.* 102 (6), 967–977. doi:10.1093/aob/mcn188
- Harpole, W. S., Ngai, J. T., Cleland, E. E., Seabloom, E. W., Borer, E. T., Bracken, M. E. S., et al. (2011). Nutrient co-limitation of primary producer communities. *Ecol. Lett.* 14, 852–862. doi:10.1111/j.1461-0248.2011.01651.x
- Harpole, W. S., Sullivan, L. L., Lind, E. M., Firm, J., Adler, P. B., Borer, E. T., et al. (2017). Out of the shadows: Multiple nutrient limitations drive relationships among biomass, light and plant diversity. *Funct. Ecol.* 31, 1839–1846. doi:10.1111/1365-2435.12967
- Harvey, E., and MacDougall, A. S. (2018). Non-interacting impacts of fertilization and habitat area on plant diversity via contrasting assembly mechanisms. *Divers. Distributions* 24 (4), 509–520. doi:10.1111/ddi.12697
- Harvey, E., and MacDougall, A. S. (2015). Spatially heterogeneous perturbations homogenize the regulation of insect herbivores. *Am. Nat.* 186 (5), 623–633. doi:10.1086/683199
- Harvey, E., and MacDougall, A. S. (2014). Trophic island biogeography drives spatial divergence of community establishment. *Ecology* 95, 2870–2878. doi:10.1890/13-1683.1
- Hinsinger, P. (2001). Bioavailability of soil inorganic P in the rhizosphere as affected by root-induced chemical changes: A review. *Plant Soil* 237, 173–195. doi:10.1023/a:1013351617532
- Hooper, D. U., and Vitousek, P. M. (1998). Effects of plant composition and diversity on nutrient cycling. *Ecol. Monogr.* 68, 121–149. doi:10.1890/0012-9615(1998)068[0121:eopcad]2.0.co;2
- Hou, E. Q., Luo, Y. Q., Kuang, Y. W., Chen, C. R., Lu, X. K., Jiang, L. F., et al. (2020). Global meta-analysis shows pervasive phosphorus limitation of aboveground plant production in natural terrestrial ecosystems. *Nat. Commun.* 11, 637. doi:10.1038/s41467-020-14492-w
- Jiang, J., Wang, Y. P., Yang, Y. H., Yu, M. X., Wang, C., and Yan, J. H. (2019). Interactive effects of nitrogen and phosphorus additions on plant growth vary with ecosystem type. *Plant Soil* 440, 523–537. doi:10.1007/s11104-019-04119-5
- Lefcheck, J. S. (2016). piecewiseSEM: piecewise structural equation modelling in R for ecology, evolution, and systematics. *Methods Ecol. Evol.* 7, 573–579. doi:10.1111/2041-210x.12512
- Li, Y., Niu, S. L., and Yu, G. R. (2016). Aggravated phosphorus limitation on biomass production under increasing nitrogen loading: A meta-analysis. *Glob. Change Biol.* 22, 934–943. doi:10.1111/gcb.13125
- Mazzorato, A. C., Esch, E. H., and MacDougall, A. S. (2022). Prospects for soil carbon storage on recently retired marginal farmland. *Sci. Total Environ.* 806, 150738. doi:10.1016/j.scitotenv.2021.150738
- McCann, K. S., Cazelles, K., MacDougall, A. S., Fussmann, G. F., Bieg, C., Cristescu, M., et al. (2021). Landscape modification and nutrient-driven instability at a distance. *Ecol. Lett.* 24 (3), 398–414. doi:10.1111/ele.13644
- Mueller, N. D., Gerber, J. S., Johnston, M., Ray, D. K., Ramankutty, N., and Foley, J. A. (2012). Closing yield gaps through nutrient and water management. *Nature* 490, 254–257. doi:10.1038/nature11420
- Niklas, K. J., Owens, T., Reich, P. B., and Cobb, E. D. (2005). Nitrogen/phosphorus leaf stoichiometry and the scaling of plant growth. *Ecol. Lett.* 8, 636–642. doi:10.1111/j.1461-0248.2005.00759.x
- Noble, D., MacDougall, A. S., and Levison, J. (2023). *Seasonal dynamics of dissolved nutrient flows in riparian farm buffers*. Netherlands: Science of the Total Environment.
- Ogdahl, M., Buyarski, C., and contributors, P. W. (2013). *Plant phosphorus protocol -sulfuric acid digestion*. Minneapolis, MN, USA: PrometheusWiki.
- Ontario Ministry of Agriculture Food and Rural Affairs (2018). *Field crop budgets 2018*. Canada: Ontario Ministry of Agriculture Food and Rural Affairs.
- Penn, C. J., and Camberato, J. J. (2019). A critical review on soil chemical processes that control how soil pH affects phosphorus availability to plants. *Agriculture* 9 (6), 120. doi:10.3390/agriculture906120
- Penuelas, J., Sardans, J., Rivas-Ubach, A., and Janssens, I. A. (2012). The human-induced imbalance between C, N and P in Earth's life system. *Glob. Change Biol.* 18, 3–6. doi:10.1111/j.1365-2486.2011.02568.x
- Pretty, J., Benton, T. G., Bharucha, Z. P., Dicks, L. V., Flora, C. B., Wratten, J., et al. (2018). Global assessment of agricultural system redesign for sustainable intensification. *Nat. Sustain.* 1, 441–446. doi:10.1038/s41893-018-0114-0
- R Core Team (2018). *R: A language and environment for statistical computing*. Vienna, Austria: R Foundation for Statistical Computing.
- Shipley, B. (2009). Confirmatory path analysis in a generalized multilevel context. *Ecology* 90, 363–368. doi:10.1890/08-1034.1
- Sobota, D. J., Compton, J. E., McCrackin, M. L., and Singh, S. (2015). Cost of reactive nitrogen release from human activities to the environment in the United States. *Environ. Res. Lett.* 10, 025006. doi:10.1088/1748-9326/10/2/025006
- Standard Methods (2005). in *4500-N(Org) C. Semi-micro-Kjeldahl. Standard methods 21st edition*
- Standard Methods (2006). in *4500-NO3- F. Automated cadmium reduction method. Standard methods online*
- Stevens, C. J., Lind, E. M., Hautier, Y., Harpole, W. S., Borer, E. T., Hobbie, S., et al. (2015). Anthropogenic nitrogen deposition predicts local grassland primary production worldwide. *Ecology* 96 (6), 1459–1465. doi:10.1890/14-1902.1
- Tilman, D., Knops, J., Wedin, D., Reich, P., Ritchie, M., and Siemann, E. (1997). The influence of functional diversity and composition on ecosystem processes. *Science* 277, 1300–1302. doi:10.1126/science.277.5330.1300
- U.S. EPA (1994). “Method 200.8: Determination of trace elements in waters and wastes by inductively coupled plasma-mass spectrometry.”. Revision 5.4.
- Weigelhofer, G., Fuchsberger, J., Teufl, B., Welti, N., and Hein, T. (2012). Effects of riparian forest buffers on in-stream nutrient retention in agricultural catchments. *J. Environ. Qual.* 41, 373–379. doi:10.2134/jeq2010.0436
- Yang, Y., Tilman, D., Lehman, C., and Trost, J. J. (2018). Sustainable intensification of high-diversity biomass production for optimal biofuel benefits. *Nat. Sustain.* 1, 686–692. doi:10.1038/s41893-018-0166-1
- You, C., Wu, F., Gan, Y., Yang, W., Hu, Z., Xu, Z., et al. (2017). Grass and forbs respond differently to nitrogen addition: A meta-analysis of global grassland ecosystems. *Sci. Rep.* 7, 1563. doi:10.1038/s41598-017-01728-x
- Ziter, C., and MacDougall, A. S. (2013). Nutrients and defoliation increase soil carbon inputs in grassland. *Ecology* 94, 106–116. doi:10.1890/11-2070.1





## OPEN ACCESS

## EDITED BY

Kaibo Wang,  
Chinese Academy of Sciences (CAS),  
China

## REVIEWED BY

Guowei Pang,  
Northwest University, China  
Saman Soleimani Kutanaei,  
Babol Noshirvani University of  
Technology, Iran

Yurui Li,  
Chinese Academy of Sciences (CAS),  
China

## \*CORRESPONDENCE

Jichang Han,  
✉ hanjc\_sxdj@126.com

RECEIVED 18 April 2023

ACCEPTED 29 May 2023

PUBLISHED 15 June 2023

## CITATION

Sun Z, Liu Z, Han J, Wang H, Zhang H and  
Yan J (2023), Long-term effects of soft  
rock amendment on changes of soil  
aggregate cementing agents of sandy soil  
by SEM-EDS.

*Front. Environ. Sci.* 11:1207781.  
doi: 10.3389/fenvs.2023.1207781

## COPYRIGHT

© 2023 Sun, Liu, Han, Wang, Zhang and  
Yan. This is an open-access article  
distributed under the terms of the  
[Creative Commons Attribution License  
\(CC BY\)](https://creativecommons.org/licenses/by/4.0/). The use, distribution or  
reproduction in other forums is  
permitted, provided the original author(s)  
and the copyright owner(s) are credited  
and that the original publication in this  
journal is cited, in accordance with  
accepted academic practice. No use,  
distribution or reproduction is permitted  
which does not comply with these terms.

# Long-term effects of soft rock amendment on changes of soil aggregate cementing agents of sandy soil by SEM-EDS

Zenghui Sun<sup>1,2,3</sup>, Zhe Liu<sup>1,4</sup>, Jichang Han<sup>1,3\*</sup>, Huanyuan Wang<sup>1,3</sup>,  
Haiou Zhang<sup>1,3</sup> and Jiakun Yan<sup>2</sup>

<sup>1</sup>Technology Innovation Center for Land Engineering and Human Settlements, Shaanxi Land Engineering Construction Group Co., Ltd., and Xi'an Jiaotong University, Xi'an, China, <sup>2</sup>College of Life Sciences, Yulin University, Yulin, China, <sup>3</sup>Key Laboratory of Degraded and Unused Land Consolidation Engineering, Ministry of Natural and Resources of China, Xi'an, China, <sup>4</sup>School of Human Settlements and Civil Engineering, Xi'an Jiaotong University, Xi'an, China

Soil aggregates are a crucial constituent of soil and have a significant function in regulating water, nutrients, air, and heat within the soil. The development of soil aggregates is influenced by various factors, including the soil's parent material and human activities. Understanding the formation and the mechanism of stabilization of soil aggregates is of great significance in the study of soil development, in regulating and managing organic carbon pools in soils, and in promoting soil fertility. In this study, aeolian sandy soil with a low degree of soil development and compound soil formed by combining soft rock and aeolian sandy soil were selected as the research objects. We selected three time points from 0 to 9 years after amendment by soft rock in order to investigate the changes of soil aggregate cementing agents. The shape of soil aggregates in both types of soils was analyzed by environmental scanning electron microscopy-energy dispersive spectroscopy (SEM-EDS), which were also used to assess the appearance of soil aggregates and quantify the composition of mineral elements on a cross section of the aggregate. The results show that when the soft rock and the aeolian sandy soil are compounded and mixed, the clay minerals in the soft rock change the microstructure of the original aeolian sandy soil from a single granular barrier to one characterized by a cumulative porous structure, indicating that clay minerals promote soil development and form aggregates with good structural properties. The cementing agents in the compounded soil aggregates are mainly clay minerals, aluminum, iron, and calcium. In comparison to aeolian sandy soils, the presence of iron and calcium in compounded soils is notably elevated. The iron oxides present in compounded soils serve a similar function to "bolts" in the formation of soil aggregates. These findings establish a theoretical foundation for investigating the process of soil aggregate formation and the mechanisms by which cementing agents contribute to their stabilization.

## KEYWORDS

aeolian sandy soil, compound soil, soil aggregate, cementing agent, environmental scanning electron microscopy

# 1 Introduction

Soil aggregates are an important component of soil and are widely regarded as the basic unit as well as an important parameter of soil structure (Barral et al, 1998; Hou et al, 2018). Aggregates play important roles in coordinating water, nutrients, air, and heat in soil, affecting the types and activities of soil enzyme, maintaining and stabilizing soil, and loosening and curing layers (Haynes et al, 1993; Jastrow et al, 1996). The formation of soil aggregates is a very complex process involving a range of physical, chemical, and biological effects that depend primarily on the quantity and nature of the various materials of composition in the soil (Chaney et al., 1986a; Janalizadeh et al, 2019b; Lado et al, 2004). During the process of soil particle aggregation, not only organic compounds play an important role in particle cementation, but inorganic compounds such as iron and aluminum oxides and hydroxides, as well as silica and calcium carbonate also play important roles (Arya et al, 1972; Falsone et al, 2007; Wiesmeier et al, 2012). The parent material is the primary material that makes up soil, and has a great influence on the composition and action of inorganic soil cementing agents (Bosch-Serra et al, 2017; Oades et al, 1993). The formation of organic cementing agents is related to the quantity of microorganisms, their activity and metabolites, plant root exudates, and organic matter input (Chaney et al., 1986b; Fakhrabadi et al, 2021; Gale et al, 2000).

Soil cementing agents may be inorganic, organic, or a combination of organic and inorganic (Giovannini et al, 1976; Shi et al, 2002). Although these three types of cementing agents may be found at the same time in different soil types, the composition of organic and inorganic cementing agents in the soil differs due to differences in parent materials, bioclimatic conditions, and agricultural management. In soils with high organic matter content and low clay and oxidized iron and aluminum, the role of organic matter is dominant (Guénet et al, 2016; Ren et al, 2011); in soils with low organic matter content, but high clay and oxidized iron and aluminum content, the formation of soil aggregates is mainly due to the cohesive force between clay particles and due to cementation by iron and aluminum oxides (Barral et al, 1998; Roshan et al, 2022; Skjemstad et al, 1993). Numerous studies have investigated the quantity, distribution, stability, and other factors that influence the formation of soil aggregates (Chaney et al., 1986a; Terpstra et al, 1990; Diaz et al, 1994; Schomburg et al, 2018). However, such studies cannot describe the internal structure of soil aggregates, explain the process of aggregate formation, or the cementation mechanism. The basic physical indicators of aggregates contain very limited information and do not reflect the complex internal structural differences of the aggregates, but it is difficult to distinguish and discriminate the shape and internal composition of soil aggregates.

Soft rock, formed in continental clastic rock system of late Paleozoic Permian, Mesozoic Triassic, Jurassic, and Cretaceous (Sun and Han, 2018), has the characteristics of low diagenetic degree, poor intergrain bond and low structural intensity and is the fundamental reason for serious water loss and soil erosion in soft rock area. To solve the problems of the sand soil sharing common root but with different qualities and that it is hard for sandy to

become soils, Han et al (2012) found that soft rock had great potentials as sandy remediating material. They prepared “new type soil” by mixing soft rock sandstone with sand at certain proportion, which not only could solve the problems of the sandy being unable to form colloidal materials due to poor resistance and fertility, but also could alleviate the trouble of nonlocal soil dressing. Applied in Mu Us Desert land consolidation projects, this technology helped increase the arable areas of more than 200,000 ha. Corns and potatoes have been planted in the “compound soil” with high yield. In this way, utilization of sand and soft rock is realized, which has increased effectively the arable areas and guaranteed food security with good ecologic, economic and social benefits (Sun et al, 2021). To study furthermore the improvement of soft rock of aeolian sandy soil as well as the formation of this new type of “artificial soil” mixed with soft rock and sand and to realize multi-purpose application of the compound soil, it is hard to diagnose and study relying only on some routine features of cross section form and the fundamental physical and chemical analysis; therefore, it requires also to study profoundly the micro morphology of the compound soil as well as the formation and development of the aggregate cementing materials in the compound soil.

With the advancement of soil morphology research, research on the structure of soil aggregates has evolved from qualitative observation by scanning electron microscopy (SEM) to quantitative analysis combined with image processing technology (Garbout et al, 2013; Hapca et al, 2015; Wang et al, 2012; Wilson et al, 2013). SEM has the characteristics of high magnification, high resolution, and large depth of field. It can be used to directly observe the original microstructure of soil aggregates and can be used together with X-ray diffraction spectroscopy to achieve simultaneous analysis of morphology at a microscopic scale and elemental composition (Sayen et al, 2009; Jiménez-Pinilla et al, 2016; Yu et al, 2017). It has become an important tool for the analysis of the morphology of clay mineral particles. The combined analysis of the qualitative and quantitative microstructure data provides information on the various nutrients, microorganisms, and cementing agents in soil aggregates and is an ideal method by which the state and mechanism of soil aggregate formation may be explored. For this research, the selected objects of study were aeolian sandy soil with low soil development and a compound soil created by combining aeolian sandy soil and soft rock. Understanding the nature of organic cementing materials, the concepts behind the formation of soil aggregates, the mechanisms of soil aggregate stability, and the mechanism for renewal and turnover can help to further explore changes in soil development and succession, organic carbon pool, water stability of soil aggregates, and other soil fertility indexes once virgin land is first opened for cultivation, as well as the mechanism of the influence of soil structure on soil fertility (Yu et al, 2017; Watteau et al, 2012; Zhang et al, 2015). The main purpose of our study is to determine, through the use of SEM-energy dispersive spectroscopy (EDS):

- the main composition of cementing agents on the surface of soil aggregates during soil development
- to quantify the distribution of major mineral elements on the surface of soil aggregates

TABLE 1 Basic characteristic of sandy soil and soft rock\*.

Material	Texture	Sand	Silt	Clay	BD	pH	CEC	Organic matter	Fe	Al	Ca
		(%)	(%)	(%)	(g cm <sup>-3</sup> )		(cmol kg <sup>-1</sup> )	(g kg <sup>-1</sup> )	(%)	(%)	(%)
Aeolian sandy soil	Sand	95.4	4.1	0.5	1.6	7.4	3.86	2.93	1.81	5.04	2.25
Soft rock	—	34.9	58.1	7	1.4	8.1	45.79	1.74	4.82	8.40	1.16

\*Percentage of clay (<0.002 mm), silt (0.002–0.05 mm), and sand (0.05–2 mm) particles, measured by Pipette Method; BD, bulk density, measured by undisturbed soil core method; soil pH was measured with a soil: water ratio of 1:2.5 using an ion pH meter; CEC, cation exchange capacity, measured by shaking 1 mm of air-dried soil with 1 M NH<sub>4</sub>OAc at pH 7.0.

TABLE 2 Mineral composition of sandy soil and soft rock.

Material	Quartz	Kaolinite	Montmorillonite	Feldspar	Calcite	Dolomite	Amphibole
	(%)						
Aeolian sandy soil	82	4	—	10	2	—	2
Soft rock	57	—	30	10	—	3	—

- to elucidate the mechanism of action of cementing agents during the formation of soil aggregates.

2 Materials and methods

2.1 Sites and soil sampling

The aeolian sandy soil and compound soil selected for the experiment were collected from the Mu Us desert, Jingkeliang, Daji Khan Village, Yuyang District, Yulin City, China (38°27'53"N, 109°28'58 E). The area is located in northwestern Shaanxi at an altitude of 1,210 m above sea level and is a typical warm temperate monsoon climate. The annual average temperature is 6.0°C–8.5°C and the annual precipitation is 400–440 mm. The compound soil is composed of materials from soft rock (also called Pisha sandstone or Feldspathic Sandstone) and aeolian sandy soil in a volume ratio of 1: 2 [Detailed field experiments design were shown in Sun et al (2018)]. The physical and chemical properties of the aeolian sandy soil and the soft rock materials are shown in Tables 1, 2. The soft rock is composed of Paleozoic Permian, Mesozoic Triassic, Jurassic and Cretaceous thick layer sandstones, sand shale, and argillaceous sandstones (Bazhenov et al, 1993; Martin et al, 1999). Its rock layer is thin, with low pressure, low diagenesis, and poor cementation between sand grains and poor structural strength (Wang et al, 2009). In recent years, some scholars have used the complementary properties of soft rock and aeolian sandy soil to form a new compound soil (the soil at this time is only at the beginning of its development) which is an improvement on aeolian sandy soil (Sun et al, 2018; Han et al, 2015; Han et al, 2012; Wang et al, 2013; Sun et al, 2019). As the years of cultivation increase, the compound soil tends to ripen. Therefore, this study selected aeolian sandy soil, compound soil that has undergone 3 years of planting, and compound soil that has undergone 9 years of planting as research materials.

Undisturbed soil was collected from topsoil and the soil samples were taken back to the laboratory and naturally air-dried. The dry sieve method was used to screen the 1–2 mm soil aggregates that were the objects of observation in this study.

2.2 SEM and X-ray diffraction methods

The German LEO1430VP scanning electron microscopy (SEM) and the OXFORD7353 energy dispersive spectrometer (EDS) were used in combination. The SEM was operated with a test voltage of 30 kV, a secondary electron resolution of 3.5 nm, and a maximum magnification of 900,000 times. The EDS was used for quantitative analysis of the mineral elements in the sample, with an error of less than 5%. SEM-EDS was used to observe and analyze the soil aggregates (1–2 mm). The relatively flat interparticle cementation was used as the location of analysis for surface cementation, which standardized the locations where analyses were performed. In this study, 10 typical cementation points were selected on the surface of each observed soil aggregate for energy spectral point element analysis.

Soil aggregates 1.0–2.0 mm were selected for cross-sectional elemental analysis. The selected aggregates were embedded and fixed with polyester resin and sample columns with a diameter of 2 cm and a height of 1 cm were cut out, and the sample was mechanically polished. The cross section of the compound soil was observed by SEM, and the elemental distribution of the soil aggregate section was analyzed using the element mapping mode of EDS. Firstly, the typical cross section of the target aggregate was found at low magnification and then the overall element distribution analysis was performed by using the mapping mode. Finally, the overall regional elements are collected and analyzed quantitatively using pattern mode analysis. The SEM was set on fast mode, working distance 10 mm, acceleration voltage 15 kv, dead time is at 30%–50%, and then the result was subjected to zaf wt% normalization and correction.

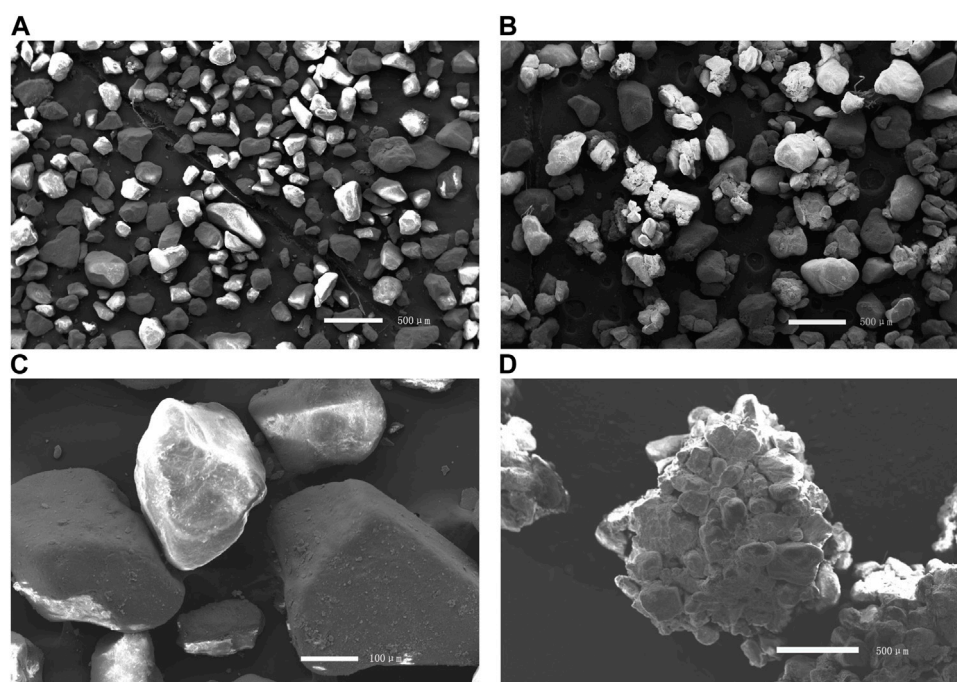


**FIGURE 1**  
Morphology features of aeolian sandy soil (A,C) and compound soil (B,D).

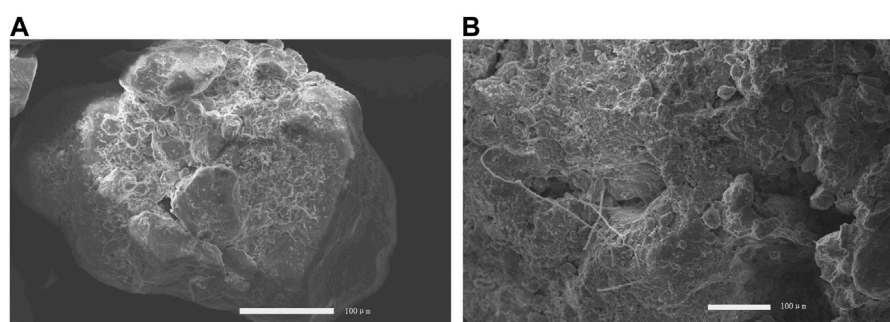


**FIGURE 2**  
Morphology features of aggregates in compound soil. (A) Surface of compound soil aggregates; (B) hyphae in soil aggregates.

## 2.3 Statistical analysis

Statistical analysis was performed using the PROC GLM process in SAS for equation analysis. The mean comparison was performed using the least significant difference (LSD) method with a significance level of  $p < 0.05$  between treatments.

## 3 Analysis result

### 3.1 Aggregate trait analysis

The microaggregates of aeolian sandy soil are mainly composed of single particles of irregular shape, with high degree of rounding, smooth

surface, almost no sharp edges and corners, and no bonding surface (Figures 1A, C). Compared with the aeolian sandy soil aggregates, the compound soil aggregates have a certain number of bridging barrier structures formed by the bonding of small mineral particles as cementing agents to the core structural particles; the coarse core structural particles are filled by fine particles, which either form filler-like junction structures filling the voids of the core structure or an envelope-like structure encapsulating core structural particles (Figures 1B, D). The differences in morphological characteristics between compound soil and aeolian sandy soil can be clearly observed on the surface of compound soil microaggregates, where 2–40  $\mu\text{m}$  morphologically different pore structures can be observed (Figure 2A). The presence of hyphae was also observed on the surface of compound soil aggregates (Figure 2B), indicating that the compound soil has a good soil aggregate structure.



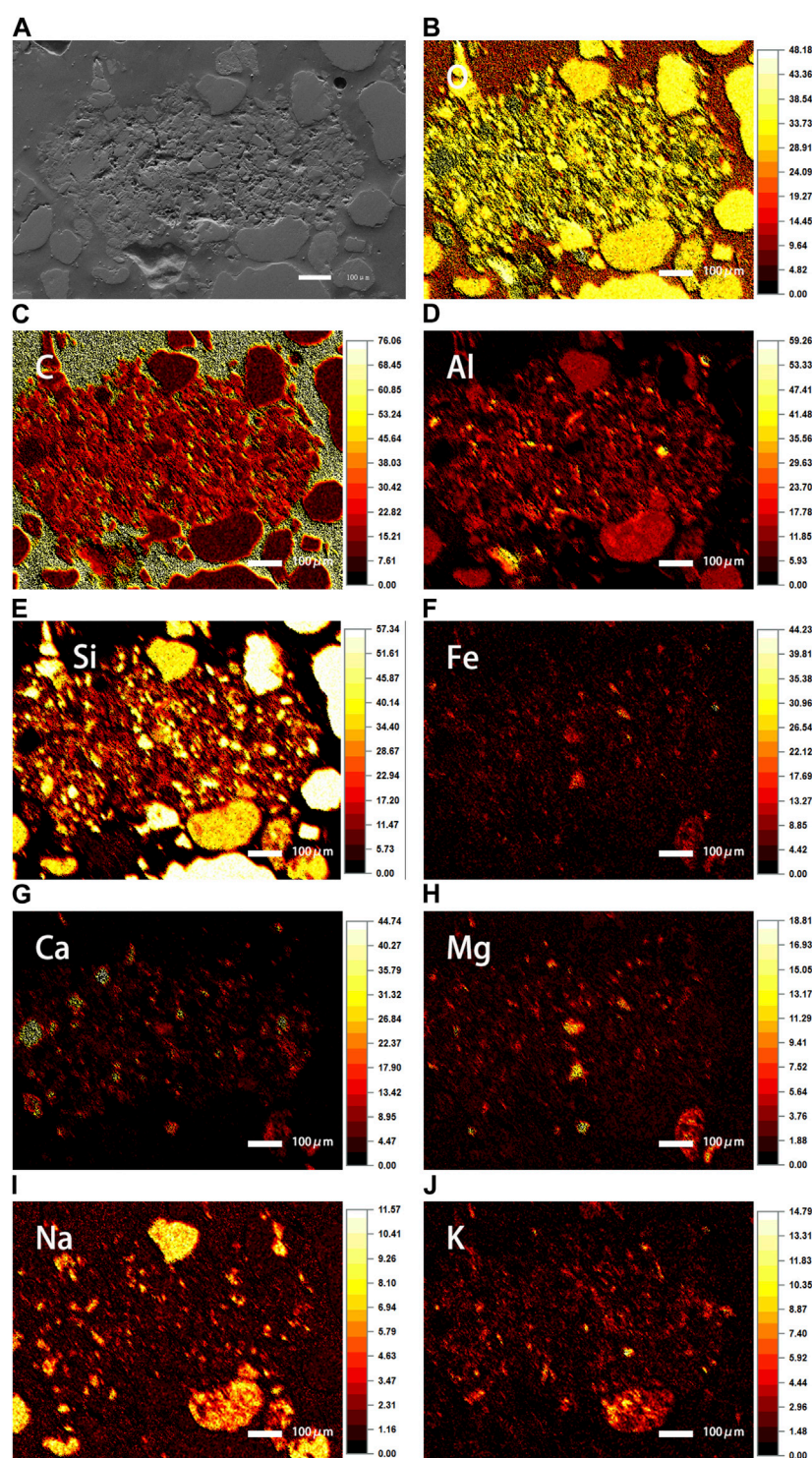


**FIGURE 3**

SEM-EDS analysis of aeolian sandy soil aggregate. SEM image of the sample (A), and corresponding X-ray maps of O (B), C (C), Al (D), Si (E), Fe (F), Ca (G), Mg (H), Na (I), and K (J).

### 3.2 Soil aggregate cross-section elemental distribution

The aeolian sandy soil aggregate section has regions of significant Si and Al enrichment, and only a small amount of Fe

and Ca (Figure 3). The distribution of Al, Ca, and Fe in aeolian sandy soil aggregates are intermittently in the soil aggregate cross section. Areas of highly concentrated Si, Al, Fe, and Ca appeared in the cross section of compound soil aggregates that has undergone 3 years of planting (Figure 4). The Al-Mg distribution zones in the



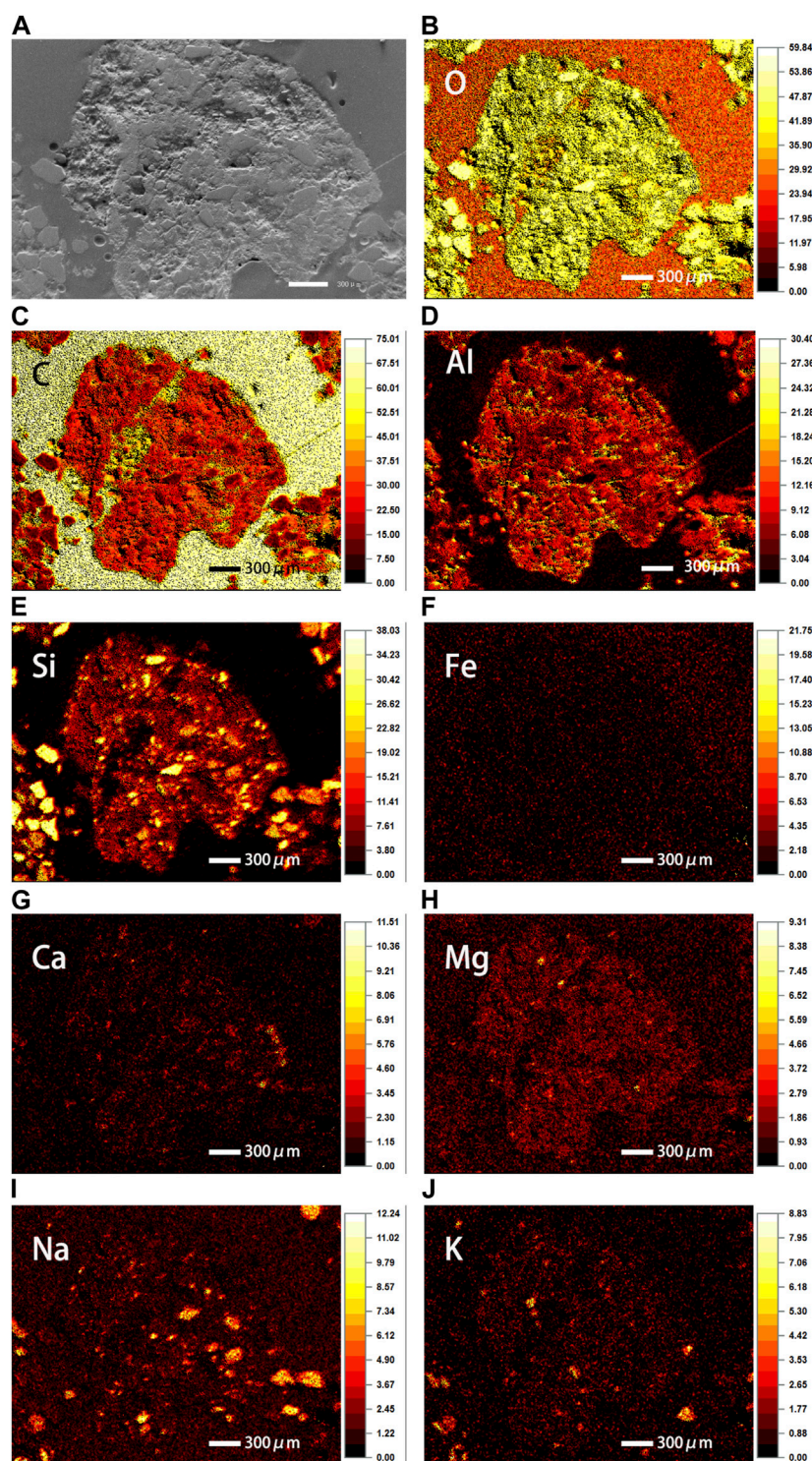


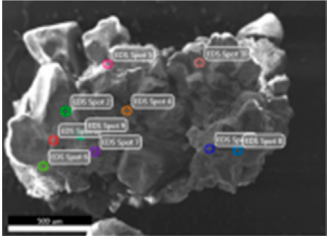
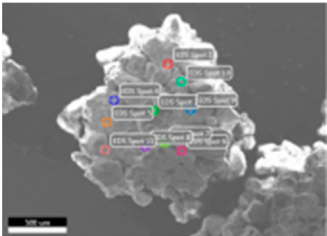
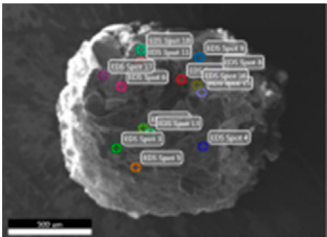
**FIGURE 4**

SEM-EDS analysis of compound soil aggregates that has undergone 3 years of planting. SEM image of the sample (A), and corresponding X-ray maps of O (B), C (C), Al (D), Si (E), Fe (F), Ca (G), Mg (H), Na (I), and K (J).

compounded soil have strong correlation and connectivity, and run through the entire soil aggregate cross section and form the basic shape of the aggregate section. Al has obvious regions of enrichment that exist mainly as semi-joined points. The areas of Al enrichment

are mostly concentrated on the pores in the cross section and at the edge of the core structural particles. Ca is distributed independently in some parts of the section, and is relatively far from the areas containing Al-Mg.

TABLE 3 Analytical results of X-ray energy spectrum characteristics of the aggregates in aeolian sandy soil and compound soils.

Treatment	Analyzed sites	Element (%)							
		O	Na	Mg	Al	Si	K	Ca	Fe
3 year aeolian sandy soil		49.98 <sup>a</sup>	0.78 <sup>a</sup>	1.91 <sup>b</sup>	11.87 <sup>a</sup>	26.93 <sup>a</sup>	2.72 <sup>a</sup>	1.73 <sup>c</sup>	4.08 <sup>c</sup>
3 year compound soil		43.56 <sup>b</sup>	1.34 <sup>a</sup>	2.72 <sup>a</sup>	11.05 <sup>a</sup>	28.50 <sup>a</sup>	2.09 <sup>a</sup>	3.47 <sup>b</sup>	7.27 <sup>b</sup>
9 year compound soil		41.07 <sup>c</sup>	0.83 <sup>a</sup>	2.52 <sup>a</sup>	10.58 <sup>a</sup>	27.26 <sup>a</sup>	2.60 <sup>a</sup>	4.40 <sup>a</sup>	10.74 <sup>a</sup>

Mean values in the table, and columns within the same soil layer and with the same letters are not significantly different at  $p < 0.05$  according to a protected LSD test.  
a, b, c: Columns within the same soil layer and with the different letters are significantly different at  $p < 0.05$  according to a protected LSD test.

3.3 Analysis of elemental content on the surface of soil aggregates

The relative contents of Fe, Ca and Mg in the compound soil aggregates were significantly higher than those in the aeolian sandy soil (Table 3). It suggests that Fe, Ca, and Mg elements play an important role in the cementation process during the formation of soil aggregates. From this, it can be inferred that compared with aeolian sandy soil, the cementing materials on the surface of compound soil aggregates mainly include ferric oxide, calcium carbonate, and magnesium carbonate. After 9 years of cultivation, there are more iron cementation points on the surface of large aggregates in compound soil, and the content of Fe super-enriched zones is higher. The relative content of Fe increased from 7.27% to 10.74% and the distribution area is more extensive and tight. The Ca enrichment area also increased and the relative content of Ca increased from 3.47% to 4.40% (Table 3).

4 Discussion

Soil minerals are important constituents of soil and can be divided into three types: primary minerals, secondary minerals, and soluble minerals (Gislason et al, 1996; Ghadakpour et al, 2020). Primary

minerals in soft rock and compound soils are silicate minerals such as quartz and feldspar. The main elements are Si, Al, and O. Secondary minerals include clay minerals, secondary oxides, and salts. The clay minerals are mostly in the form of cementing agents (Afrakoti et al, 2020; Roshan et al, 2020). The elemental composition is mostly Si, Al, O, Mg, K, Ca, and Fe. Secondary oxides are iron oxide or oxidized alumina, and its elemental composition is mostly O, Fe, and Al. Salt minerals include carbonates and other substances, the main elements of which are O, C, and Ca. In this study, the resin embedding technique was used for the cross-section analysis of the soil aggregates. The constituent elements of the resin were C and O. Therefore, C and O were not analyzed in this study.

This study analyzed the mapped image of the elements found on the cross-section of 1–2 mm soil aggregates in compound soil. According to the distribution characteristics of the Fe-rich region using iron oxide as the indicator, iron oxide is mainly in the form of an organic-inorganic composite formed by the iron oxide cemented by adsorption or co-precipitation with organic matter, and is mostly present around the core structural particles of the soil aggregate and at the pores as a clear semi-continuous envelope (Janalizadeh et al, 2019a; Koutenaei et al, 2021). Iron oxides act like “bolts” in the development of compound soil aggregates. In addition, the high degree of association between Fe-Ca distribution zones and Fe



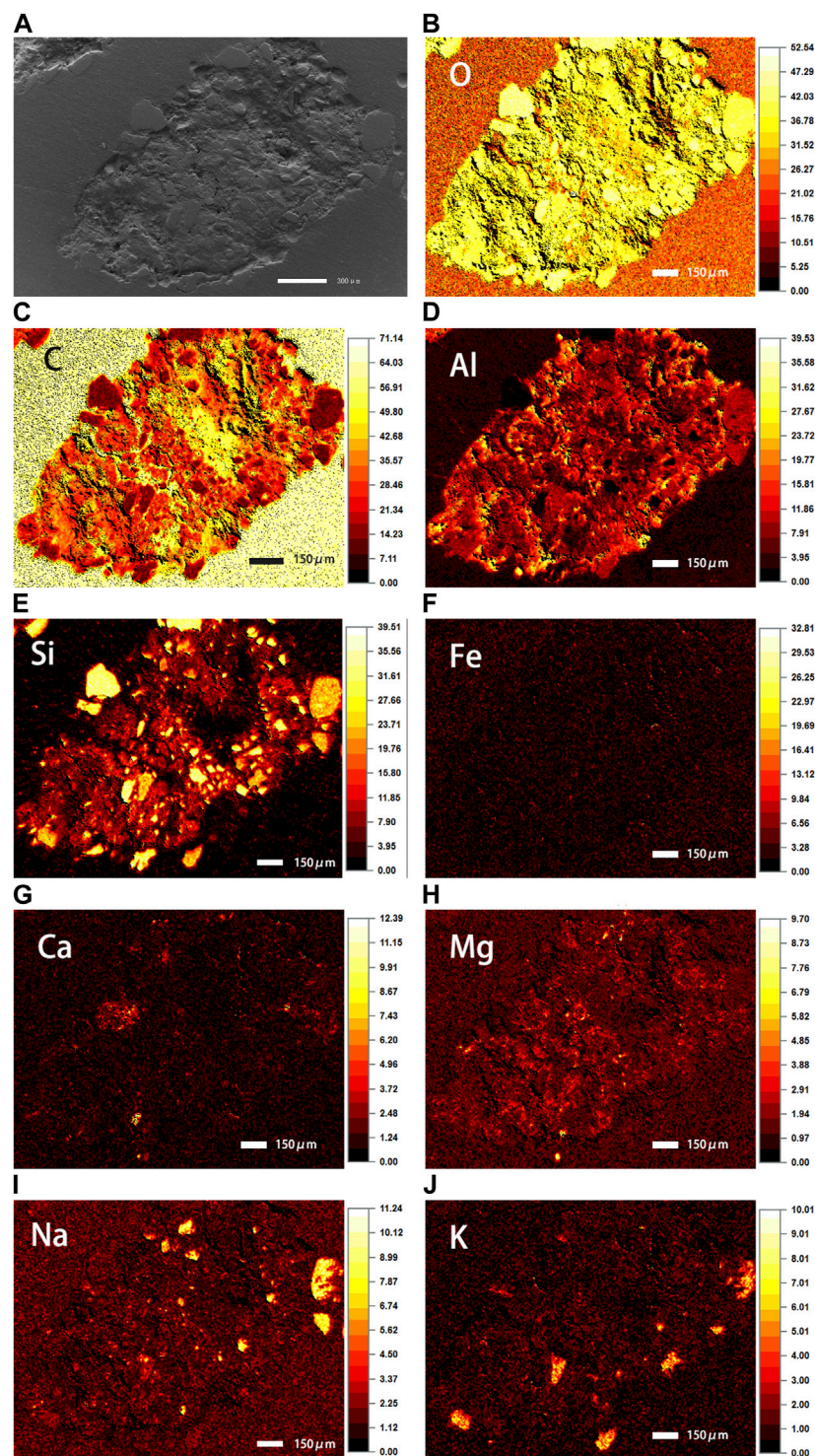


**FIGURE 5**

SEM-EDS analysis of compound soil aggregates that has undergone 9 years of planting. SEM image of the sample (A), and corresponding X-ray maps of O (B), C (C), Al (D), Si (E), Fe (F), Ca (G), Mg (H), Na (I), and K (J).

enrichment zones in the cross section of compound soil aggregates cultivated for 3 and 9 years indicates that good clay mineral-metal oxide-organic matter composite cementing agents is formed in the compound soil (Figures 4, 5). The composite cementing system is more stable as the years of cultivation increases.

The interaction between iron-aluminum oxide and clay minerals is closely related to the cementation of soil aggregates (Barral et al, 1998; Amézketa et al, 1999; Duiker et al, 2003; Molina et al, 2001). For the new “artificial soil” with low organic matter content and high content of clay minerals and iron-aluminum oxides ( $Al_2O_3$ ;

**TABLE 4 Analytical results of cementing materials content in aeolian sandy soil and compound soils<sup>a</sup>**

Treatment	Al <sub>f</sub>	Fe <sub>f</sub>	Al <sub>c</sub>	Fe <sub>c</sub>	Clay mineral content (%)	Relative content of clay minerals (%)			
	g/kg		mg/kg			I/S	Illite	Kaolinite	Chlorite
3 year aeolian sandy soil	0.59	5.06	0.61	1.03	13.7	45	27	12	16
3 year compound soil	0.48	7.66	2.17	4.92	21.2	47	28	12	13
9 year compound soil	0.08	7.42	2.07	3.97	12.9	52	24	11	13

<sup>a</sup>Al<sub>f</sub> is free aluminum oxide, Fe<sub>f</sub> is free iron oxide, Al<sub>c</sub> is complex aluminum, Fe<sub>c</sub> is complex iron, I/S is illite smectite mixed layers.

2.17–2.07 mg/kg; Fe<sub>c</sub>: 4.92–3.97 mg/kg) in the compound soil (Table 4), the formation of soil aggregates mainly depends on the cohesive force within the clay and the cementation of iron-aluminum oxide (Barral et al, 1998; Choobbasti et al, 2017; Skjemstad et al, 1993). This study found that iron oxides have obvious distribution characteristics in the compound soil aggregates: Fe is mainly concentrated at the outside of the aggregates, and the surface Fe aggregates become more and more abundant with increased years of cultivation (Figure 5). The free iron oxide in the compound soil aggregates showed a small downward trend with the increase in years of cultivation (Table 4). This is mainly because the soft rock contains minerals rich in Fe, adding the soft rock to the aeolian sandy soil increases the content of free iron oxide in the compound soil. Since iron oxide is very active in the soil environment and can move, under the continuous action of soil roots, leaching and redox, free iron oxide continuously enters the soil solution and adsorbs to the surface of the aggregate, effectively promoting the cementation of soil aggregates (Choobbasti et al, 2015; Muggler et al, 1999; Barberis et al, 1991). On the other hand, as a redox sensitive element, Fe is continuously enriched at the surface of the aggregate due to the difference of redox conditions on the inside and the outside of the compound soil aggregates and due to the lack of pores in the aggregate (Yaghi et al, 2013; Huang et al, 2016). This also leads to positively charged iron oxides on the surface of the compound soil aggregates becoming more easily cemented together with the negatively charged aggregates by electrostatic forces, causing the soil aggregate particle size to increase (Choobbasti et al, 2018). With increased years of cultivation, the free iron oxide in the compound soil ages, the free iron oxide is continuously reduced, and the iron oxide in the cemented state is gradually increased, which also reveals the soil formation process of the compound soil. In general, iron plays an important role as a “bridge builder” in the development of compound soil aggregates (Giovannini et al, 1976; Jiang et al, 2015).

Compared with compound soil, the distribution characteristics of clay minerals and aluminum oxides in aeolian sandy soils are not significantly different, but iron oxides exhibit a certain distribution on the surface and inside of aeolian sandy soil aggregates (Table 3), showing the difference in the distribution of cementing agents between the aeolian sandy soil and compound soil. The content of free iron oxide and complexed iron oxide is small, indicating that the aggregate cementation strength in aeolian sandy soil is low, which also illustrates in a different way the difference between the redox system and the pore channels inside soil aggregates from aeolian sandy soil and compound soil. When soft rock is compounded and mixed with the aeolian sandy soil, the micro-

structural characteristics of the original aeolian sandy soil with a single-grain barrier are changed, which promotes the development of “new man-made soil” to form bridges, fill microaggregates, and promote good structural characteristics, mainly due to the positive effect of the cementing materials in the soft rock on soil formation and development of the compound soil.

With the same number of cultivation years, the clay mineral content in the compound soil is higher than that in the aeolian sandy soil, and the clay minerals in the compound soil and the aeolian sandy soil are mainly water-sensitive illite smectite mixed layers. This is mainly because soft rock contains abundant water-sensitive clay minerals (Li et al, 2014; Ma et al, 2016). These clay minerals have strong hydrophilicity, specific surface area and cation exchange capacity (Van et al, 1995; Joussein et al, 2004). The surface of the clay particles has strong hydrophilicity, which can absorb water and nutrients in the soil, forming a cohesive substance and promoting the formation of soil aggregates (Ghadakpour et al, 2020). In addition, clay particles can also provide support force to promote the stability of soil aggregates. After soft rock is used as a remediation material and compounded and mixed with aeolian sandy soil, under the action of continuous leaching and weathering, the soft rock gradually disintegrates, and the clay minerals are continuously released and redistributed (Li et al, 2017; Ribeiro et al, 2018). The clay minerals adsorb to the minerals in the aeolian sandy soil and improve its surface characteristics, which promotes the development of microaggregates in compound soil.

## 5 Conclusion

In this study, SEM-EDS was used to characterize the microstructure and elemental distribution of soil aggregates in aeolian sandy soils and compound soil containing a mixture of soft rock and aeolian sandy soil, and the formation and development and aggregation of cemented materials in compound soil aggregates were studied. The results show that when soft rock and aeolian sandy soil are compounded and mixed, the micro-structure of the original aeolian sandy soil, which is primarily single granular barrier, is changed, promoting the formation and development of soil and forms soil aggregates with good structural characteristics. Compared with aeolian sandy soil, the cementing agents in the compound solid aggregates are mainly clay minerals, aluminum cements, iron cements, and calcium cements. During soil development, many aggregates are further cemented into larger soil aggregates. Iron oxides are fixed by combining with organic matter, which further

strengthens the stability and development of soil aggregates. The iron oxides in the compounded soil play a role similar to “bolts” during the development of soil aggregates. This study provides a theoretical basis for the study of the formation process and stabilization mechanism of soil aggregates driven by cementing agents. This study also has some shortcomings. It only analyzed the surface morphology characteristics of the complex soil, and did not detect the structures below the surface. Quantitative research needs to be strengthened in future studies.

## Data availability statement

The original contributions presented in the study are included in the article/Supplementary Material, further inquiries can be directed to the corresponding author.

## Author contributions

ZS and ZL wrote the main manuscript. JH and ZS designed the experiment. ZL performed the experiments and collected the data. HW and HZ prepared the figures. ZS and JY contributed the statistical analyses. All authors contributed to the article and approved the submitted version.

## Funding

This research was supported by the Fund for Less Developed Regions of the National Natural Science Foundation of China (No. 42167039), the Technology Innovation Center for Land Engineering and Human Settlement Environment, Shaanxi Land Engineering

Construction Group Co., Ltd., and Xi'an Jiaotong University (2021WHZ0091), and the Scientific Research Item of Shaanxi Provincial Land Engineering Construction Group (DJTD 2022-3, DJNY 2022-15, and DJNY 2022-35).

## Acknowledgments

The authors gratefully acknowledge researchers at the Shaanxi Provincial Land Engineering Construction Group, for their help with the field experiments.

## Conflict of interest

Authors ZS, ZL, JH, HW, and HZ were employed by Shaanxi Land Engineering Construction Group Co., Ltd.

The authors declare that this study received funding from Shaanxi Land Engineering Construction Group Co., Ltd. The funder had the following involvement in the study: study design and preparation of the manuscript.

The remaining author declares that the research was conducted in the absence of any commercial or financial relationships that could be construed as a potential conflict of interest.

## Publisher's note

All claims expressed in this article are solely those of the authors and do not necessarily represent those of their affiliated organizations, or those of the publisher, the editors and the reviewers. Any product that may be evaluated in this article, or claim that may be made by its manufacturer, is not guaranteed or endorsed by the publisher.

## References

- Afrakoti, M. T. P., Choobbasti, A. J., Ghadakpour, M., and Kutanaei, S. S. (2020). Investigation of the effect of the coal wastes on the mechanical properties of the cement-treated sandy soil. *Constr. Build. Mater.* 239, 117848. doi:10.1016/j.conbuildmat.2019.117848
- Amézqueta, E. (1999). Soil aggregate stability: A review. *J. Sustain. Agric.* 14, 83–151. doi:10.1300/j064v14n02\_08
- Arya, L. M., and Blake, G. R. (1972). Stabilization of newly formed soil aggregates. *Agron. J.* 64, 177–180. doi:10.2134/agronj1972.00021962006400020015x
- Barberis, E., Marsan, F. A., Boero, V., and Arduino, E. (1991). Aggregation of soil particles by iron oxides in various size fractions of soil b horizons. *J. Soil Sci.* 42, 535–542. doi:10.1111/j.1365-2389.1991.tb00100.x
- Barral, M., Arias, M., and Guerif, J. (1998). Effects of iron and organic matter on the porosity and structural stability of soil aggregates. *Soil Tillage Res.* 46, 261–272. doi:10.1016/s0167-1987(98)00092-0
- Bazhenov, M. L., Chauvin, A., Audibert, M., and Levashova, N. (1993). Permian and triassic paleomagnetism of the southwestern tien Shan: Timing and mode of tectonic rotations. *Earth Planet. Sci. Lett.* 118, 195–212. doi:10.1016/0012-821x(93)90168-9
- Bosch-Serra, A. D., Yagüe, M., Poch, R. M., Molner, M., Junyent, B., and Boixadera, J. (2017). Aggregate strength in calcareous soil fertilized with pig slurries. *Eur. J. Soil Sci.* 68, 449–461. doi:10.1111/ejss.12438
- Chaney, K., and Swift, R. S. (1986b). Studies on aggregate stability 11 The effect of humic substances on the stability of re-formed soil aggregates. *Eur. J. Soil Sci.* 37, 337–343. doi:10.1111/j.1365-2389.1986.tb00036.x
- Chaney, K., and Swift, R. (1986a). Studies on aggregate stability. I. Re-formation of soil aggregates. *J. Soil Sci.* 37, 329–335. doi:10.1111/j.1365-2389.1986.tb00035.x
- Choobbasti, A. J., and Kutanaei, S. S. (2017). Microstructure characteristics of cement-stabilized sandy soil using nanosilica. *J. Rock Mech. Geotechnical Eng.* 9 (5), 981–988. doi:10.1016/j.jrmge.2017.03.015
- Choobbasti, A. J., Vafaei, A., and Kutanaei, S. S. (2015). Mechanical properties of sandy soil improved with cement and nanosilica. *Open Eng.* 5, 111–116. doi:10.1515/eng-2015-0011
- Choobbasti, A. J., Vafaei, A., and Soleimani, K. S. (2018). Static and cyclic triaxial behavior of cemented sand with nanosilica. *J. Mater. Civ. Eng.* 30 (10), 04018269. doi:10.1061/(ASCE)MT.1943-5533.0002464
- Diaz, E., Roldan, A., Lax, A., and Albaladejo, J. (1994). Formation of stable aggregates in degraded soil by amendment with urban refuse and peat. *Geoderma* 63, 277–288. doi:10.1016/0016-7061(94)90069-8
- Duiker, S. W., Rhoton, F. E., Torrent, J., Smeck, N. E., and Lal, R. (2003). Iron (hydr) oxide crystallinity effects on soil aggregation. *Soil Sci. Soc. Am. J.* 67, 606–611. doi:10.2136/sssaj2003.6060
- Fakhrabadi, G. A., Ghadakpour, M., Choobbasti, A. J., and Kutanaei, S. S. (2021). Evaluating the durability, microstructure and mechanical properties of a clayey-sandy soil stabilized with copper slag-based geopolymer against wetting-drying cycles. *Bull. Eng. Geol. Environ.* 80, 5031–5051. doi:10.1007/s10064-021-02228-z
- Falsone, G., Celi, L., and Bonifacio, E. (2007). Aggregate formation in chloritic and serpentinitic alpine soils. *Soil Science* 172, 1019–1030. doi:10.1097/ss.0b013e31815778a0
- Guénet, H., Davranche, M., Vantelon, D., Pédrot, M., Al-Sid-Cheikh, M., Dia, A., et al. (2016). Evidence of organic matter control on as oxidation by iron oxides in riparian wetlands. *Chem. Geol.* 439, 161–172. doi:10.1016/j.chemgeo.2016.06.023



- Gale, W., Cambardella, C., and Bailey, T. (2000). Root-derived carbon and the formation and stabilization of aggregates. *Soil Sci. Soc. Am. J.* 64, 201–207. doi:10.2136/sssaj2000.641201x
- Garbout, A., Munkholm, L. J., and Hansen, S. B. (2013). Temporal dynamics for soil aggregates determined using x-ray ct scanning. *Geoderma* 204, 15–22. doi:10.1016/j.geoderma.2013.04.004
- Ghadakpour, M., Choobasti, A. J., and Kutanaei, S. S. (2020). Experimental study of impact of cement treatment on the shear behavior of loess and clay. *Arabian J. Geoscience* 13 (4), 184. doi:10.1007/s12517-020-5181-7
- Giovannini, G., and Szqui, P. (1976). Iron and aluminium as cementing substances of soil aggregates: I. Acetylacetone in benzene as an extractant of fractions of soil iron and aluminium. *J. Soil Sci.* 27, 140–147. doi:10.1111/j.1365-2389.1976.tb01984.x
- Gislason, S. R., Arnórsson, S., and Armannsson, H. (1996). Chemical weathering of basalt in southwest Iceland; effects of runoff, age of rocks and vegetative/glacial cover. *Am. J. Sci.* 296, 837–907. doi:10.2475/ajs.296.8.837
- Han, J., Liu, Y., and Zhang, Y. (2015). Sand stabilization effect of feldspathic sandstone during the fallow period in mu us sandy land. *J. Geogr. Sci.* 25, 428–436. doi:10.1007/s11442-015-1178-7
- Han, J., Xie, J., and Zhang, Y. (2012). Potential role of feldspathic sandstone as a natural water retaining agent in mu us sandy land, northwest China. *Chin. Geogr. Sci.* 22, 550–555. doi:10.1007/s11769-012-0562-9
- Hapca, S., Baveye, P. C., Wilson, C., Lark, R. M., and Otten, W. (2015). Three-dimensional mapping of soil chemical characteristics at micrometric scale by combining 2d sem-edx data and 3d x-ray ct images. *PLoS One* 10, e0137205. doi:10.1371/journal.pone.0137205
- Haynes, R., and Francis, G. (1993). Changes in microbial biomass c, soil carbohydrate composition and aggregate stability induced by growth of selected crop and forage species under field conditions. *J. Soil Sci.* 44, 665–675. doi:10.1111/j.1365-2389.1993.tb02331.x
- Hou, T., Berry, T. D., Singh, S., Hughes, M. N., Tong, Y., Papanicolaou, A. T., et al. (2018). Control of tillage disturbance on the chemistry and proportion of raindrop-liberated particles from soil aggregates. *Geoderma* 330, 19–29. doi:10.1016/j.geoderma.2018.05.013
- Huang, X., Jiang, H., Li, Y., Ma, Y., Tang, H., Ran, W., et al. (2016). The role of poorly crystalline iron oxides in the stability of soil aggregate-associated organic carbon in a rice-wheat cropping system. *Geoderma* 279, 1–10. doi:10.1016/j.geoderma.2016.05.011
- Janalizadeh, D. C., Soleimani, K. S., and Taslimi, P. A. M. (2019a). Modeling of compressive strength of cemented sandy soil. *J. Adhesion Sci. Technol.* 33 (8), 791–807. doi:10.1080/01694243.2018.1548535
- Janalizadeh, F., Choobasti, A., Farrokhzad, F., Nadimi, A., and Soleimani, K. S. (2019b). Effects of copper sludge on cemented clay using ultrasonic pulse velocity. *J. Adhesion Sci. Technol.* 33 (4), 433–444. doi:10.1080/01694243.2018.1471842
- Jastrow, J. (1996). Soil aggregate formation and the accrual of particulate and mineral-associated organic matter. *Soil Biol. Biochem.* 28, 665–676. doi:10.1016/0038-0717(95)00159-x
- Jiang, X., Bol, R., Willbold, S., Vereecken, H., and Klumpp, E. (2015). Speciation and distribution of p associated with Fe and Al oxides in aggregate-sized fraction of an arable soil. *Biogeochemistry* 12, 6443–6452. doi:10.5194/bg-12-6443-2015
- Jiménez-Pinilla, P., Mataix-Solera, J., Arcenegui, V., Delgado, R., Martín-García, J. M., Lozano, E., et al. (2016). Advances in the knowledge of how heating can affect aggregate stability in mediterranean soils: A xdr and sem-edx approach. *Catena* 147, 315–324. doi:10.1016/j.catena.2016.07.036
- Joussein, E., Kruyts, N., Righi, D., Petit, S., and Delvaux, B. (2004). Specific retention of radiocesium in volcanic ash soils devoid of micaceous clay minerals. *Soil Sci. Soc. Am. J.* 68, 313–319. doi:10.2136/sssaj2004.3130
- Koutanaei, E. R. Y., Choobasti, A. J., and Kutanaei, S. S. (2021). Triaxial behaviour of a cemented sand reinforced with Kenaf fibres. *Eur. J. Environ. Civ. Eng.* 25 (7), 1268–1286. doi:10.1080/19648189.2019.1574607
- Lado, M., Ben-Hur, M., and Shainberg, I. (2004). Soil wetting and texture effects on aggregate stability, seal formation, and erosion. *Soil Sci. Soc. Am. J.* 68, 1992–1999. doi:10.2136/sssaj2004.1992
- Li, C., Zhang, T., and Wang, L. (2014). Mechanical properties and microstructure of alkali activated pisha sandstone geopolymer composites. *Constr. Build. Mater.* 68, 233–239. doi:10.1016/j.conbuildmat.2014.06.051
- Li, T., Wang, H., Chen, X., and Zhou, J. (2017). Soil reserves of potassium: Release and availability to liliom perenne in relation to clay minerals in six cropland soils from eastern China. *Land Degrad. Dev.* 28, 1696–1703. doi:10.1002/ldr.2701
- Ma, W., and Zhang, X. (2016). Effect of pisha sandstone on water infiltration of different soils on the Chinese loess plateau. *J. Arid Land* 8, 331–340. doi:10.1007/s40333-016-0122-8
- Martin, M. W., Clavero, J., and Mpodozis, C. (1999). Late paleozoic to early jurassic tectonic development of the high andean principal cordillera, el indio region, Chile (29–30 s). *J. S. Am. Earth Sci.* 12, 33–49. doi:10.1016/s0895-9811(99)00003-6
- Molina, N., Caceres, M., and Pietroboni, A. (2001). Factors affecting aggregate stability and water dispersible clay of recently cultivated semiarid soils of Argentina. *Arid Land Res. Manag.* 15, 77–87. doi:10.1080/15324980118369
- Muggler, C. C., van Griethuysen, C., Buurman, P., and Pape, T. (1999). Aggregation, organic matter, and iron oxide morphology in oxisols from minas gerais, Brazil. *Soil Sci.* 164, 759–770. doi:10.1097/00010694-199910000-00007
- Oades, J. (1993). The role of biology in the formation, stabilization and degradation of soil structure. *Geoderma* 56, 377–400. doi:10.1016/0016-7061(93)90123-3
- Ren, W., Wang, M., and Zhou, Q. (2011). Adsorption characteristics and influencing factors of chlorimuron-ethyl in two typical Chinese soils. *Soil Sci. Soc. Am. J.* 75, 1394–1401. doi:10.2136/sssaj2010.0228
- Ribeiro, S. P. d. S., Cescon, L. d. S., Ribeiro, R. Q. C. R., Landesmann, A., Esteve, L. R. d. M., and Nascimento, R. S. V. (2018). Effect of clay minerals structure on the polymer flame retardancy intumescent process. *Appl. Clay Sci.* 161, 301–309. doi:10.1016/j.clay.2018.04.037
- Roshan, H. K., Choobasti, A. J., and Kutanaei, S. S. (2020). Evaluation of the impact of fiber reinforcement on the durability of lignosulfonate stabilized clayey sand under wet-dry condition. *Transp. Geotech.* 23, 100359. doi:10.1016/j.trgeo.2020.100359
- Roshan, H. K., Choobasti, A. J., Kutanaei, S. S., and Fakhrabadi, A. (2022). The effect of adding polypropylene fibers on the freeze-thaw cycle durability of lignosulfonate stabilised clayey sand. *Cold Regions Sci. Technol.* 193, 103418. doi:10.1016/j.coldregions.2021.103418
- Sayen, S., Mallet, J., and Guillon, E. (2009). Aging effect on the copper sorption on a vineyard soil: Column studies and sem-eds analysis. *J. Colloid Interface Sci.* 331, 47–54. doi:10.1016/j.jcis.2008.11.049
- Schomburg, A., Verrecchia, E. P., Guenat, C., Brunner, P., Sebag, D., and Le Bayon, R. C. (2018). Rock-eval pyrolysis discriminates soil macro-aggregates formed by plants and earthworms. *Soil Biol. Biochem.* 117, 117–124. doi:10.1016/j.soilbio.2017.11.010
- Shi, Y., Chen, X., and Shen, S. (2002). Mechanisms of organic cementing soil aggregate formation and its theoretical models. *J. Appl. Ecol.* 13, 1495–1498.
- Skjemstad, J., Janik, L. J., Head, M., and McClure, S. G. (1993). High energy ultraviolet photo-oxidation: A novel technique for studying physically protected organic matter in clay- and silt-sized aggregates. *J. Soil Sci.* 44, 485–499. doi:10.1111/j.1365-2389.1993.tb00471.x
- Sun, Z., and Han, J. (2018). Effect of soft rock amendment on soil hydraulic parameters and crop performance in mu us sandy land, China. *Field Crops Res.* 222, 85–93. doi:10.1016/j.fcr.2018.03.016
- Sun, Z., Han, J., and Wang, H. (2019). Soft rock for improving crop yield in sandy soil in the mu us desert, China. *Arid Land Res. Manag.* 33, 136–154. doi:10.1080/15324982.2018.1522385
- Sun, Z. H., Han, J. C., Wang, H. Y., Zhang, R. Q., Sun, Y. Y., Wei, J., et al. (2021). Use and economic benefit of soft rock as an amendment for sandy soil in Mu Us Sandy Land, China. *Arid Land Res. Manag.* 35, 15–31. doi:10.1080/15324982.2020.1765221
- Terpstra, R. (1990). Formation of new aggregates and weed seed behaviour in a coarse- and in a fine-textured loam soil. A laboratory experiment. *Soil Tillage Res.* 15, 285–296. doi:10.1016/0167-1987(90)90085-r
- Van Oss, C., and Giese, R. (1995). The hydrophilicity and hydrophobicity of clay minerals. *Clays Clay minerals* 43, 474–477. doi:10.1346/ccmn.1995.0430411
- Wang, N., Xie, J., and Han, J. (2013). A sand control and development model in sandy land based on mixed experiments of arsenic sandstone and sand: A case study in mu us sandy land in China. *Chin. Geogr. Sci.* 23, 700–707. doi:10.1007/s11769-013-0640-7
- Wang, W., Kravchenko, A., Smucker, A., Liang, W., and Rivers, M. (2012). Intra-aggregate pore characteristics: X-ray computed microtomography analysis. *Soil Sci. Soc. Am. J.* 76, 1159–1171. doi:10.2136/sssaj2011.0281
- Wang, Y., Zheng, J., Zhang, X., and Zhang, Y. (2009). A structure-based investigation on the binding interaction of hydroxylated polycyclic aromatic hydrocarbons with DNA. *Acta Agrestia Sin.* 17, 250–257. doi:10.1016/j.tox.2009.06.015
- Watteau, F., Villemin, G., Bartoli, F., Schwartz, C., and Morel, J.-L. (2012). 0–20 µm aggregate typology based on the nature of aggregative organic materials in a cultivated silty topsoil. *Soil Biol. Biochem.* 46, 103–114. doi:10.1016/j.soilbio.2011.11.021
- Wiesmeier, M., Steffens, M., Mueller, C., Kölbl, A., Reszkowska, A., Peth, S., et al. (2012). Aggregate stability and physical protection of soil organic carbon in semi-arid steppe soils. *Eur. J. Soil Sci.* 63, 22–31. doi:10.1111/j.1365-2389.2011.01418.x
- Wilson, C., Cloy, J. M., Graham, M. C., and Hamlet, L. (2013). A microanalytical study of iron, aluminium and organic matter relationships in soils with contrasting hydrological regimes. *Geoderma* 202, 71–81. doi:10.1016/j.geoderma.2013.03.020
- Yaghi, N., and Hartikainen, H. (2013). Enhancement of phosphorus sorption onto light expanded clay aggregates by means of aluminum and iron oxide coatings. *Chemosphere* 93, 1879–1886. doi:10.1016/j.chemosphere.2013.06.059
- Yu, X., Fu, Y., and Lu, S. (2017). Characterization of the pore structure and cementing substances of soil aggregates by a combination of synchrotron radiation x-ray micro-computed tomography and scanning electron microscopy. *Eur. J. Soil Sci.* 68, 66–79. doi:10.1111/ejss.12399
- Zhang, Y., Zhao, S., Wang, Z., Li, X., Li, M., Du, C., et al. (2015). Karyopherin alpha 2 is a novel prognostic marker and a potential therapeutic target for colon cancer. *J. Soil Water Conservation* 13, 145–150. doi:10.1186/s13046-015-0261-3



## OPEN ACCESS

EDITED BY  
Jianping Li,  
Ningxia University, China

REVIEWED BY  
Junzhuo Liu,  
Chinese Academy of Sciences (CAS),  
China  
Yangquanwei Zhong,  
Northwestern Polytechnical University,  
China

\*CORRESPONDENCE  
Chunyu Li,  
✉ chunyu\_li@snnu.edu.cn

<sup>†</sup>These authors have contributed equally  
to this work and share first authorship

RECEIVED 31 May 2023  
ACCEPTED 10 July 2023  
PUBLISHED 20 July 2023

CITATION  
Wang Y, Li Q and Li C (2023). Organic  
fertilizer has a greater effect on soil  
microbial community structure and  
carbon and nitrogen mineralization than  
planting pattern in rainfed farmland of the  
Loess Plateau.  
*Front. Environ. Sci.* 11:1232527.  
doi: 10.3389/fenvs.2023.1232527

COPYRIGHT  
© 2023 Wang, Li and Li. This is an open-  
access article distributed under the terms  
of the [Creative Commons Attribution  
License \(CC BY\)](https://creativecommons.org/licenses/by/4.0/). The use, distribution or  
reproduction in other forums is  
permitted, provided the original author(s)  
and the copyright owner(s) are credited  
and that the original publication in this  
journal is cited, in accordance with  
accepted academic practice. No use,  
distribution or reproduction is permitted  
which does not comply with these terms.

# Organic fertilizer has a greater effect on soil microbial community structure and carbon and nitrogen mineralization than planting pattern in rainfed farmland of the Loess Plateau

Yi Wang<sup>1†</sup>, Qianxue Li<sup>2†</sup> and Chunyu Li<sup>2\*</sup>

<sup>1</sup>State Key Laboratory of Loess and Quaternary Geology, Institute of Earth Environment, Chinese Academy of Sciences, Xi'an, China, <sup>2</sup>School of Geography and Tourism, Shaanxi Normal University, Xi'an, China

Agricultural ecosystem is the largest artificial ecosystem on Earth and provide 66% of the world's food supply. Soil microorganisms are an engine for carbon and nutrient cycling. However, the driving mechanism of soil microbial community structure and carbon and nitrogen transformation mediated by fertilization and planting pattern in rainfed agricultural ecosystems is still unclear. The research was conducted at the Changwu Agricultural Ecology Experimental Station in Shaanxi Province, China. Seven different fertilization and planting pattern were designed. The Phosphate fatty acids (PLFAs) were used to explore the effects of fertilization and plating pattern on the soil microbial community structure and the relationship with soil carbon and nitrogen transformation. The results showed that there were significant differences in soil physical and chemical properties among treatments. Organic fertilizer significantly increased the soil carbon and nitrogen and decreased the soil pH. The contents of total PLFAs and microbial groups in the wheat and corn rotation treatment were the highest. Compared with the change in planting pattern, organic fertilizer had a greater impact on PLFA content and soil ecological processes. The soil microbial community structure has a significantly positive correlation with soil organic carbon (SOC), total carbon (TC), total nitrogen (TN), and total phosphorus (TP). Compared with applying NP fertilizer, applying organic fertilizer significantly increased the soil respiration rate and mineralized nitrogen content while decreasing the soil microbial biomass carbon (MBC). The correlation analysis showed that soil respiration was significantly positively correlated with SOC and TP, and mineralized nitrogen was significantly positively correlated with SOC, nitrate nitrogen, TN and MBC. Structural equation modeling (SEM) showed that the soil respiration rate was significantly positively affected by TC and negatively affected by SWC and explained 63%, whereas mineralized nitrogen was significantly positively influenced by TN and explained 55% of the total variance.

## KEYWORDS

rainfed farmland, soil respiration, nitrogen mineralization, fertilization, cropping pattern, soil microbe

# 1 Introduction

Soil microorganisms are not only widely involved in various biochemical reactions with element cycling but are also an important medium connecting plants and soil (Zhang Q. et al., 2022). The agricultural ecosystem provides nearly 66% of the food supply, and agricultural soil acts as an important matrix linking crops and underground ecosystem processes (Zhang J. Y. et al., 2022). Agricultural soil microorganisms are of great significance to soil fertility, and their biomass nitrogen and phosphorus are important sources of crop nutrients (Chen et al., 2017). The quality of the soil environment can directly affect the composition of the microbial community and thereby affect crop growth and health (Li et al., 2021). A suitable microbial community structure in agricultural ecosystems could promote crop growth, and the change in soil microbial community structure could be used as an important indicator of soil health and crop growth (Liu Z. H. et al., 2021).

Agricultural crop planting pattern affect soil physicochemical properties and microbial properties (Rashid et al., 2016). Agricultural crop planting pattern mainly include continuous cropping and crop rotation. Research has shown that the biotic and abiotic environments in the soil are significantly different between different crops under the same planting pattern or between different planting patterns of the same crop (Li et al., 2021). The reason is mainly because different planting patterns could affect the physical structure, nutrients, and microbial community structure of the soil (Aimaierjiang et al., 2022). Continuous cropping may lead to a decline in soil fertility and the transformation of soil microorganisms, causing abnormal crop growth (Ma et al., 2004; Pradeep et al., 2010). Crop rotation could balance the utilization of soil nutrients and increase the variety and quantity of beneficial microorganisms in the soil (Asuming-Brempong et al., 2008). For example, soybean rotation can significantly increase bacterial PLFA content, and avoid the process of microbial groups transforming to fungi caused by continuous cropping (Yao et al., 2015). Therefore, scientifically and reasonably selecting crop planting pattern is beneficial for improving the soil environment and promoting the healthy growth of crops.

Fertilization is an important factor affecting crop growth and soil health. Long-term application of chemical nitrogen and phosphorus fertilizers significantly increases soil organic carbon (SOC), total phosphorus (TP), and available phosphorus (AP) (Gao et al., 2021). Fertilization can also alter soil microbial properties, and organic fertilizers or organic–inorganic combinations can effectively increase the number and activity of microorganisms (Li et al., 2005; Wu et al., 2020). In humid and warm climate conditions, organic fertilizer has a great effect on soil microbial properties and leads to greater microbial diversity and a more stable microbial community (Wang et al., 2017). The combination of organic and inorganic fertilizers increased the number of bacteria and decreased fungi (Nanda et al., 1998). Although chemical fertilizers can effectively improve crop productivity (Liu Z. et al., 2020; Liu J. A. et al., 2021), excessive application of inorganic fertilizers can cause damage to the soil environment, which not only leads to soil quality degradation but also has a negative impact on soil microecological balance

(Tiziano et al., 2011; Kour et al., 2020; Yu et al., 2020). It is of great significance to explore the effects of fertilization on soil physicochemical and microbial properties to improve agricultural safety.

Soil organic carbon and nitrogen and their turnover processes determine soil fertility and sustainability (Morales-Rodriguez et al., 2019). Soil carbon and nitrogen mineralization is affected by environmental factors, and generally, the rate of soil organic carbon mineralization increases with increasing temperature (Ma et al., 2016). In addition to temperature, changes in planting and fertilization pattern also cause changes in soil carbon mineralization, which in turn affects crop growth. Nitrogen fertilizer application can prohibit soil carbon mineralization by inhibiting microbial biomass and extracellular enzyme activity (Keeler et al., 2009), while significantly improving soil microbial net nitrogen mineralization (NNM) (Wang et al., 2014). Organic fertilization could increase carbon mineralization by 52%–117% more than chemical inputs in soil, and significantly enhance NNM under no-tillage management in humid conditions (Wang et al., 2011). There has been a report that fertilization has a greater impact on soil microbial community structure than crop rotation (Guo et al., 2020). However, there are still few reports on the effects of fertilization and planting pattern on soil microorganisms and carbon and nitrogen mineralization in rainfed farmland.

The rainfed farmland in the Chinese Loess Plateau is an important agricultural ecosystem and produces vital food for the local people (Lian et al., 2021). To explore the effects of fertilization and planting pattern on soil microbial community structure and microbe-mediated ecological processes of carbon and nitrogen cycling. We used long-term field experiments to address these uncertainties and we hypothesized that 1) fertilization and planting pattern mainly affect the soil carbon and nitrogen contents and affect the microbial community structure and 2) compared with the change in planting pattern, fertilization had a greater influence on the structure and composition of the microbial community. To test these assumptions, the changes in the microbial community and carbon and nitrogen mineralization were tested by the traditional biochemical method. Determining the influence mechanism of fertilization and planting pattern on soil carbon and nitrogen mineralization and soil microbial properties will help to set an effective and safe fertilization pattern under different planting scenarios.

## 2 Materials and methods

### 2.1 Site description

The research site is selected in the Changwu Agricultural Ecology Experimental Station of the Chinese Academy of Sciences, Shaanxi Province, China. Geographic coordinates are 107°41'E, 35°14'N, with an altitude of 1,220 m. It belongs to a semihumid continental monsoon climate. The average annual precipitation is 580 mm, the average annual temperature is 9.1°C, and the frost-free period is 171 days. The loose and higher permeability soil is Heilu soil (Cumulic Haplustoll, USDA). The long-term field experiment in this research began in 1984. The initial soil nutrient status was as follows: organic matter = 10.50 g·kg<sup>-1</sup>,

total nitrogen = 0.80 g·kg<sup>-1</sup>, total phosphorus = 1.26 g·kg<sup>-1</sup>, and pH = 8.10.

## 2.2 Experimental treatment and design

This experimental design had 7 different fertilization and planting pattern treatments: 1) wheat continuous cropping without fertilization (W-CK); 2) wheat continuous cropping with NP fertilizer (W-NP); 3) wheat continuous cropping with NP and organic fertilizer (W-NPM); 4) wheat and corn rotation with NP fertilizer (WC-NP); 5) wheat and corn rotation with NP and organic fertilizer (WC-NPM); 6) wheat, millet and pea rotation with NP fertilizer (WMP-NP); and 7) wheat, millet and pea rotation with NP fertilizer and organic fertilizer (WMP-NPM). The fertilization amounts of the three fertilizers were as follows: N (120 kg·ha<sup>-1</sup>·y<sup>-1</sup> CH<sub>4</sub>N<sub>2</sub>O), P (90 kg·ha<sup>-1</sup>·y<sup>-1</sup> P<sub>2</sub>O<sub>5</sub>), and M (7.5 × 10<sup>4</sup> kg·ha<sup>-1</sup>·y<sup>-1</sup> manure with 10.6% organic matter content). Each treatment had 3 replicates with a 36 m<sup>2</sup> (4 m × 9 m) plot area. Field activities such as weeding and spraying were carried out according to local field management habits.

## 2.3 Soil sample collection

In June 2019, soil samples were collected after crop harvest. After clearing the dead branches and leaves on the soil surface, a soil sample of 0–20 cm was taken using the five point sampling method. The same treated soil samples in each plot were mixed and bagged, stored at 4°C and taken back to the laboratory. After removing the visible sand, gravel, animal and plant residues, the soil was passed through a 2 mm stainless sieve. The screened soil sample was divided into 3 parts. One part was placed into a 4°C refrigerator to determine the soil microbial biomass and soil respiration, one part was stored at -86°C to test PLFAs, and the third part was used to determine the soil physical and chemical properties after air drying with protection from sunlight.

## 2.4 Measurement items and methods

### 2.4.1 Determination of soil physical and chemical properties

The soil water content (SWC) was determined using the oven drying method; total carbon (TC) in soil was measured using a carbon analyzer (Vario TOC, Elemental, Hanau, Germany); soil organic carbon (SOC) was measured using the potassium dichromate external heating method; total phosphorus (TP) in soil was measured using the Olsen method; a fully automatic Kjeldahl nitrogen analyzer was used to measure soil total nitrogen (TN); ammonium nitrogen (NH<sub>4</sub><sup>+</sup>-N) and nitrate nitrogen (NO<sub>3</sub><sup>-</sup>-N) in soil were extracted with K<sub>2</sub>SO<sub>4</sub> solution and measured using a continuous flow analyzer (Autoanalyzer 3, Bran Luebbe, Germany); available phosphorus (AP) in soil was measured using the Olsen method; the organic phosphorus (OP) in the soil was determined by the high-temperature burning method; soil pH (water/soil at 2.5:1) was measured by a glass electrode pH meter; soil particle composition was measured using the Malvern 2000 laser particle size analyzer; and mineralized nitrogen was measured using the biological culture method (Bao, 2000).

### 2.4.2 Determination of soil microbial community structure and microbial indicators

The phosphate fatty acid (PLFA) method was used to determine the soil microbial community structure. 8 g of freeze-dried soil was weighed for the test. After operating with the protocol, phospholipid fatty acids were extracted and determined using a gas chromatograph (Agilent GC-7890B) combined with the MIDI microbial identification system Sherlock 6.2 (Frosteg et al., 1991). Bacteria were represented with 15:0, 17:0, 15:0iso, 15:0anteiso, 16:0iso, 16:1w7c, 17:0iso, 17:0anteiso, 17:0cyclo7c, 18:1w7c and 18:1w5c (Tunlid et al., 1989; Frosteg et al., 1993). Fungi were represented with 16:1w5c, 18:1w9c, 18:2w6c and 20:1w9c (Federle et al., 1986; Baath, 2003). Arbuscular mycorrhizal fungi (AMF) were represented with 16:1w5c (Nordby et al., 1981; Olsson, 1999). Actinomycete were represented with 10Me16:0, 10Me17:0 and 10Me18:0 (Zelles, 1997). Gram-positive bacteria (G<sup>+</sup>) were represented with 15:0iso, 15:0anteiso, 16:0anteiso, 17:0iso, 17:1isow9c, 18:0iso, 16:0iso, 17:0anteiso and 17:1anteisow7c. Gram-negative bacteria (G<sup>-</sup>) were represented with 19:0cyclo7c, 12:1w5c, 16:1w7c, 18:1w5c, 17:1w8c, 12:1w8c, 16:1w9c, 17:0cyclo7c, 19:0cyclo7c and 21:1w9c (Frosteg and Baath, 1996; Zelles, 1997).

Soil microbial biomass carbon (MBC) and microbial biomass nitrogen (MBN) were extracted and measured using the chloroform fumigation method. Soil respiration and mineralized nitrogen were measured by alkali absorption titration. The samples were incubated continuously at 25°C for 28 days and removed on days 1, 3, 7, and 14 to calculate the soil respiration rate during the incubation process by titration. At 28 days, the soil nitrate nitrogen (NO<sub>3</sub><sup>-</sup>-N) and ammonium nitrogen (NH<sub>4</sub><sup>+</sup>-N) contents before and after cultivation were measured using a continuous flow analyzer (Autoanalyzer 3, Bran Luebbe, Germany), and the soil mineralization nitrogen, soil net nitrification rate, and net mineralization rate were calculated as follows:

Soil microbial respiration entropy (d<sup>-1</sup>) = soil basic respiration / MBC

$$\begin{aligned} A_{\text{nit}} &= c(\text{NO}_3^- - \text{N})_2 - c(\text{NO}_3^- - \text{N})_1 \\ A_{\text{min}} &= c(\text{NH}_4^+ - \text{N})_2 + c(\text{NO}_3^- - \text{N})_2 - c(\text{NH}_4^+ - \text{N})_1 - c(\text{NO}_3^- - \text{N})_1 \\ V_{\text{nit}} &= A_{\text{nit}} / d \end{aligned}$$

In the formula, d refers to the cultivation days of the soil used for measuring mineralized nitrogen, which in this research is 28 days. c(NO<sub>3</sub><sup>-</sup>-N)<sub>1</sub>, c(NO<sub>3</sub><sup>-</sup>-N)<sub>2</sub>, c(NH<sub>4</sub><sup>+</sup>-N)<sub>1</sub> and c(NH<sub>4</sub><sup>+</sup>-N)<sub>2</sub> represent the concentrations of NO<sub>3</sub><sup>-</sup>-N and NH<sub>4</sub><sup>+</sup>-N before and after incubation. A<sub>nit</sub> and A<sub>min</sub> represent the net accumulation of nitrate nitrogen and mineralized nitrogen content, respectively. V<sub>nit</sub> and V<sub>min</sub> represent the net nitrification rate and net mineralization rate of nitrogen, respectively.

## 2.5 Statistical analysis

Data Processing System (DPS) software was used for data analysis (Tang and Zhang, 2013). One-way ANOVA was performed with least significant difference (LSD) analysis. Structural equation modeling (SEM) was used to analyze the effect of different treatments on mineralized nitrogen and soil respiration by soil microbial community structure. The maximum likelihood estimation method was used with Amos V18.0 (IBM, Chicago, IL, United States). R software was used to draw figures. The data in this research are expressed as the average ± standard deviation.

**TABLE 1 Soil physical and chemical properties in different treatments.**

Treatment	SOC (g·kg <sup>-1</sup> )	TC (g·kg <sup>-1</sup> )	NH <sub>4</sub> <sup>+</sup> -N (mg·kg <sup>-1</sup> )	NO <sub>3</sub> <sup>-</sup> -N (mg·kg <sup>-1</sup> )	TN (g·kg <sup>-1</sup> )	OP (mg·kg <sup>-1</sup> )	AP (mg·kg <sup>-1</sup> )	TP (mg·kg <sup>-1</sup> )	pH (2.5:1)	SWC (%)	Physical clay (%)	Clay (%)
W-CK	8.05 ± 0.62b	21.88 ± 1.15a	0.28 ± 0.04c	10.99 ± 0.99e	1.11 ± 0.13bcd	150.67 ± 16.65bc	8.82 ± 0.68e	892.33 ± 5.03d	8.18 ± 0.05a	12.44 ± 0.07a	36.60 ± 3.20c	10.04 ± 1.14ab
W-NP	7.91 ± 0.98b	18.39 ± 0.52bc	0.26 ± 0.03c	57.72 ± 2.08c	1.08 ± 0.02cd	160.67 ± 5.03bc	15.58 ± 1.88d	1035.67 ± 8.39c	7.91 ± 0.07b	11.94 ± 0.07b	39.50 ± 0.88abc	10.09 ± 1.18ab
W-NPM	9.82 ± 0.73a	23.97 ± 0.60a	0.40 ± 0.04b	50.55 ± 2.51c	1.29 ± 0.10ab	157.33 ± 6.11bc	35.38 ± 2.30b	1229.33 ± 13.61a	7.89 ± 0.02b	10.25 ± 0.12cd	36.93 ± 1.57bc	10.83 ± 0.23a
WC-NP	8.56 ± 0.16b	17.72 ± 0.39c	0.52 ± 0.04a	29.28 ± 0.65d	1.21 ± 0.07bc	171.33 ± 11.02ab	16.78 ± 0.89d	1044.33 ± 95.44c	7.84 ± 0.03bc	10.42 ± 0.25c	41.01 ± 1.14a	8.85 ± 0.89b
WC-NPM	10.12 ± 0.08a	21.64 ± 3.93a	0.28 ± 0.03c	89.84 ± 10.54a	1.42 ± 0.07a	157.33 ± 13.01bc	41.28 ± 2.95a	1198.67 ± 18.90a	7.70 ± 0.01d	10.01 ± 0.24d	38.16 ± 0.94abc	9.27 ± 1.06ab
WMP-NP	8.47 ± 0.37b	18.40 ± 0.63bc	0.50 ± 0.06a	70.99 ± 3.76b	1.05 ± 0.10cd	190.00 ± 20.30a	21.58 ± 1.79c	1129.00 ± 3.00b	7.77 ± 0.04cd	8.89 ± 0.18e	39.66 ± 0.74ab	9.39 ± 0.66ab
WMP-NPM	9.13 ± 0.91ab	20.95 ± 0.61ab	0.26 ± 0.01c	36.82 ± 1.92d	0.95 ± 0.19d	144.67 ± 2.31c	35.78 ± 1.41b	1202.33 ± 9.61a	7.79 ± 0.02c	10.46 ± 0.19c	39.12 ± 1.37abc	8.56 ± 0.67b

Note: The same letter in each column indicates no significant difference ( $p > 0.05$ ); different letters indicate significant differences ( $p < 0.05$ ). The same below. A significant difference was obtained by one-way ANOVA, and LSD, test. SOC, soil organic carbon; TC, total carbon; TN, total nitrogen; OP, organic phosphorus; AP, available phosphorus; TP, total phosphorus; SWC, soil water content.



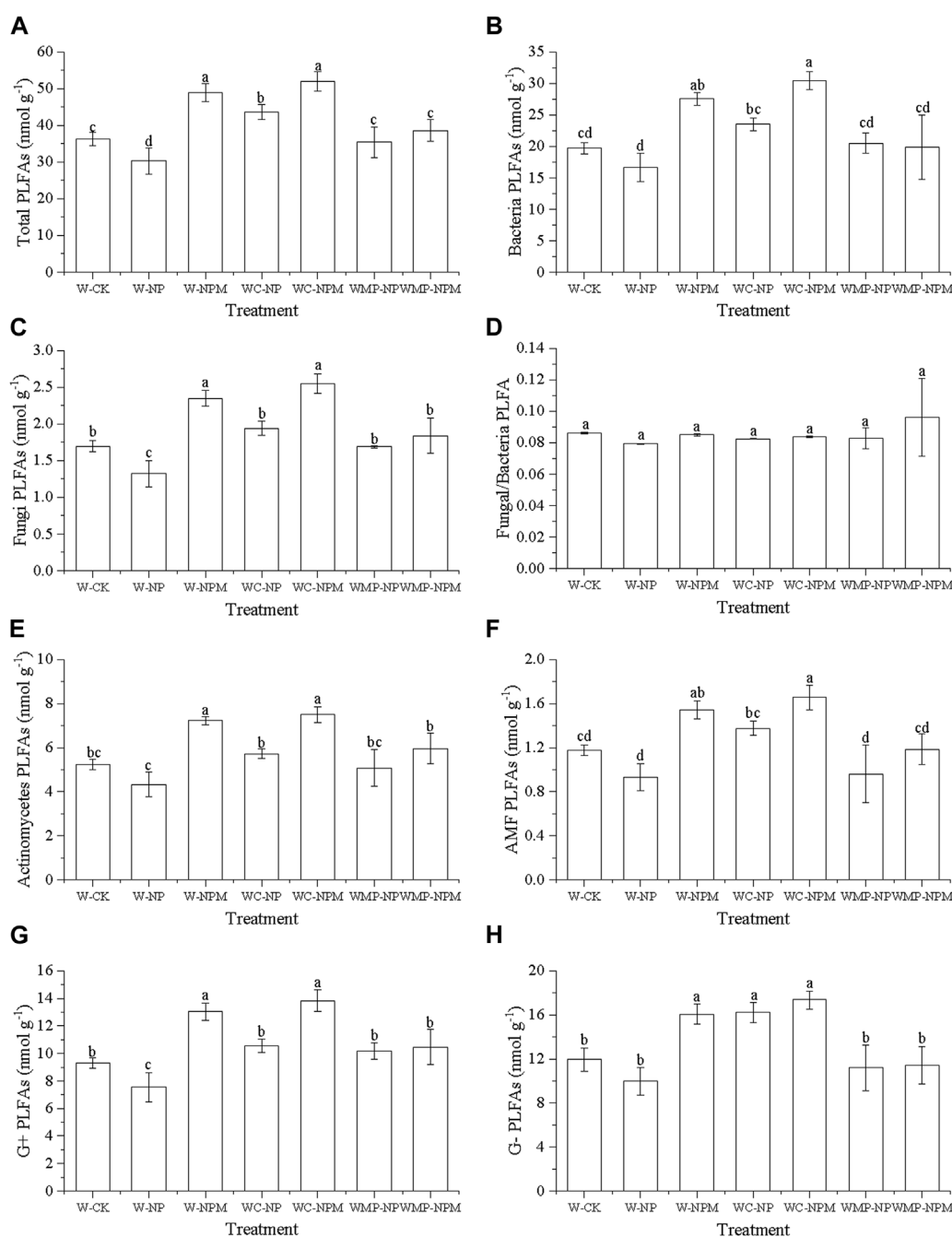


FIGURE 1

Trends of Total PLFAs (A), Bacteria PLFAs (B), Fungi PLFAs (C), Fungi/Bacteria PLFAs (D), Actinomycete PLFAs (E), AMF PLFAs (F), Gram positive bacteria PLFAs (G) and Gram negative bacteria PLFAs (H) in soil microbial communities under different treatments. The same letter above each column indicates no significant difference ( $p > 0.05$ ); different letters indicate significant difference ( $p < 0.05$ ).

### 3 Results

#### 3.1 Soil physical and chemical properties under different treatments

Planting pattern and fertilization treatments had significant effects on soil physical and chemical properties (Table 1).

Compared with the W-CK, SOC was significantly increased in the W-NPM and WC-NPM ( $p < 0.05$ ), whereas TC was significantly decreased in the W-NP, WC-NP and WMP-NP ( $p < 0.05$ ). All treatments significantly enhanced  $\text{NO}_3^-$ -N, while only W-NPM, WC-NP and WMP-NP increased  $\text{NH}_4^+$ -N and WC-NPM increased TN ( $p < 0.05$ ). AP and TP were significantly higher than those in the W-CK in all other treatments, and OP was only

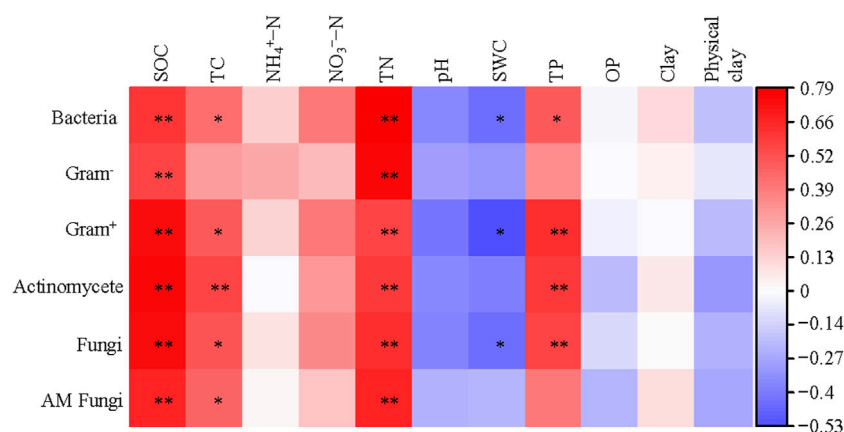


FIGURE 2

Correlation analysis of soil microbial PLFAs with soil physical and chemical properties.

significantly higher in the WMP-NP treatment ( $p < 0.05$ ). The pH and SWC both significantly decreased in all the treatments, but the physical clay content only increased in the WC-NP treatment ( $p < 0.05$ ).

In the wheat continuous treatment, SOC, TC, NH<sub>4</sub><sup>+</sup>-N, TN, AP and TP were significantly higher in the organic fertilizer used plot whereas SWC had a reverse trend ( $p < 0.05$ ). The wheat and corn rotation plot with organic fertilizer had significantly higher SOC, TC, NO<sub>3</sub><sup>-</sup>-N, TN, AP and TP, and significantly lower NH<sub>4</sub><sup>+</sup>-N, pH and SWC than the chemical fertilizer plot ( $p < 0.05$ ). The plot with wheat, millet and pea rotation and organic fertilizer obviously enhanced AP, TP and SWC but abated NH<sub>4</sub><sup>+</sup>-N, NO<sub>3</sub><sup>-</sup>-N and OP ( $p < 0.05$ ).

In the chemical fertilizer treatment, AP and TP significantly increased with the number of rotations whereas SWC decreased ( $p < 0.05$ ). NH<sub>4</sub><sup>+</sup>-N and NO<sub>3</sub><sup>-</sup>-N were significantly influenced by rotational management with a reverse trend ( $p < 0.05$ ). In the organic fertilizer plot, NH<sub>4</sub><sup>+</sup>-N significantly decreased with the number of rotations, pH decreased first and then increased, and NO<sub>3</sub><sup>-</sup>-N, TN and AP had a reverse trend ( $p < 0.05$ ).

## 3.2 Soil microbial community structure in different treatments

Planting pattern and fertilization had a significant effect on the soil microbial community structure (Figure 1). Compared with W-CK, the total PLFA content was significantly decreased in W-NP and significantly increased in W-NPM, WC-NP and WC-NPM ( $p < 0.05$ ). There was no obvious difference among the W-CK, WMP-NP and WMP-NPM (Figure 1A). The trend of bacteria, fungi, actinomycete, AMF, G<sup>+</sup> and G<sup>-</sup> PLFAs all showed a similar pattern with the total PLFAs. The Fungal/Bacteria ratio was not significantly different.

The plot with organic fertilizer had higher microbial PLFAs than the chemical fertilizer treatment, and this effect was weakened in the wheat, millet and pea rotation scenario. As the rotation number increased, all the microbial PLFAs first increased then decreased. Overall, the application of organic fertilizers has a

greater impact on soil microbial PLFAs than rotation management.

A heatmap was used to show the correlation between soil physical and chemical properties and soil microbial communities (Figure 2). The PLFAs of bacteria, gram positive bacteria and fungi were significantly correlated with SOC, TC, TN, SWC and TP ( $p < 0.05$ ). The PLFAs of actinomycete and AM fungi were significantly correlated with SOC, TC and TN ( $p < 0.05$ ). Gram negative bacteria were only correlated with SOC and TN ( $p < 0.05$ ).

## 3.3 Soil microbial biomass under different treatments

Fertilization and planting pattern have significant effects on soil microbial biomass. Compared with W-CK, W-NP and WMP-NP significantly increased MBC, whereas WC-NPM and WMP-NPM decreased MBC ( $p < 0.05$ ). The organic fertilizer had a negative effect on MBC and the effect obviously increased as the rotation number increased (Figure 3A). The MBN was significantly decreased in the W-NP and WMP-NP treatments but increased in WC-NPM ( $p < 0.05$ ). Contrary to MBC, MBN was positively influenced by organic fertilizer and the effect was lower in the wheat and corn rotation treatment (Figure 3B).

## 3.4 Mineralization of soil C and N under different treatments

### 3.4.1 Soil respiration rate of different treatments

Fertilization and rotation significantly affected the soil respiration rate (Figure 4A). Compared with the W-CK, the soil respiration rate was significantly increased in the W-NPM, WC-NPM, WMP-NP and WMP-NPM ( $p < 0.05$ ). Under the same planting pattern, organic fertilizer significantly increased the soil respiration rate in the wheat continuous cropping, and wheat and corn rotation treatments ( $p < 0.05$ ), whereas a converse trend was observed in the wheat, millet and pea rotation treatments, although

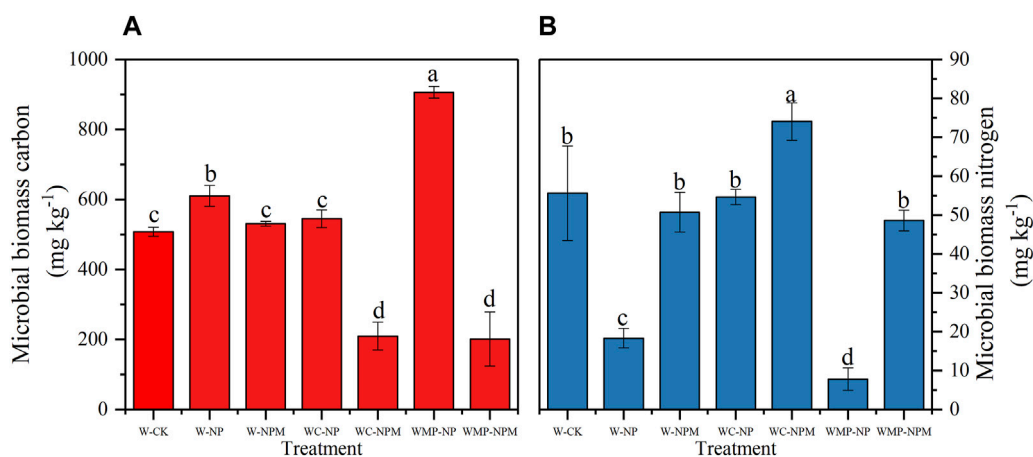


**FIGURE 3**  
Soil microbial biomass C (A) and N (B) content under different treatments.

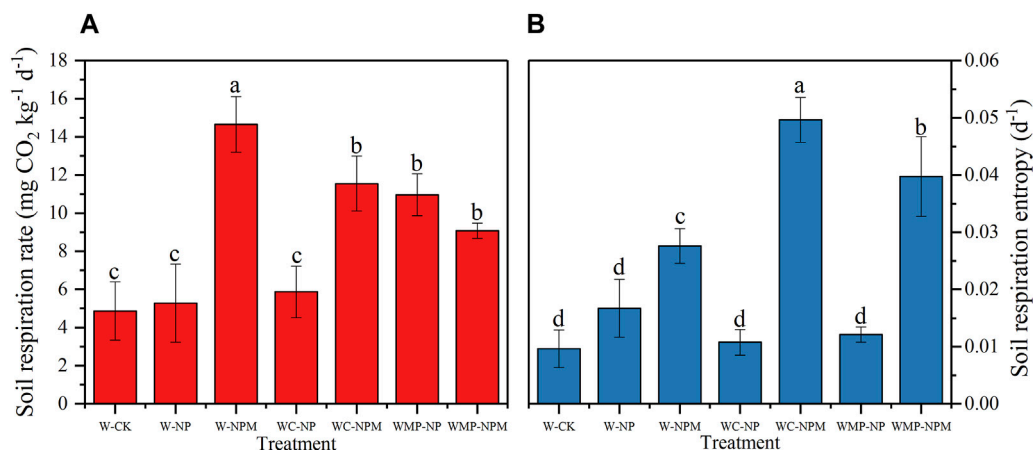


**FIGURE 4**  
Soil respiration rate (A) and respiration entropy (B) in different treatments.

it was not statistically significant. Under the chemical fertilizer scenario, the soil respiration rate increased as the rotation number increased, while this trend reversed when the organic fertilizer was applied.

There were significant differences in the soil respiration entropy among the different treatments (Figure 4B). The soil respiration entropy in the W-NPM, WC-NPM and WMP-NPM treatments was significantly higher than that in the W-CK treatment ( $p < 0.05$ ). Under the same planting pattern, organic fertilizer significantly enhanced soil respiration entropy, and the wheat and corn rotation system was the most sensitive treatment ( $p < 0.05$ ). Under the same fertilization treatment, chemical fertilizer had no obvious effect on the soil respiration entropy under different rotation plots, whereas the soil respiration entropy first increased and then decreased with increasing rotation number in the plot with organic fertilizer ( $p < 0.05$ ).

The soil respiration rate was significantly positively correlated with SOC,  $\text{NO}_3^-$ -N and TP, and negatively correlated with pH and

SWC ( $p < 0.05$ ). Soil respiration entropy was significantly positively correlated with SOC,  $\text{NO}_3^-$ -N, TP and MBN, and negatively correlated with  $\text{NH}_4^+$ -N, pH and MBC,  $p < 0.05$  (Figure 5).

### 3.4.2 Mineralization of soil nitrogen under different treatments

The field management practice, fertilization and planting rotation, significantly affected soil mineralized nitrogen, net nitrogen mineralization rate and net nitrification rate with a similar trend (Figure 6). Compared with the W-CK, the soil mineralized nitrogen, net nitrogen mineralization rate and net nitrification rate were all significantly increased in the W-NPM, WC-NP and WC-NPM ( $p < 0.05$ ). Under the same planting pattern, the soil mineralized nitrogen, net nitrogen mineralization rate and net nitrification rate were significantly higher in the plot with organic fertilizer but this effect was not significant in the wheat, millet and pea rotation treatment ( $p < 0.05$ ). Under the same fertilization treatment, the soil mineralized nitrogen, net nitrogen mineralization rate and net

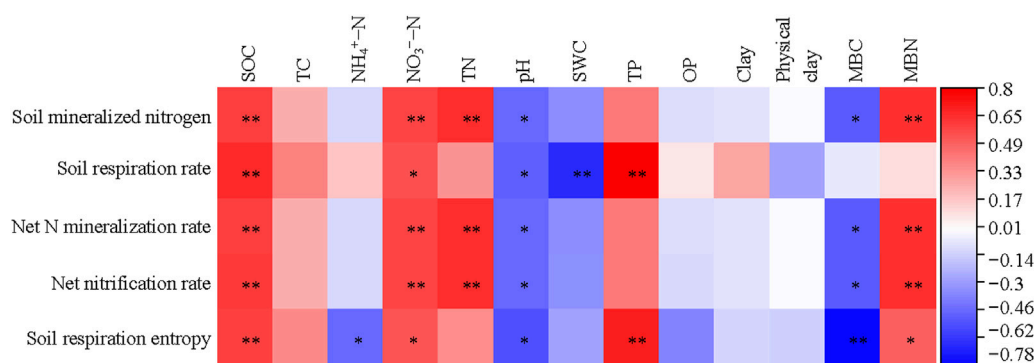


FIGURE 5

Correlation analysis of soil carbon and nitrogen mineralization with soil physiochemical and microbial properties.

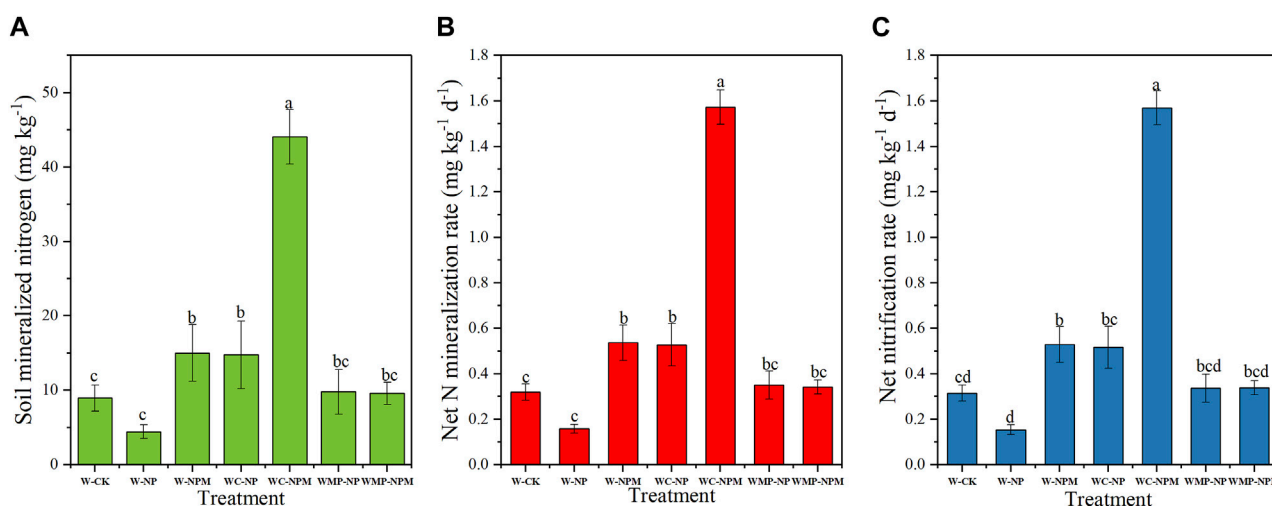


FIGURE 6

Soil mineralization nitrogen (A), net N mineralization rate (B) and net nitrification rate (C) in different treatments.

nitrification rate all increased from the wheat continuous cropping to wheat and corn rotation treatment, and then decreased in the wheat, millet and pea rotation treatment ( $p < 0.05$ ).

Soil mineralized nitrogen, net nitrogen mineralization rate and net nitrification rate were all significantly positively correlated with SOC, NO<sub>3</sub><sup>-</sup>-N, TN and MBN, and negatively correlated with pH and MBC,  $p < 0.05$ , (Figure 5).

### 3.5 Effect of fertilization and planting pattern on soil microbial community structure and soil carbon and nitrogen mineralization

Based on structural equation modeling, the driving mechanisms of different treatments on mineralized nitrogen and soil respiration rate were analyzed (Figure 7,  $\chi^2 = 17.175$ ,  $df = 10.000$ ,  $p = 0.071$ , CFI = 0.916, GFI = 0.839, RMSEA = 0.189, AIC = 69.175). The results of the SEM showed that both TN and SOC directly positively affected total PLFAs and explaining 58% of the total variance with TC and SWC. The fungi/

bacteria PLFAs were significantly negatively influenced by TN with  $-0.65$  standardized path coefficients, and significantly positively affected by SOC with  $0.63$  standardized path coefficients. The combination of TC, TN, SOC and SWC explained 84% of its total variance. Mineralized nitrogen was significantly positively affected by TN, and 55% of the total variance was explained by soil environmental factors and soil microbial community structure. The soil respiration rate was significantly positively affected by TC and negatively affected by SWC and was explained 63% by soil physical, chemical and microbial properties.

## 4 Discussion

### 4.1 Effects of fertilization and planting pattern on soil physical and chemical properties

Fertilization and planting pattern, as important field management practices, can affect soil nutrients and alter soil

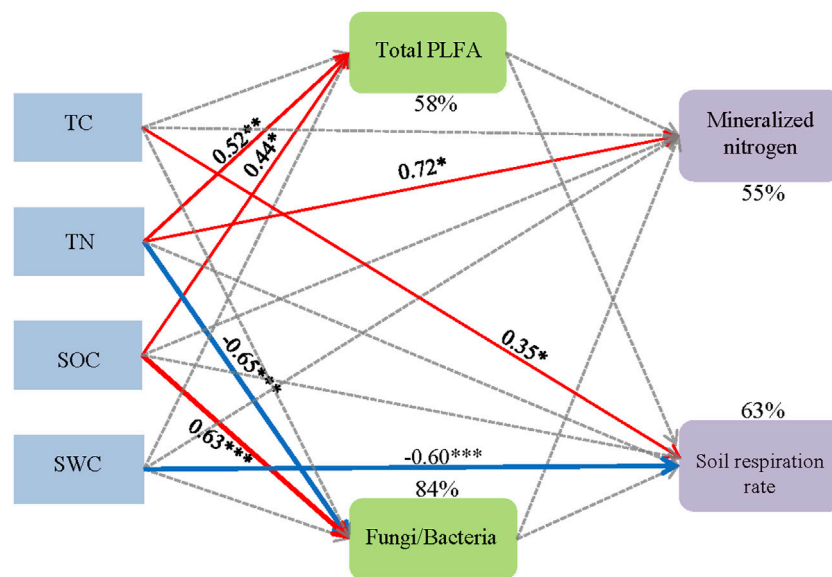


FIGURE 7

Structural equation model shows the effect of fertilization and planting pattern on soil microbial community structure and soil carbon and nitrogen mineralization. Note: The model fits:  $\chi^2 = 17.175$ ,  $df = 10.000$ ,  $p = 0.071$ , CFI = 0.916, GFI = 0.839, RMSEA = 0.189, AIC = 69.175. The numbers on the arrows are standardized path coefficients (correlation coefficients), and asterisks following the numbers indicate significant relationships (\*\* $p < 0.001$ , \* $p < 0.01$ , \* $p < 0.05$ ). Red solid arrows indicate significant positive relationships, blue solid arrows indicate significant negative relationships, and gray dashed arrows indicate path coefficients  $> 0.05$ . The width of the arrows shows the strength of the relationship. Percentages ( $R^2$ ) close to endogenous variables indicate the variance explained by the soil factors.

physicochemical characteristics (Wang W. et al., 2015; Cai et al., 2019). Soil nutrients are the main source for crop nutrition, and the level of soil nutrient content affects the survival and health of crops. Similar to other research, fertilization can significantly increase soil  $\text{NH}_4^+\text{-N}$ ,  $\text{NO}_3^-\text{-N}$ , TN, AP, TP, and clay content, and reduce soil pH and SWC in the wheat continuous cropping treatment (Guo et al., 2010; Sun et al., 2014; Lusiba et al., 2017; Liu J. et al., 2020; Lin et al., 2022). The reason for this change in soil physicochemical properties may be that fertilizers contain a large amount of nitrogen and phosphorus. The application of fertilizers can quickly supplement the nutrient elements, thereby greatly increasing the available nitrogen and phosphorus. The increased available nutrients could enhance microbial activity and accelerate the transformation of nutrients (Zhang et al., 2013). The hydrolysis of urea causes a short-term and rapid decrease in soil pH, and lower pH and sufficient urea hydrolysates ( $\text{NH}_4^+\text{-N}$ ) significantly stimulate nitrification in soils (Zhao et al., 2014). This is consistent with the significant increase in nitrate nitrogen content and the opposite trend of nitrate and ammonia nitrogen changes after fertilization in this study. Soil pH is an important factor affecting soil quality. Nitrogen in fertilizer promotes the absorption of soil cations by crop roots, resulting in the production of more hydrogen ions and a decrease in the soil pH value with soil acidification (Cai et al., 2019; Dong et al., 2021b). In addition, the  $\text{H}^+$  produced by nitrification will also reduce the pH (Dong et al., 2021a).

Compared with the application of inorganic fertilizers, the application of chemical with organic fertilizers can increase SOC and reduce SWC and pH. After being applied to the soil, organic fertilizers increase the rate of soil nutrient accumulation, improve

the soil physical structure, and create a rich microenvironment, which is conducive to microbial reproduction and ultimately drives the carbon nitrogen cycle and is more conducive to the accumulation of organic carbon components (Chen et al., 2019). The decrease in pH may be due to the combination of organic and inorganic fertilizers regulating the carbon nitrogen ratio of soil, promoting microbial growth, increasing soil microbial diversity, stimulating soil enzyme activity, promoting organic matter degradation, and generating more low molecular organic acids such as acetic acid ( $\text{CH}_3\text{COOH}$ ) (Zhang et al., 2021). This research also found that under the same fertilizer conditions, the soil nutrient content was also affected by planting pattern. Under the same fertilization conditions, the SOC, TN, AP, and TP of the wheat corn rotation were higher than those of the wheat continuous cropping. This may be due to differences in nutrient absorption among different crops in rotation. Reasonable crop rotation can achieve balanced utilization of soil nutrients and achieve the effect of land nutrition. Meanwhile, compared to wheat continuous cropping, the SWC of wheat corn rotation decreases, possibly due to the more developed corn roots and high water demand, resulting in a decrease in SWC (Wu et al., 2021).

## 4.2 Effects of fertilization and planting pattern on microbial community structure

Soil microorganisms are an important component of soil ecosystems and play a notable role in maintaining soil ecosystem function and services. Fertilization significantly affects the abundance and diversity of soil microorganisms (Chinnadurai



et al., 2014; Tamilselvi et al., 2015). In this research, compared with no fertilization, the application of chemical with organic fertilizer significantly increased the content of total PLFAs, bacteria, fungi,  $G^+$ ,  $G^-$ , AMF and actinomycete PLFAs in the wheat continuous cropping treatment, whereas the NP fertilizer had the opposite effect. The application of organic fertilizer can provide a suitable survival environment for microorganisms (Wang et al., 2020). The application of organic fertilizers could increase the organic matter content of the soil, improve the soil physicochemical traits and the structure of the soil, improve the soil fertility, provide a suitable environment for microbial growth and promote microbial activity, and they also directly introduced microorganisms in organic fertilizers into the soil and played the roles of “inoculating” and “importing” (Zeng et al., 2007; Dong et al., 2014). Long-term application of inorganic fertilizers alters soil physicochemical traits and inhibits the activity of soil microorganisms; at the same time, exogenous organic carbon sources are insufficiently supplemented, and there is not enough energy to satisfy the growth and development of microorganisms, resulting in a decline in the number of microorganisms, while the input of organic fertilizers exactly complements this shortcoming, thereby increasing soil microbial PLFA contents (Li et al., 2020).

With the same fertilization, the PLFA content was different among the different rotation systems. In this research, the PLFA content in the wheat millet pea rotation treatment was lower than that in the wheat corn rotation treatment, indicating that rotation has a certain impact on the soil microbial community structure. Compared with the effect of fertilization, the planting pattern has a smaller impact on the soil microbial community structure, which may be because the application of organic fertilizer allows microorganisms to obtain a large amount of nutrients, or the presence of a large number of different microbial groups in the organic fertilizer. The differences in soil microbial community structure among different treatments are mainly related to whether organic fertilizers are applied, and although planting pattern have an impact on microbial community structure, the effect is relatively small.

### 4.3 Effects of fertilization and planting pattern on soil carbon and nitrogen mineralization

Soil microbial biomass serves as both a reservoir of available nutrients and a driving force for soil nutrient cycling and organic matter transformation (Yang et al., 2017). MBN is a key interconversion of inorganic and organic N in soils and often serves as a sensitive indicator for the evolution of soil fertility status and soil quality. Previous studies have shown that the application of chemical fertilizers can enhance MBC and MBN (Daniel and Kate, 2014). The results of this study differed in that, compared with no fertilization, the application of NP and organic manure had no significant effect on MBC and MBN, but the application of NP significantly increased the MBC content and decreased the MBN content. This may be due to the difference in the amount of NP applied compared to other studies, or it may be related to soil cultivation methods or background physicochemical

indicators, resulting in the application of NP affecting microorganisms and causing a decrease in MBN. In addition, research has found that compared to applying NP, applying NP and organic fertilizer significantly reduces MBC content and increases MBN content. This may be due to unreasonable chemical fertilizer application, resulting in insufficient carbon sources. The increase in MBN may be due to the long-term input of exogenous organic materials, which can regulate the soil nitrogen supply (Liu et al., 2012).

Soil respiration is often used to measure the total activity of soil microorganisms and to evaluate soil fertility and is affected by fertilization and planting pattern. Compared with no fertilization, fertilization can significantly improve soil respiration, except when chemical fertilizer is applied in wheat continuous and wheat and corn rotation systems. This may be because fertilizer improves the availability of nitrogen in the soil, promotes the growth of crop roots and their secretions, and increases microbial respiration (Ding et al., 2006; Li et al., 2010). Compared with applying NP, applying NP and organic fertilizer can significantly improve soil respiration in wheat continuous and wheat and corn rotation systems. In addition, by comparing W-NP, W-NPM, WC-NP and WC-NPM, although rotation had an impact on soil respiration, the impact was far less than that of the combined application of organic fertilizer. The main reason may be that the combination of organic and inorganic fertilizers significantly increases the soil organic matter content and thus increases the number of soil microorganisms, thereby increasing  $CO_2$  emissions from microbial respiration (Han et al., 2008). Different soil microenvironments lead to different soil respiration (Raich and Tufekciogul, 2000), and changes in fertilization and planting pattern can change soil physical and chemical properties, which indirectly affect soil respiration by affecting the number and distribution of microorganisms (Zhou et al., 2011).

The nitrogen required by crops comes not only from the input of exogenous fertilizer but also from the inorganic nitrogen released by soil organic nitrogen mineralization. Therefore, studying the changes in soil nitrogen mineralization under different fertilization and planting pattern is crucial for the nitrogen supply to crops (Zhang et al., 2019). In this study, the trends of changes in soil mineralization nitrogen content, soil net nitrification rate, and soil net mineralization rate were the same among the different treatments. When the fertilization was the same, the wheat and corn rotation treatment had the highest soil mineralization nitrogen content, soil net mineralization rate, and soil net nitrification rate. The combination of organic fertilizer and wheat and corn rotation has a promoting effect on soil N transformation. According to the heatmap analysis in Figure 5, there is a highly significant positive correlation between soil mineralization nitrogen content and SOC, nitrate nitrogen, TN, and MBN, indicating that the richer the soil organic carbon, nitrate nitrogen, TN, and MBN content, the more substrates and more conducive to mineralization (He et al., 2005; Wang S. C. et al., 2015). Soil urease and protease are key enzymes for soil nitrogen conversion, and their activity is closely related to the intensity of soil nitrogen conversion and soil nitrogen supply capacity (Wang et al., 2010). It is speculated that the impact mechanism of fertilization and planting pattern on N mineralization is, on the one hand, by changing the mineralization substrate and the number of related microorganisms, and on the other hand, it may

affect enzyme activity by changing soil physical and chemical properties, thereby affecting nitrogen mineralization.

## 5 Conclusion

There were significant differences in soil physicochemical factors and microbial community structure among the different fertilization and planting pattern. Compared with applying NP fertilizer, applying organic fertilizer significantly increased soil organic matter and nutrients and decreased SWC and soil pH. The wheat and corn rotation treatment had the highest content of total PLFAs and microbial groups. Applying organic fertilizer can significantly increase the content of PLFAs in the soil. Increasing organic fertilizer mainly affects the content of various microorganisms and total PLFAs in the soil by changing the content of SOC and TN. Compared with applying organic fertilizer, changes in the planting pattern had less impact on the structure of the soil microbial community. Both increasing organic fertilizer application and changing planting pattern can affect soil respiration and soil mineralized nitrogen content. Overall, increasing the application of organic fertilizers has a greater impact on soil ecological processes than changes in planting pattern. The soil microbial community structure (fungi:bacteria) was significantly negatively correlated with total nitrogen and positively correlated with soil organic carbon. Soil respiration was negatively affected by soil water content and positively affected by total carbon. Soil mineralized nitrogen was positively influenced by total nitrogen. In summary, compared to applying NP fertilizer, applying organic fertilizer has a more significant effect on improving soil quality in agricultural ecosystems. Compared with the planting pattern, the application of organic fertilizer has a higher impact on soil properties.

## Data availability statement

The original contributions presented in the study are included in the article/Supplementary Material, further inquiries can be directed to the corresponding author.

## References

- Aimaierjiang, A., Huang, J., Xu, H. Q., Chen, F. L., Xiao, J. X., Cheng, Z. J., et al. (2022). Effects of different planting patterns on soil physicochemical properties and microbial characteristics. *J. South. Agric.* 53, 3369–3379. doi:10.3969/j.issn.2095-1191.2022.12.008
- Asuming-Brempong, S., Gantner, S., Adiku, S. G. K., Archer, G., Edusei, V., and Tiedje, J. M. (2008). Changes in the biodiversity of microbial populations in tropical soils under different fallow treatments. *Soil Biol. biochem.* 40, 2811–2818. doi:10.1016/j.soilbio.2008.08.010
- Baath, E. (2003). The use of neutral lipid fatty acids to indicate the physiological conditions of soil fungi. *Microb. Ecol.* 45, 373–383. doi:10.1007/s00248-003-2002-y
- Bao, S. D. (2000). *Soil and agricultural chemistry analysis*. Beijing: China Agriculture Press.
- Cai, A. D., Xu, M. G., Wang, B. R., Zhang, W. J., Liang, G. P., Hou, E. Q., et al. (2019). Manure acts as a better fertilizer for increasing crop yields than synthetic fertilizer does by improving soil fertility. *Soil till. Res.* 189, 168–175. doi:10.1016/j.still.2018.12.022
- Chen, J., Liang, G. Q., Zhou, W., Wang, X. B., Sun, J. W., Liu, D. H., et al. (2019). Responses of soil organic carbon and nitrogen fractions to long-term organic fertilization under rice-wheat rotation. *J. Plant Nutr. Fertilizers* 25, 36–44. doi:10.11674/zwyf.18138
- Chen, J., Zheng, M. J., Pang, D. W., Yin, Y. P., Han, M. M., Li, Y. X., et al. (2017). Straw return and appropriate tillage method improve grain yield and nitrogen efficiency of winter wheat. *J. Integr. Agric.* 16, 1708–1719. doi:10.1016/s2095-3119(16)61589-7
- Chinnadurai, C., Gopalaswamy, G., and Balachandar, D. (2014). Impact of long-term organic and inorganic nutrient managements on the biological properties and eubacterial community diversity of the Indian semi-arid Alfisol. *Arch. Agron. Soil Sci.* 60, 531–548. doi:10.1080/03650340.2013.803072
- Daniel, G., and Kate, M. S. (2014). Long-term effects of mineral fertilizers on soil microorganisms – a review. *Soil Biol. biochem.* 75, 54–63. doi:10.1016/j.soilbio.2014.03.023
- Ding, W. X., Meng, L., Yin, Y. F., Cai, Z. C., and Zheng, X. H. (2006). CO<sub>2</sub> emission in an intensively cultivated loam as affected by long-term application of organic manure and nitrogen fertilizer. *Soil Biol. biochem.* 39, 669–679. doi:10.1016/j.soilbio.2006.09.024
- Dong, W. Y., Zhang, X. Y., Dai, X. Q., Fu, X. L., Yang, F. T., Liu, X. Y., et al. (2014). Changes in soil microbial community composition in response to fertilization of paddy soils in subtropical China. *Appl. Soil Ecol.* 84, 140–147. doi:10.1016/j.apsoil.2014.06.007
- Dong, Y., Yang, J. L., Zhao, X. R., Yang, S. H., Jan, M., Peter, D., et al. (2021a). Seasonal dynamics of soil pH and N transformation as affected by N fertilization in subtropical China: An *in situ* <sup>15</sup>N labeling study. *Sci. Total Environ.* 816, 151596. doi:10.1016/j.scitotenv.2021.151596

## Author contributions

YW conceptualized the experiment, wrote and edited the manuscript. QL wrote the first original draft. CL designed the research experiment and edited the manuscript. All authors contributed to the article and approved the submitted version.

## Funding

This work was funded by the project of Science and Technology Department of Shaanxi Province (2022NY-074), the National Natural Science Foundation of China (41501255 and 41671269), the Xi'an Science and Technology Project (21NYF0033) and the Fundamental Research Funds for the Central Universities (SYJS202224).

## Acknowledgments

The authors would like to thank YX for performing the experiments and collecting the data.

## Conflict of interest

The authors declare that the research was conducted in the absence of any commercial or financial relationships that could be construed as a potential conflict of interest.

## Publisher's note

All claims expressed in this article are solely those of the authors and do not necessarily represent those of their affiliated organizations, or those of the publisher, the editors and the reviewers. Any product that may be evaluated in this article, or claim that may be made by its manufacturer, is not guaranteed or endorsed by the publisher.

- Dong, Y., Yang, J. L., Zhao, X. R., Yang, S. H., and Zhang, G. L. (2021b). Contribution of different proton sources to the acidification of red soil with maize cropping in subtropical China. *Geoderma* 392, 114995. doi:10.1016/j.geoderma.2021.114995
- Federle, T. W., Dobbins, D. C., Thornton-Manning, J. R., and Jones, D. D. (1986). Microbial biomass, activity, and community structure in subsurface soils. *Groundwater* 24, 365–374. doi:10.1111/j.1745-6584.1986.tb01013.x
- Frosteg, R. D., Å., Tunlid, A., and Baath, E. (1991). Microbial biomass measured as total lipid phosphate in soils of different organic content. *J. Microbiol. Methods* 14, 151–163. doi:10.1016/0167-7012(91)90018-1
- Frosteg, R. D., Å., Tunlid, A., and Baath, E. (1993). Phospholipid fatty acid composition, biomass, and activity of microbial communities from two soil types experimentally exposed to different heavy metals. *Appl. Environ. Microbiol.* 59, 3605–3617. doi:10.1128/aem.59.11.3605-3617.1993
- Frosteg, R. D. A., and Baath, E. (1996). The use of phospholipid fatty acid analysis to estimate bacterial and fungal biomass in soil. *Biol. Fertil. Soils* 22, 59–65. doi:10.1007/bf00384433
- Gao, X. F., Yan, B. S., Wu, C. X., and Wang, G. L. (2021). Effects of long-term fertilization on soil quality and millet yield on slope farmland in loess hilly areas. *Agric. Res. Arid Areas* 39, 76–83. doi:10.7606/j.issn.1000-7601.2021.05.10
- Guo, J. H., Liu, X. J., Zhang, Y., Shen, J. L., Han, W. X., Zhang, W. F., et al. (2010). Significant acidification in major Chinese croplands. *Science* 327, 1008–1010. doi:10.1126/science.1182570
- Guo, Z. B., Wan, S. X., Hua, K. K., Yin, Y., Chu, H. Y., Wang, D. Z., et al. (2020). Fertilization regime has a greater effect on soil microbial community structure than crop rotation and growth stage in an agroecosystem. *Appl. Soil Ecol.* 149, 103510. doi:10.1016/j.apsoil.2020.103510
- Han, G. X., Zhou, G. S., and Xu, Z. Z. (2008). Research and prospects for soil respiration of farmland ecosystems in China. *Chin. J. Plant Ecol.* 32, 719–733. doi:10.3773/j.issn.1005-264x.2008.03.022
- He, F. Y., Yin, B., Cai, G. X., Jin, X. X., and Li, H. X. (2005). Comparison of nitrogen mineralization and nitrification in vegetable and dry grain soils. *Chin. J. Soil Sci.* 36, 41–44. doi:10.19336/j.cnki.trtb.2005.01.012
- Keeler, B. L., Hobbie, S. E., and Kellogg, L. E. (2009). Effects of long-term nitrogen addition on microbial enzyme activity in eight forested and grassland sites: Implications for litter and soil organic matter decomposition. *Ecosystems* 12, 1–15. doi:10.1007/s10021-008-9199-z
- Kour, D., Rana, K. L., Yadav, A. N., Yadav, N., Kumar, M., Kumar, V., et al. (2020). Microbial biofertilizers: Bioresources and eco-friendly technologies for agricultural and environmental sustainability. *Biocatal. Agric. Biotechnol.* 23, 101487. doi:10.1016/j.bcab.2019.101487
- Li, J. M., Ding, W. X., and Cai, Z. C. (2010). Effects of nitrogen fertilization on soil respiration during maize growth season. *Chin. J. Appl. Ecol.* 21, 2025–2030. doi:10.13287/j.1001-9332.2010.0293
- Li, L. R., Feng, J. L., Liu, M. M., Mei, H., Kang, Z. Y., and Cai, Q. N. (2021). Effect of crop planting patterns on soil microorganisms and crop pests in farmland. *Chin. Agric. Sci. Bull.* 37, 99–106. doi:10.11924/j.issn.1000-6850.casb2020-0789
- Li, M. L., Chen, Y. T., Hong, X. F., Qiao, Y. Y., Wang, Q. X., Chen, X. J., et al. (2020). Effects of nitrogen management on soil microbial community structure in paddy fields. *Acta Agric. Zhejiangensis* 32, 308–316. doi:10.3969/j.issn.1004-1524.2020.02.15
- Li, X. Y., Zhao, B. Q., Li, X. H., Li, Y. T., Sun, R. L., Zhu, L. S., et al. (2005). Effects of different fertilization systems on soil microbe and its relation to soil fertility. *Sci. Agric. Sin.* 38, 1591–1599. doi:10.3321/j.issn:0578-1752.2005.08.014
- Lian, X., Piao, S., Chen, A., Huntingford, C., Fu, B., Li, L. Z. X., et al. (2021). Multifaceted characteristics of dryland aridity changes in a warming world. *Nat. Rev. Earth Env.* 2, 232–250. doi:10.1038/s43017-021-00144-0
- Lin, X., Chen, X. L., Wan, S. M., Wang, S. A., Zhang, L., Wang, X. J., et al. (2022). Socket shield technique: A systemic review and meta-analysis. *Soils Crops* 11, 226–235. doi:10.11689/j.issn.2095-2961.2022.02.012
- Liu, J. A., Shu, A. P., Song, W. F., Shi, W. C., Li, M. C., Zhang, W. X., et al. (2021a). Long-term organic fertilizer substitution increases rice yield by improving soil properties and regulating soil bacteria. *Geoderma* 404, 115287. doi:10.1016/j.geoderma.2021.115287
- Liu, J., Li, C. Y., Xing, Y. W., Wang, Y., Xue, Y. L., Wang, C. R., et al. (2020a). Effects of long-term fertilization on soil organic phosphorus fractions and wheat yield in farmland of Loess Plateau. *Chin. J. Appl. Ecol.* 31, 157–164. doi:10.13287/j.1001-9332.202001.028
- Liu, Y. R., Yu, J., Li, X., Xu, Y. C., and Shen, Q. R. (2012). Effects of combined application of organic and inorganic fertilizers on soil microbiological characteristics in a wheat-rice rotation system. *J. Agro-Environment Sci.* 31, 989–994. (in Chinese with English abstract).
- Liu, Z., Guo, Q., Feng, Z. Y., Liu, Z. D., Li, H. Y., Sun, Y. F., et al. (2020b). Long-term organic fertilization improves the productivity of kiwifruit (*Actinidia chinensis* Planch) through increasing rhizosphere microbial diversity and network complexity. *Appl. Soil Ecol.* 147, 103426. doi:10.1016/j.apsoil.2019.103426
- Liu, Z. H., Huang, F. Y., Li, J. L., Zhang, P., Yang, B. P., Ding, R. X., et al. (2021b). Effects of farmland mulching patterns on soil microbial diversity and community structure in dryland. *Acta Ecol. Sin.* 41, 2750–2760. doi:10.5846/stxb201904130739
- Lusiba, S., Odhiambo, J., and Ogola, J. (2017). Effect of biochar and phosphorus fertilizer application on soil fertility: Soil physical and chemical properties. *Arch. Agron. Soil Sci.* 63, 477–490. doi:10.1080/03650340.2016.1218477
- Ma, C. M., Tang, Y. Z., and Ji, S. N. (2004). Long term experimental study on crop positioning rotation system (II) - effect of different rotation methods on soil microbial biomass in soybean fields. *J. Northeast Agric. Univ.* 35, 645–650. doi:10.19720/j.cnki.issn.1005-9369.2004.06.001
- Ma, T. E., Wei, Y. C., Yang, X. L., Wei, X. R., Wang, Y. H., Hao, M. D., et al. (2016). Mineralization characteristics of soil organic carbon under long-term fertilization management. *Chin. J. Eco-Agriculture* 24, 8–16. doi:10.13930/j.cnki.cjea.150740
- Morales-Rodriguez, C., Anslan, S., Auger-Rozenberg, M.-A., Augustin, S., Baranchikov, Y., Bellahirech, A., et al. (2019). Forewarned is forearmed: Harmonized approaches for early detection of potentially invasive pests and pathogens in sentinel plantings. *Neobiota* 47, 95–123. doi:10.3897/neobiota.47.34276
- Nanda, S. K., Das, P. K., and Behera, B. (1998). Effects of continuous manuring on microbial population, ammonification and CO<sub>2</sub> evolution in a rice soil. *Oryza* 25, 413–416.
- Nordby, H. E., Nemeć, S., and Nagy, S. (1981). Fatty acids and sterols associated with citrus root mycorrhizae. *J. Agric. Food Chem.* 29, 396–401. doi:10.1021/jf00104a043
- Olsson, P. A. (1999). Signature fatty acids provide tools for determination of the distribution and interactions of mycorrhizal fungi in soil. *FEMS Microbiol. Ecol.* 29, 303–310. doi:10.1111/j.1574-6941.1999.tb00621.x
- Pradeep, K. S., Meenakshi, S., and Deepak, V. (2010). Biocontrol of fusarium wilt of chickpea using arbuscular mycorrhizal fungi and rhizobium leguminosorum biovar. *Caryologia* 63, 349–353. doi:10.1080/00087114.2010.10589745
- Raich, J. W., and Tufekcioglu, A. (2000). Vegetation and soil respiration: Correlations and controls. *Biogeochemistry* 48, 71–90. doi:10.1023/a:1006112000616
- Rashid, M. I., Mujawar, L. H., Shahzad, T., Almeelbi, T., Ismail, I. M. I., and Oves, M. (2016). Bacteria and fungi can contribute to nutrients bioavailability and aggregate formation in degraded soils. *Microbiol. Res.* 183, 26–41. doi:10.1016/j.micres.2015.11.007
- Sun, C. L., Xue, S., Liu, G. B., and Ding, S. N. (2014). Effects of long-term fertilization on soil particles and microaggregate distribution in the loess area. *J. Plant Nutr. Fertilizers* 20, 550–561. doi:10.11674/zwyl.2014.0305
- Tamilselvi, S. M., Chinnadurai, C., Ilamurugu, K., Arulmozhiselvan, K., and Balachandrar, D. (2015). Effect of long-term nutrient managements on biological and biochemical properties of semi-arid tropical Alfisol during maize crop development stages. *Ecol. Indic.* 48, 76–87. doi:10.1016/j.ecolind.2014.08.001
- Tang, Q., and Zhang, C. (2013). Data Processing System (DPS) software with experimental design, statistical analysis and data mining developed for use in entomological research. *Insect Sci.* 20, 254–260. doi:10.1111/j.1744-7917.2012.01519.x
- Tiziano, G., David, P., and Maurizio, G. P. (2011). Environmental impact of different agricultural management practices: Conventional vs. organic agriculture. *Crit. Rev. Plant Soil* 30, 95–124. doi:10.1080/07352689.2011.554355
- Tunlid, A., Hoitink, H. A., Low, C., and White, D. C. (1989). Characterization of bacteria that suppress rhizoctonia damping-off in bark compost media by analysis of fatty acid biomarkers. *Appl. Environ. Microb.* 55, 1368–1374. doi:10.1128/aem.55.6.1368-1374.1989
- Wang, C. H., Zhu, F., Zhao, X., and Dong, K. H. (2014). The effects of N and P additions on microbial N transformations and biomass on saline-alkaline grassland of Loess Plateau of Northern China. *Geoderma* 213, 419–425. doi:10.1016/j.geoderma.2013.08.003
- Wang, C. T., Long, R. J., Wang, Q. L., Liu, W., Jing, Z. C., and Zhang, L. (2010). Fertilization and litter effects on the functional group biomass, species diversity of plants, microbial biomass, and enzyme activity of two alpine meadow communities. *Plant Soil* 331, 377–389. doi:10.1007/s11104-009-0259-8
- Wang, J. W., Zhang, G. Y., and Yu, C. Q. (2020). A Meta-analysis of the effects of organic and inorganic fertilizers on the soil microbial community. *J. Resour. Ecol.* 11, 298–303.
- Wang, S. C., Zhou, J. B., Chen, Z. J., and Man, J. (2015a). Effects of temperature on soil nitrogen mineralization in solar greenhouses with different cultivation years. *J. Plant Nutr. Fertilizers* 21, 121–127. (in Chinese with English abstract).
- Wang, W., Lai, D. Y. F., Wang, C., Pan, T., and Zeng, C. (2015b). Effects of rice straw incorporation on active soil organic carbon pools in a subtropical paddy field. *Soil Till. Res.* 152, 8–16. doi:10.1016/j.still.2015.03.011
- Wang, Y., Li, C., Tu, C., Hoyt, G. D., Deforest, J. L., and Hu, S. (2017). Long-term no-tillage and organic input management enhanced the diversity and stability of soil microbial community. *Sci. Total Environ.* 609, 341–347. doi:10.1016/j.scitotenv.2017.07.053

- Wang, Y., Tu, C., Cheng, L., Li, C., Gentry, L. F., Hoyt, G. D., et al. (2011). Long-term impact of farming practices on soil organic carbon and nitrogen pools and microbial biomass and activity. *Soil Till. Res.* 117, 8–16. doi:10.1016/j.still.2011.08.002
- Wu, E., Sun, P. L., Sa, Q. R. G., Cao, C. L., Tian, X. Y., and He, Q. (2021). Effects of different rotation patterns on the physical and chemical properties and enzyme activities of Black soil in Northeast China. *China Agric. Technol. Ext.* 37, 70–75+80. doi:10.3969/j.issn.1002-381X.2021.06.027
- Wu, R., Liu, S. J., Sun, H., Li, Y. X., Ma, L., and Bai, Y. (2020). Effects of long-term fertilization on soil fertility and microbial characteristics. *Soil Fertilizer Sci. China* 37, 12–16. (in Chinese with English abstract). doi:10.3760/cma.j.issn.1003-9406.2020.01.004
- Yang, T., Adams, J. M., Shi, Y., He, J. S., Jing, X., Chen, L., et al. (2017). Soil fungal diversity in natural grasslands of the Tibetan plateau: Associations with plant diversity and productivity. *New Phytol.* 215, 756–765. doi:10.1111/nph.14606
- Yao, Q., Xu, Y. L., Song, J., and Wei, W. (2015). Characteristics of phospholipid fatty acids of soil microorganism under different plant patterns of soybean. *Soybean Sci.* 34, 442–448. doi:10.11861/j.issn.1000-9841.2015.03.0442
- Yu, C., Li, Y., Mo, R., Deng, W., Zhu, Z., Liu, D., et al. (2020). Effects of long-term straw retention on soil microorganisms under a rice-wheat cropping system. *Arch. Microbiol.* 202, 1915–1927. doi:10.1007/s00203-020-01899-8
- Zelles, L. (1997). Phospholipid fatty acid profiles in selected members of soil microbial communities. *Chemosphere* 35, 275–294. doi:10.1016/s0045-6535(97)00155-0
- Zeng, L. S., Liao, M., Chen, C. L., and Huang, C. Y. (2007). Effects of lead contamination on soil enzymatic activities, microbial biomass, and rice physiological indices in soil-lead-rice (*Oryza sativa* L.) system. *Ecotox. Environ. Safe.* 67, 67–74. doi:10.1016/j.ecoenv.2006.05.001
- Zhang, J. Y., Song, Y., and Wang, J. (2022a). Spatiotemporal patterns of gross ecosystem product across China's cropland ecosystems over the past two decades. *Front. Ecol. Evol.* 10-2022, 959329. doi:10.3389/fevo.2022.959329
- Zhang, Q., Wang, C., Sun, Z. S., Li, S. Y., and Liang, Y. J. (2022b). Research progress on influencing factors of soil microbial biomass and diversity. *North. Hortic.* 503, 116–121. doi:10.11937/bfy.20213763
- Zhang, X., Wang, H., Hui, X. L., Wang, Z. H., and Liu, J. S. (2019). Effects of different fertilization and fallowing practices on soil carbon and nitrogen mineralization in a dryland soil with low organic matter. *J. Soil Sci. Plant Nut.* 19, 108–116. doi:10.1007/s42729-019-0016-x
- Zhang, Y., Sheng, Z. E., Wang, Y. N., Su, S. M., Bai, L. Y., Wu, C. X., et al. (2021). Long-term manure application enhances the stability of aggregates and aggregate-associated carbon by regulating soil physicochemical characteristics. *Catena* 203, 105342. doi:10.1016/j.catena.2021.105342
- Zhang, Z. S., Cao, C. G., Cai, M. L., and Li, C. F. (2013). Crop yield, P uptake and soil organic phosphorus fractions in response to short-term tillage and fertilization under a rape-rice rotation in central China. *J. Soil Sci. Plant Nut.* 13, 0–882. doi:10.4067/s0718-95162013005000069
- Zhao, X., Wang, S. Q., and Xing, G. X. (2014). Nitrification, acidification, and nitrogen leaching from subtropical cropland soils as affected by rice straw-based biochar: Laboratory incubation and column leaching studies. *J. Soil. Sediment.* 14, 471–482. doi:10.1007/s11368-013-0803-2
- Zhou, H. H., Li, W. H., Yang, Y. H., Cao, Z. C., and Li, Z. (2011). Diurnal variation of soil respiration and its influencing factors under different land use patterns in arid areas. *Sci. Geogr. Sin.* 31, 190–196. doi:10.13249/j.cnki.sgs.2011.02.019



## OPEN ACCESS

## EDITED BY

Kaibo Wang,  
Chinese Academy of Sciences (CAS),  
China

## REVIEWED BY

Aliza Pradhan,  
National Institute of Abiotic Stress  
Management (ICAR), India  
Thirol Fall,  
University of Florida, United States

## \*CORRESPONDENCE

Guang-Na Zhang,  
✉ gnzhang@lyu.edu.cn  
Zhen Wang,  
✉ wangzhen@lyu.edu.cn

RECEIVED 19 April 2023

ACCEPTED 29 June 2023

PUBLISHED 27 July 2023

## CITATION

Lin X-J, Zhang G-N, Wang Z, Han Q-D  
and Leng P (2023), Phosphatase activities  
and available nutrients in soil aggregates  
affected by straw returning to a  
calcareous soil under the maize–wheat  
cropping system.  
*Front. Environ. Sci.* 11:1208323.  
doi: 10.3389/fenvs.2023.1208323

## COPYRIGHT

© 2023 Lin, Zhang, Wang, Han and Leng.  
This is an open-access article distributed  
under the terms of the [Creative  
Commons Attribution License \(CC BY\)](#).  
The use, distribution or reproduction in  
other forums is permitted, provided the  
original author(s) and the copyright  
owner(s) are credited and that the original  
publication in this journal is cited, in  
accordance with accepted academic  
practice. No use, distribution or  
reproduction is permitted which does not  
comply with these terms.

# Phosphatase activities and available nutrients in soil aggregates affected by straw returning to a calcareous soil under the maize–wheat cropping system

Xiang-Jie Lin<sup>1,2</sup>, Guang-Na Zhang<sup>1\*</sup>, Zhen Wang<sup>3\*</sup>,  
Qing-Dian Han<sup>1</sup> and Peng Leng<sup>4</sup>

<sup>1</sup>Shandong Provincial Key Laboratory of Water and Soil Conservation and Environmental Protection, College of Agriculture and Forestry Science, Linyi University, Linyi, China, <sup>2</sup>Philippine Christian University Center for International Education, Manila, Philippines, <sup>3</sup>School of Pharmacy, Linyi University, Linyi, China, <sup>4</sup>Linyi Academy of Agricultural Sciences, Linyi, China

The objective of this study was to investigate the effects of different rates of straw returning on soil aggregate stability, phosphatase activities, and the available nitrogen (N) and phosphorus (P) within different soil aggregate sizes. The experiment included five treatments: 1) no straw returning and no chemical fertilizer, 2) chemical fertilizer only (150 kg N ha<sup>-1</sup>, 75 kg P ha<sup>-1</sup>, and 75 kg K ha<sup>-1</sup>), 3) 20% straw returning with chemical fertilizer, 4) 60% straw returning with chemical fertilizer, and 5) 100% straw returning with chemical fertilizer. Soil samples were collected 3.5 years after the start of the experiment and separated into four aggregate sizes (<0.25 mm, 0.25–1 mm, 1–2 mm, and 2–7 mm) using the dry sieving method. Soil acid phosphomonoesterase (AcP) and alkaline phosphomonoesterase (AlP); phosphodiesterase (PD); pyrophosphatase (PrA) activities; and soil NO<sub>3</sub><sup>-</sup>-N, NH<sub>4</sub><sup>+</sup>-N, and resin-P were determined within soil aggregates. The results showed that straw returning rates did not significantly impact soil aggregate distribution. However, straw returning increased soil AcP, AlP, and PD in <2 mm aggregates, and high rates of straw returning led to high enzyme activities. Soil phosphatase activities were also higher in 1–2 mm aggregates. All straw returning and chemical fertilization treatments increased soil NO<sub>3</sub><sup>-</sup>-N and resin-P concentrations but had much less effect on soil NH<sub>4</sub><sup>+</sup>-N concentrations. Additionally, the study revealed that soil pH, the concentrations of NH<sub>4</sub><sup>+</sup>-N, NO<sub>3</sub><sup>-</sup>-N, resin-P, and CaCO<sub>3</sub> significantly influenced soil phosphatase activities, but their impact varied across different sizes of aggregates.

## KEYWORDS

straw returning, soil aggregate, phosphomonoesterase, phosphodiesterase, pyrophosphatase



# 1 Introduction

The intensive winter wheat–summer maize cropping system in the central North China Plain is known for high inputs of chemical fertilizers, inadequate organic matter, high crop yields, and large amounts of crop residues (Zhang et al., 2016; Lu et al., 2020). Traditionally, both wheat and maize straws were used as fuel for cooking or burned on the farm to clean the field for planting the next crop. Since the on-farm straw burning practice was banned in 2008, a large quantity of straw must be incorporated into the soil. Straw returning has been shown to increase soil organic matter (SOM) and available soil nutrients (Tan et al., 2015), improve soil porosity and structure (Yao et al., 2015), reduce soil bulk density, and enhance soil enzyme activities (Wang et al., 2018). However, the straw return was challenging due to the lack of appropriate field equipment in some hilly areas, where straws are currently removed from fields. As a consequence, intensive farming has led to soil quality degradation (i.e., lack of SOM, low soil fertility, poor nutrient use, subsequently low yield, and degraded soil structure) (Liu and Diamond, 2005), which greatly influences the long-term productive capacity of the soil (Vitousek et al., 2019).

Soil aggregates are vital for soil structure and fertility (Mrquez et al., 2019), and the associated soil characteristics within and between aggregates are essential for soil quality (Lehmann et al., 2017). Straw returning has been shown to increase the proportion of soil macroaggregates larger than 0.25 mm (Alidad et al., 2012; Zhang et al., 2018; Zhao et al., 2018; Cao et al., 2021). Additionally, the distribution of soil aggregates and the mean weight diameter (MWD) also differed from the straw returning mode (Ma et al., 2020). However, the effects of straw returning on phosphorus (P) distribution among soil aggregates remain unclear. For instance, soil P could be enriched in soil macroaggregates or microaggregates due to different soil types (Ahmed et al., 2017). Studies have shown that 80% of soil total P was contained in soil macroaggregates (>2 mm) (Zhang et al., 2021), while soil total P or available P concentrations were highest in <0.053 mm soil aggregates (Cheng et al., 2019; Deng et al., 2021). Additionally, different sizes of soil aggregates also affect P loss from soil (Garland et al., 2018; Li et al., 2020; Cao et al., 2021). Therefore, the input of exogenous organic materials can potentially impact the structure of soil aggregates and P distribution among aggregates.

Phosphatase enzymes are responsible for mineralization of organic matter to release phosphate ions ( $\text{H}_2\text{PO}_4^-$  and  $\text{HPO}_4^{2-}$ ) in soil (Crique and Braud, 2008). Soil acid phosphomonoesterase (AcP), alkaline phosphomonoesterase (AlP), phosphodiesterase (PD), and pyrophosphatase (PrA) are specific enzymes that facilitate this process. Studies have shown that straw returning significantly increased soil alkaline phosphatase activity (Wang et al., 2018), and phosphatase activity decreased with decreasing aggregate size (Tian et al., 2022), but the effect of straw returning on soil phosphatase activities may not be long term (Stegarescu et al., 2021). Furthermore, the turnover of nutrients is closely related to soil aggregates and soil structure (Six et al., 2000; Galantini et al., 2004) because soil aggregates can provide physical protection for nutrients from microbial decomposition (Six

et al., 2004; Barthès et al., 2008), and the availability of nutrients would conversely influence phosphatase activities. Thus, straw returning may cause a difference in soil phosphatase activities and P availability among soil aggregates.

The existing research on soil aggregates following straw returning to the field has mainly focused on water-stable aggregates (Meng et al., 2014; Garbuz et al., 2016). Although studies have primarily centered on soil carbon status among aggregates (Wang et al., 2015; He et al., 2018; Wang et al., 2018), few have investigated the concentration of available P and phosphatase activities after straw returning to the field. The study was conducted in a typical Yimeng mountainous area in Northern China, where cinnamon soil (Calcaric Cambisol, FAO) accounts for up to 50% of the land area. Straw returning is not common practice in this area, and the soils often suffer from erosion and low P nutrients. The objective of this study was to determine the effects of straw returning on the structure and internal available P and other nutrients and phosphatase activities of soil aggregates in a calcareous soil under a maize–wheat cropping system.

## 2 Materials and methods

### 2.1 Site description and experimental design

The field experiment was conducted on cinnamon soil (Calcaric Cambisols in FAO classification) at Fei County (117°54' E and 35°13' N), Shandong Province, Northern China. The region has a temperate continental monsoon climate; the annual mean temperature and precipitation are 14.1°C and 849 mm, respectively; and 60%–80% of the annual precipitation occurs during the maize-growing season in summer. The initial soil properties in the study area were 8.05 pH, 1.12% TC, 0.16% TN, and 548 mg kg<sup>-1</sup> TP. Winter wheat was planted in early or mid-October with a seeder and harvested in early June of the following year. Then, summer maize was planted after the wheat harvest and harvested in early October. Five treatments were as follows: 1) CK (control - no fertilizer and no straw), 2) C (chemical fertilizer only), 3) SR20 (20% straw returning with chemical fertilizer), 4) SR60 (60% straw returning with chemical fertilizer), and 5) SR100 (100% amount of straw returning with chemical fertilizer). The chemical fertilizer treatment consisted of 150 kg N ha<sup>-1</sup> urea and with about 5.48 kg N from  $\text{NH}_4\text{H}_2\text{PO}_4$ , 45 kg P ha<sup>-1</sup> as  $\text{NH}_4\text{H}_2\text{PO}_4$ , and 45 kg K ha<sup>-1</sup> as KCl. Each plot was 3 m × 4 m in size with a 1-m buffer zone between plots. All treatments were replicated four times, except CK (three times due to limited experimental area), and plots were arranged according to a single-factor, completely randomized experiment design. Prior to the initiation of this experiment, no straw returning was performed to the soil in this field previously. For this study, only maize straw was returned to the field, and the amount of the maize straw that was returned based on the average straw weight (8,700 kg/ha dry weight) in the field. The nutrient contents of straws returned to the fields were 687 g TC kg<sup>-1</sup>, 9.16 g TN kg<sup>-1</sup>, and 2.83 g TP kg<sup>-1</sup>. Maize straw was chopped into 1-cm-long pieces and disked into 0–20 cm soil layer.

## 2.2 Soil sampling

Intact soil core samples were collected from each plot by pushing a plastic frame (10 cm long, 10 cm wide, and 20 cm deep) into the soil after the wheat harvest, 3.5 years after the initiation of the experiment. After being transported to the laboratory, the soil cores were gently broken into small clods according to the natural texture and dried at 4 °C in a refrigerated cabinet until the soil water content was around 8%. After being sieved through a 7-mm sieve, soil aggregates were measured with the dry screening method (Zhang et al., 2013). The dry sieving method was chosen in our study as aggregates divided by the wet-sieving method can hardly be used for the determination of soil nutrient contents and soil phosphatase activities. A sub-sample was sieved (<2 mm) and stored at 4 °C for analysis of enzyme activities within a week. Another subsample was air-dried, sieved, and analyzed for basic soil properties.

## 2.3 Soil aggregate fractionation measurement

Cold air-dried soil samples (100 g) were agitated by a mechanical shaker (OA SS203, Ortoalresa, Spain) at 50 Hz frequency for 2 min on a stack of sieves (2–7 mm, 1–2 mm, 0.25–1 mm, and <0.25 mm) until soil aggregate samples were enough for further analysis. The aforementioned procedure was repeated several times. All soil aggregate samples were weighed and stored at 4 °C until further analysis. The MWD of soil aggregates was calculated using the following formula (Kemper and Rosenau, 1986):

$$MWD = \sum_{i=1}^n X_i W_i.$$

where  $X_i$  is the mean diameter (mm) and  $W_i$  is the weight proportion of each size fraction.

## 2.4 Soil properties

Soil pH was measured using a glass electrode (soil/water ratio of 1.0:2.5). Soil carbonate content was measured with a sieved air-dried sample (<100 mesh) using the pressure calcimeter method: 1.0 g of soil and 2 mL of 6 M HCl containing 3% by weight of  $\text{FeCl}_2 \cdot 4\text{H}_2\text{O}$  are placed at the bottom of a 100-mL sealing reaction vessel; the acid was mixed with soil by turning the vessel sideways; an 18-gauge hypodermic needle was inserted, which is attached to the pressure transducer and voltage meter, the results were recorded; and then  $\text{CO}_2$  concentration was calculated using a calibration curve to obtain carbonate content (Loeppert and Suarez, 1996). Soil organic carbon (SOC) content was measured with sieved air-dried soil (<100 mesh) using the dichromate oxidation method, and SOM content was calculated based on  $\text{OM} = 1.724 \times \text{SOC}$  (Nelson and Sommers, 1996).

Soil available nitrogen (N) and P concentrations were determined for all grades of soil aggregates. Ammonium N and nitrate N concentrations were determined by the colorimetric method after being extracted with 1: 5 2 M KCl solutions (Mulvaney, 1996). The

content of available P in soil was determined by the anionic exchange resin strips combined with molybdenum blue method, and the blue color was detected at 700 nm using the Agilent Cary 100 UV–Vis spectrophotometer (Sharpley, 2000).

## 2.5 Soil phosphatase assay

Soil acid phosphomonoesterase activities (EC 3.1.3.2, AcP), alkaline phosphomonoesterase activities (EC 3.1.3.1, ALP), and the phosphodiesterase activities (PD) were determined by the method of Tabatabai et al. (1994). Briefly, soil acid phosphomonoesterase activities were determined as follows: a fresh soil sample (1.0 g) was mixed with 1 mL of 50 mM disodium phenyl phosphate in 4 mL of modified universal buffer at pH 6.5 and 0.2 mL of toluene before incubating for 1 h at 37 °C. The alkaline phosphomonoesterase activities were determined using the same procedure, except the universal buffer pH was adjusted to 11. Universal buffer was prepared by mixing 12.1 g of Tris (hydroxymethyl) aminomethane, 11.6 g of succinic acid, 14.0 g of citric acid, and 6.3 g of boric acid in 488 mL of sodium hydroxide solution [ $\text{C}(\text{NaOH}) = 1 \text{ mol L}^{-1}$ ], then diluting to 1 L, and storing at low temperature for future use. Modified universal buffer can be obtained by diluting the universal buffer from 200 mL to 1 L and modifying it to the needed pH of 6.5 for AcP and 11.0 for ALP. After incubation, 1 mL  $0.5 \text{ mol L}^{-1} \text{ CaCl}_2$  and 4 mL  $\text{mol L}^{-1} \text{ NaOH}$  were added to terminate the reaction. Phosphodiesterase activities (PD) were determined by incubating 1.0 g fresh soil with 1 mL of 50 mM sodium bis (*p*-nitrophenyl) phosphate and 4 mL of pH 8.0 buffer prepared by dissolving 6.1 g of Tris-base, adjusting to pH 8.0 with sulfuric acid solution, and then fixing the volume to 1 L. To stop phosphodiesterase activities, 1 mL  $0.5 \text{ mol L}^{-1} \text{ CaCl}_2$  and 4 mL of  $\text{CaCl}_2$ -Tris (hydroxymethyl aminomethane) were used. Fluorescence produced by the aforementioned enzymatic reactions was measured colorimetrically at 410 nm using the Agilent Cary 100 UV–Vis spectrophotometer. For the aforementioned enzyme assays, controls were included for each soil sample. Pyrophosphatase activities (EC 3.6.1.1, PrA) were also assayed following the method of Tabatabai et al. (1994). Fresh soil (1.0 g) was mixed with 3 mL of 50 mM sodium pyrophosphate, and after incubating for 1 h at 37 °C, 25 mL of 0.5 M  $\text{H}_2\text{SO}_4$  and 3 mL of pH 8.0 modified universal buffer (the same universal buffer as phosphomonoester activities modified with pH 8.0) were added and shook using a horizontal oscillator for 3 min, and then centrifuged to obtain the supernatant. About 2 mL of the supernatants was taken in 50-mL volumetric flasks, the developers were added, the volume fixed, and the color compared at 700 nm using the UV–Vis spectrophotometer (Agilent, Santa Clara, CA) after 15 min of color development.

## 2.6 Statistical analyses

The differences among treatments or grades were tested by one-way ANOVA using SPSS 16.0 (SPSS Inc., Chicago, Ill., United States). Mean separation was determined using Tukey's or Dunnett's T3 test based on the results of

**TABLE 1** Effects of different rates of maize straw returning on soil chemical properties, aggregate distribution, and MWD.

Treatment	pH	SOM	CaCO <sub>3</sub>	Soil aggregate distribution (%)				MWD (mm)
		g kg <sup>-1</sup>	g kg <sup>-1</sup>	2–7 mm	1–2 mm	0.25–1 mm	<0.25 mm	
CK	7.98 ± 0.11a	16.8 ± 0.77 ab	30.1 ± 1.31a	30.6 ± 1.13aAB	27.6 ± 1.00aB	33.2 ± 1.37aA	8.59 ± 1.41aC	2.02 ± 0.07a
C	7.77 ± 0.17a	16.0 ± 0.15 b	27.0 ± 1.42a	32.5 ± 0.80aA	26.9 ± 0.79aB	34.5 ± 0.97aA	6.05 ± 0.68aC	2.09 ± 0.03a
SR20	8.03 ± 0.08a	19.1 ± 0.70 ab	27.3 ± 0.87a	28.4 ± 1.80aB	28.4 ± 0.53aB	35.7 ± 1.61aA	7.55 ± 1.31aC	1.94 ± 0.07a
SR60	7.97 ± 0.05a	18.7 ± 0.85 ab	12.6 ± 0.53b	32.2 ± 0.57aA	27.8 ± 0.67aB	34.6 ± 0.60aA	5.37 ± 0.79aC	2.09 ± 0.02a
SR100	7.68 ± 0.04a	19.1 ± 0.89 a	13.2 ± 0.44b	31.8 ± 0.80aA	27.1 ± 0.36aB	34.6 ± 1.01aA	6.46 ± 0.38aC	2.06 ± 0.03a

Note: Values are shown as mean ± standard error. Different lowercase letters represent the difference between the different treatments within the same aggregate size, and the different capital letters indicate differences in particle size distribution within the same treatment. Treatments were CK (no chemical fertilizer and no straw), C (chemical fertilizer), SR20 (20% straw returning with chemical fertilizer), SR60 (60% straw returning with chemical fertilizer only), and SR100 (100% full amount of straw returning with chemical fertilizer).

homogeneity of variances ( $p$ -value < 0.05). A detrended correspondence analysis (DCA) was applied, and the lengths of the gradients were less than 3. Then, a redundancy analysis (RDA) was used to identify the effects of soil properties on soil phosphatase activities among treatments and soil aggregates using Canoco Software 4.5 (Microcomputer Power, Ithaca, NY, United States). The soil factors were standardized by error variance when RDA was performed. All soil properties included in the RDA analysis were D standardized as Z-scores to remove the unit's influence. Soil phosphatase activity scores were “divided by standard deviation,” soil phosphatase activity data chose the “do not transform” item, soil samples were “standardized by norm,” and the phosphatase activities were “standardized by error variance” when RDA was carried out. The Monte Carlo permutation test (999 permutations) was used to select factors that significantly influenced soil phosphatase activities. Figures were prepared using SigmaPlot 10 (SYSTAT, Point Richmond, CA, United States).

### 3 Results

#### 3.1 Effect of different rates of maize straw returning on soil pH, SOM, carbonate, and soil aggregate distribution

Compared to the use of chemical fertilizer alone, the maximum straw returning treatment (SR100) significantly increased SOM by 19% and reduced carbonate concentration by 51% (Table 1). The second highest straw returning treatment (SR60) significantly reduced carbonate concentration but did not significantly increase SOM. The low rate of straw returning (SR20) neither significantly affected the contents of organic matter nor those of carbonate. In addition, no significant changes in soil pH were found among treatments.

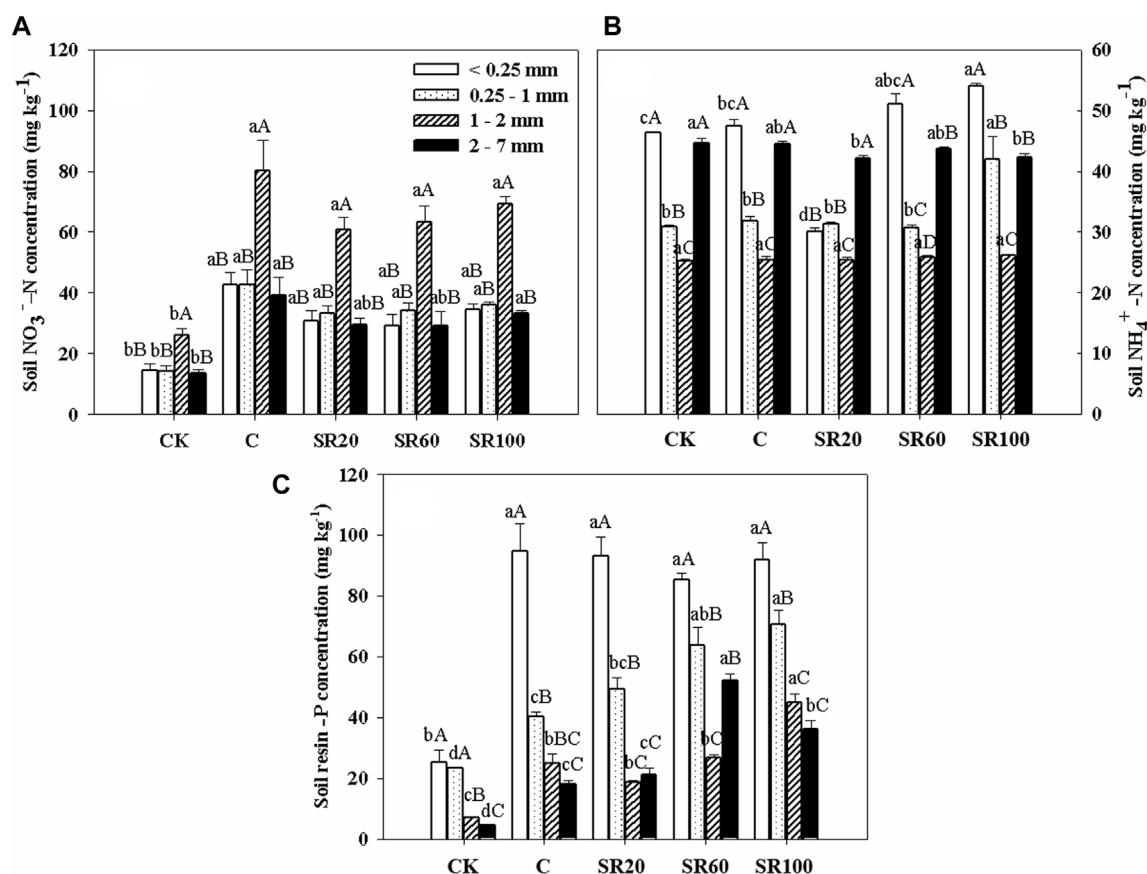
The soil aggregates in the CK sample were almost equally distributed among small macroaggregates (33.2%, 0.25–1 mm), medium macroaggregates (27.6%, 1–2 mm), and large macroaggregates (30.6%, 2–7 mm); the microaggregates (<0.25 mm) were relatively small (8.6%). As for 2–7 mm aggregates, results showed that SR20 treatment significantly

decreased the proportion of 2–7 mm aggregates compared to other treatments. Except for that, no significant differences were observed among treatments within the same size of aggregate. In addition, different treatments did not affect the soil MWD.

#### 3.2 Effects of straw returning rate on the available N, P concentration among soil aggregates

All sizes of soil aggregates under CK treatment had significantly lower NO<sub>3</sub><sup>-</sup>-N concentrations than those of other treatments, while medium macroaggregates (1–2 mm) showed significantly higher NO<sub>3</sub><sup>-</sup>-N concentrations than those of other sizes of aggregates under the same treatments (Figure 1A). The high concentrations of NH<sub>4</sub><sup>+</sup>-N were found in microaggregates (<0.25 mm), while the low concentrations were from medium macroaggregates (1–2 mm) for all treatments (Figure 1B). The NH<sub>4</sub><sup>+</sup>-N concentration in <0.25 mm soil aggregates showed that SR100 treatment had the highest and SR20 treatment had the lowest NH<sub>4</sub><sup>+</sup>-N contents, significantly different with C and CK treatments. For 0.25–1 mm aggregates, only the SR100 treatment had significantly higher NH<sub>4</sub><sup>+</sup>-N contents than the other treatments. No significant difference was observed for NH<sub>4</sub><sup>+</sup>-N contents associated with 1–2 mm aggregates among treatments. For 2–7 mm aggregates, the CK sample had the highest NH<sub>4</sub><sup>+</sup>-N contents, which were significantly higher than those of the SR20 and SR100 treatments. Under the same treatment, NH<sub>4</sub><sup>+</sup>-N contents ordinarily followed the sequence from high to low as < 0.25 mm > 2–7 mm > 0.25–1 mm > 1–2 mm. Only the SR20 treatment showed that NH<sub>4</sub><sup>+</sup>-N was significantly high in 2–7 mm, followed by < 0.25 mm and 1–2 mm, and at last, 1–2 mm.

The order of resin-P concentration was <0.25 mm aggregates > 0.25–1 mm aggregates > 1–2 mm aggregates = 2–7 mm aggregates under CK, C, SR20, and SR100 treatments (Figure 1C). Only SR60 treatment showed that resin-P in 2–7 mm aggregates was significantly higher than that in 1–2 mm aggregates. Within the same aggregate, no clear trend was shown among treatments, but resin-P followed the order of SR100 > SR60 > SR20 > C > CK from high to low in

**FIGURE 1**

Soil aggregate-associated available NO<sub>3</sub><sup>-</sup>-N (A), NH<sub>4</sub><sup>+</sup>-N (B), and phosphorus (C) under different treatments [CK (no chemical fertilizer and no straw), C (chemical fertilizer only), SR20 (20% straw returning with chemical fertilizer), SR60 (60% straw returning with chemical fertilizer), and SR100 (100% full amount of straw returning with chemical fertilizer)]. Values are shown as the mean ± standard error. Different lowercase letters represent the difference among different treatments within the same aggregate size, and different capital letters indicate the difference among the grain levels of the same processing different aggregates.

0.25–1 mm and 1–2 mm aggregates. Furthermore, the higher returning rate of straw had positive effects on soil resin-P concentration.

### 3.3 Effects of maize straw returning rate on soil aggregate-associated AcP, AIP, PD, and PrA

As shown in Figure 2A, AcP in <0.25 mm microaggregates under CK and SR20 treatments was significantly lower than those under SR100 and SR60 treatments. Within 0.25–1 mm aggregates, only SR100 treatment significantly increased AcP. As for 1–2 mm aggregates, SR20 treatment had the lowest AcP, which was significantly lower than that in SR100. For AcP in 2–7 mm aggregates, there was no significant difference among treatments. As seen from CK treatment, 1–2 mm aggregates showed the highest AcP, whereas SR60 treatment showed the highest AcP in both 1–2 mm and <0.25 mm aggregates. The rest of the treatments showed that <0.25 mm aggregates had the highest AcP. All

treatments showed that aggregates of 0.25–1 mm had the lowest AcP.

Soil AIP was higher in 1–2 mm aggregates than in 2–7 mm aggregates under C and CK treatments (Figure 2B). Straw returning increased soil AIP associated with 1–2 mm aggregates, while only SR100 and SR60 treatments increased AIP associated with 0.25–1 mm and 2–7 mm aggregates. As for AIP within <0.25 mm aggregates, only SR100 had higher AIP than CK and C treatments. The soil AIP associated with 1–2 mm and 0.25–1 mm aggregates were higher than that associated with <0.25 mm and 2–7 mm aggregates under SR100, SR60, and SR20 treatments, while soil AIP within 1–2 mm aggregates were even more higher than within 0.25–1 mm aggregates under SR60 treatment. Furthermore, soil AIP in 1–2 mm aggregates was only higher than that in 2–7 mm aggregates under CK and C treatments.

As shown in Figure 2C, PD of <0.25 mm, 0.25–1 mm, and 1–2 mm aggregates under SR100 treatment was significantly higher than that under C, CK, and SR20 treatments. Soil PD in 2–7 mm aggregates under SR100 treatment was significantly higher than that under C treatment, and there was no significant difference



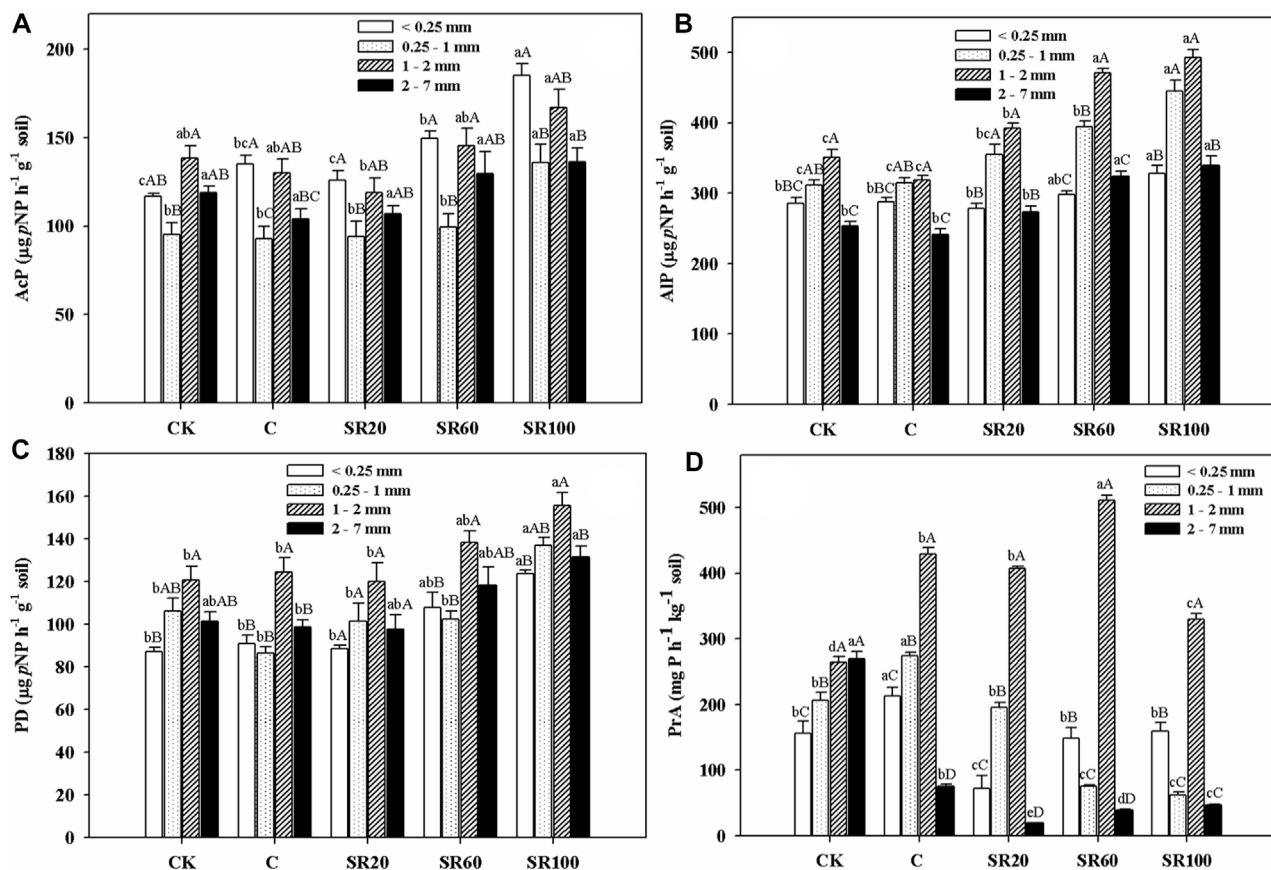


FIGURE 2

Soil aggregate-associated AcP (A), AIP (B), PD (C) and PrA (D) under different treatments [CK (no chemical fertilizer and no straw), C (chemical fertilizer only), SR20 (20% straw returning with chemical fertilizer), SR60 (60% straw returning with chemical fertilizer), and SR100 (100% full amount of straw returning with chemical fertilizer)]. Values are shown as mean  $\pm$  standard error. Different lowercase letters represent the difference among the different treatments within the same aggregate size, and the different capital letters indicate the difference among the grain levels of the same processing different aggregates.

compared with other treatments. Considering the same treatment, PD under SR20 treatment had no significant difference among aggregates. Under other four treatments, 1–2 mm aggregates had higher PD than other aggregates, and <0.25 mm or 0.25–1 mm showed the lowest value.

Unlike other soil phosphatase activities, soil PrA was significantly affected by treatments and among aggregates (Figure 2D). Soil PrA associated with <0.25 mm and 0.25–1 mm aggregates was significantly higher under C treatment than under other treatments. Soil PrA in 0.25–1 mm aggregates was highest under SR60 treatment, followed by C and SR20 treatments, and then SR100, and CK treatments. It is worth noting that CK treatment had the highest PrA in 2–7 mm aggregates, followed by C, SR100, SR60, and SR20 treatments. Under the same treatment, soil macroaggregates had higher PrA than microaggregates.

### 3.4 Multivariate analysis of soil phosphatase activities and soil properties

Redundancy analysis was conducted to investigate the relationships between soil phosphatase activities in different soil

aggregates. In aggregates <0.25 mm, soil phosphatase activities were significantly related to soil available nitrogen (N) concentration, soil organic matter (SOM), and carbonate contents (Figure 3A). The soil properties explained 77.5% of the variation in soil phosphatase activities ( $F = 12.3$ ,  $P = 0.001$ ), with the first (RDA1) and second (RDA2) axes explaining 57.0% and 66.3% of the accumulated variation in soil phosphatase activities, respectively. The RDA1 explained 73.6% of the variation in the relationship between the soil phosphatase activities and soil properties ( $F = 18.1$ ,  $P = 0.001$ ), while the RDA2 explained 98.4% of the accumulated variation ( $F = 20.6$ ,  $P = 0.001$ ).

In aggregates 0.25–1 mm, soil phosphatase activities were significantly related to SOM and carbonate contents (Figure 3B). The soil properties explained 70.2% of the variation in soil phosphatase activities ( $F = 21.5$ ,  $P = 0.001$ ), with the first (RDA1) and second axes (RDA2) explaining 68.8% and 70.2% of the accumulated variation in soil phosphatase activities, respectively. The RDA1 explained 98% of the variation in the relationship between the soil phosphatase activities and soil properties ( $F = 40.6$ ,  $P = 0.001$ ), while the RDA2 explained 100% of the accumulated variation ( $F = 2.09$ ,  $P = 0.312$ ).



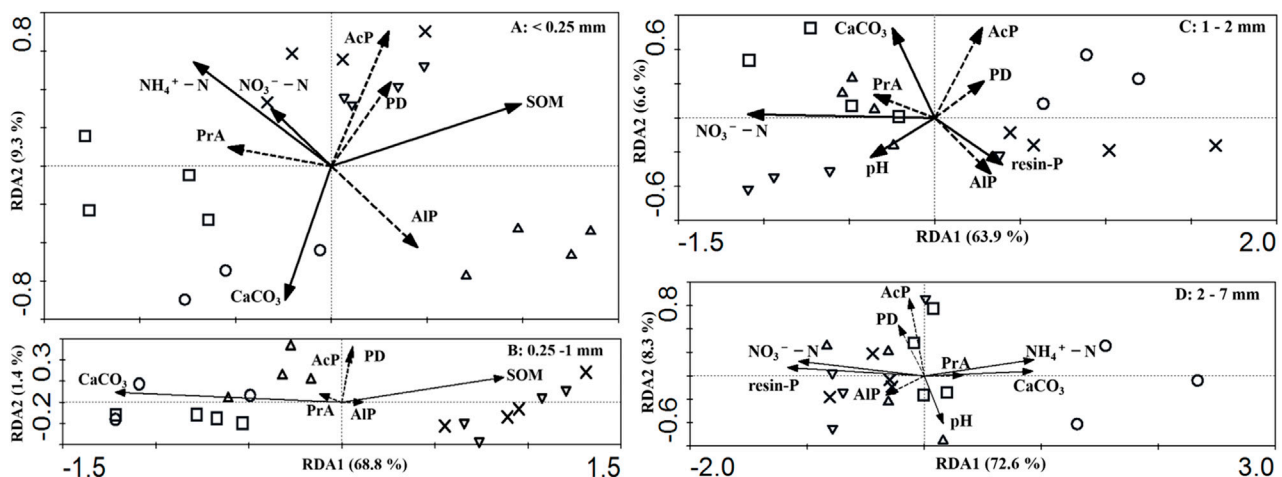


FIGURE 3

Redundancy analysis of ordination triplot of soil phosphatase activities in different soil aggregates. Samples are displayed as points, and soil variables are shown as arrows. The direction of the arrow shows the increase in environmental factors: CK (O)—no chemical fertilizer and no straw; C (□)—chemical fertilizer only; SR20 (Δ)—20% straw returning with chemical fertilizer; SR60 (▽)—60% straw returning with chemical fertilizer; and SR100 (X)—100% full amount of straw returning with chemical fertilizer.

In 1–2 mm aggregates, soil phosphatase activities were significantly related to  $\text{NO}_3^-$ -N, resin-P,  $\text{CaCO}_3$ , and pH (Figure 3C). The soil properties explained 73.4% of the variation in soil phosphatase activities ( $F = 9.68$ ,  $P = 0.001$ ), with the RDA1 and RDA2 axes explaining 63.9% and 70.5% of the accumulated variation in soil phosphatase activities, respectively. The RDA1 explained 87.1% of the variation in the relationship between the soil phosphatase activities and soil properties ( $F = 24.9$ ,  $P = 0.001$ ), while the RDA2 explained 96% of the accumulated variation ( $F = 6.28$ ,  $P = 0.111$ ).

In 2–7 mm aggregates, soil phosphatase activities were significantly related to  $\text{NO}_3^-$ -N, resin-P,  $\text{CaCO}_3$  contents, and pH (Figure 3D). The soil properties explained 81.3% of the variation in soil phosphatase activities ( $F = 10.5$ ,  $P = 0.001$ ), with the RDA1 and RDA2 explaining 72.6% and 80.9% of the accumulated variation in soil phosphatase activities, respectively. The RDA1 explained 89.3% of the variation in the relationship between the soil phosphatase activities and soil properties ( $F = 29.9$ ,  $P = 0.001$ ), while the RDA2 explained 99.4% of the accumulated variation in the aforementioned relationship ( $F = 11.5$ ,  $P = 0.001$ ).

## 4 Discussion

### 4.1 Soil pH, SOM, and carbonate concentration

Unlike previous studies that found returning straw could decrease (Sahrawat, 2005; Bai et al., 2013; Cheng et al., 2023) or increase (Wang et al., 2013) soil pH, this study showed no significant change in soil pH during 3.5 years of the experiment. This could be attributed to the high soil-buffering capacity due to the high concentration of  $\text{CaCO}_3$  in the soil (Wang et al., 2013; Zamanian and Kuzyakov, 2019). Straw returning treatments with high

percentages (60% and 100%) led to a reduction of approximately 50% in carbonate concentration within 3.5 years. Continuation of the straw returning practice might eventually neutralize all or most carbonate, leading to a reduction in soil pH. The increase in soil organic matter (SOM) resulting from straw returning may take longer and require larger amounts of straw. Although many studies reported an increase in SOM (0–20 cm soil depth) due to straw returning (Ma et al., 2020), significant results may take several years to emerge, as reported by Zhao et al. (2018) who observed a positive influence on SOC after 7 years. Chemical fertilization, mainly with N inputs, might cause reduction in SOM (Zhao et al., 2018), likely the same situation as observed under the C treatment. Additionally, straw returning can lead to priming effects, increasing microbial activity and causing SOM depletion (Fang et al., 2018). The decrease in  $\text{CaCO}_3$  content in SR60 and SR100 can be attributed to two reasons. First, organic acids released during the decomposition of the high rate of straw residue (Sahrawat, 2005; Cao et al., 2021) through root exudates and microbial respiration (Sahrawat, 2005; Wang et al., 2013) can contribute to the decrease. Second, the high rate of straw returning treatments can improve soil water permeability (Alidad et al., 2012; Gorokhova and Chursin, 2021), and the presence of  $\text{H}_2\text{O}$  and  $\text{CO}_2$  could accelerate  $\text{CaCO}_3$  dissolution (Gorokhova and Chursin, 2021).

### 4.2 Soil aggregate distribution and associated available N and P concentrations

The mean weight diameter (MWD), an important index for assessing soil aggregate size distribution, can reveal the physical structure of soil and reflect soil quality (Ma et al., 2020). Previous studies have shown that straw returning increased MWD (Huang et al., 2017; Ma et al., 2020; Cao et al., 2021), but we found no significant change in MWD in our study, likely due to the use of the

dry sieving method, which differs from the wet sieving method used in previous studies. As seen in Table 1, 2–7 mm soil aggregates were increased by the C, SR60, and SR100 treatments, but not the SR20 treatment. High rates of straw returning increased the proportion of >2 mm soil aggregates, consistent with previous reports (Wang et al., 2015; Ma et al., 2020), showing that fresh SOC can stimulate microbial activity to produce soil binders (Six et al., 2000), so it is easy for soil aggregate agglomeration. The C treatment also increased the proportion of >2 mm soil aggregates, which may be caused by the same reason, but the carbon source for microbial activity came from the depletion of soil original SOM. The low proportion of >2 mm soil aggregates under SR20 treatment showed high microbial activity but inadequate soil fresh carbon input.

The concentration of  $\text{NO}_3^-$ -N within all sizes of aggregates in C and straw returning treatments was higher than that in the CK treatment, likely due to the chemical fertilization of N (Nagatake et al., 2018). Furthermore, straw returning could increase soil cation exchange capacity (Cheng et al., 2023) and decrease N leaching in soil (Yang et al., 2016), which could also increase  $\text{NO}_3^-$  adsorption to soil aggregates and  $\text{NO}_3^-$ -N concentration. Our study also found that within the same treatment,  $\text{NO}_3^-$  was strongly associated with 1–2 mm soil aggregates.

Previous studies have suggested that straw returning could increase soil N availability due to N input from straw (Wang et al., 2018), immobilizing soil mineral N, and releasing N from straw decomposition (Takahashi et al., 2003; Thuy et al., 2008). However, few studies have investigated  $\text{NO}_3^-$ -N and  $\text{NH}_4^+$ -N distribution among different soil aggregates. We found that the SR100 treatment significantly increased  $\text{NH}_4^+$ -N concentration in <0.25 mm and 0.25–1 mm aggregates. The reasons might be that the SR100 treatment increased soil organic carbon content, which decreased  $\text{NH}_4^+$  adsorption to the soil caused by reduced exchange sites for  $\text{NH}_4^+$  (Zhang et al., 2022). All treatments showed that  $\text{NH}_4^+$ -N concentrations were higher in <0.25 mm and 2–7 mm aggregates but lower in 0.25–1 mm and 1–2 mm aggregates. Soil aggregates of <0.25 mm showed the highest  $\text{NH}_4^+$ -N concentration, likely due to their large surface area, which has been reported in previous studies to accumulate nutrients (Adesodun et al., 2007; Wang W. et al., 2011; Mitran et al., 2018).  $\text{NH}_4^+$ -N concentration was also high in 2–7 mm aggregates, possibly due to  $\text{CaCO}_3$  content shown by RDA analysis (Figure 3D).  $\text{CaCO}_3$  content has been reported to have positive effects on soil macroaggregates (Ge et al., 2019), which provide physical protection for soil organic carbon content from microbial decomposition (Wei et al., 2013), which was proved to be important for  $\text{NH}_4^+$  retention in soil (Baldock and Nelson, 2000).

The application of chemical fertilizer alone or combined with straw returning was shown to increase soil available P due to P release from the fertilizer (Wang W. et al., 2011; Ahmed et al., 2017) or organic matter mineralization (Chen et al., 2018; Cheng et al., 2019; Cao et al., 2021). Previous studies reported that a high rate of straw returning has positive effects on soil available P in aggregates, indicating that more nutrients are contained in straw (Ma et al., 2020). This study found that resin-P concentrations generally increased as aggregate size decreased, which is consistent with previous findings and might be caused by the increasing surface area with decreasing size of aggregates (Mitran et al., 2018; Cheng et al., 2019).

### 4.3 Soil aggregate-associated phosphatase activities

Phosphatase activities play a crucial role in soil P availability. This study found that straw returning had positive treatment effects on soil acid phosphomonoesterase activities (AcP) in aggregates <2 mm and alkaline phosphomonoesterase activities (AlP) and phosphodiesterase activities (PD) in all aggregates. These findings were consistent with those of previous studies, which suggested that the increasing substrate availability caused by straw returning (Li et al., 2022), and cumulative effects on soil enzyme activities from annual straw incorporation, might contribute to the significant effects of a high rate of straw returning (Wang et al., 2018; Li et al., 2022). The high AcP, AlP, and PD in 1–2 mm aggregates indicate those aggregates provide a more suitable environment for microbial population, and soil enzymes due to the suitable environment probably had higher phosphomonoesterase and phosphodiesterase activities.

Pyrophosphatase in soil plays a role in catalyzing pyrophosphate to orthophosphate (Tabatabai et al., 1994). Pyrophosphatase activities (PrA) are negatively related to soil pH (Tabatabai and Dick, 1979), but no significance of soil pH was found in this study. The study also found that the activities of pyrophosphatase are closely related to substrate (pyrophosphate) content, which correlated positively with microbial P (Reitzel and Turner, 2014), especially with soil fungal communities (Bünemann et al., 2004; Makarov et al., 2005; Koukol et al., 2008). The previous studies showed that straw returning affects fungal communities, resulting in more fungal communities under medium and high levels of straw returning (Wang et al., 2021). The high activities of PrA in 1–2 mm aggregates under C, SR20, SR60, and SR100 treatments might show more fungal microbial biomass, which provided more pyrophosphate as substrates.

### 4.4 Relationships among straw returning, soil properties, soil aggregates, and soil phosphatase activities

Only four significant factors could influence <0.25 mm soil aggregates associated with phosphatase activities. Soil AcP, AlP, and PD positively related to soil organic matter, and PrA positively correlated with  $\text{NH}_4^+$ -N and  $\text{NO}_3^-$ -N concentration. Soil AcP, AlP, and PD positively related to soil organic carbon, which had been found previously (Saha et al., 2008; Wang J. B. et al., 2011; Wei et al., 2015) due to substrate effect and more favorable environmental factors for enzymes (Zhang et al., 2012; Zhang et al., 2016).

For 0.25–1 mm soil aggregates associated with phosphatase activities, only SOM and  $\text{CaCO}_3$  contents significantly influenced enzyme activities. SOM positively influences AlP, PrA, and soil  $\text{CaCO}_3$ . Soil organic carbon increasing phosphatase activities were extensively reported (Tabatabai and Dick, 1979; Saha et al., 2008; Wang J. B. et al., 2011; Wei et al., 2015). Unlike the report of soil  $\text{CaCO}_3$  negatively related to soil PrA (Tabatabai and Dick, 1979), this study found a positive relationship between  $\text{CaCO}_3$  and PrA (also in 1–2 and 2–7 mm aggregates, Figures 3C, D). This was possible because the soil pH in this study still ranged in the optimum pH for soil PrA (Dick and Tabatabai, 1978), which covered the effect of  $\text{CaCO}_3$ .

Soil pH,  $\text{NO}_3^-$ -N, resin-P, and  $\text{CaCO}_3$  were considered significant factors influencing soil phosphatase activities in 1–2 mm aggregates. Soil pH negatively correlated with soil AcP and PD, while soil AIP was attributed to soil resin-P concentration. Through the data analysis, the study found that alkaline phosphomonoesterase was a determining factor for P availability in 1–2 mm aggregates in calcareous soils and a high rate of straw returning had higher alkaline phosphatase activities.

The study found that soil pH,  $\text{NH}_4^+$ -N,  $\text{NO}_3^-$ -N, resin-P, and  $\text{CaCO}_3$  are significant factors that influence soil phosphatase activities in 2–7 mm aggregates. Similar to those in 1–2 mm aggregates, soil pH negatively correlated with soil AcP and PD, while soil AIP positively related to soil resin-P and  $\text{NO}_3^-$ -N concentration.  $\text{NH}_4^+$ -N and  $\text{CaCO}_3$  had a positive effect on soil PrA. Soil available nitrogen concentration positively correlated with soil PrA or soil AIP, except for 0.25–1 mm aggregates. This can be explained by soil biota secreting more enzymes to enhance the supply of N and P when soil nutrition is limited (Zhang et al., 2012). Soil pH was considered to have a negative effect on soil PrA, but the effect would be weak in neutral and alkaline soil (Tabatabai and Dick, 1979); thus, we found a slight influence between soil pH and PrA (Figures 3C, D). In addition, the soil pH in our study had no difference among treatments.

## 5 Conclusion

Straw returning with chemical fertilizer could increase soil phosphatase activities, and a high rate of straw returning treatment could be more desirable. The phosphatase activities within <0.25 mm, 0.25–1 mm, 1–2 mm, and 2–7 mm aggregates were influenced differently by soil properties under different treatments, with significant factors including soil pH,  $\text{NH}_4^+$ -N,  $\text{NO}_3^-$ -N, resin-P, SOM, and  $\text{CaCO}_3$ . These factors can be classified into 1) SOM, which influences the substrate of phosphatase, and 2) soil pH, available N and P, and  $\text{CaCO}_3$ , which influence the environment and soil biota. More research should be conducted on straw returning to calcareous soils, especially on soil aggregates and their associated enzyme activities, as they have not been extensively studied.

In conclusion, the short term (3.5 years) of maize straw returning to the field had no significant influence on the calcareous soil

aggregate distribution. However, a high rate of straw returning significantly increased SOM and activities of soil enzymes (acid phosphomonoesterase, alkaline phosphomonoesterase, and phosphodiesterase). The soil pyrophosphatase activities showed a different trend from the other three enzymes and were significantly influenced by soil available N and  $\text{CaCO}_3$  concentration. Therefore, a high rate of straw returning is recommended to improve soil nutrition and phosphatase activities in calcareous soils.

## Data availability statement

The original contributions presented in the study are included in the article/Supplementary Material; further inquiries can be directed to the corresponding authors.

## Author contributions

X-JL: conceptualization, data curation, and original draft preparation. G-NZ: design of methodology and supervision. ZW: writing—review and editing. Q-DH: validation. PL: resources and supervision. All authors contributed to the article and approved the submitted version.

## Conflict of interest

The authors declare that the research was conducted in the absence of any commercial or financial relationships that could be construed as a potential conflict of interest.

## Publisher's note

All claims expressed in this article are solely those of the authors and do not necessarily represent those of their affiliated organizations, or those of the publisher, the editors, and the reviewers. Any product that may be evaluated in this article, or claim that may be made by its manufacturer, is not guaranteed or endorsed by the publisher.

## References

- Adesodun, J. K., Adeyemi, E. F., and Oyegoke, C. O. (2007). Distribution of nutrient elements within water stable aggregates of two tropical agro-ecological soils under different land uses. *Soil Tillage Res.* 92, 190–197. doi:10.1016/j.still.2006.03.003
- Ahmed, E. H., Anjum, S. I., and Zhang, M. K. (2017). Effects of fertilization on phosphorus distribution in water-stable aggregates of soils with different properties. *Toxicol. Environ. Chem.* 99 (1), 32–47. doi:10.1080/02772248.2016.1172584
- Alidad, K., Mehdi, H., Sadegh, A., Hassan, R., and Sanaz, B. (2012). Organic resource management: Impacts on soil aggregate stability and other soil physico-chemical properties. *Agric. Ecosyst. Environ.* 148, 22–28. doi:10.1016/j.agee.2011.10.021
- Bai, Y., Gu, C., Tao, T., Chen, G., and Shan, Y. (2013). Straw incorporation increases solubility and uptake of cadmium by rice plants. *Acta Agric. Scand. Sect. B Soil Plant Sci.* 63, 193–199. doi:10.1080/09064710.2012.743582
- Baldock, J. A., and Nelson, P. N. (2000). "Soil organic matter," in *Handbook of soil science*. Editor M. E. Sumner (Boca Raton, USA: CRC Press).
- Barthès, B. G., Kouakoua, E., Larré-Larrouy, M. C., Razafimbelo, T. M., de Luca, E. F., Azontonde, A., et al. (2008). Texture and sesquioxide effects on water-stable aggregates and organic matter in some tropical soils. *Geoderma* 143 (1), 14–25. doi:10.1016/j.geoderma.2007.10.003
- Bünemann, E. K., Smernik, R. J., Marschner, P., and McNeill, A. M. (2004). Microbial synthesis of organic and condensed forms of phosphorus in acid and calcareous soils. *Soil Biol. biochem.* 40, 932–946. doi:10.1016/j.soilbio.2007.11.012
- Cao, D. Y., Lan, Y., Sun, Q., Yang, X., Chen, W. F., Meng, J., et al. (2021). Maize straw and its biochar affect phosphorus distribution in soil aggregates and are beneficial for improving phosphorus availability along the soil profile. *Eur. J. Soil Sci.* 72 (5), 2165–2179. doi:10.1111/ejss.13095
- Chen, Y., Camps-Arbestain, M., Shen, Q., Singh, B., and Cayuela, M. L. (2018). The long-term role of organic amendments in building soil nutrient fertility: A meta-analysis and review. *Nutr. Cycl. Agroecosyst.* 111, 103–125. doi:10.1007/s10705-017-9903-5
- Cheng, R., Da, P. G., Tian, Q. B., Yan, Q. G., Xi, W. S., and Li, Y. G. (2023). Straw return alleviates the negative effects of saline sodic stress on rice by improving soil chemistry and reducing the accumulation of sodium ions in rice leaves. *Agri. Ecosyst. Environ.* 342, 108253. doi:10.1016/j.agee.2022.108253

- Cheng, Z. B., Chen, Y., Gale, W. J., and Zhang, F. H. (2019). Inorganic phosphorus distribution in soil aggregates under different cropping patterns in northwest China. *J. Soil Sci.* 19, 157–165. doi:10.1007/s42729-019-00022-1
- Criquet, S., and Braud, A. (2008). Effects of organic and mineral amendments on available P and phosphatase activities in a degraded Mediterranean soil under short-term incubation experiment. *Soil Tillage Res.* 98, 164–174. doi:10.1016/j.still.2007.11.001
- Deng, X., Xu, T. L., Dong, W. W., Zhang, Q., and Liang, Y. J. (2021). Distribution of organic phosphorus in soil aggregates from apple-pear Orchard of China. *Eurasian Soil Sci.* 54 (1), 72–79. doi:10.1134/s1064229321010038
- Dick, W. A., and Tabatabai, M. A. (1978). Inorganic pyrophosphatase activity of soils. *Soil Biol. biochem.* 10, 58–65. doi:10.1016/0038-0717(78)90011-1
- Fang, Y., Nazaries, L., Singh, B. K., and Singh, B. P. (2018). Microbial mechanisms of carbon priming effects revealed during the interaction of crop residue and nutrient inputs in contrasting soils. *Glob. Chang. Biol.* 24, 2775–2790. doi:10.1111/gcb.14154
- Galantini, J. A., Senesi, N., Brunetti, G., and Roselli, R. (2004). Influence of texture on organic matter distribution and quality and nitrogen and sulphur status in semiarid Pampean grassland soils of Argentina. *Geoderma* 123 (1), 143–152. doi:10.1016/j.geoderma.2004.02.008
- Garbuz, S. A., Yaroslavtseva, N. V., and Kholodov, V. A. (2016). Enzymatic activity inside and outside of water-stable aggregates in soils under different land use. *Eurasian Soil Sci.* 49 (3), 367–375. doi:10.1134/s1064229316030030
- Garland, G., Bünenmann, E. K., Oberson, A., Frossard, E., Snapp, S., Chikowo, R., et al. (2018). Phosphorus cycling within soil aggregate fractions of a highly weathered tropical soil: A conceptual model. *Soil Biol. biochem.* 116, 91–98. doi:10.1016/j.soilbio.2017.10.007
- Ge, N., Wei, X. R., Xiang, W. C., Liu, X. T., Shao, M. G., Jia, X. X., et al. (2019). Soil texture determines the distribution of aggregate-associated carbon, nitrogen and phosphorus under two contrasting land use types in the Loess Plateau. *Catena* 172, 148–157. doi:10.1016/j.catena.2018.08.021
- Gorokhova, N., and Chursin, I. N. (2021). Carbonates in irrigated soils of the Caspian depression. *Arid. Ecosyst.* 11, 193–199. doi:10.1134/s2079096121020062
- He, Y. T., He, X. H., Xu, M. G., Zhang, W. J., Yang, X. Y., and Huang, S. M. (2018). Long-term fertilization increases soil organic carbon and alters its chemical composition in three wheat-maize cropping sites across central and south China. *Soil Tillage Res.* 177, 79–87. doi:10.1016/j.still.2017.11.018
- Huang, R., Lan, M. L., Liu, J., and Gao, M. (2017). Soil aggregate and organic carbon distribution at dry land soil and paddy soil: The role of different straws returning. *Environ. Sci. Pollut. Res.* 24, 27942–27952. doi:10.1007/s11356-017-0372-9
- Kemper, W. D., and Rosenau, R. C. (1986). “Aggregate stability and size distribution,” in *Methods of soil analysis. Part 1. Physical and mineralogical methods. Agronomy monograph*. Editor A. Klute 2nd ed. (Madison, USA: American Society of Agronomy and Soil Science Society of America).
- Koukol, O., Novák, F., and Hrabal, R. (2008). Composition of the organic phosphorus fraction in basidiocarps of saprotrophic and mycorrhizal fungi. *Soil Biol. biochem.* 40, 2464–2467. doi:10.1016/j.soilbio.2008.04.021
- Lehmann, A., Leifheit, E. F., and Rillig, M. C. (2017). “Mycorrhizas and soil aggregation,” in *Mycorrhizal mediation of soil*. Editors N. C. Johnson, C. Gehring, and J. Jansa (Amsterdam, Netherlands: Elsevier).
- Li, F. Y., Liang, X. Q., Li, H., Jin, Y. B., Jin, J. W., He, M. M., et al. (2020). Enhanced soil aggregate stability limits colloidal phosphorus loss potentials in agricultural systems. *Environ. Sci. Eur.* 32, 17. doi:10.1186/s12302-020-0299-5
- Li, X. D., Mao, N., Jiang, H., Jiang, X. Y., Li, C., Gong, X., et al. (2022). Synergistic effects of straw and earthworm addition on microbial diversity and microbial nutrient limitation in a subtropical conservation farming system. *Soil Tillage Res.* 224, 105500. doi:10.1016/j.still.2022.105500
- Liu, J., and Diamond, J. (2005). China's environment in a globalizing world. *Nature* 435 (7046), 1179–1186. doi:10.1038/4351179a
- Loeppert, R. H., and Suarez, G. L. (1996). “Carbonates and gypsum,” in *Methods of soil analysis part 3 chemical methods*. Editors D. L. Sparks, A. L. Page, and P. A. Helmke (Madison, USA: American Society of Agronomy and Soil Science Society of America).
- Lu, H., Hu, L., Zheng, W., Yao, S., and Qian, L. (2020). Impact of household land endowment and environmental cognition on the willingness to implement straw incorporation in China. *J. Clean. Prod.* 262, 121479. doi:10.1016/j.jclepro.2020.121479
- Ma, S. T., Kan, Z. R., Qi, J. Y., and Zhang, H. (2020). Effects of straw return mode on soil aggregates and associated carbon in the North China Plain. *Agronomy* 10, 61. doi:10.3390/agronomy10010061
- Makarov, M. I., Haumaier, L., Zech, W., Marfenina, O. E., and Lysak, L. V. (2005). Can  $^{31}\text{P}$  NMR spectroscopy be used to indicate the origins of soil organic phosphates? *Soil Biol. biochem.* 37, 15–25. doi:10.1016/j.soilbio.2004.07.022
- Meng, Q. F., Sun, Y. T., Zhao, J., Zhou, L. R., Ma, X. F., Zhou, M., et al. (2014). Distribution of carbon and nitrogen in water-stable aggregates and soil stability under long-term manure application in solonchets soils of the Songnen plain, northeast China. *J. Soils Sediments* 14 (6), 1041–1049. doi:10.1007/s11368-014-0859-7
- Mitran, T., Mani, P. K., Bandyopadhyay, P. K., and Basak, N. (2018). Effects of organic amendments on soil physical attributes and aggregate-associated phosphorus under long-term rice-wheat cropping. *Pedosphere* 28, 823–832. doi:10.1016/s1002-0160(17)60423-5
- Mrquez, C. O., García, V. J., Schultz, R. C., and Isenhardt, T. M. (2019). A conceptual framework to study soil aggregate dynamics. *Eur. J. Soil Sci.* 70 (3), 466–479. doi:10.1111/ejss.12775
- Mulvaney, R. L. (1996). “Nitrogen-inorganic forms,” in *Methods of soil analysis part 3 chemical methods*. Editors D. L. Sparks, A. L. Page, and P. A. Helmke (Madison, USA: American Society of Agronomy and Soil Science Society of America).
- Nagatake, A., Mukumbuta, I., Yasuda, K., Shimizu, M., Kawai, M., and Hatano, R. (2018). Temporal dynamics of nitrous oxide emission and nitrate leaching in renovated grassland with repeated application of manure and/or chemical fertilizer. *Atmosphere* 9, 485. doi:10.3390/atmos9120485
- Nelson, D. W., and Sommers, L. E. (1996). “Total carbon, organic carbon, and organic matter,” in *Methods of soil analysis part 3 chemical methods*. Editors D. L. Sparks, A. L. Page, and P. A. Helmke (Madison, USA: American Society of Agronomy and Soil Science Society of America).
- Reitzel, K., and Turner, B. (2014). Quantification of pyrophosphate in soil solution by pyrophosphatase hydrolysis. *Soil Biol. biochem.* 74, 95–97. doi:10.1016/j.soilbio.2014.03.001
- Saha, S. V., Prakash, S., Kundu, N., Kumar, B. L., Eur, J., and Mina, B. L. (2008). Soil enzymatic activity as affected by long term application of farm yard manure and mineral fertilizer under a rainfed soybean-wheat system in N-W Himalaya. *Eur. J. Soil Biol.* 44, 309–315. doi:10.1016/j.ejsobi.2008.02.004
- Sahrawat, K. L. (2005). Fertility and organic matter in submerged rice soils. *Curr. Sci.* 88, 735–739.
- Sharpley, A. (2000). “Bioavailable phosphorus in soil,” in *Methods of phosphorus analysis for soils, sediments, residuals and waters*. Editor G. M. Pierzynski (North Carolina, USA: North Carolina State University).
- Six, J., Bossuyt, H., Degryze, S., and Deneef, K. (2004). A history of research on the link between (micro) aggregates, soil biota, and soil organic matter dynamics. *Soil Tillage Res.* 79 (1), 7–31. doi:10.1016/j.still.2004.03.008
- Six, J., Elliott, E. T., and Paustian, K. (2000). Soil macroaggregate turnover and microaggregate formation: A mechanism for C sequestration under no-tillage agriculture. *Soil Biol. biochem.* 32, 2099–2103. doi:10.1016/s0038-0717(00)00179-6
- Stegarescu, G., Reintam, E., and Tönutare, T. (2021). Cover crop residues effect on soil structural stability and phosphatase activity. *Acta Agr. Scand. B-S p.* 71 (9), 992–1005. doi:10.1080/09064710.2021.1973083
- Tabatabai, M. A., Angel, S., Bottomley, P., Bezdicke, D., Smith, S., Tabatabai, A., et al. (1994). “Soil enzymes,” in *Method of soil analysis*. Editors S. H. Mickelson and J. M. Bigham (Madison, USA: American Society of Agronomy and Soil Science Society of America).
- Tabatabai, M. A., and Dick, W. A. (1979). Distribution and stability of pyrophosphatase in soils. *Soil Biol. biochem.* 11, 655–659. doi:10.1016/0038-0717(79)90035-x
- Takahashi, S., Uenosono, S., and Ono, S. (2003). Short- and long-term effects of rice straw application on nitrogen uptake by crops and nitrogen mineralization under flooded and upland conditions. *Plant Soil* 251, 291–301. doi:10.1023/a:1023006304935
- Tan, C. J., Cao, X., Yuan, S., Wang, W. Y., Feng, Y. Z., and Qiao, B. (2015). Effects of long-term conservation tillage on soil nutrients in sloping fields in regions characterized by water and wind erosion. *Sci. Rep.* 5, 17592. doi:10.1038/srep17592
- Thuy, N. H., Shan, Y. H., Bija, S., Wang, K. R., Cai, Z. C., Yadvinder, S., et al. (2008). Nitrogen supply in rice-based cropping systems as affected by crop residue management. *Soil Sci. Soc. Am. J.* 72, 514–523. doi:10.2136/sssaj2006.0403
- Tian, S. Y., Wang, M. W., Jiang, Y. J., Zhang, C. Z., Li, D. M., Chen, X. Y., et al. (2022). Organic fertilization promotes crop productivity through changes in soil aggregation. *Soil Biol. biochem.* 165, 108533. doi:10.1016/j.soilbio.2021.108533
- Vitousek, P. M., Naylor, R., Crews, T., David, M. B., Drinkwater, L. E., Holland, E., et al. (2019). Nutrient imbalances in agricultural development. *Science* 324 (5934), 1519–1520. doi:10.1126/science.1170261
- Wang, E. Z., Lin, X. L., Tian, L., Wang, X. G., Li, J., Jin, F., et al. (2021). Effects of short-term rice straw return on the soil microbial community. *Agriculture* 11, 561. doi:10.3390/agriculture11060561
- Wang, J. B., Chen, Z. H., Chen, L. J., Zhu, A. N., and Wu, Z. J. (2011a). Surface soil phosphorus and phosphatase activities affected by tillage and crop residue input amounts. *Plant Soil Environ.* 57, 251–257. doi:10.17221/437/2010-pse
- Wang, W., Chen, W. C., Wang, K. R., Xie, X. L., Yin, C. M., and Chen, A. L. (2011b). Effects of long-term fertilization on the distribution of carbon, nitrogen and phosphorus in water-stable aggregates in paddy soil. *Agri. Sci. China* 10, 1932–1940. doi:10.1016/s1671-2927(11)60194-6
- Wang, X. J., Jia, Z. K., Liang, L. Y., Yang, B. P., Ding, R. X., Nie, J. F., et al. (2015). Maize straw effects on soil aggregation and other properties in arid land. *Soil Tillage Res.* 153, 131–136. doi:10.1016/j.still.2015.05.001
- Wang, X. J., Jia, Z. K., Liang, L. Y., Zhao, Y. F., Yang, B. P., Ding, R. X., et al. (2018). Changes in soil characteristics and maize yield under straw returning system in dryland farming. *Field Crop Res.* 218, 11–17. doi:10.1016/j.fcr.2017.12.003



- Wang, Y., Tang, C., Wu, J., Liu, X., and Xu, J. (2013). Impact of organic matter addition on pH change of paddy soils. *J. Soils Sediments* 13, 12–23. doi:10.1007/s11368-012-0578-x
- Wei, T., Zhang, P., Wang, K., Ding, R., Yang, B., Nie, J., et al. (2015). Effects of wheat straw incorporation on the availability of soil nutrients and enzyme activities in semiarid areas. *PLoS One* 10, e0120994. doi:10.1371/journal.pone.0120994
- Wei, X., Li, X., Jia, X., and Shao, M. (2013). Accumulation of soil organic carbon in aggregates after afforestation on abandoned farmland. *Biol. Fertil. Soils* 49, 637–646. doi:10.1007/s00374-012-0754-6
- Yang, H. S., Xu, M. M., Koide, R. T., Liu, Q., Dai, Y. J., Liu, L., et al. (2016). Effects of ditch-buried straw return on water percolation, nitrogen leaching and crop yields in a rice-wheat rotation system. *J. Sci. Food Agr.* 96, 1141–1149. doi:10.1002/jsfa.7196
- Yao, S., Teng, X., and Zhang, B. (2015). Effects of rice straw incorporation and tillage depth on soil puddlability and mechanical properties during rice growth period. *Soil Tillage Res.* 146, 125–132. doi:10.1016/j.still.2014.10.007
- Zamanian, K., and Kuzyakov, Y. (2019). Contribution of soil inorganic carbon to atmospheric CO<sub>2</sub>: More important than previously thought. *Glob. Change Biol.* 25, e1–e3. doi:10.1111/gcb.14463
- Zhang, A. M., Chen, Z. H., Zhang, G. N., Chen, L. J., and Wu, Z. J. (2012). Soil phosphorus composition determined by 31P NMR spectroscopy and relative phosphatase activities influenced by land use. *Eur. J. Soil Biol.* 52, 73–77. doi:10.1016/j.ejsobi.2012.07.001
- Zhang, P., Chen, X., Wei, T., Yang, Z., Jia, Z., Yang, B., et al. (2016). Effects of straw incorporation on the soil nutrient contents, enzyme activities, and crop yield in a semiarid region of China. *Soil Tillage Res.* 160, 65–72. doi:10.1016/j.still.2016.02.006
- Zhang, S. X., Li, Q., Lü, Y., Zhang, X. P., and Liang, W. J. (2013). Contributions of soil biota to C sequestration varied with aggregate fractions under different tillage systems. *Soil Biol. biochem.* 62, 147–156. doi:10.1016/j.soilbio.2013.03.023
- Zhang, W. Z., Chen, X. Q., Wang, H. Y., Wei, W. X., and Zhou, J. M. (2022). Long-term straw return influenced ammonium ion retention at the soil aggregate scale in an Anthrosol with rice-wheat rotations in China. *J. Integr. Agr.* 21, 521–531. doi:10.1016/s2095-3119(20)63592-4
- Zhang, X. F., Xin, X. L., Zhu, A. N., Yang, W. L., Zhang, J. B., Ding, S. J., et al. (2018). Linking macroaggregation to soil microbial community and organic carbon accumulation under different tillage and residue managements. *Soil Tillage Res.* 178, 99–107. doi:10.1016/j.still.2017.12.020
- Zhang, Y. Q., Dalal, R. C., Bhattacharyya, R., Meyer, G., Wang, P., Menzies, N. W., et al. (2021). Effect of long-term no-tillage and nitrogen fertilization on phosphorus distribution in bulk soil and aggregates of a Vertisol. *Soil Tillage Res.* 205, 104760. doi:10.1016/j.still.2020.104760
- Zhao, H. L., Shar, A. G., Li, S., Chen, Y. L., Shi, J. L., Zhang, X. Y., et al. (2018). Effect of straw return mode on soil aggregation and aggregate carbon content in an annual maize-wheat double cropping system. *Soil Tillage Res.* 175, 178–186. doi:10.1016/j.still.2017.09.012



# Frontiers in Environmental Science

Explores the anthropogenic impact on our natural world

An innovative journal that advances knowledge of the natural world and its intersections with human society. It supports the formulation of policies that lead to a more inhabitable and sustainable world.

## Discover the latest Research Topics

[See more →](#)

### Frontiers

Avenue du Tribunal-Fédéral 34  
1005 Lausanne, Switzerland  
[frontiersin.org](https://frontiersin.org)

### Contact us

+41 (0)21 510 17 00  
[frontiersin.org/about/contact](https://frontiersin.org/about/contact)

